Investigating the transcriptional response of rDNA to hypoxia

Natalie Ng

Trinity College

Thesis submitted to the University of Oxford in accordance with the requirements for the degree of Doctor of Philosophy

Michaelmas Term 2020
University of Oxford

Word Count: 33000 words

Acknowledgements

What a wild ride these 4+ years have been. I owe my experience to a huge number of people, without many of whom my experience would have been entirely different.

To my supervisors Ester, I could not have asked for a better person to guide me through this DPhil. I am grateful for the in-depth discussions that we had, no matter how brain-aching the topic and a relentless supply of energy to keep me motivated, even through a global pandemic. I have learnt a lot through working with Ester, in particular, the align function in PowerPoint, but also in becoming a better scientist and for that I am extremely grateful. Without your support, none of this would have been possible.

To my research thesis committee, Andy Blackford and Rob Chapman, thank you for all the discussions and comments with the progress of the project. Also, Tim Humphrey and Nic Denko for help with the manuscript.

To the amazing Hammond lab past and present – Sam, this DPhil has been our Mount Doom and we're nearly at the summit. Whether it was KFC, losing multiple points on the board through squash bets or nearly getting locked up in Greece, I couldn't have asked for a person so sick to start and finish with. Thank you for being the best friend and fellow comrade I could have ask for. It is fair to say I wouldn't have enjoyed my time quite as much had it not been for you.

Shaliny, my shining moon. Transcription is abhorrent and your long, long stories about nothing in particular are going to be sorely missed. Tiffany, it has been a pleasure being your *Senpai*. Ania, you've been my pillar of support in the form of polish sausage and also true friendship, best regards. Liz, thank you for all the marvelous times spent goofing around in the lab. We live in isolation… Hannah, Joe, Hasan, Kasia, Eva, GG, Karin, Greg, Ishna, Sarah, Ewen, Ryan, Juan, Athena, Jutta, Anna.

To the legends who have helped me along the way – Sovan, Ihor, Eliot, Greg Blow, Egon, Manon, Graham, Rhod, Lisa, Carol, Jamie, Andy Ryan, Asmita, Sam Hume, Timo, from German beers in the park to delving into career chats. The heroes of the oncology facilities team - Caroline, Andy, Pash, Charles. To all the Trin folk especially Owain, sorry for stealing your room.

To my better half, Jen, where would I be without you. I'm so grateful for the support, laughs and love over the past few years. I don't think I could have been luckier to meet such a selfless, wonderful person during the most challenging of times to get through them together. Also, special thank you to Jen's family, Chris, Peter & Marianne for taking me under their wing.

Finally, to my incredible parents for being the pillar of support for all my endeavours and always telling me not to give up. From home-visits to recuperate from busy Oxford life to real-life advice, I am eternally grateful for everything you've done and I owe all my successes to them.

Abstract

Hypoxic conditions initiate a multitude of transcriptional adaptations including increased expression of a family of well-characterised stress-inducible genes by hypoxia-dependent transcription factors. In contrast, the mechanisms of transcriptional repression in hypoxia have not been well characterised. Here, I show that hypoxia leads to global transcriptional repression, including at the site of ribosomal DNA (rDNA) transcription in the membraneless subcellular organelle, the nucleolus. Transcriptional repression occurs in both cancer and non-cancer cell lines in an oxygen-dependent manner. Both transcription of the rDNA and processing of the pre-ribosomal RNA (pre-rRNA) is repressed in hypoxic conditions. I describe the rapid accumulation of DNA/RNA hybrids, also known as R-loops, in hypoxia and demonstrate that these R-loops are most prominent in the nucleolus. Mechanistically, neither hypoxia-mediated activation of the DNA damage response kinases ATM or ATR, nor the nucleoprotein TCOF1 contribute to rDNA transcriptional repression in hypoxia. Instead, it was determined that R-loops rapidly accumulate on the rDNA in hypoxia and that this limits RNA polymerase I mediated transcription. Finally, I show that R-loop formation increases heterochromatin formation, specifically H3K9me3 on the rDNA and that R-loop accumulation is mediated by the RNA/DNA helicase senataxin (SETX) at rDNA loci, suggesting a chromatin-based mechanism that contributes to hypoxia-mediated repression of rDNA transcription. Together, these findings shed light on the control of RNPI transcription in response to hypoxic conditions and presents a unique mechanism of RNPI shutdown in response to stress.

Contents

Abstract 1
List of Figures 6
List of tables 8
List of Abbreviations 9
1 Chapter 1 16
Introduction 16
1.1 Cancer 16
1.2 Sources of genome instability 18
1.2.1 The tumour microenvironment 26
1.3 Hypoxia 26
1.3.1 The origins of tumour hypoxia 26
1.3.2 Acute, chronic, cycling hypoxia 27
1.4 Hypoxia and resistance to therapy 28
1.5 The biological response to hypoxia 30
1.5.1 Hypoxia inducible factor (HIF) 31
1.5.2 Unfolded protein response (UPR) activation in hypoxia 32
1.5.3 DNA damage response (DDR) activation in hypoxia 36
1.5.4 The repression of gene transcription in hypoxia 39
1.6 RNPI mediated transcription 44
1.6.1 rRNA processing 53
1.6.2 5'ETS processing 56
1.6.3 Stress induced repression of rDNA transcription 62
1.6.4 How are R-loops linked to RNPI 68
1.7 RNPI in hypoxia 70
1.8 Aims of this study 71
2 Chapter 2 73
Materials and Methods 73
2.1 Cell lines and Reagents 73
2.2 Freezing and thawing cells 73
2.3 Mycoplasma test 73
2.4 Hypoxia 74
2.5 Short interfering RNA (siRNA) transfection 74
2.6 Bacterial transformation 75

2.7 Plasmid purification 75
2.8 DNA Plasmid transfection 76
2.9 5’ethynyl uridine (EU) staining 76
2.10 RNA preparation 77
2.11 Complementary DNA (cDNA) synthesis 77
2.12 Quantitative PCR (qPCR) 77
2.13 PAPAS detection using PCR 79
2.14 Protein lysate preparation 80
2.15 Western blotting 81
2.16 Puromycin incorporation assay 84
2.17 Immunofluorescence (IF) 84
2.18 Nucleotide (NTP) measurement 85
2.19 R-loop detection by S9.6 immunofluorescence 85
2.20 RNA gel electrophoresis 86
2.21 Poly-nucleotide Kinase (PNK) radio-end labelling probe preparation 86
2.22 Northern blotting 86
2.23 DNA purification using columns 87
2.24 DNA/RNA immunoprecipitation (DRIP) 88
2.25 Slot blot assay for R-loop detection 89
2.26 Chromatin immunoprecipitation (ChIP) 89
2.27 Statistical analysis 90
3 Chapter 3 91
The effect of hypoxia on the rDNA transcription response 91
3.1 Introduction 91
3.2 Hypoxia induces the DDR 91
3.3 Hypoxia leads to global transcriptional repression in cancer cells 93
3.4 Transcriptional repression in hypoxia occurs in non-cancer cells 94
3.5 Global transcriptional repression in hypoxia occurs in a HIF1α-independent manner 95
3.6 Global transcriptional repression in hypoxia occurs independently of p53 96
3.7 Transcription of ribosomal RNA is repressed in an oxygen dependent manner in hypoxia 98
3.8 rDNA transcription is repressed rapidly in hypoxia 99
3.9 Total levels of 18S and 28S rRNA are maintained in hypoxia 100
3.10 Protein synthesis is repressed in hypoxia 101

3.11 Hypoxia leads to an rRNA processing defect at A0 on the 5'ETS 103
3.12 Downstream processing of pre-rRNA is on the ITS1 and ITS2 region in hypoxia 104
3.13 snoRNA expression is maintained in hypoxia 106
3.14 PNRC1 is upregulated in an oxygen-dependent manner 107
3.15 Discussion 108
4 Chapter 4 110
Mechanisms of rDNA transcriptional repression 110
4.1 Introduction 110
4.2 Nucleotide levels are reduced in hypoxia 111
4.3 Nucleotide supplementation does not affect rRNA transcription in hypoxia 112
4.4 POLR1A and POLR1B subunits are repressed at the mRNA level in prolonged hypoxia 114
4.5 The expression of RNPI associated factors 115
4.6 Fibrillarin and nucleolin change localisation in prolonged periods of hypoxia 116
4.7 TCOF1 is not involved in rDNA repression in hypoxia 117
4.8 RNA polymerase II CTD levels do not change in acute hypoxia 121
4.9 RNA polymerase II inhibitors lead to decreased RNPI activity 121
4.10 PAPAS expression does not change in hypoxia 122
4.11 Transcriptional repression of rDNA occurs independently of p53 124
4.12 Transcriptional repression of rDNA occurs independently of ATM 124
4.13 Transcriptional repression of rDNA occurs independently of ATR 127
4.14 Transcriptional repression of rDNA occurs independently of PERK 129
4.15 Discussion 131
5 Chapter 5 133
Hypoxia leads to R-loop formation in the nucleolus which impact rDNA transcription 133
5.1 Introduction 133
5.2 R-loops impact the biological response to hypoxia 134
5.3 R-loops accumulate in hypoxic conditions in the nucleolus 136
5.4 Transcription of rDNA can be rescued by RNase H1 overexpression in hypoxia 137
5.5 RNase H1 overexpression does not affect pre-rRNA processing in hypoxia 138
5.6 C-MYC repression is not rescued by RNase H1 overexpression in hypoxia 139
5.7 R-loops form on the rDNA in hypoxia 140
5.8 Senataxin knockdown leads to reduced R-loops on the rDNA in hypoxia 141
5.9 Heterochromatin forms on the rDNA in hypoxia 143
5.10 Heterochromatin formation on the rDNA is RNase H1-sensitive in hypoxia 144

5.11 Discussion 145
6 Chapter 6 147
Discussion and conclusions 147
7 References 157
8 Appendix 184
8.1 Copyright details 184
8.2 Publications from this thesis 185
8.3 Awards and Prizes 185
8.4 Presentations 185

List of Figures

Figure 1.1. 1 The Hallmarks of cancer. 16
Figure 1.2. 1. Fork reversal and degradation upon encounter with a blockade. 19
Figure 1.2. 2. DNA/RNA hybrids (R-loops) are potential sources of genome instability. 20
Figure 1.2.3. The orientation of TRC affects R-loops and DDR signalling. 24
Figure 1.3.1.1. A gradient of decreasing oxygen tensions in a tumour occur due to insufficient vasculature. 27
Figure 1.5.1.1. The regulation of HIF1α under normoxic and hypoxic conditions. 32
Figure 1.5.2.1. Schematic of the unfolded protein response (UPR). 34
Figure 1.5.2.2. Pharmacological activation of the UPR restricts rDNA transcription in a PERK/EIF2α dependent manner. 35
Figure 1.5.4.1. A schematic of the transcriptional cycle of RNPII. 41
Figure 1.6. 1. Schematic of ribosome biogenesis. 46
Figure 1.6.2. The nucleolar compartments in a cell. 47
Figure 1.6. 3. The formation of the PIC for rDNA transcription. 50
Figure 1.6.1 1. Pre-rRNA processing pathways in humans. 54
Figure 1.6.2. 1. Uridine and pseudouridine (Ψ) chemical structure. 56
Figure 1.6.2. 2. U3 snoRNA base pairing with the 5'ETS of the pre-rRNA. 58
Figure 1.6.2. 3. PNRC1 blocks rRNA maturation. 59
Figure 1.6.2. 4. The exosome complex degrades many RNA species. 60
Figure 1.6.2. 5. 5'ETS elimination by the exosome complex 62
Figure 1.6.3.1.1. Schematic of the rDNA DSB-induced mechanism of transcriptional repression. 65
Figure 1.6.3.2. 1. Schematic of the mechanism of mild hypoosmotic stress induced R-loop stabilisation to block RNPI. 67
Figure 1.6.4. 1. RNPII drives ribosome biogenesis through R-loop formation. 70
Figure 2.1. Schematic of PAPAS detection experimental procedure. 80
Figure 3.2. The DDR is activated in an oxygen dependent manner. 92
Figure 3.3. Transcription is repressed in an oxygen dependent manner in cancer cells. 94
Figure 3.4. Transcriptional repression occurs in non-cancer cells in hypoxia. 95
Figure 3.5. Transcriptional repression in hypoxia occurs in a HIF1α-independent manner. 96
Figure 3.6. Transcriptional repression in hypoxia occurs in a p53-independent manner. 97
Figure 3.7. Transcription of rDNA is repressed in an oxygen dependent manner. 99
Figure 3.8. Transcription of rDNA is repressed rapidly in hypoxia. 100
Figure 3.9. The levels of 18S and 28S are maintained in hypoxia. 101

Figure 3.10. Protein translation is reduced significantly in prolonged hypoxia. 102
Figure 3.11. Processing at the A0 site of the 5'ETS pre-rRNA occurs aberrantly in hypoxia. 104
Figure 3.12. Processing at the ITS1 and ITS2 region of pre-rRNA occurs aberrantly in hypoxia.....105
Figure 3.13. SnoRNA expression panel in hypoxia.....106
Figure 3.14. PNRC1 is upregulated in hypoxic conditions. 108
Figure 4.2. NTP levels are reduced in hypoxia.....112
Figure 4.3. Nucleoside supplementation in hypoxia restores NTP levels. 114
Figure 4.4. POLR1A and POLR1B are repressed after prolonged hypoxia. 115
Figure 4.5. RNPI-associated factors expression in hypoxia. 116
Figure 4.6. The nucleolus undergoes nucleolar reorganisation in hypoxia. 117
Figure 4.7. TCOF1 does not translocate to the nucleolus in hypoxia.....120
Figure 4.8. RNPII CTD phosphorylation of S2 and S5 levels in hypoxia.....121
Figure 4.9. RNPII inhibitors decrease RNPI activity. 122
Figure 4.10. PAPAS expression in hypoxia.....123
Figure 4.11. rDNA transcriptional repression occurs independently of p53 in hypoxia. 124
Figure 4.12. rDNA transcriptional repression occurs independently of ATM in hypoxia. ...126
Figure 4.13. rDNA transcriptional repression occurs independently of ATR in hypoxia. 128
Figure 4.14. Initial rDNA transcriptional repression occurs independently of PERK in hypoxia.....130
Figure 5.2. RNase H1 overexpression impacts the biological response in hypoxia. 136
Figure 5.3. R-loops accumulate in the nucleolus in hypoxia.....137
Figure 5.4. RNase H1 overexpression results in higher levels of 47S production in hypoxia. 138
Figure 5.5. RNase H1 overexpression does not affect processing at A0 on the 5'ETS in hypoxia.....139
Figure 5.6. RNase H1 overexpression does not rescue C-MYC repression in hypoxia. 140
Figure 5.7. R-loops accumulate on the rDNA in hypoxia. 141
Figure 5.8. Senataxin knockdown in hypoxia leads to reduced R-loops on the rDNA. 142
Figure 5.9. Heterochromatin accumulates on the rDNA in hypoxia. 143
Figure 5.10. Heterochromatin accumulation on the rDNA is RNase H1-sensitive. 144

List of tables

Table 1.6 1 RNPI subunits in yeast and in human. 49

Table 2. 1. siRNA sequences 75
Table 2. 2. Primer sequences 78
Table 2. 3. PAPAS detection primer sequences 80
Table 2.4. Primary antibodies 81
Table 2.5. Secondary antibodies 83
Table 2. 6. Northern blot probes 87
Table 2. 7. DRIP primer sequences 88

List of Abbreviations

Abbreviation	Full Name
°C	°Celsius
53BP1	p53-binding protein 1
AA	Alpha amanitin
AID	Activation-induced cytidine deaminase
ANOVA	Analysis of variance
ATCC	American Type Culture Collection
ATF6	Activating transcription factor 6
ATM	Ataxia-telangiectasia mutated
ATP	Adenosine triphosphate
ATR	ATM- and Rad3-Related
ATRIP	ATR interacting protein
BER	Base excision repair
BPB	Bromophenol blue
BRCA	Breast Cancer gene
BRCT	BRCA1 C-terminal
BSA	Bovine serum albumin
Ca^{2+}	Calcium ions
CAIX	Carbonic anhydrase IX
CD	Co-directional
CDK	Cyclin dependent kinase
cDNA	Complementary DNA
CHK	Checkpoint protein
CP	Core promoter
CPT	Camptothecin
CRISPR	clustered regularly interspaced short palindromic repeats
Cas9	CRISPR associated protein 9

CSR	Class switch recombination
CTD	C-terminal domain
CTP	Cytosine triphosphate
DAPI	4',6-diamidino-2-phenylindole
DCP2	Decapping complex
DDR	DNA damage response
DDX19	Dead-box helicase 19
DEC1/2	Deleted in oesophageal cancer 1 and 2
DEPC	Diethyl pyrocarbonate
DFC	Dense fibrillar centre
DMEM	Dulbecco's modified eagle's medium
DMSO	Dimethyl sulfoxide
DNA	Deoxyribonucleic acid
dNTP	Deoxynucleotide
DSB	Double strand break
DOC	Sodium deoxycholate
DRB	5,6-dichloro-1-beta-D-ribofuranosylbenzimidazole
dsDNA	Double stranded DNA
dsRNA	Double stranded RNA
EDTA	Ethylenediaminetetraacetic acid
eIF2	Elongation initiation factor 2
ER	Endoplasmic reticulum
ERCC1	Excision Repair 1
ETAA1	Ewing’s tumour-associated antigen 1
ETS	External transcribed spacer
FBS	Fetal bovine serum
FC	Fibrillar centre
G4	G-quadruplex
GC	Granular compartment

GDP	Guanosine diphosphate
GTP	Guanosine triphosphate
H3	Histone H3
H3K4	Histone 3 lysine 4
H3K9me3	Histone 3 lysine 9 trimethylation
H3S10	Histone 3 Serine 10
HCl	Hydrochloric acid
HDAC	Histone deacetylase
HIF1α	Hypoxia-inducible factor 1α
HO	Head-on
HP1	Heterochromatin protein 1
HR	Homologous recombination
HRE	Hypoxia response element
HU	Hydroxyurea
IF	Immunofluorescence
Ig	Immunoglobulin
IGS	Intergenic region spacer
IP	Immunoprecipitation
I-PpoI	Intron-encoded endonuclease
IR	Ionising radiation
IRE1	Inositol requiring enzyme 1
ITS	Internal transcribed spacer
JmjC	Jumonji C
KAP-1	Krüppel-associated box domain associated protein 1
KDM	Lysine histone demethylase
LiCl	Lithium chloride
LSU	Large ribosomal subunit
m_3G	Tri-methylated 5' cap
m^7G	Mono-methylated 5' cap

MB	Methylene blue
MDC1	Mediator of DNA damage checkpoint 1
MDM2	Mouse double minute 2 homolog
MKI67	Marker of proliferation Ki-67
mmHg	Millimetres of mercury
MMR	Mismatch repair
M-MTIF	Microphthalmia-associated transcription factor
MRN	Mre11-Rad50-Nbs1
mRNA	Messenger RNA
mTOR	Mammalian target of rapamycin
Na_2PO_4	Bisodium phosphate
NaCl	Sodium chloride
$NaHCO_3$	Sodium carbonate
NBS	Nibrin
NCS	Neocarzinostatin
NER	Nucleotide excision repair
NHEJ	Non-homologous recombination
NMD	Nonsense mediated decay
NoRC	Nucleolar remodelling complex
NTP	Nucleotide
O_2	Oxygen
ODD	Oxygen dependent degradation
OGG1	8-Oxoguanine glycosylase
p53	Tumour protein p53
PAPAS	Promoter associated pre-rRNA antisense
PARP	Poly-ADP ribose phosphorylation
PAS	Per-ARNT-Sim
PBS	Phosphate buffered saline
PCNA	Proliferating cell nuclear antigen

PDI	Protein disulphide isomerases
PERK	protein kinase RNA-like endoplasmic reticulum kinase
PFA	Paraformalydehyde
PHD	Prolyl hydroxylase
PIC	Pre-initiation complex
PNK	Polynucleotide kinase
PNRC1	Proline-rich nuclear receptor coactivator 1
PO_2	Partial pressure of oxygen
PCR	Polymerase chain reaction
P-TEFB	Positive elongation factor B
PTRF	RNA polymerase I and transcript release factor
qPCR	Quantitative PCR
rDNA	Ribosomal DNA
REST	Repressor element-1 silencing transcription factor
RFB	Replication fork barrier
RNA	Ribonucleic acid
RNAi	RNA interference
RNPI	RNA polymerase I
RNPII	RNA polymerase II
RNPIII	RNA polymerase III
ROS	Reactive oxygen species
RP	Ribosomal protein
RPA	Replication protein A
RRM1	Ribonucleotide reductase catalytic subunit M1
RRM2B	Ribonucleotide-diphosphate reductase subunit B
RRN3	RNA polymerase I-specific transcription initiation factor
rRNA	Ribosomal RNA
RRP6	rRNA processing protein 6
RT	Room temperature

S.E.M	Standard error of mean
SD	Standard deviation
SDS	Sodium dodecyl sulfate
SETX	Senataxin
sincRNA	Sense induced non-coding RNA
siRNA	Short interfering RNA
SIRT6	Sirtuin 6
SL1	Selectivity factor 1
snoRNA	Small nucleolar RNA
snoRNP	small nucleolar ribonucleoprotein
SSC	Sodium saline citrate
ssDNA	single-stranded DNA
SSU	Small ribosomal subunit
TAF	Transcription associated factor
TBS	Tris buffered saline
TC-NER	Transcription coupled-nucleotide exchange repair
TCOF1	Treacher collins factor 1
TFIIA	Transcription factor II A
TFIIB	Transcription factor II B
TFIIE	Transcription factor II C
TME	Tumour microenvironment
Top1	Topoisomerase 1
Top2	Topoisomerase 2
TopBP1	DNA topoisomerase 2-binding protein 1
TRAMP	Trf4/Air2/Mtr4p Polyadenylation
TRC	Transcription-replication conflict
tRNA	Transfer RNA
TTF1	Transcription termination factor 1
Ub	Ubiquitin

UBF	Upstream binding factor 1
UCE	Upstream control element
UPR	Unfolded protein response
UTB	Urea tris buffer
UTP	Uridine triphosphate
UTP-A	U-3 associated protein-A
UTR	Untranslated region
UV	Ultraviolet
VHL	von Hippel-Landau
WB	Western blot
XBP1	X-box binding protein 1
XPG	xeroderma pigmentosum complementation group G
XRN2	5'-3' Exoribonuclease 2

Chapter 1

Introduction

1.1 Cancer

Cancer is a term used to describe a diverse group of neoplastic diseases. Despite a huge amount of research, cancer still caused 9.6 million deaths in 2018 (Cancer Research UK). Although the death rate of cancer remains high, there are some types of cancer that are now manageable by early detections through national screening initiatives and improvements in treatments that allow for a longer and, in some cases, better quality of life. This diverse group of diseases share common characteristics; Hanahan and Weinberg discuss in their seminal paper 'the Hallmarks of Cancer', a set of six capabilities that cells acquire to progress to a neoplastic state (Hanahan and Weinberg, 2000). An updated addition to the original paper, 'The Hallmarks of Cancer: the Next Generation' include a set of emerging hallmarks and enabling characteristics which are summarised in the diagram in **Figure 1.1.1** (Hanahan and Weinberg, 2011).

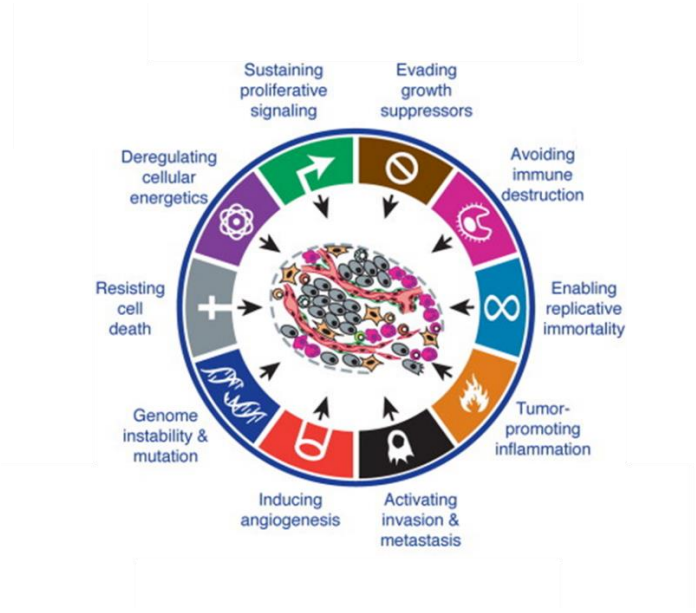


Figure 1.1. 1 The Hallmarks of cancer.
A diagram to show the capabilities of cancer cells to progress described originally in by Hanahan and Weinberg in 2000, with a set of emerging hallmarks and characteristics updated in 2011. Adapted with permission from (Hanahan and Weinberg, 2011). Copyright details in Appendix.

The authors identify that sustained proliferative growth is arguably the most fundamental characteristic of cancer cells. Normal cells can control the production and release of growth signals and instructions to ensure cell division and cell number lie within the constraints of the tissues structure and function. Dysregulation of growth signals allows cancer cells to sustain proliferation. Cells have evolved ways to prevent or circumvent uncontrolled cell proliferation programs, many of which are conducted by the expression of tumour suppressor genes (Brady et al., 2011). Furthermore, it is widely accepted that for cancer cells to divide, their replicative potential must be unlimited. Normal cells are limited to a number of rounds of cell-growth and division; the Hayflick limit (Hayflick, 1965). Cellular programs that limit replicative potential include senescence, a non-proliferative but viable state, or those involving cell death (Rodier et al., 2009; Villunger et al., 2003). However, some cells circumvent these barriers and exhibit unlimited replicative potential, a term known as immortalisation (Bryan et al., 1995). Notably among the hallmarks, a characteristic that drives cancer cell progression is the increase in genome instability which allows for the acquisition of mutations that confer a selective survival advantage enabling a subpopulation of cells to proliferate and develop into a tumour (Alexandrov et al., 2013). The increased proliferative activity and unlimited replicative potential of tumour cells gives rise to a situation where the oxygen supply is insufficient (hypoxia) to support the rapidly dividing cancer cell population and dysregulated replication may give rise to more replicative errors, which lead to increased genome instability (Coquelle et al., 1998; Hammond et al., 2002; Reynolds et al., 1996). Severe levels of hypoxia (<0.1% O_2) lead to a set of adaptations that are designed to limit genome instability and understanding how these occur are pivotal questions to this study.

1.2 Sources of genome instability

Multiple genome maintenance systems are adopted in normal circumstances to limit spontaneous mutations from occurring. The mutational burden in cancer cells is due to an increase in sensitivity to mutagenic agents or a loss or breakdown of genome maintenance machinery to resolve the defects on the DNA (Lin et al., 2009; Lopez de Mesa et al., 2002; Sugasawa et al., 1998).

Cells must carry out numerous processes precisely to proliferate and preserve the fidelity of the DNA sequence. DNA replication is a process by which an exact copy of DNA is duplicated (Batrakou et al., 2020; Duriez et al., 2019). Inaccurate or incomplete rounds of DNA replication are a potential threat to genome stability (Tomasetti and Vogelstein, 2015). During DNA synthesis, the replication machinery must overcome numerous obstacles, including tightly bound DNA-protein complexes, non-B form DNA structures and lesions that interfere with fork progression. Failure to overcome these barriers may lead to a break in the DNA in the form of a double strand break (DSB), the repair of which is essential to prevent deleterious outcomes for the genome (Zellweger et al., 2015).

In addition to DNA replication, transcription is another endogenous source of genome stability (Donahue et al., 1994; Saponaro et al., 2014). As both DNA replication and transcription occur on the same DNA template, transcription complexes can impede fork progression and as a result, transcription-replication conflicts (TRCs) can occur (Hamperl et al., 2017). The stalling or backtracking of the replication fork when it encounters an obstacle such as an RNA polymerase leads to DNA damage in the form of a double strand break (DSB), the mechanisms of which are summarised in (**Figure 1.2.1**).

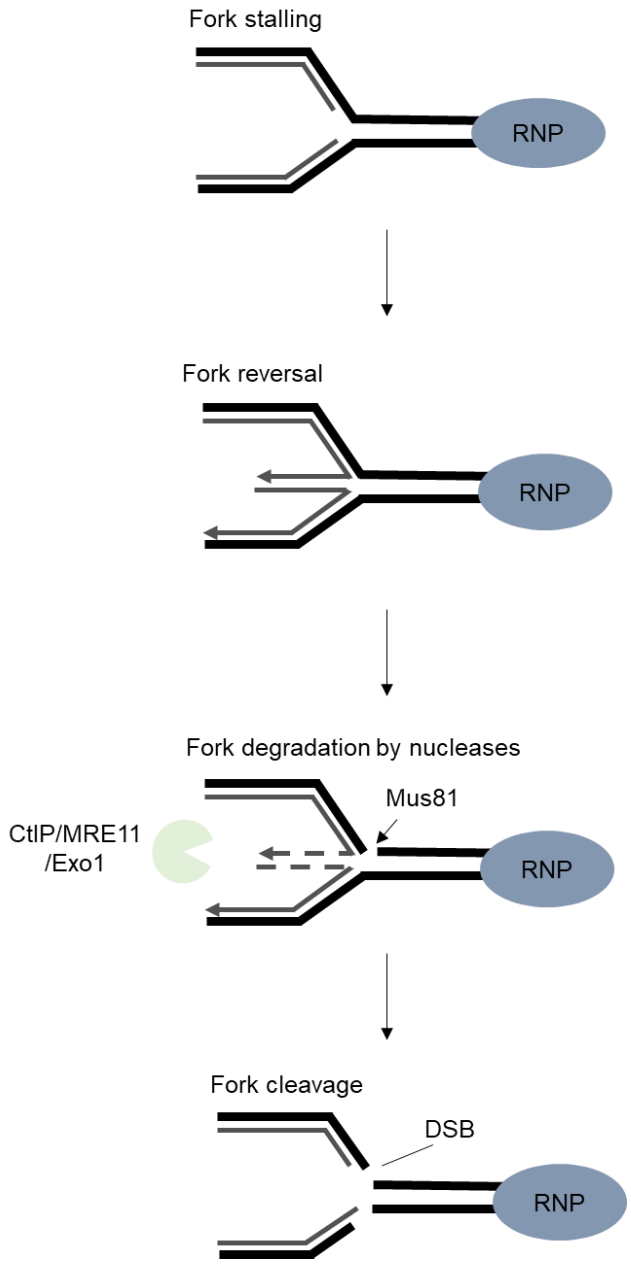


Figure 1.2. 1. Fork reversal and degradation upon encounter with a blockade.
When a replisome encounters an obstacle, such as an RNA polymerase (RNP), fork stalling or reversal can lead to a DSB or fork degradation through nuclease activity e.g. Mus81/CtIP/MRE11/Exo1 (Lemacon et al., 2017).

Overcoming or avoiding a TRC event is crucial to prevent DNA replication-fork stalling, DNA recombination, DNA breaks and mutations. DNA/RNA hybrids, also known as R-loops, can lead to TRCs where they can form as a product of transcription. R-loops form when an RNA polymerase binds and unwinds the double stranded DNA (dsDNA) and begins to transcribe the template DNA. The nascent RNA transcript then hybridises with the template DNA strand and

displaces the non-template strand as single stranded DNA (ssDNA), which can subsequently be coated in replication protein A (RPA) and results in the formation of an R-loop **(Figure 1.2.2**) (Thomas et al., 1976). R-loops participate in regulatory processes but they are also sources of DNA damage if their turnover is deregulated and are therefore a potential source of genome instability.

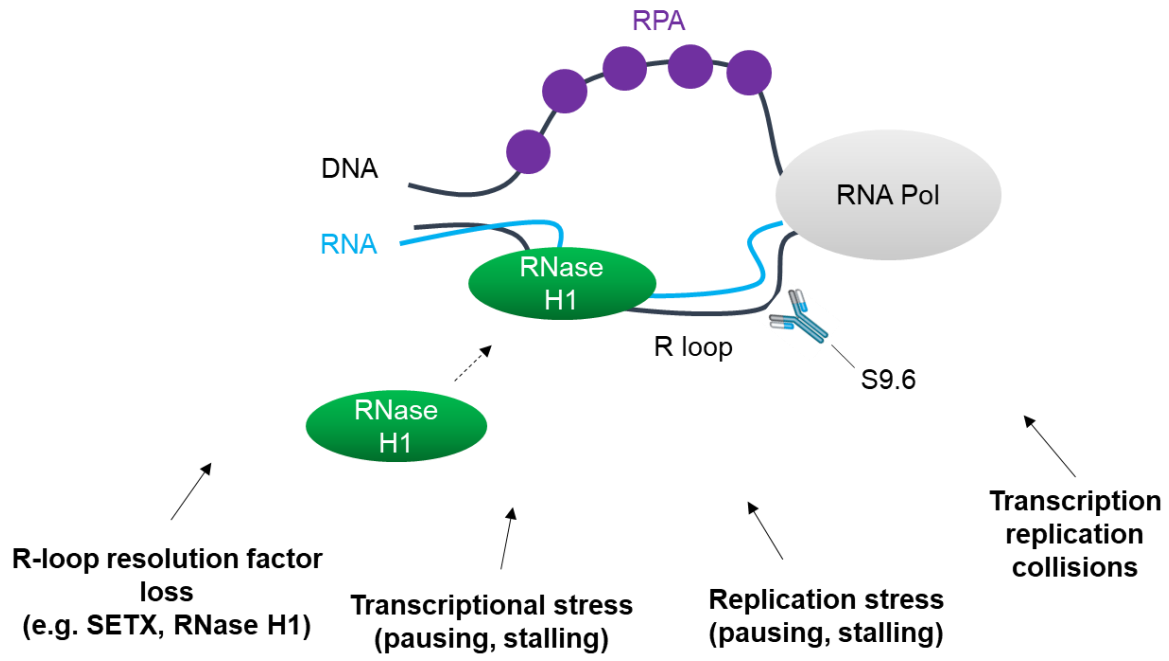


Figure 1.2. 2. DNA/RNA hybrids (R-loops) are potential sources of genome instability. Reasons that R-loops arise include transcriptional stress, replication stress, TRCs or loss of function of R-loop resolving factors. R-loops are nucleic acid structures that form during the transcriptional process. RNA polymerase unwinds the DNA helix which leaves the single stranded DNA (ssDNA) exposed. RPA coats the ssDNA non-template strand, allowing the nascent RNA to hybridise with the template DNA and form a stable hybrid. RNase H1 is an enzyme that binds and degrades the RNA component of the R-loop. The S9.6 antibody is used in a number of molecular biology techniques to detect R-loops.

The generation of an antibody that specifically detects R-loops (S9.6) has allowed for the study of R-loops in different biological settings (Boguslawski et al., 1986). Methods using the S9.6 antibody include DNA/RNA immunoprecipitation (DRIP) which allows for the detection of R-loops on gene loci when combined with polymerase chain reaction (PCR). DRIP combined

with next generation sequencing (DRIP-seq) and its variations, such as S1 nuclease DRIP, have shed light on the prevalence and location of R-loops across the genome (Nadel et al., 2015; Wahba et al., 2016). RNase H is an enzyme that specifically degrades the RNA component of the R-loop by hydrolysis of the phosphodiester bond of the RNA when bound to DNA (Stein and Hausen, 1969). R-ChIP is another technique that allows for R-loop detection which utilises an enzymatically dead mutant of RNase H which is retained at R-loops on the chromatin but does not degrade the RNA strand in the DNA:RNA hybrid (Chen et al., 2017). Relevant to our study, genome-wide analyses have shown that repetitive and/or intergenic regions of the genome such as ribosomal DNA (rDNA) are hot-spots for R-loops in bacteria, yeast and mammals and therefore, R-loops on the rDNA may represent sources of increased mutation and genome instability (El Hage et al., 2010; Masse et al., 1997; Nadel et al., 2015). A hallmark of R-loop forming regions is a high local density of RNA polymerase, which suggests R-loops lead to stalling or pausing (Sanz et al., 2016). Alternatively, it is possible that RNA polymerase stalling may promote R-loop formation. R-loops can lead to genome instability by excessive RNA polymerase stalling, pausing or backtracking, a condition known as transcriptional stress (Saponaro et al., 2014). Importantly, there are several factors including nucleases, helicases, RNA binding proteins and signalling factors that assist in the careful regulation and resolution of R-loops such as the PIF1, RTEL1 and the DNA/RNA helicase, senataxin (SETX). SETX has been shown to resolve R-loops over G-rich transcriptional pause sites to allow the access of exosome component, XRN2 to carry out 3' transcript degradation and RNA polymerase II (RNPII) termination (Skourti-Stathaki et al., 2011). The resolution of an R-loop is in many cases, essential to protect genome stability. For example, R-loops have been shown to form over the *C-MYC* locus in the absence of topoisomerase IIIB which leads to increased genome instability (Yang et al., 2014). Topoisomerase IIIIB acts by reducing negative supercoiling and resolving R-loops on *C-MYC*. Therefore, transcription can resume which protects against DNA

damage, ultimately resulting in less chromosomal rearrangements (Yang et al., 2014). Additionally, transcription-coupled nucleotide excision repair (TC-NER) factors that are usually required to remove bulky DNA lesions can also non-canonically resolve R-loops which can lead to a DSB (Sollier et al., 2014). Therefore, R-loop processing can cause DNA damage. Breast cancer associated gene 1 and 2 (BRCA1/2) are also implicated in the resolution of R-loops by recruiting SETX to termination sites which reduces DNA damage and mutations (Hatchi et al., 2015; Shivji et al., 2018).

The majority of R-loop-induced DNA damage occurs during DNA replication in S-phase when TRCs occur (Gan et al., 2011; Hamperl et al., 2017; Wellinger et al., 2006). The Fanconi anaemia group of proteins such as FANCD2 repress DNA damage caused by R-loops during TRCs by resolving intra-strand cross links (Garcia-Rubio et al., 2015). In addition, RNase H1 overexpression reduces DNA damage and fork slowing in response to oncogene-induced RS suggesting that R-loops interfere with DNA replication (Kotsantis et al., 2016). Advances in the tools to precisely control TRCs in both bacteria and mammalian episomal systems have enabled scientists to closely study the molecular mechanisms that lead to the causes and consequences when TRCs occur (Hamperl et al., 2017; Lang et al., 2017). Studies have demonstrated that the orientation of collision, either head on (HO) or co-directional (CD), affects the physiological outcome of the TRC. R-loops that block DNA replication in a HO orientation promoted genome instability, whereas TRCs that occur CD were more tolerable. Interestingly, HO TRCs promote higher levels of R-loops, whereas CD TRCs reduce R-loops (**Figure 1.2.3**). It is possible that the torsional stress created through HO TRCs may impact genome stability (Promonet et al., 2020). These studies suggest that the orientation of how the replication fork encounters R-loops is a contributing factor which impacts genome instability.

As R-loops expose ssDNA and impede fork progression, the DNA damage kinases, ataxia telangiectasia mutated (ATM) and ATM and RAD3-related (ATR), which orchestrate the

cellular DNA damage response (DDR), can also be activated in response to R-loop formation. Additionally, R-loop processing can also induce DSBs which activate ATM signalling. However, not all R-loops lead to ATM signalling. Mutations in splicing factors, which lead to R-loops, have been demonstrated to activate ATR signalling (Chen et al., 2018). Recent studies have identified that HO-associated R-loops activate ATR, while CD-associated R-loops activate ATM (**Figure 1.2.3**) (Hamperl et al, 2017). Additionally, a recent study found that ATR phosphorylates RPA at the transcriptional termination sites that are replicated in a HO-directional manner relative to the transcriptional direction leading to DSBs at R-loop containing loci in topoisomerase I (top1) depleted cells (Promonet et al., 2020). Another recent study demonstrated that ATR activation in response to R-loops protects the genome by repressing TRCs by promoting replication fork recovery, thereby limiting R-loop induced DSB formation and enforcing a G2/M cell cycle arrest (Matos et al., 2020). The mechanism of R-loop activation of ATM/ATR is not well understood. Interestingly, the DDR kinases also regulate R-loop level. In support of the DDR kinases importance in regulating R-loops, ATM and ATR activation have been shown to promote SETX recruitment to TRCs (Yuce and West, 2013). Furthermore, ATR activation in response to DSBs results in the RNA DNA helicase DDX19 recruitment into the nucleus to unwind R-loops and prevent TRCs (Hodroj et al., 2017). In this way, the activation of ATM/ATR in response to R-loops may trigger activation of certain targets that regulate and resolve R-loops (Matsuoka et al., 2007). Although the precise reason why ATM is activated in response to CD-associated R-loops is not clear, there is evidence that to show that ATM is involved in the repair of transient DSBs that occur during the xeroderma pigmentosum complementation group G (XPG)-dependent resolution of R-loops in Werner syndrome protein deficient cells (Marabitti et al., 2019). Taken together, the transient DSBs associated with the resolution of pre-existing R-loops in the CD collision may act as a stimulus for ATM activation.

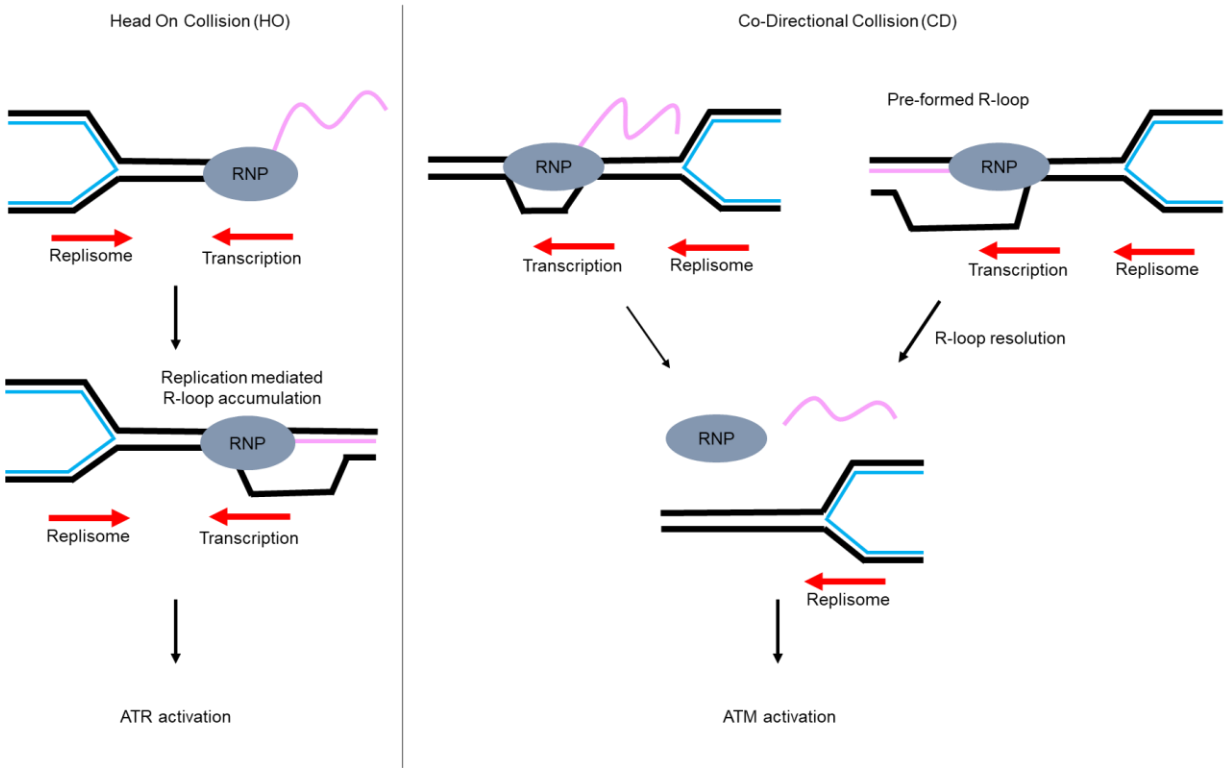


Figure 1.2.3. The orientation of TRC affects R-loops and DDR signalling.
When a replisome travelling in in the opposite direction to a transcription complex encounter one another in a head on (HO) collision, R-loops accumulate, and ATR signalling is activated. When a replisome is travelling in the same direction as the transcription complex and collides in the same direction, also known as a co-directional (CD) collision, the RNA polymerase is evicted from the chromatin, R-loops are reduced, and ATM is activated. The red arrows indicate the direction of the process. The RNA component is depicted in pink.

R-loops are also important regulators of gene expression. Genome-wide mapping demonstrated an abundance of R-loops that transiently form over RNPII gene promoters (Chen et al., 2017; Chen et al., 2015). R-loops at promoters may facilitate transcription by inhibiting the accessibility of DNA methyltransferase binding to the promoter and increasing RNA polymerase gene occupancy, subsequently suppressing DNA methylation-associated transcriptional silencing (Takeshima et al., 2009). Additionally, R-loops may also inhibit transcription by blocking the binding of transcription factors or chromatin remodellers associated with transcriptional activation. It is unclear what distinguishes the activating or repressive nature of an R-loop on transcription. Importantly, although R-loops form transiently,

they can also act as epigenetic marks which can send a signal to proteins such as chromatin remodellers to effect longer-lived changes in chromatin state (Skourti-Stathaki et al., 2014).

R-loop formation is essential for some key biological processes. For example, R-loop formation over the switch (S) region of the immunoglobulin heavy-chain (IgH) locus is essential for activation-induced cytidine deaminase (AID)-mediated class-switch recombination (CSR). Here, the act of transcription creates short strands of ssDNA at the transcription bubble, which can be detected by AID. The RNA strand that is G-rich forms G-quadruplex (G4) structures over the S-region (Ribeiro de Almeida et al., 2018). Deadbox helicase 1 (DDX1), an RNA helicase, binds to the G4 and converts it to an R-loop (Huang et al., 2007). The formation of an R-loop leaves the top strand of G-rich DNA as long single stranded stretches, rendering it targetable for deamination by AID.

The finding that R-loops are a source of DNA damage is somewhat paradoxical in that they also play beneficial roles in the cell. The key determinants between ‘bad’ and ‘good’ R-loops are yet to be fully understood, although it appears that HO TRCs are a likely but not exclusive factor by which R-loops cause DNA damage. HO collisions in human cells have been shown to be a particular threat to genome stability. Interestingly, in yeast, genome instability is only evident when R-loops are in the context of histone 3 serine 10 (H3S10) phosphorylation (Garcia-Pichardo et al., 2017). Therefore, the chromatin environment in which an R-loop forms may be important in preventing genome instability. An alternative hypothesis is that the ‘good’ R-loops are kept within a critical threshold. The deregulation of the pathways that preserve this threshold could cause the normally ‘good’ R-loops to affect the transcriptional or replicative process, leading to more DNA damage.

1.2.1 The tumour microenvironment

Cancer cells in solid tumours reside in a milieu of secreted factors, blood vessels and immune cells which compose the tumour microenvironment (TME). The TME is highly dynamic and heterogenous with a propensity for aggressive phenotypes associated with a negative clinical outcome. The physical and chemical interactions of the TME influences both tumourigenesis and response to treatment (Jahanban-Esfahlan et al., 2018). TME constituents and cancer cells continually adapt to the environmental conditions, influencing overall tumour growth, response to therapy and ultimately clinical outcome. The TME includes the interplay between the cancer cells and neighbouring cells such as immune cells. The rapid growth of the tumour triggers several conditions that include hypoxia, which will be the focus of this study.

1.3 Hypoxia

The tumour vasculature is characterised by excessive and convoluted vessel branching, distorted and enlarged vessels, erratic blood flow, leakiness, and abnormal levels of endothelial cell proliferation and apoptosis (Baluk et al., 2005; Nagy et al., 2010). Oxygen levels differ vastly from tissue to tissue, and even within the same tissue. For example, arterial blood has an oxygen partial pressure (PO_2) of 100 mmHg whereas venous blood has a PO_2 of 40 mmHg (Carreau et al., 2011). Therefore, hypoxia is a term that should be used to refer to the relative cell or tissue type's normal physiological oxygen concentration (normoxia/physoxia).

1.3.1 The origins of tumour hypoxia

The fundamental reason that hypoxia occurs is that the supply of oxygen to the tumour cannot meet the demand. The tumour proliferates rapidly, outgrowing the vasculature needed to supply adequate oxygen tensions to the cells. Shown schematically in **Figure 1.3.1.1**, cancer cells near a blood vessel have enough oxygen to proliferate. However, cells further away from a blood vessel have restricted access to oxygen and are therefore denoted as hypoxic.

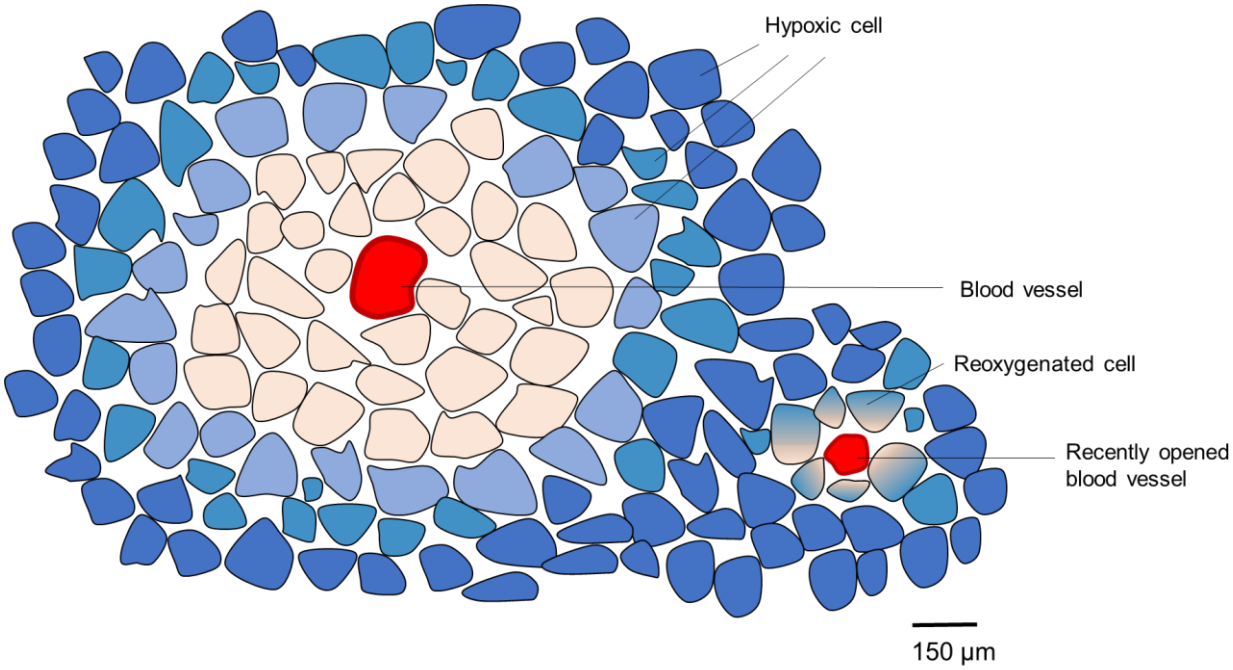


Figure 1.3.1.1. A gradient of decreasing oxygen tensions in a tumour occur due to insufficient vasculature.
Well-oxygenated cells (pink) exist within the diffusion distance of oxygen through tissue (150 µm). The cells that are furthest away from a blood vessel are more hypoxic and resistant to therapy (shades of blue). Newly formed blood vessels or unblocked vessels in tumours can reoxygenate cells in hypoxia which increases DNA damage leading to more genome instability (Pires et al., 2010b).

1.3.2 Acute, chronic, cycling hypoxia

Hypoxia can be sub-divided into categories based on duration and severity. Acute hypoxia is characterised by a transient reduction in oxygen content in blood vessels which can occur due to fluctuations of red blood cell flux or a temporary shutoff of flow (Chaplin et al., 1986). Cycling hypoxia, also known as intermittent acute hypoxia, results from transient fluctuations in tumour perfusion (Brown, 1979; Cardenas-Navia et al., 2008; Dewhirst, 2009; Kimura et al., 1996). Areas of tumours experiencing cycling hypoxia, are subject to periods of hypoxia and reoxygenation shown in **Figure 1.3.1.1.** Cancer cells undergoing cycling hypoxia can lead to increased levels of reactive oxygen species (ROS) which induce DNA damage in the cell (Han et al., 2001). In contrast to acute hypoxia, chronic hypoxia exists in cancer cells that surpass the distance that oxygen travels in actively metabolising tissue and is typically

associated with reduced cell proliferation. Each of these types of hypoxia can occur within a solid tumour and confer a negative prognosis on clinical outcome (Cairns and Hill, 2004; Chaplin et al., 1986). Importantly, acute and chronic hypoxia may have different biological consequences as a function of changes in the global landscape of transcription, protein translation and cell cycle signalling cascades. Cell survival and biology may be different in cells that are treated after exposure to longer durations of chronic hypoxia compared to those exposed to short term acute hypoxia (Koritzinsky et al., 2001). Therefore, the current state of research in tumour biology necessitates further investigation into understanding the differences in cellular mechanisms involved in the response to hypoxic conditions.

1.4 Hypoxia and resistance to therapy

The presence of oxygen is required for the hydrolysis of water upon exposure to ionising radiation. The splitting of water releases free radicals to induce damage to DNA and other cellular organelles. Based on histological assessment, the presence of hypoxia in human tumours and its role in treatment resistance was first postulated by Thomlinson and Gray (Thomlinson and Gray, 1955). Studies have demonstrated that, at PO_2 below 10 mm Hg, tumour cells become relatively resistant to radiotherapy (Knocke et al., 1999; Nordsmark et al., 2005). This is important because radiotherapy is the primary therapy for many cancers. Resistance to chemotherapy is often due to poor drug delivery due to fluctuating blood flow, drug diffusion distance and reduced cell proliferation. Furthermore, DNA damage-inducing agents such as cisplatin are less effective in inducing cell death in hypoxic tumours cells, in part due to decreased free-radical generation (Matsushima et al., 1998). Hypoxic tumours are also frequently associated with a lower pH which may reduce the activity of some chemotherapeutic agents.

Among the hallmarks of cancer, hypoxia can drive a mutational phenotype in tumours through an increased mutation rate and increased genomic instability (Nelson et al., 2004; Reynolds et al., 1996). A source of genome instability in severe hypoxia (<0.1% oxygen) is brought about through the induction of a G1 and intra-S phase (DNA replication) arrest. Acute hypoxia limits S phase progression, which stimulates activation of the ATM and ATR kinases, but does not lead to DNA damage. However, reoxygenation after hypoxia rapidly induces DNA damage as a result of a burst of free radical generation which could potentially lead to an accumulation of unrepaired DNA lesions and increased genome instability (Pires et al., 2010b). These studies highlight the critical role of hypoxia in tumour progression where cycles of acute hypoxia may increase genome instability. Additionally, the ability of cells under hypoxia to evade cell death may lead to an increase in mutations (Nelson et al., 2004). Tumours that adapt to fluctuating hypoxic conditions gain a growth and survival advantage that leads to a subpopulation of cells that are resistant following irradiation or chemotherapy with the potential to metastasise and proliferate (Young et al., 1988).

An increase in genome instability in hypoxic conditions has been proposed to be exacerbated due to the inhibition of DNA repair pathway proteins involved in homologous recombination (HR) and mismatch repair (MMR) that are crucial to repair DNA breaks and maintain the fidelity of the genome (Bindra et al., 2005; Bindra and Glazer, 2007; Meng et al., 2005; Mihaylova et al., 2003). Factors involved in HR such as Rad51 and BRCA2 have been found to be repressed through selective inhibition of mRNA translation in hypoxia (Chan et al., 2008). However, it is currently unclear how hypoxia impacts the regulation of DNA repair pathways such as base excision repair (BER).

Hypoxia has been demonstrated to promote chromosomal instability at fragile sites that are prone to chromosomal breakage and rearrangements during replication stress (Coquelle et al., 1998; Zhu et al., 2006). Pioneering studies identified DNA over-replication in hypoxia as a

link to gene amplification and metastasis (Young et al., 1988). In support of this concept, a study has shown that hypoxia-induced fragile sites drive the formation and insertion of double mini chromosomes, common features of gene amplification (Coquelle et al., 1998).

The altered DNA repair landscape and checkpoint control may lead to increased mutations in hypoxic conditions. For example, a study using a chromosomally integrated reporter has demonstrated that hypoxic cells exhibit 5-fold more mutations in the tumour microenvironment compared to that of cells in culture (Reynolds et al., 1996). Similarly, a different study showed a 2-fold increase in mutation frequency using a transgene construct in mammary epithelial cells and transformed mammary cells transplanted as a xenograft in response to 24 hours of hypoxia (Papp-Szabo et al., 2005).

Strategies to exploit hypoxia-associated genetic instability and faulty DNA repair might be a target for novel cancer therapies to improve the therapeutic ratio. A term known as synthetic lethality arises between two genes when the perturbation of either gene alone is viable, but the perturbation of both genes simultaneously results in the loss of viability. For example, hypoxic cells exposed to periods of reoxygenation experience impaired DNA repair through reduced homologous recombination (HR) protein expression and function. As HR-defects are synthetically lethal with poly(ADP-ribose) polymerase 1 (PARP) inhibitors, PARP inhibition in HR-deficient hypoxic cells was shown to lead to contextual synthetic lethality (Chan et al., 2010).

1.5 The biological response to hypoxia

Maintaining oxygen homeostasis is essential for survival. The cellular response to low oxygen levels involve both proteomic and genomic changes. These adaptive protein changes may increase a hypoxic cells potential to initiate signalling to reduce cell proliferation, inhibit the cell cycle and become necrotic and apoptose. Alternatively, the signalling pathways that are

activated could also stimulate tumour growth and metastasis in an effort to survive the hostile hypoxic environment. This section will highlight the molecular mechanisms that control the response to decreasing oxygen tensions.

1.5.1 Hypoxia inducible factor (HIF)

Deprivation of oxygen triggers cells to adapt and initiate many survival pathways. Perhaps the most well characterised is the HIF1 response to hypoxia. HIF1 is a heterodimeric transcription factor which consists of a constitutively expressed β-subunit and an oxygen-associated α-subunit. Both HIF1α and HIF1β subunits have helix-loop-helix motifs and a Per-ARNT-Sim (PAS) domain that aid dimerisation once bound to DNA (Wang et al., 1995). The HIF1α subunit contains an oxygen-dependent degradation (ODD) domain, which is hydroxylated by prolyl-hydroxylase-2 (PHD-2) under normal oxygen conditions (**Figure 1.5.1.1**) (Appelhoff et al., 2004). In an adequate oxygen supply, the HIF1α subunit is recognised by the von Hippel-Landau tumour suppressor protein (VHL), an E3-ligase ubiquitin factor, resulting in α subunit degradation by the proteasome (Maxwell et al., 1999). In the absence of oxygen, the α subunit is no longer hydroxylated or recognised by VHL and is subsequently stabilised. The stabilisation of HIF1α allows for subsequent binding to HIF1β. The HIF1 heterodimer binds to gene promoters via hypoxia regulatory elements (HREs) which results in the upregulation of a specific set of genes. HIF1 activation plays a crucial role in the adaptive response to hypoxia by activating well over 100 genes involved in the regulation of angiogenesis, glucose uptake, cell proliferation and tumour survival/progression. For example carbonic anhydrase IX (CAIX) is important for the control of cellular pH, or VEGF allow for an increase in the formation of blood vessels in response to hypoxia (Liu et al., 2012a). In this way, the HIF1 response allows for a vast reorganisation of the transcriptional response to promote the carcinogenic properties of a tumour.

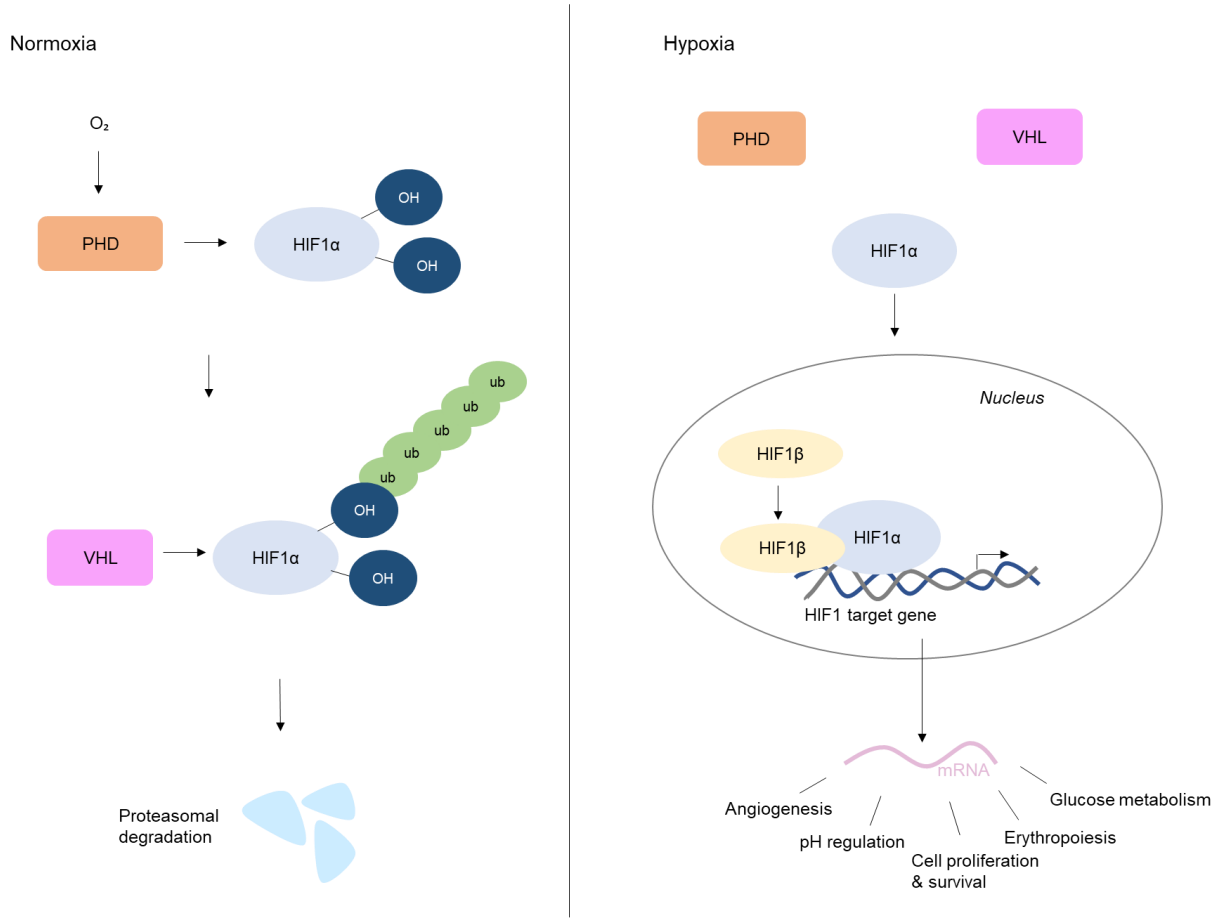


Figure 1.5.1.1. The regulation of HIF1α under normoxic and hypoxic conditions. Under normoxic conditions, oxygen activates the PHD enzymes which hydroxylate the HIF1α subunit. VHL then targets the HIF1α subunit for proteasomal degradation via a ubiquitin (ub)-mediated mechanism. In hypoxia, HIF1α is stabilised and translocates to the nucleus to form a heterodimer with HIF1β at HIF response elements at HIF1 target genes leading to upregulation of gene products to adapt to the hypoxic environment and increase tumourigenesis.

1.5.2 Unfolded protein response (UPR) activation in hypoxia

Secreted and membrane proteins are folded and mature in the lumen of the endoplasmic reticulum (ER) before being transported to the cell surface where they may be extracellularly released or remain integral to the cell membrane. The unfolded protein response (UPR) is a stress responsive network that monitors the conditions in the ER. The misfolding of proteins in the ER is sensed by the UPR which leads to a gene expression control program to maintain homeostasis by limiting the flux of protein entering the ER lumen (Koumenis et al., 2002).

The UPR pathway is transduced through the three ER transmembrane proteins, activating transcription factor 6 (ATF6), double-stranded RNA-activated protein kinase (PKR)–like ER kinase (PERK) and inositol requiring enzyme 1 (IRE1), that represent the three main branches of the UPR (**Figure 1.5.2.1**). Each branch operates through unique signal transduction mechanisms in parallel. Misfolded proteins are sensed by GRP78 which dissociates from each ER transmembrane protein of the UPR (Bertolotti et al., 2000; Nadanaka et al., 2007). ATF6 is a transcription factor that contains a large ER-luminal domain (Nadanaka et al., 2007). Misfolded protein accumulation triggers ATF6 vesicular transport to the Golgi apparatus, where protease activity liberates the N-terminal domain into the nucleus to activate UPR target genes. Monomeric, inactive PERK forms an active dimer and phosphorylates both itself and the translation initiation factor eukaryotic initiation factor 2 α (eIF2α), indirectly inactivating eIF2 and inhibiting translation (Koumenis et al., 2002; Wang et al., 2018). IRE1 is a bifunctional endoribonuclease and kinase that uses a unique mechanism of mRNA splicing to transmit the UPR signal (Cox et al., 1993). Activation of IRE1 cleaves the mRNA encoding X-box binding protein 1 (XBP1), a UPR-specific transcription factor, resulting the removal of an intron (Calfon et al., 2002; Lee et al., 2002; Romero-Ramirez et al., 2004). The spliced exons are ligated to form an XBP isoform encoding for active XBP1. Activation of each branch leads to the production of transcription factors, which work alone or together to activate UPR target genes and decrease the load of misfolded proteins in the ER. If misfolded proteins continue to accumulate, a process known as 'proteotoxicity', the cell undergoes apoptosis (Kohanski et al., 2008). The mechanism of ER-related apoptosis is known to be due, in part to the release of calcium ions (Ca^{2+}) involved in cellular signalling from the ER that activate caspases that mediate cell death (Deniaud et al., 2008).

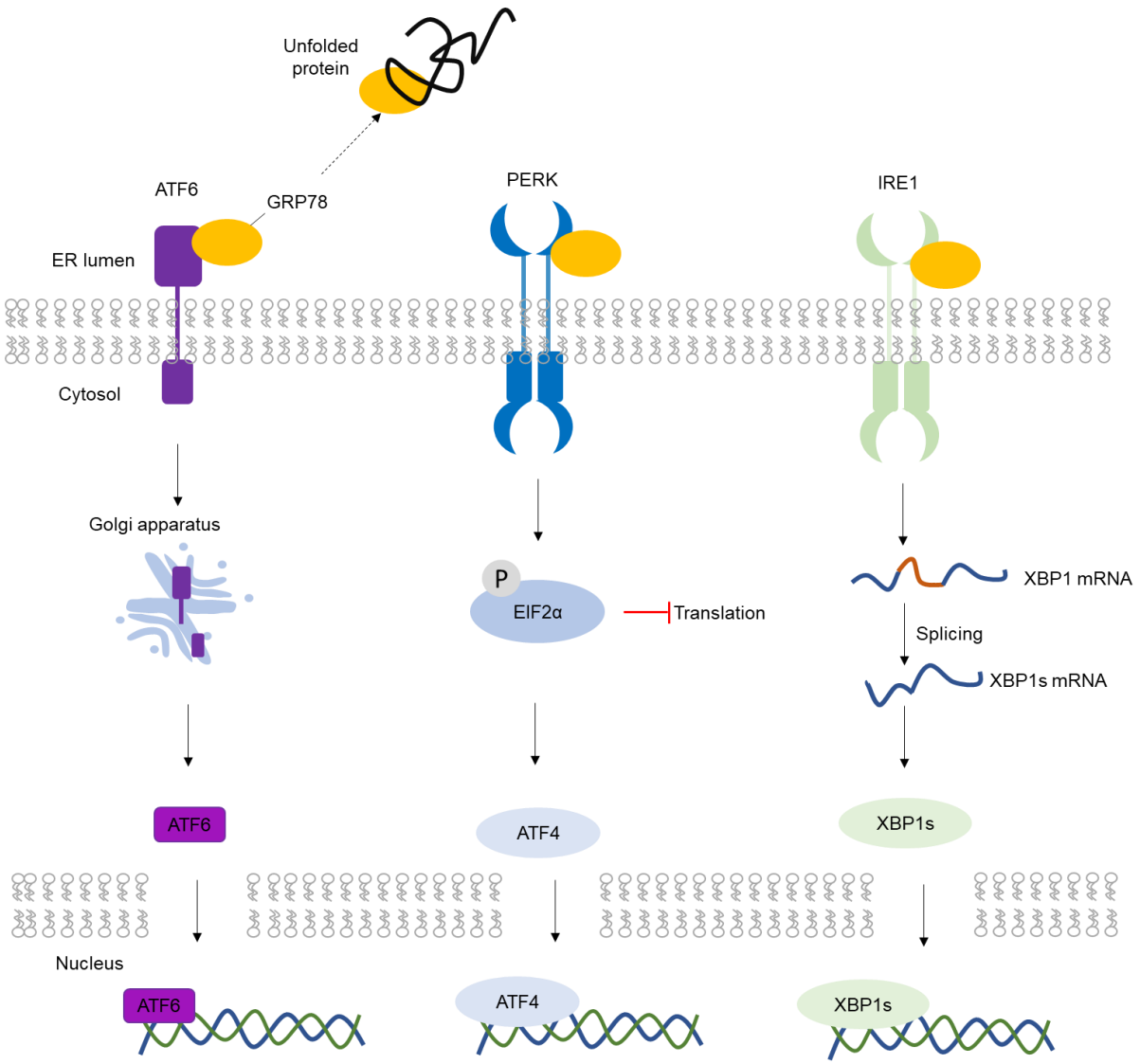


Figure 1.5.2.1. Schematic of the unfolded protein response (UPR).
Three branches of the UPR are conducted through the ER transmembrane proteins ATF6, PERK and IRE1 which are each bound by GRP78. PERK monomers form dimers to initiate trans-activation of the PERK arm. An unfolded protein triggers GRP78 to dissociate from the transmembrane proteins and sequester the unfolded protein. Signal transduction pathway are initiated in the cytosol to activate transcription factors which bind to gene promoters involved in the downregulation of global translation.

In addition to the control of translation in response to an accumulation of misfolded proteins, the PERK branch of the UPR has been demonstrated to limit the transcription of rDNA in response to pharmacological activation of the UPR by thapsigargin and tunicamycin which block the ability of the sarcoplasmic ER calcium ion pump and block N-linked glycosylation by preventing oligosaccharide addition to the nascent polypeptide, respectively (DuRose et al.,

2009) (**Figure 1.5.2.2**). The PERK-dependent phosphorylation of eIF2α leads to abrogation of the recruitment of the RNPI-specific transcription initiation factor, RRN3. In this way, the PERK/eIF2α branch of the UPR limits the production of rRNA which, in turn, restricts ribosome biogenesis and protein translation.

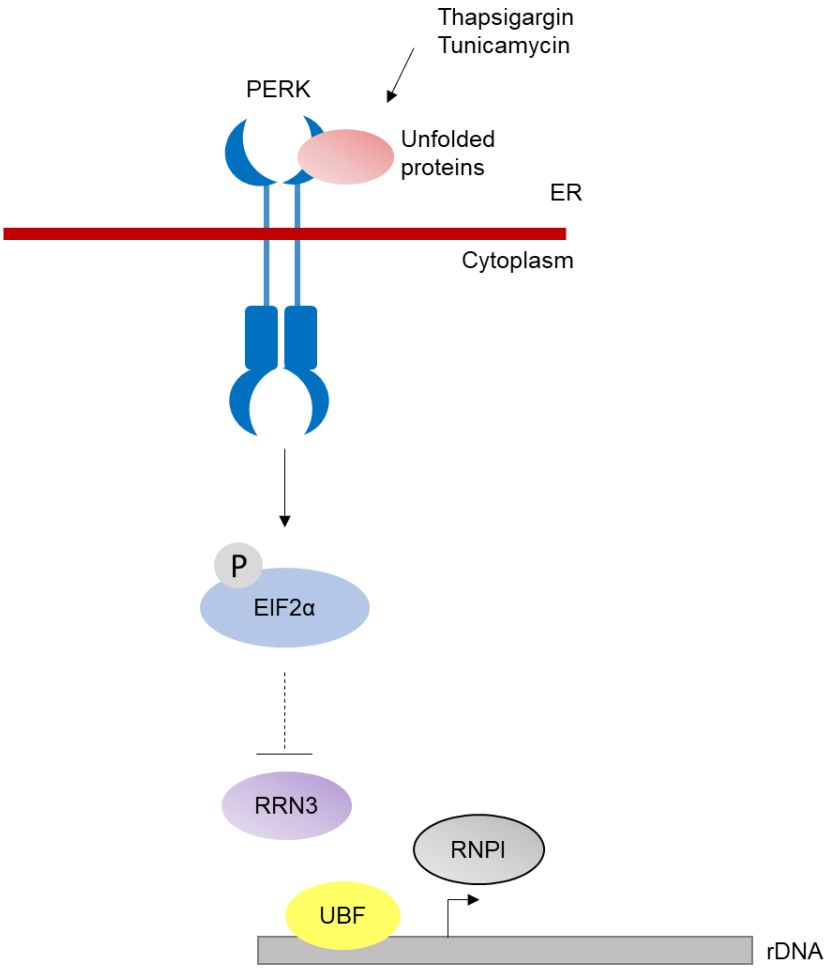


Figure 1.5.2.2. Pharmacological activation of the UPR restricts rDNA transcription in a PERK/EIF2α dependent manner.
Thapsigargin and tunicamycin activation the UPR and trigger PERK phosphorylation of EIF2α. RRN3, a transcriptional initiation factor is prevented from translocating to the rDNA, restricting rDNA transcription.

Under hypoxic conditions, changes in protein synthesis are largely accounted for by changes in translation. Activation of the UPR is crucial to limit the energetically demanding process of translation and protein folding (Buttgereit and Brand, 1995). Disulphide bonds that are

necessary for protein folding form by a redox relay reaction that involves protein disulphide isomerases (PDIs), oxidases, and oxygen as a terminal electron acceptor (Koritzinsky et al., 2013). The impaired formation of disulphide bonds in hypoxia is the underlying trigger for UPR activation in hypoxia (Koritzinsky et al., 2013). The severity and duration of hypoxic stress influences the stress response pathways which are important for cancer cell survival. In contrast to the HIF1 response which is activated in mild hypoxic conditions (2% O_2), the activation of the UPR has been demonstrated only in response to more severe hypoxia (<0.1% O_2). eIF2α is phosphorylated rapidly under severe hypoxia indicating UPR activation leading to decreased protein synthesis (Koumenis et al., 2002).

1.5.3 DNA damage response (DDR) activation in hypoxia

DNA replication stress (RS) is defined as the stalling or slowing of replication fork progression. Stretches of exposed ssDNA are initially coated with replication protein A (RPA) which initiates the ataxia telangiectasia and RAD3-related (ATR) mediated pathway through the recruitment of ATR-interacting protein (ATRIP). Interaction and recruitment of several proteins such as DNA topoisomerase II binding protein 1 (TopBP1) and Ewing tumour-associated antigen (ETAA1) are required for ATR activation (Bass et al., 2016; Haahr et al., 2016). Activation of ATR signalling initiates a cascade of downstream signalling to prevent mis-replicated DNA progressing through the cell cycle. DSBs that form from RS can occur through fork breakage or in the event of a fork reversal, an endonuclease can cut the fork, for example, Mus81 as described in **Figure 1.2.1**. There are two main pathways that ensure the repair of DSBs, firstly, non-homologous end joining (NHEJ) occurs in all cell cycle phases but is an error-prone form of DNA repair. Secondly, HR is less error prone and only occurs in S and G2 phase. Ataxia telangiectasia mutated (ATM) kinase is the primary responder to DSBs (Bakkenist and Kastan, 2003; Canman et al., 1998; Savitsky et al., 1995). DNA-dependent protein kinase, catalytic subunit (DNA-PKcs) activation occurs when DSBs are repaired

through the NHEJ pathway. It is generally considered that ATR is activated in response to RS, and ATM and DNA-PK are DSB responsive. However, this notion is not a strict rule as ATM and ATR share many common targets and therefore there is significant cross over in their signalling pathways (Matsuoka et al., 2007). ATM activation has been demonstrated in the absence of DNA damage, for example in response to hypoxia, hypoosmotic stress and oxidative stress (Bencokova et al., 2009; Guo et al., 2010; Velichko et al., 2019).

A gradient of oxygen tensions occurs throughout tumours, reaching near anoxia in areas adjacent to necrotic regions. These extremely low oxygen tensions have been associated with the induction of RS and the subsequent activation of the DDR pathway (Hammond et al., 2002; Hammond et al., 2004; Hammond and Giaccia, 2004; Olcina et al., 2013; Pires et al., 2010a). Strikingly, evidenced by the tumour suppressor p53-binding protein 1 (53BP1) foci assay and comet assay, even prolonged periods of hypoxia do not lead to detectable DNA damage (Bencokova et al., 2009; Olcina et al., 2013; Pires et al., 2010b). Unsurprisingly, RS in hypoxia leads to activation of ATR (Hammond et al., 2003). Hypoxic cells demonstrate increased sensitivity to pharmacological inhibition of ATR (Hammond and Giaccia, 2006; Leszczynska et al., 2016a; Pires et al., 2012). Hypoxic conditions lead to ATM activation, despite the lack of detectable DNA damage, as evidenced by ATM-dependent phosphorylation of downstream targets such as KAP-1 (Bencokova et al., 2009). ATM activation in hypoxia occurs independently of the DSB-associated Mre11-Rad50-Nbs1 (MRN) complex, further confirming the lack of DNA damage in these conditions. ATM activation in hypoxia was demonstrated to be partially dependent on the combination of H3K9me3 formation in response to RS (Olcina et al., 2013).

Previous studies indicate that nucleotide imbalance leads to RS in hypoxia. The biosynthesis of deoxyribonucleotides (dNTPs) and ribonucleotides (NTPs) involves *de novo* and salvage pathways. The reduction of NTPs to dNTPs requires the activity of ribonucleotide reductase

(RNR). RNR is an enzyme consisting of two homodimeric subunits, ribonucleotide reductase catalytic subunit M1 (RRM1) and RRM2 or RRM2B. The RRM1 dimer contains the catalytic site and constitutes the large α subunit, whereas the β subunit is encoded by either *RRM2* or *RRM2B*. Crucially, the β subunit contains an oxygen-requiring di-iron tyrosyl radical site essential for catalysis. Previous work in the Hammond laboratory demonstrated that RNR switches isoforms from RRM2 to RRM2B allowing ongoing replication in hypoxic conditions (Foskolou et al., 2017). The functional activity of RNR in hypoxia is retained through increased oxygen-entering frequency and increased stabilisation of the tyrosyl radical in the RRM2B subunit. This activity of RNR allows for the preservation of fork integrity through maintaining replication rates, albeit significantly slower than normal. Inhibition of the RRM2B subunit in hypoxic conditions results in DNA damage and proves detrimental to a hypoxic cell fate.

Although a DDR is active in hypoxic conditions, as mentioned in section **1.4**, concomitant repression of some DNA repair genes results in decreased activity of some DNA repair pathways. Although hypoxia has effects on HR pathways, its effects on other major repair pathways such a NHEJ are less well known. Factors involved in the NHEJ pathway have been shown to be repressed on the mRNA level. However the profile of NHEJ factors on the protein level is yet to be determined (Fanale et al., 2013). Contradictory studies have reported that NHEJ proteins stay the same, increase or decrease (Bindra et al., 2005; Jongen et al., 2017; Madan et al., 2012; Ren et al., 2013). The exact effects of hypoxic on NHEJ are yet to be elucidated. However, it is likely that multiple mechanisms regulate the repair factor dynamics and that these mechanisms may be affected by cell-line specificity as well as the nature of the hypoxic conditions reported. Similarly, the effects of hypoxia on nucleotide excision repair (NER), a pathway involved in the removal of bulky DNA lesions, are unclear. Some reports have indicated that NER is downregulated in hypoxia, for example hypoxia has been shown to

reduce NER repair capacity leading to increased mutagenesis (Yuan et al., 2000). In another study the NER repair factor ERCC1 was found to be downregulated at the mRNA and protein levels in response to hypoxia (Dudas et al., 2014). On the other hand, NER has been shown to be upregulated in response to milder hypoxic conditions and that HREs exist in the promoters of NER-encoding genes (Liu et al., 2012b; Rezvani et al., 2010). Other repair pathways essential for maintaining genome stability in response to stress include the BER pathway. mRNA levels of factors involved in BER including ATMIN, OGG1, PCNA and MYH have been found to be downregulated in hypoxia (Chan et al., 2014; Leszczynska et al., 2016b). In contrast, the translesion synthesis pathway, which uses specialised DNA polymerases ι, κ and ζ to bypass DNA lesions in an effort to prevent replication fork stalling albeit in an error-prone manner, has some evidence towards being utilised in hypoxia. For example, DNA polymerase ι has been demonstrated to be induced through HIF1α (Ito et al., 2006). In addition, translesion synthesis may play an important role in the response to radiation in hypoxia as cells that lack the catalytic subunit of DNA polymerase ζ have been shown to have reduced cell survival and increased chromosomal breaks in response to ionising radiation in hypoxia (Shimizu et al., 2015). However, it is unclear what the exact effects of hypoxia are on translesion synthesis. It is unclear why hypoxia-induced reprogramming of the transcriptional landscape of DNA repair occurs. However this change is likely to lead to increased genome instability, tumourigenesis and resistance to therapy.

1.5.4 The repression of gene transcription in hypoxia

As discussed in section **1.5.1**, hypoxia leads to well characterised gene induction. Interestingly, in these same conditions, concomitant transcriptional repression occurs. Characterising and understanding the whole transcriptional landscape is necessary to understand the biological response to hypoxic conditions. The steady state level of RNA is determined by RNA synthesis and stability. Studies have often focussed on the repression of specific genes but generally, the

mechanisms of gene repression are not well understood. A study demonstrated that in mild, long periods (>22 hours) of hypoxia (1% O_2), global RNA levels, including mRNA levels, are reduced in a HIF1α independent manner (Johnson et al., 2008). A more recent study demonstrated mRNA degradation in long periods (16 hours) of hypoxia (1% O_2) increases whereas, the levels of nascent RNA synthesis was similar to normoxia which suggests that mRNA decay as opposed to mRNA synthesis is responsible for an overall reduction in total cellular mRNA content in these hypoxic conditions (Tiana et al., 2020). This study seems to suggest that less mRNA is used in translation by the ribosome and are therefore targeted for degradation. The mechanism by which mRNA in hypoxia is degraded is unclear and warrants further investigation. Hypoxia has been shown to increase the stabilisation of a subset of mRNAs including that of the angiogenic growth factor VEGF, which has been shown to rely on a 40 base pair (bp) stretch in the 3'untranslated region (UTR) typically containing AU rich sequences, which are bound and stabilised by RNA binding proteins (Levy et al., 1996). Interestingly, a study has shown that nonsense mediated decay (NMD), a cellular mechanism that targets mRNA for degradation, is inhibited in hypoxia which promotes the stability of mRNAs important for the stress response (Gardner, 2008). Overall, these studies suggest that although there are mRNAs that are upregulated in hypoxia e.g. HIF targets, there is concomitant repression of other genes.

RNPII is a DNA-dependent RNA polymerase consisting of 12 subunits. The C-terminal domain (CTD) of RNPII contains multiple hepta-peptide repeats (Y1 S2 P3 T4 S5 P6 S7) which are dynamically phosphorylated at specific residues to control transcriptional activity (**Figure 1.5.4.1**). Formation of the pre-initiation complex (PIC) requires the recruitment of several factors including transcription factor II D (TFIID), TFIIB, TFIIF, TFIIE, and TFIIH. Unphosphorylated RNPII is recruited to core promoter elements which may contain a TATA binding sequence located 25 nucleotides upstream of the transcriptional start site. Serine 5 of

the CTD is phosphorylated by the CDK7 kinase upon promoter binding facilitating promoter escape. The transition to productive elongation is mediated through the phosphorylation of serine 2 by CDK9 of the positive elongation factor B (P-TEFB) family. Lastly, transcription is terminated by the loss of serine 5 phosphorylation and subsequent activity of factors such as 5'-3' exoribonuclease 2 (XRN2) to release the nascent RNA transcript and complete the transcriptional process (Skourti-Stathaki et al., 2011).

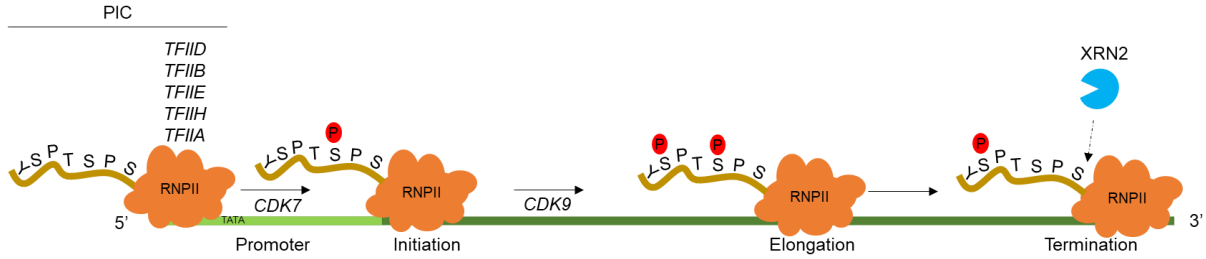


Figure 1.5.4.1. A schematic of the transcriptional cycle of RNPII.
The Y1 S2 P3 T4 S5 P6 S7 repeat of the CTD is phosphorylated to regulate the transcriptional activity of RNPII. Unphosphorylated RNPII is recruited to the promoter to bind the TATA control element. Promoter escape is stimulated by binding of several TFs (TFIID, B, E, H, A) and by CDK7-dependent phosphorylation of S5 of the CTD. The transition from initiation to elongation involves phosphorylation by CDK9 and S2 of the CTD. Transcriptional termination of RNPII releases the nascent RNA transcript through XRN2 activity and dephosphorylation of S5.

Studies have demonstrated using *in vitro* transcription assays that hypoxic cell extracts are unable to form the preinitiation complex (PIC) but are capable of elongating (Denko et al., 2003). However, elongation competence was also proved to be diminished in hypoxia *in vivo* through inactivation of CDK9 (Safronova et al., 2014). The repression of CDK9 in hypoxia was associated with a reduction in the post-translational modifications including acetylation of CDK9 and cyclin T1. The PIC and elongation incompetence identified in these studies were identified after prolonged periods of hypoxia (>18 hours). Therefore, the conclusion from this literature suggests that long periods of hypoxia decrease the global transcriptional ability of RNPII through multiple mechanisms.

Transcriptional repressors are a large and diverse group of proteins that can disrupt transcription through different mechanisms. Repressors can inhibit the RNA polymerase basal machinery, inhibit transcriptional activators or remodel the chromatin (Levine and Manley, 1989; Pengue and Lania, 1996). RNPII-transcribed genes have been shown to decrease in hypoxia through the activity of repressors such as repressor element-1 silencing transcription factor (REST), which was shown to repress over 200 specific genes (Cavadas et al., 2016). REST is recruited to genes that contain a 21 bp nucleotide repressor element 1 (RE1) sequence and disrupts the basal RNPII machinery and chromatin environment to inhibit transcription of neuronal genes. Other hypoxia responsive transcriptional repressors have been reported to play a role in specific gene silencing in hypoxic conditions. Negative cofactor protein 2 (NC2α/β) was found to bind the core promoter of a certain set of genes in hypoxia to influence the transcriptional output (Denko et al., 2003). These studies show that the hypoxic impairment of RNPII activity may also be impacted by transcriptional repressors at specific gene control elements.

As mentioned earlier in this section, some DNA repair pathways are repressed in hypoxic conditions, the mechanisms of which vary but include the repression of key repair factors. For example DEC1/2 (deleted in oesophageal cancer 1 and 2) is a HIF1-inducible gene which regulates a key mismatch repair (MMR) gene, *MLH1* (Nakamura et al., 2008). DEC1 or DEC2 binds directly to the *MLH1* promoter resulting in transcriptional repression leading to impaired MMR function in hypoxic conditions.

The chromatin environment influences transcriptional activity through generating barriers to progression of the transcriptional machinery. The significant changes in gene expression in hypoxia is accompanied by profound changes in chromatin structure and function (Batie et al., 2019; Johnson et al., 2008). Histone methylation can create binding sites over regions for specific proteins and can contribute to both gene activation and gene repression. Histone

methylation can occur at either arginine or lysine residues on histone H3 or H4, this methylation pattern determines the chromatin structure and therefore the transcriptional status of specific genes. Mono-, di- and tri-methylation of lysine 9 on histone H3 (H3K9) is associated with transcriptionally inactive states (heterochromatin), whereas methylated lysine 4 or 36 of H3 are associated with transcriptional activity. Hypoxia is known to regulate heterochromatin formation through oxygen dependent mechanisms (Beyer et al., 2008; Chen et al., 2006; Krieg et al., 2010; Pollard et al., 2008). Global levels of di and tri- methylated K9 have been shown to increase in both mild hypoxia (2% O_2) and more severe hypoxia (<0.1% O_2) (Olcina et al., 2013). Global levels of H3K4, H3K27, H3K36 and H3K79 methylation have also been shown to increase in hypoxic conditions (Johnson et al., 2008; Tausendschon et al., 2011; Zhou et al., 2010). H3K9 methylation is deposited by the recruitment of heterochromatin protein (HP1) and histone methyltransferases such as G9a and SUV39h2 which add methyl groups to histones and has been shown to be post-translationally upregulated in hypoxia (Chen et al., 2006; Olcina et al., 2013). Increased H3K9me3 levels were associated with the repression of DNA repair genes, for example, *BRCA1* (Lu et al., 2011). How the hypoxic cell achieves specificity of heterochromatin formation across the genome is not fully understood.

Epigenetic regulation also involves histone demethylases which remove methyl groups from histones. The Jumonji-C (JmjC) histone demethylases (KDMs) are molecular dioxygenases which require oxygen as well as iron and 2-oxoglutarate for activity (Hancock et al., 2017). The oxygen dependency of methyltransferase activity of these enzymes confers an important regulatory mechanism in the response to changing oxygen levels and are required for widespread formation of heterochromatin across many genes (Couture et al., 2007; Krieg et al., 2010; Tsukada et al., 2006). It is plausible that the epigenetic changes in the chromatin landscape allow for a flexible adaptation to the hypoxic microenvironment (Gomez-Schiavon and Buchler, 2019).

Although these studies provide specific examples of transcriptional repression of RNPII-transcribed genes and an insight into how the transcriptional process is altered, our overall knowledge of global transcriptional repression of all RNA categories in hypoxia is not well characterised. A study has shown that RNA polymerase III (RNPIII) activity is repressed in hypoxia (1% O_2) through abrogated recruitment of transcription factor III B (TFIIIB) to RNPIII promoters (Ernens et al., 2006). The same study demonstrated that some transfer RNA (tRNA) are also repressed in these same conditions. Further investigation into the mechanisms of global transcriptional repression are pivotal to understand the biological response to hypoxia.

1.6 RNPI mediated transcription

rRNA are the most abundant RNA species in the cell, comprising approximately 80% of total RNA (Blobel and Potter, 1967). The rRNA is produced by the enzyme complex known as RNA polymerase I (RNPI). RNPI transcribes ribosomal DNA (rDNA) which are found in the largest sub-cellular membrane-less organelle, the nucleolus. Nucleolar organiser regions (NORs) form around 400 human rDNA tandem repeat arrays which are located on the p-arms of acrocentric chromosomes 13-15, 21 and 22. Each rDNA repeat is around 43 kilo-base (kb) long and includes regulatory elements within an intergenic spacer (IGS) of approximately 30 kb and a 47S coding region of around 13 kb (**Figure 1.6.1**). The regulatory elements in the IGS contain a promoter for the 47S, origins of DNA replication, repetitive enhancer elements, and termination elements that can bind transcription termination factor 1 (TTF1) and replication fork barriers (RFBs). The NORs, containing tandemly repeated rDNA, contribute to formation of the nucleolus. The ribosome consists of two subunits; the large subunit (LSU) is around twice the size of the small subunit (SSU). The SSU functions to bring together the tRNA and mRNA to translate the genetic code. The LSU contains the peptidyl transferase centre (PTC) which catalyses peptide bond formation. Ribosome biogenesis is a process which involves the incorporation of RNPI-transcribed rRNA and RNA polymerase III (RNPIII)-transcribed

rRNA, the 5S, small nucleolar RNAs (snoRNA) and over 200 ribosomal proteins (RPs) (summarised in **Figure 1.6.1**). rRNA are sometimes referred to ribozymes or catalytic RNA to reflect their function in the catalysis of peptide bond formation during protein synthesis (Erlacher et al., 2006). rRNA positions the mRNA molecule by sequence complementarity to direct protein synthesis. snoRNA are short 60-300 nucleotide non-coding RNA that primarily regulate rRNA modifications by binding to regions of the pre-rRNA by complementary base-pairing which recruits a multiprotein snoRNP complex to post transcriptionally modify the rRNA. For example, C/D box snoRNAs such as *SNORD27* guide 2'-O methylation at specific residues of the 18S by the methyltransferase fibrillarin which may assist secondary structure folding (Falaleeva et al., 2016). RPs assist in ribosome maturation, for example, depletion of RPs result in decreased levels of mature ribosome subunits (Robledo et al., 2008).

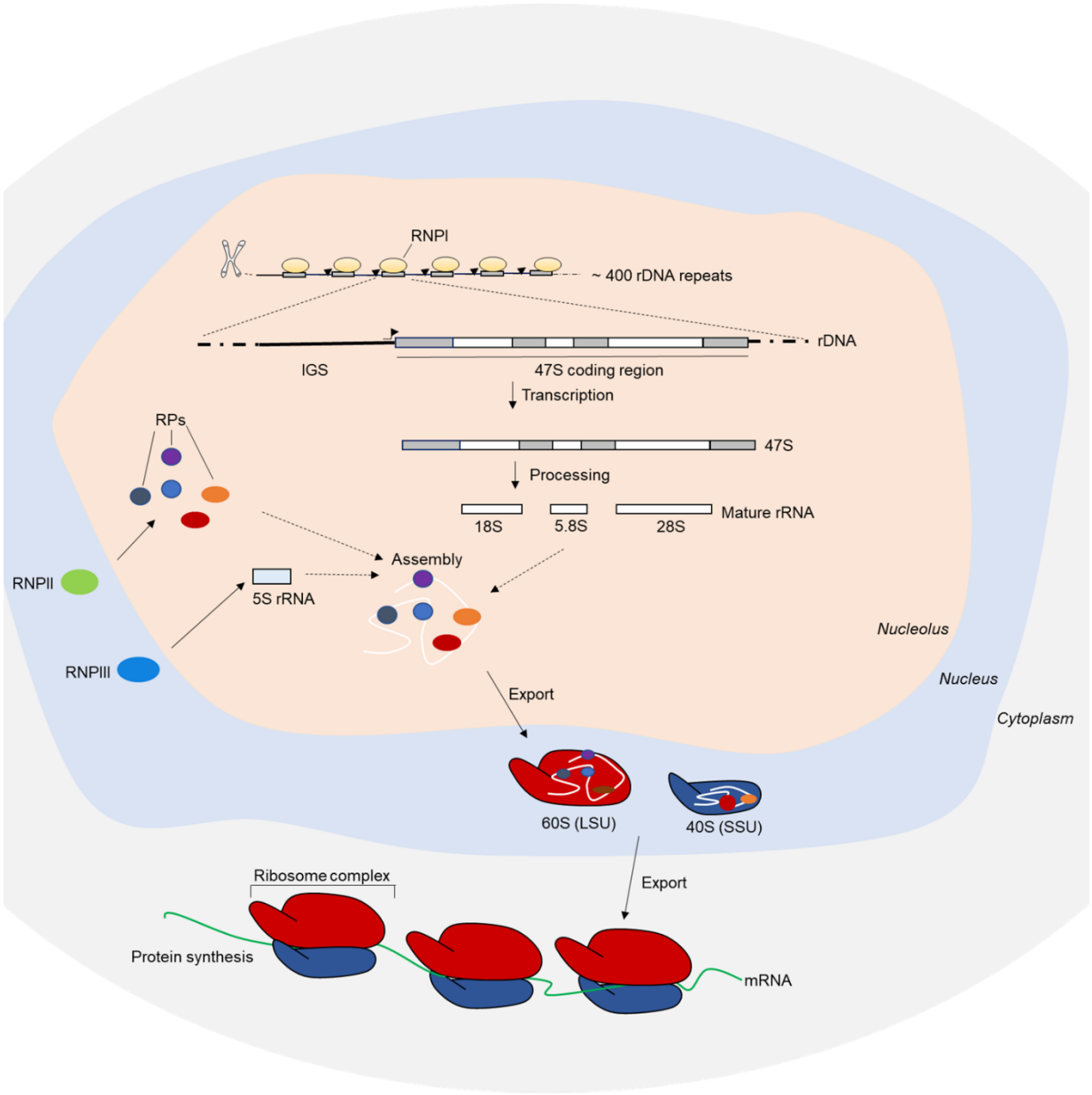


Figure 1.6. 1. Schematic of ribosome biogenesis.
Around 400 rDNA repeats are found on the acrocentric arms of 5 different chromosomes in the nucleolus in humans. A high density of RNA polymerase I (RNPI) loading on the rDNA allows for a high rate of rDNA transcription. Each 43 kb rDNA is made up of a 30 kb intergenic spacer region (IGS) which contains regulatory element and a 13 kb 47S coding region. RNPI transcription produces the precursor rRNA, the 47S. Processing of the nascent transcript involves a series of cleavages and rRNA modifications to yield the mature 18S, 5.8S and 28S rRNA. RNPII transcribes genes encoding for ribosome proteins (RPs) in the nucleus which are assembled with the RNPIII-transcribed 5S rRNA and the RNPI mature rRNAs. The ribosome complex is exported to the nucleus for further maturation into the 60S large ribosome subunit (LSU) and 40S small ribosome subunit (SSU) and is finally released into the cytoplasm where the mRNA is translated into protein.

The nucleolus is divided into three compartments which reflect different stages of ribosome biogenesis (**Figure 1.6.2**). Fibrillar centres (FCs) contain the proportion of rDNA sequences that are kept in an inactive state (Prieto and McStay, 2007). rDNA transcription occurs between the FC and the surrounding dense fibrillar centre (DFC) where the early stages of rRNA processing takes place. The surrounding granular compartment (GC) is the site of the late stages of rRNA processing, containing the 18S, 5.8S, 28S which are assembled into ribosomal subunits.

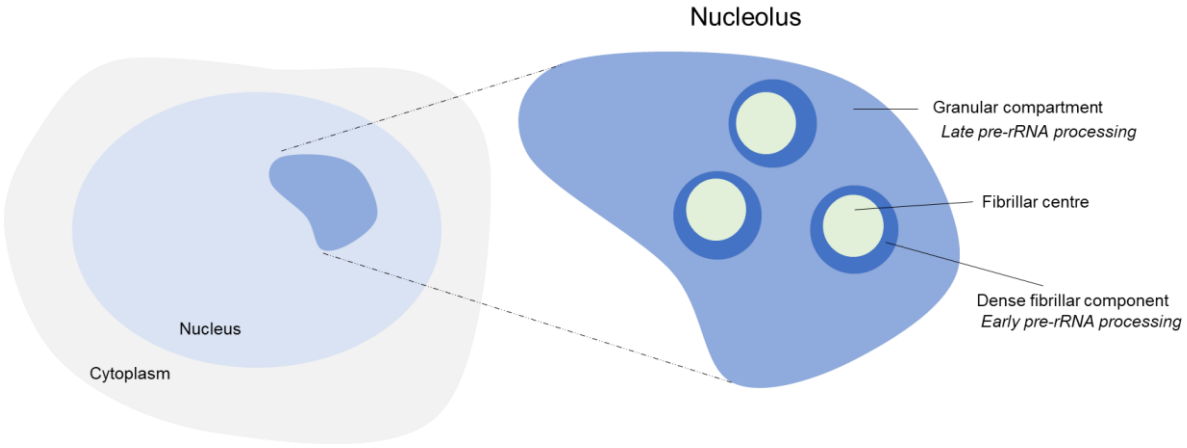


Figure 1.6.2. The nucleolar compartments in a cell.
The fibrillar centre (FC) contains the rDNA repeats. The interface between the dense fibrillar centre (DFC) and the FC are the sites where transcription of rDNA takes place. The early stages of pre-rRNA processing occur in the DFC. The granular compartment (GC) allows for the late stages of rRNA processing to take place.

The nucleolus and its compartments allow for the distinct separation of many proteins and rRNAs from one another in response to certain stimuli. Nucleolar cap formation is a phenomenon that allows for the sorting to nucleolar components such as fibrillarin and upstream binding factor (UBF) to the periphery of the GC of the nucleolus to ensure transcriptional silencing in response to stress. This process has been proposed to allow access of extra-nucleolar DNA repair factors to rDNA DSBs which is critical for transcriptional silencing (Korsholm et al., 2019; Shav-Tal et al., 2005; Siebenwirth et al., 2019). It has been

proposed that the nucleolus regulates cellular processes unrelated to ribosome biogenesis, including the DDR, cell cycle progression and maintenance of genome stability (Lindstrom et al., 2018). Furthermore, the nucleolus has been proposed to act as a phase-separated storage unit for proteins that need to be sequestered from other parts of the cell, including for example p53 (Gjerset and Bandyopadhyay, 2006). Stresses such as hypoxia, DNA damage and heat shock result in nucleolar stress which is characterised by diverse nucleolar structural and functional abnormalities. Nucleolar stress triggers the binding of several RPs, including L5 and L11, to bind to mouse double minute 2 homolog (MDM2), which is the E3 ligase responsible for the degradation of p53 (Bursac et al., 2012; Momand et al., 1992). Binding of the RPs to MDM2 inhibits the ubiquitination function of MDM2, leading to p53 stabilisation and release from the nucleolus to elicit cell cycle checkpoint activation (Lohrum et al., 2003; Marechal et al., 1994). The ability to purify nucleoli, combined with important advances in the identification and analysis of proteins using mass spectrometry, has provided a wealth of information regarding the nucleolar proteome (Andersen et al., 2002; Scherl et al., 2002; Stenstrom et al., 2020). For example, Stenstrom *et al*., took an antibody-based immunofluorescence approach to spatiotemporally profile 1318 nucleolar proteins. From this same study, the authors proposed that the nucleolar rim is a dynamic sub-compartment with a distinct composition of proteins such as the marker of proliferation Ki-67 (MKI67), a protein found to be essential for temporal partitioning (Stenstrom et al., 2020). Intriguingly, these studies have identified the nucleolar proteome as highly dynamic as opposed to static and contains a number of proteins that are not only related to ribosome biogenesis which may suggest that the nucleolar proteome may be much more diverse than previously expected.

RNPI-mediated transcription is a highly dynamic process that requires multiple factors to accurately and efficiently synthesise rRNA. RNPI has 14 subunits in yeast (*S. cerevisiae*), 13 of which have homologs identified in mammals and humans shown in **Table 1.6.1**. These

specific RNPI subunits function at multiple stages in the RNPI transcription cycle, playing important roles in promoter escape and elongation. Ten of these subunits form a catalytic core, which are homologous or shared with subunits found in RNPII or RNPIII. Six of these subunits are specific to RNPI shown in bold.

Human RNPI subunits	***S. cerevisiae* RNPI subunits**	**Human Homologues in RNPII/RNPIII**
hRPB5	RPB5 (ABC27, POLR2E)	shared
hRPB6	RPB6 (ABC23, POLR2F)	shared
hRPB8	RPB8 (ABC14.5, POLR2H)	shared
hRPB10	RPB10 (ABC10β, POLR2L)	shared
hRPB12	RPB12 (ABC10α, POLR2K)	shared
hRPA40	RPA40 (AC40, POLR1C)	RPB3/shared
hRPA19	RPA19 (AC19, POLR1D)	RPB11/shared
hRPA190	RPA190 (A190, POLR1A)	RPB1/RPC160
hRPA135	RPA135 (A135, POLR1B)	RPB2/RPC128
hRPA43	RPA43 (A43, POLR1F)	RPB7/RPC25
N/A	RPA14 (A14)	RPB4/RPC17
hRPA12	RPA12 (A12.2, POLR1H)	RPB9/RPC11
PAF53	RPA49 (A49, POLR1E)	TFIIF/TFIIE-β
CAST (PAF49)	RPA34.5 (A34.5, POLR1G)	TFIIF/RPC53

Table 1.6 1 RNPI subunits in yeast and in human.
The RNPI complex in humans is made up of 13 subunits. The subunits highlighted in bold indicate those that are specific to RNPI, the others are shared between RNPII. The yeast RNPI complex has 14 identified subunits. Table adapted from (Goodfellow and Zomerdijk, 2013).

In addition to the RNPI subunits listed in **Table 1.6**, there are multiple RNPI-associated transcription factors that assist recurrent rounds of transcription initiation, elongation and termination. The first stage of transcription by RNPI is the formation of the pre-initiation complex (PIC) at the core promoter (**Figure 1.6.3**). The selectivity factor 1 (SL1) complex is essential for RNPI PIC formation transcription and is made up of several transcription-associated factors (TAFs); TAF_I110 (TAF1C), TAF_I63 (TAF1B), TAF_I48 (TAF1A), TAF_I41 (TAF1D) and TAF12. SL1 confers promoter selectivity by binding to the core promoter element on the rDNA which results in the recruitment of RNPI to the rDNA core promoter and

stabilises the interaction between UBF and RNPI. UBF bound to the upstream control element (UCE) on the rDNA and interacts with components of the RNPI complex such as PAF53 and PAF49 subunits to promote PIC formation. Another important initiation factor, RRN3, interacts directly with SL1 and RNPI, through its hRPA43 subunit and is assisted by PAF53 binding. Therefore, RRN3 facilitates PIC formation by connecting RNPI with the rDNA promoter through an essential promoter binding factor.

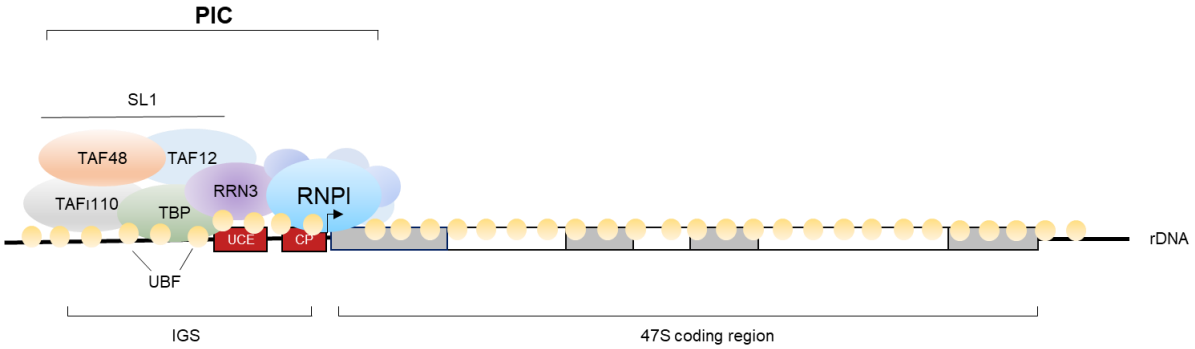


Figure 1.6. 3. The formation of the PIC for rDNA transcription.
UBF is bound across the rDNA region including the upstream control element (UCE). The RNPI complex is bound to the core promoter (CP). The SL1 complex forms when multiple transcription factors such as TAF48, TAF12, TAF$_I$110 are recruited to the rDNA transcriptional control elements in the intergenic region (IGS). The grey boxes represent the spacer-encoding regions of the 47S on the rDNA.

As RNPI escapes the core promoter, UBF and SL1 remain bound to the rDNA poised and ready to re-initiate the next RNPI complex to support multiple rounds of transcription and high density of RNPI loading on the rDNA. Elongation of RNPI is augmented by UBF which is evenly distributed along the 47S coding region (O'Sullivan et al., 2002). Topological strains with positive supercoils ahead of RNPI and negative supercoils behind the elongating RNPI can be resolved by DNA topoisomerases, Topoisomerase 1 (Top1) or Topoisomerase 1 (Top 2) which transiently break and enable unwinding of the supercoiled DNA (Brill et al., 1987). Interestingly, Top1 has been shown to be essential to prevent R-loop formation on the rDNA during transcription, ensuring genome stability (El Hage et al., 2010).

Following elongation, transcription termination elements are located towards the 3' end of the rDNA repeat are bound by termination factors to carry out the final stage of RNPI transcription. The RNPI-specific TTF1 binds and bends the 3' end of the rDNA forcing transcription to pause (Evers et al., 1995; Grummt et al., 1986). Coordination with RNPI and Transcript Release Factor, PTRF, a release factor, enables dissociation of the RNPI complex from the transcript resulting in transcriptional termination (Jansa and Grummt, 1999).

Many other factors promote and regulate rDNA transcription. Mammalian target of rapamycin (mTOR) is a key responder to growth factor and nutrient availability which controls a variety of cellular processes such as cell growth, transcription, translation and protein degradation (Brown et al., 1994; Holz et al., 2005). mTOR signalling leads to the phosphorylation and activation of RRN3 at serine 44 (S44) which enhances the interaction of RNPI with SL1, thus facilitating RNPI recruitment to the rDNA promoter resulting in increased rRNA synthesis (Mayer et al., 2004). In contrast, mTOR signalling also regulates RRN3 inactivation by phosphorylation of serine 199 (S199), therefore decreasing rRNA synthesis. Thus, mTOR kinase-dependent activity can both upregulate and decrease rRNA synthesis.

The RNase, Dicer, is most well-known to function in the RNA interference (RNAi) pathway where it cleaves a hairpin-loop double stranded RNA (dsRNA) leading to argonaut (AGO) dependent degradation (Bernstein et al., 2001; Liu et al., 2004). Non-canonical functions of dicer in the nucleus have been identified which include the control of rDNA transcription in mammals. In human and mouse cell lines, dicer was found to bind to the 47S coding region of the rDNA (Sinkkonen et al., 2010). Furthermore, the genetic depletion of *dicer* in these cells lead to a reduction in rDNA transcription which suggests that dicer is an important factor involved in rRNA synthesis (Sinkkonen et al., 2010). Interestingly, Dicer has been shown to be repressed in hypoxia, however, the impact of dicer loss in hypoxia on rDNA transcription is unknown (Ho et al., 2012; van den Beucken et al., 2014).

The oncogene encoding for C-MYC is another factor involved in the transcription of genes associated with cell growth and proliferation. C-MYC binds downstream of the rDNA transcriptional start site and activates RNPI in response to mitogenic signals to upregulate the production of rRNA (Arabi et al., 2005). Intriguingly, C-MYC has been shown to be repressed in hypoxic conditions (Wong et al., 2013; Zhang et al., 2007). Therefore, it is conceivable that the loss of C-MYC impacts the level of rDNA transcription in hypoxia, although this has not yet been explored.

Interestingly, half of the rDNA repeats are kept in a constitutively-inactive state, presumably to ensure that a portion of rDNA repeats are preserved and protected against processes that threaten genome stability such as the high rate of transcription (Ide et al., 2010). Another potential reason that half of the rDNA repeats lie dormant could be that these repeats can be reactivated when necessary to quickly start ribosome biogenesis, although our general understanding of this phenomenon is not well understood (Wittner et al., 2011). Active rDNA genes exhibit hypomethylated promoters and methylation on histone H3 on lysine 4 (H3K4), as well as acetylation on histone H3 and H4 tails. The regulation of chromatin is essential for controlling rDNA transcription. For example, methylation by fibrillarin (encoded by *NOP1* in yeast) of glutamine 104 on histone H2A in humans and glutamine 105 in yeast is proposed as a nucleolar-specific histone epigenetic mark that regulates rRNA synthesis and impairs RNPI transcription (Tessarz et al., 2014). Furthermore, the mechanism of methylation of histone H2A by fibrillarin was itself found to be epigenetically regulated through sirtuin 6 (SIRT6) deacetylation (Iyer-Bierhoff et al., 2018).

In contrast, silent rDNA genes have heterochromatic marks such as mono-, di- and tri-methylation on histone H3 on lysine 9 (H3K9me1, H3K9me2, H3K9me3) (Zentner et al., 2011). The transition from an active to silent state is mediated by the nucleolar remodelling complex (NoRC), which recruits the DNA methyltransferase (DNMT) and histone deacetylase

(HDAC) activities to the rDNA, triggering heterochromatin formation and transcriptional silencing (Santoro and Grummt, 2005). Intriguingly, deletion of tightly packed, inactive rDNA copies, even though they are not transcribed, triggers the DDR and renders cells more sensitive to mutagen inducing DNA damage agents, which suggests that rDNA heterochromatin formation may have a role in DNA damage signalling (Paredes and Maggert, 2009; Xu et al., 2017). On the other hand, the activation of rDNA repeats occurs epigenetically through UBF, a protein that recruits RNPI to the rDNA promoter but is also important for binding to hypo-methylated, pseudo-silent rDNA repeats to convert them to an active state (Diesch et al., 2019). The activation of dormant rDNA repeats during malignant transformation has been proposed as a mechanism that contributes to the changes in gene expression that regulate cell growth and differentiation (Diesch et al., 2019).

1.6.1 rRNA processing

Proper rRNA processing provides the cell with layers of quality control to fine-tune the availability and steady state levels of mature rRNA, which will ultimately determine translational output. RNPI transcription produces a single long precursor transcript, the 47S. This precursor transcript contains the 18S, 5.8S and 28S rRNAs, which are separated by the 5'external transcribed spacer (5'ETS), internal transcribed spacer 1 (ITS1), internal transcribed spacer 2 (ITS2) and 3'external transcribed spacer (3'ETS) (**Figure 1.6.1.1**). Each spacer region contains sites which are cleaved in a complicated, multi-staged and precise fashion. The pre-rRNA processing pathways differ significantly between taxa, which may be due to the highly divergent sequences of the primary spacer regions between organisms which contain the processing sites. In addition, the length of the spacer regions is longer in humans than in yeast and so contain specific cleavage sites that only exist in human organisms. An overview of pre-rRNA processing is reviewed in the following reference (Henras et al., 2015). In humans, the 47S is primarily cleaved at site A' at nucleotide 414 on the 5'ETS and then at site 02 of the

3’ETS (Kass et al., 1987; Lazdins et al., 1997). The following cleavage step occurs on the A0 site of the 5’ETS. The subsequent cleavage after A’ occurs at site 2 on the ITS1 which indicates an alternative processing pathway. Following A0 cleavage, the next cleavage step occurs at site 1 on the 5’ETS (Sloan et al., 2013). Subsequent cleavages occur in a stepwise manner to degrade the ITS1 and ITS2 to generate the mature rRNA which is exported from the nucleus to the cytoplasm to carry out the catalysis of peptide bond formation in protein translation (Gordon et al., 2019; Preti et al., 2013).

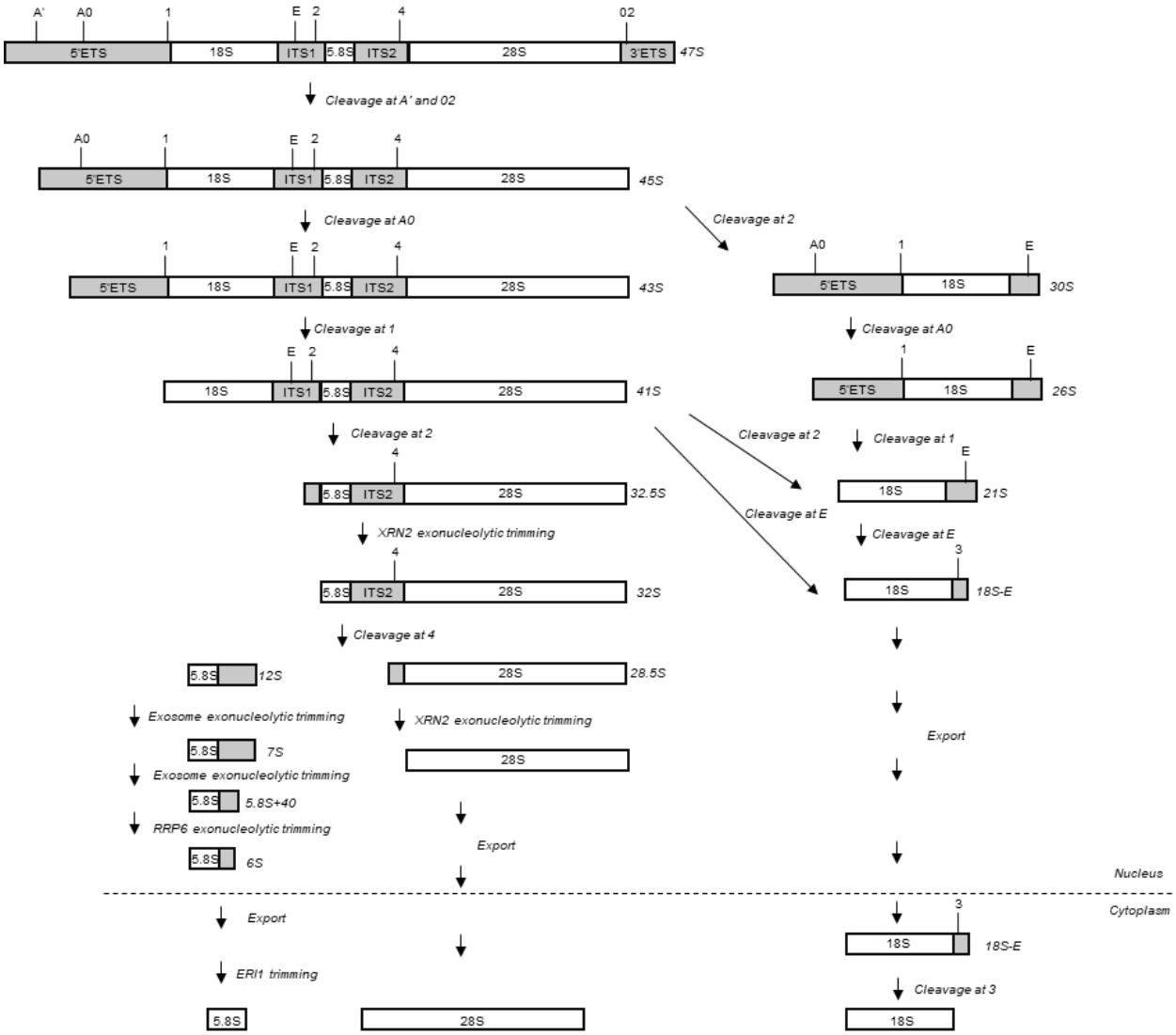


Figure 1.6.1 1. Pre-rRNA processing pathways in humans.
The product of RNPI transcription, the 47S is cleaved first at site A’ and 02 on the 5’ETS and 3’ETS region, respectively. Subsequent cleavages occur at sites located on the grey spacer regions leading to the maturation and cytoplasmic export of the 18S, 5.8S and 28S.

Improper rRNA processing has been described previously in ribosomal disorders, known as ribosomopathies, such as Treacher Collins syndrome which results from a mutation in the *TCOF1* gene. Treacher Collins syndrome leads to facial and developmental deformities, depending on the severity which can vary from mild to severe and ultimately leads to dysregulated ribosome function. Another example of a ribosomopathy includes dyskeratosis congenita, which is an inherited bone marrow failure syndrome that manifests with some somatic abnormalities. The most common form of dyskeratosis congenita is the X-linked form, which has been established to be due to mutations in the *DKC1* gene, encoding the nucleolar factor dyskerin, a protein associated with rRNA modifications and ribosome biogenesis (Heiss et al., 1998). Dyskerin has also been shown to bind to the telomerase RNA, an integral part of the telomerase enzyme complex that acts as a template for the synthesis of the TTAGGG repeats that are found at the telomeres of chromosomes. Therefore, mutations in *DKC1* lead to telomere shortening through reduced levels of telomerase RNA (Wong and Collins, 2006).

Interestingly, with the exception of Treacher Collins syndrome, ribosomopathies including dyskeratosis congenita have been found to increase susceptibility to cancer (Edwards et al., 1997). The dysregulation of protein translation in cancers has been shown to drive cell proliferation (Barna et al., 2008; Johnson et al., 1976). Therefore, it is possible that the predisposition to cancer could be triggered by abnormal ribosome biogenesis during the onset of the ribosomopathy, possibly through the mutation of essential genes associated with ribosome function. The link between impaired ribosome biogenesis in ribosomopathies and increased occurrence of cancer is inherently paradoxical as cancer usually relies on an increase in translation and many cancers upregulate RPs. The relationship between ribosomopathies and cancer is poorly understood and how dysregulation of ribosomes regulates disease progression in cancer is a largely undefined.

1.6.2 5’ETS processing

Pre-rRNA processing requires many auxiliary factors which include a range of nucleolar proteins and RNA species. A group of RNAs known as snoRNA assist with the modification and catalysis of the 2’-O-ribose methylation or pseudouridinylation of rRNA. snoRNA consist of two major families which are based on their structure and function. The first family of snoRNA are the H/ACA which forms a small nucleolar ribonucleoprotein (snoRNP) complex to isomerise specific uridine ribonucleotides in the target RNA to pseudouridines (Ψ) (**Figure 1.6.2.1).** Pseudouridine is an isomer of uridine in which the uracil is attached by a carbon-carbon bond instead of a nitrogen-carbon bond. The presence of an extra hydrogen bond in its non-Watson Crick base-pairs (also known as wobble base pairing) donor endows Ψ with biochemical and biophysical properties that are distinct from that of uridine. In particular, Ψ provides greater rigidity to the phosphodiester backbone of the RNA and, in comparison to U-A base-pairing, increases the stabilisation of Ψ-A base-pairing.

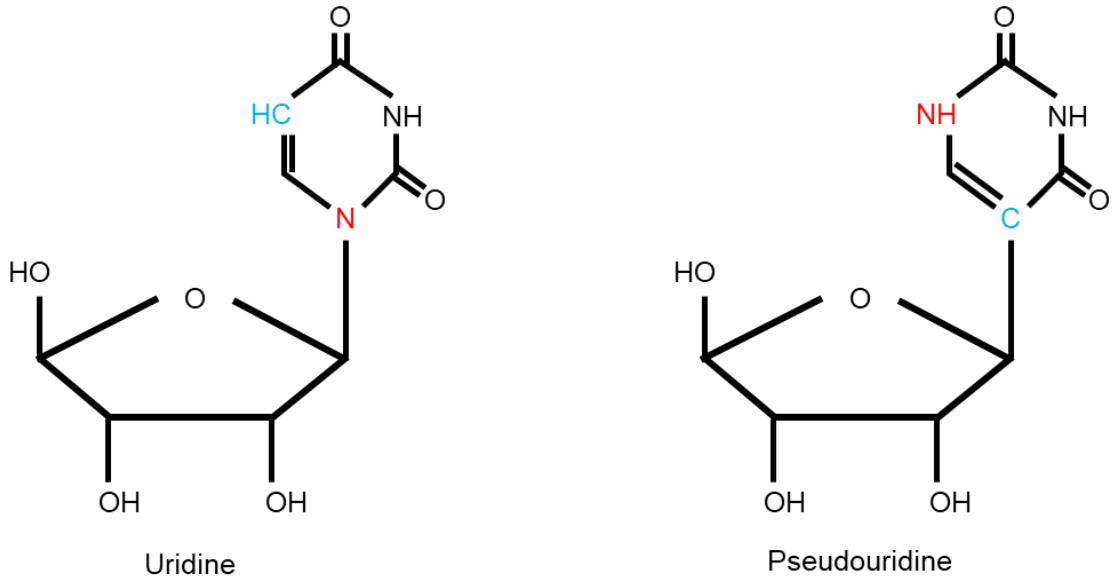


Figure 1.6.2. 1. Uridine and pseudouridine (Ψ) chemical structure.
Pseudouridine is an isomer of uridine in which the uracil is attached by a carbon-carbon bond instead of a nitrogen-carbon bond. Uridines in rRNA are often modified post-transcriptionally into pseudouridines which assist in rRNA stability.

The H/ACA motif of the snoRNA consists two conserved sequence elements; the Hinge box (H) and an ACA sequence towards the 3' end of the RNA. The second group, the C/D snoRNA act as a guide RNA for site-specific 2'-O-methylation. The C/D box motif is characterised by two terminal box sequences; box C (AUGAUGA) and box D (CUGA) and two internal C/D motifs. The RNA component of the snoRNP allows for sequence specificity through complementary base pairing to the target RNA, but do not possess any inherent catalytic activity. C/D box snoRNAs, including U3, U8, U14 and U22 are associated with pre-rRNA cleavage and processing (Langhendries et al., 2016; Tycowski et al., 1994). The U3 snoRNA is essential for the primary cleavage site A' in metazoans through base pairing with the pre-rRNA immediately downstream of the A' site (Kass et al., 1990). The U3 snoRNA are associated with four common proteins, fibrillarin, Nop56, Nop58 and 15.5K which assemble to form the multiprotein U3 snoRNP complex. In addition to the crucial role of fibrillarin in the methylation of rDNA, fibrillarin's methyltransferase activity is also directed at the methylation of rRNA when in the U3 snoRNP. Additionally, in box C/D snoRNAs, the target region hybridises adjacent to a D or D′ box and the rRNA nucleotide five base pairs from the D or D′ is methylated by fibrillarin (Galardi et al., 2002) (**Figure 1.6.2.2**). Moreover, U-three associated protein complexes also arrange around the 5'ETS which aid in folding and further maturation. Specifically, it has been demonstrated that U-3 associated protein-A (UTP-A) is essential for cleavage at site A' in humans (Sloan et al., 2014). Therefore, the U3 and potentially other snoRNPs are essential for efficient processing of the 5'ETS of the pre-rRNA.

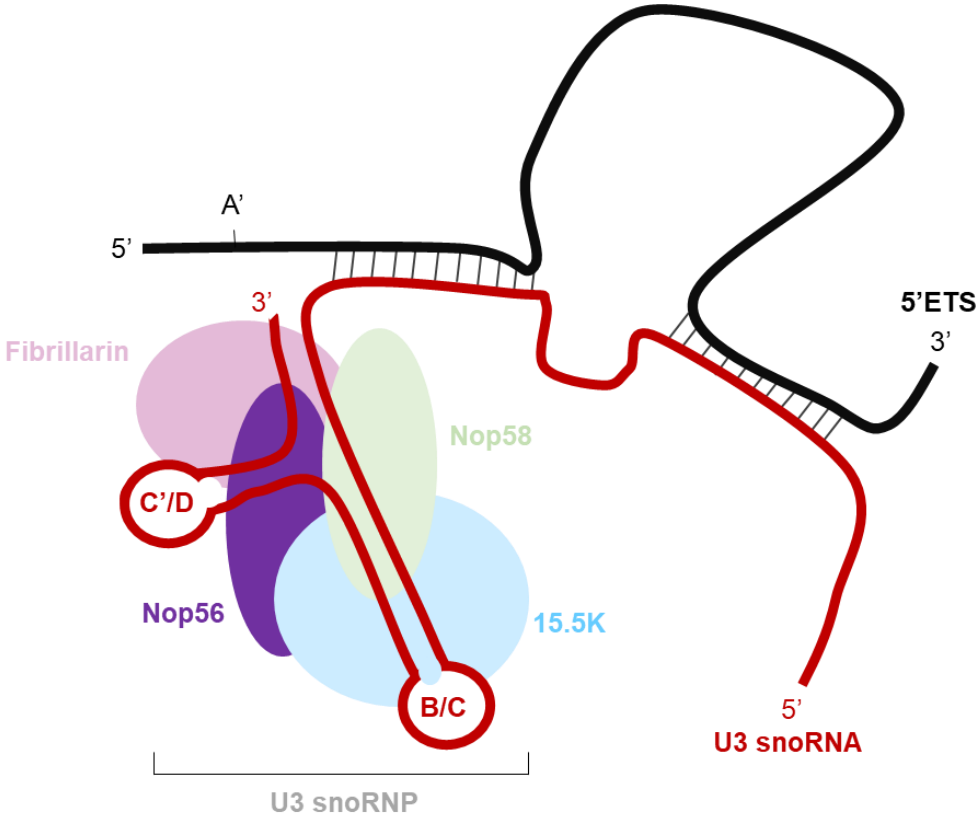


Figure 1.6.2. 2. U3 snoRNA base pairing with the 5'ETS of the pre-rRNA.
The U3 snoRNA (red) hybridises through complementary base pairing to a region downstream on the A' primary cleavage site on the 5'ETS (black). A complex of proteins containing fibrillarin, Nop56, Nop58 and 15.5K form the U3 snoRNP which assists with pre-rRNA modifications and processing.

Both U3 and U8 snoRNAs are transcribed by RNPII and receive a mono-methylated (m^7G) 5′ cap that is further converted into a tri-methylated cap structure (m_3G) during their maturation (**Figure 1.6.2.3**). The m_3G caps of the snoRNAs are targets for the decapping complex which results in impaired snoRNA maturation and improper pre-rRNA processing. Proline-rich nuclear receptor coactivator 1 (PNRC1) is a putative tumour suppressor gene that is frequently lost in cancers (Gaviraghi et al., 2018). A previous report demonstrated that PNRC1 blocks rRNA maturation by inhibiting snoRNA maturation (Gaviraghi et al., 2018). Briefly, PNRC1 recruits the DCP2/DCP1α decapping complex to the nucleolus which leads to the decapping of U3 and U8 snoRNA and abrogates rRNA processing.

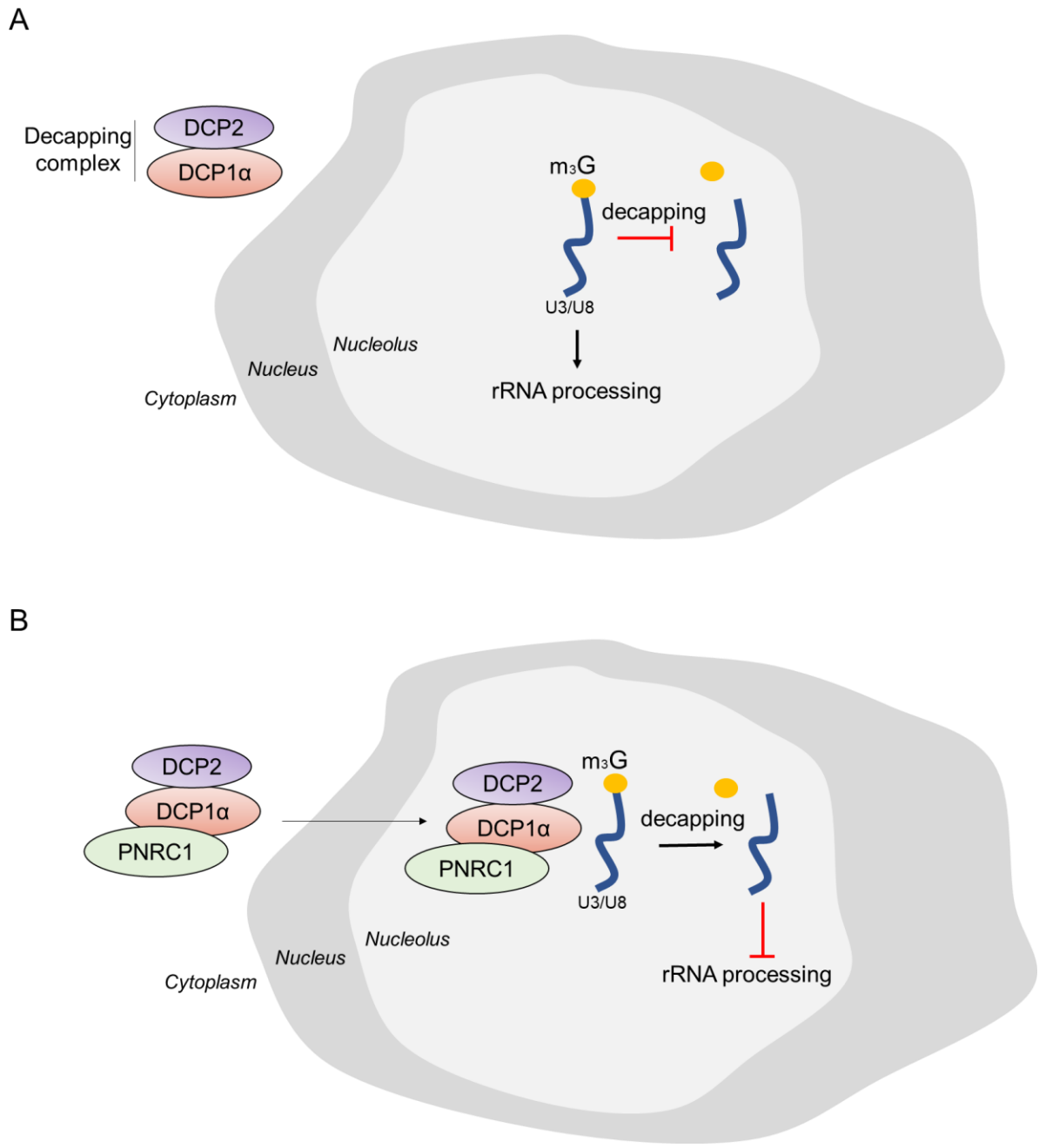


Figure 1.6.2. 3. PNRC1 blocks rRNA maturation.
A. In the absence of PNRC1, the cytoplasmic decapping complex is absent from the nucleolus. Methylation of the guanosine caps (m3G) of U3 and U8 snoRNA are required for proper snoRNA maturation and rRNA maturation. B. When the expression of PNRC1 increases, PNRC1 translocates with the decapping complex to the nucleolus resulting in decapping activity towards the snoRNA. The decapped snoRNA is no longer functional resulting in impaired rRNA processing and maturation.

The high rate of rDNA transcription results in significant amounts of pre-rRNA processing by-products which require degradation and elimination as accumulation of these by-products could

impact cellular homeostasis. Thus, 5' to 3' and 3' to 5' exoribonucleases exert rRNA quality control over aberrant pre-rRNA intermediates and include the XRN family of exonucleases (**Figure 1.6.2.4**). Sloan et al., demonstrated that XRN2 depletion resulted in the accumulation of the large 47S pre-rRNA species which suggested that A' cleavage was XRN2-dependent (Sloan et al., 2014). The authors also identified the factor MTR4, a member of the Trf4/Air2/Mtr4p polyadenylation (TRAMP) complex to play a role in A' cleavage. Furthermore, the authors demonstrated that XRN2 is involved the cleavage steps at A0 and 1 on the 5'ETS. Additionally, XRN2 is linked to transcription termination by RNPI and to the surveillance of the pre-rRNA transcripts and turnover of premature transcription termination products (Wang and Pestov, 2011). Therefore, XRN2 may provide a link to couple the transcriptional termination process with the processing of pre-rRNA.

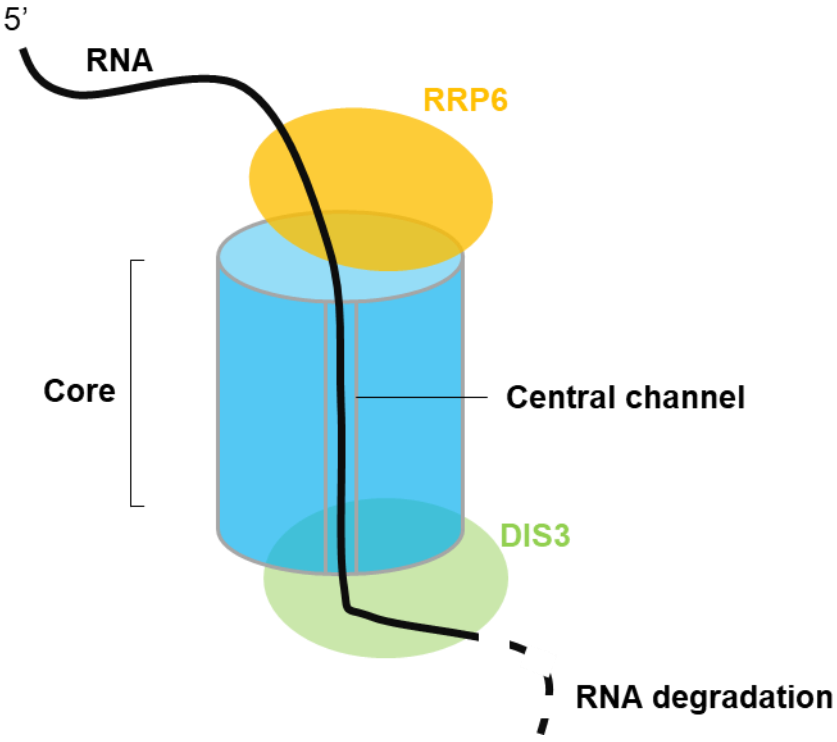


Figure 1.6.2. 4. The exosome complex degrades many RNA species.
RRP6 and DIS3 are positioned on the top and bottom of the core complex, respectively. RRP6 carries out the initial trimming of the RNA. The core of the complex contains a central channel where the RNA passes through and DIS3 carries out the catalytic activity to degrade the RNA transcript.

In contrast, elimination of the 5'ETS has been shown to be dependent on the exonucleolytic and endonucleolytic characteristics of DIS3 and rRNA processing protein 6 (RRP6), which are members of the exosome, a complex involved in the degradation of a wide variety of RNA species, the subcellular location of which depicts the specialised function through distinct exosome isoforms (**Figure 1.6.2.5**) (Kobylecki et al., 2018; Sloan et al., 2014). DIS3 is a 3' to 5' exoribonuclease that comprises the catalytic subunit of the exosome alongside DISL3 and RRP6, another exoribonuclease (Wasmuth and Lima, 2012).

Kobylecki et al., demonstrated that the processing of the fragment from A'-A0 does not depend on XRN2, but relies on the cooperative activity of DIS3 and RRP6 (**Figure 1.6.2.5**) (Kobylecki et al., 2018). The initial trimming of this product is carried out by an unknown factor which is subsequently mediated first by RRP6 followed by DIS3. Sloan et al., did not identify DIS3 as a factor involved in the processing of the 5'ETS. It is unclear why specific fragments of the 5'ETS require different nucleases for processing (Sloan et al., 2014). Efforts to understand how nucleases are regulated in rRNA processing will provide important insights into the complexity of the process of ribosome biogenesis.

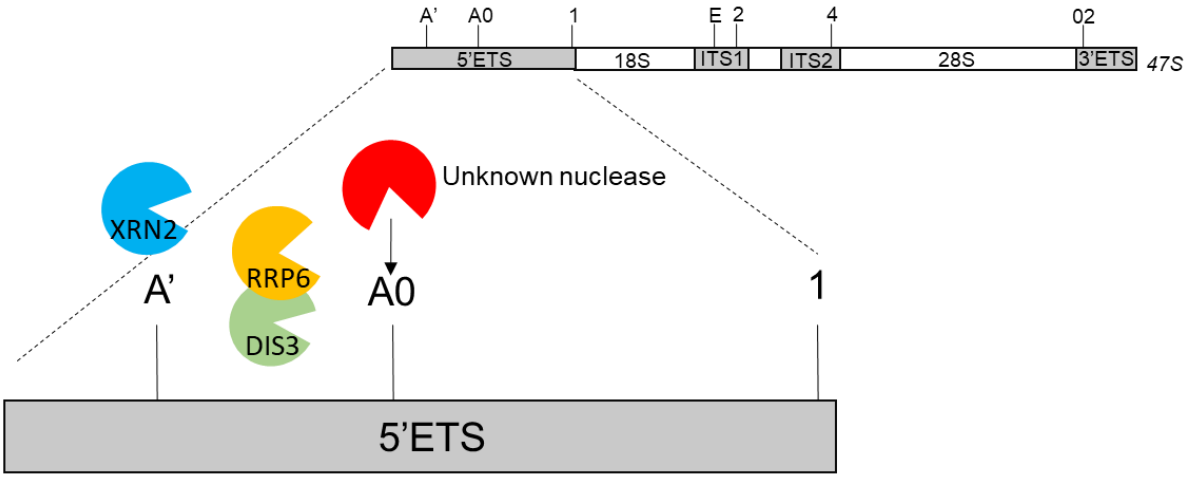


Figure 1.6.2. 5. 5'ETS elimination by the exosome complex.
Exonuclease XRN2, DIS3 and RRP6 have all been implication in the elimination of 5'ETS fragments. XRN2 is involved in cleavage at A' of the 5'ETS. DIS3 and RRP6 cooperate to degrade the A'/A0 pre-rRNA by-product using their exonucleolytic activity. The initial nuclease at site A0 is currently unknown.

1.6.3 Stress induced repression of rDNA transcription

1.6.3.1 DSB induced repression of rDNA transcription

Shutdown of rDNA transcription in response to a DSB on the rDNA is necessary to allow the DDR to repair. The nucleolar response to DSBs is distinct from that of a conventional nuclear DDR. Studies that induce DSBs directly to the 28S coding region of the rDNA using the homing Intron-encoded endonuclease (I-PpoI) endonuclease from *Physarum* or through clustered regularly interspaced short palindromic repeats (CRISPR)-CRISPR associated protein 9 (Cas9) have been demonstrated to block RNPI progression on the rDNA through nucleolar recruitment of DDR factors and nucleolar segregation/cap formation which may move nucleolar components such as the damaged rDNA repeats to the nucleolar periphery to gain access to DNA repair factors such as BRCA1 or Rad51 (**Figure 1.6.3.1.1**) (Harding et al., 2015). Although the mechanism of rDNA DSB repair and transcriptional repression remains unclear, studies have shown that rDNA transcriptional repression and DSB repair rely on ATM and ATR (Kruhlak et al., 2007; Mooser et al., 2020). rDNA DSBs result in ATM activation

which leads to TCOF1 phosphorylation, a phosphoprotein involved in nucleolar trafficking. The direct interaction between TCOF1 and Nijmegen breakage syndrome 1 (NBS1), in the context of the Mre11-Rad50-Nbs1 (MRN) complex, mediates their recruitment into the nucleoli which suggests that the MRN complex is an essential upstream component of rDNA transcriptional repression and nucleolar segregation. The MRN complex is proposed to act upstream of ATR activation through its essential role in DNA end resection which produces ssDNA, the main trigger for ATR activation. Therefore, the authors investigated the role of DNA resection in the mechanism of ATR activation in response to rDNA DSBs (Mooser et al., 2020). RPA2, phosphorylated on serine 4 and 8, a well-established marker of resection, was found to be enriched in the nucleoli before and during nucleolar cap formation which suggests that resection occurs before the rDNA repeats are moved to the nucleolar periphery. Interestingly, RPA2 foci were abrogated upon ATM and ATR inhibition in response to rDNA DSBs indicating that DNA resection is not required for ATR activation in the nucleoli. This finding highlighted a key difference between the regulation of rDNA DSB repair and other DSBs in the genome that are not reliant on ATR activity for repair.

Having determined that DNA resection does not provide the signal for ATR activation, Mooser et al., determined whether TopBP1 was the ATR activator, as previous studies have shown that overexpression of TopBP1 was shown to activate ATR and rDNA transcriptional repression, even in the absence of DNA damage (Mooser et al., 2020; Sokka et al., 2015). Interestingly, TopBP1 foci were found in the nucleolus in response to rDNA DSBs upon ATR inhibition, which indicated that TopBP1 localisation occurs upstream of ATR activation. However, ATM/ATR inhibition abrogated TopBP1 nucleolar segregation to the nucleolar caps in response to rDNA DSBs, which suggests that TopBP1 segregation as opposed to its nucleolar recruitment is reliant on ATM/ATR activity. Together, these findings suggest that TopBP1

accumulation is essential for rDNA DSB repair through nucleolar segregation and rDNA transcriptional repression.

Having found that TopBP1 is necessary for ATR activation, Mooser et al., showed that TopBP1 is recruited with TCOF1 to the nucleolus through a phosphorylation-dependent interaction which involves the BRCA1 C-terminal (BRCT) domains of TopBP1 and conserved serine/threonine residues of the C-terminal domain of TCOF1. Therefore, nucleolar recruitment of TopBP1 activates ATR signalling to supress RNPI transcription through nucleolar segregation of the damaged rDNA repeats to the nucleolar caps (Mooser et al., 2020; Sokka et al., 2015). Together, these studies demonstrate the importance of ATM/ATR kinase activity and TCOF1 and TopBP1 recruitment in the repair of rDNA DSBs through nucleolar segregation and rDNA transcriptional repression. In addition to ATM and ATR, another DNA damage kinase, DNA-PK and repair factor PARP1 have been demonstrated to block RNPI in response to cisplatin-induced DNA damage during S phase, although the precise mechanism of this repression remains elusive (Calkins et al., 2013).

It is likely that a direct modification of RNPI transcriptional machinery by ATM or ATR may be involved, as several key RNPI transcription factors have been shown to be PIKK targets (Matsuoka et al., 2007). However, as transcriptional inhibition relies on ATM and ATR as well as downstream signalling events such as CHK1, it is likely that more than one effector is responsible for transcriptional inhibition.

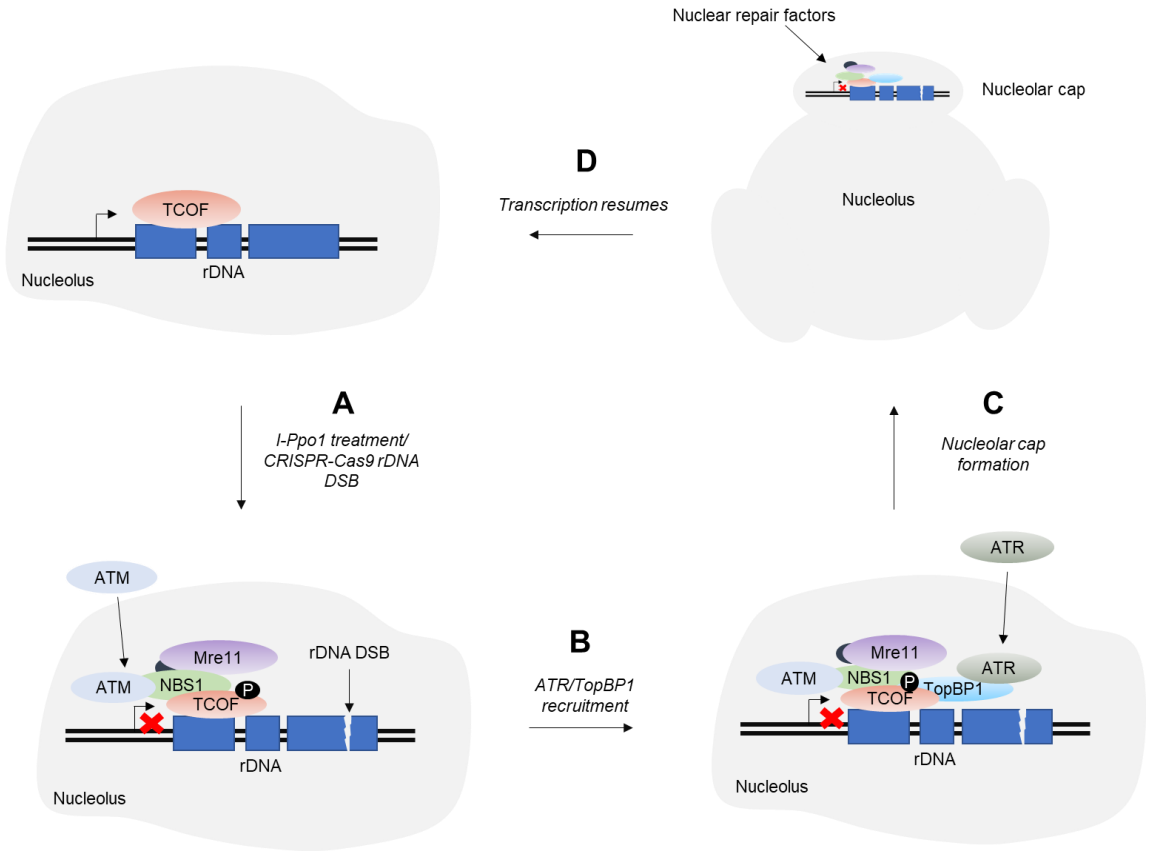


Figure 1.6.3.1.1. Schematic of the rDNA DSB-induced mechanism of transcriptional repression.
A. Treatment with the I-Ppo1 homing endonuclease targeting the 28S encoding region of the rDNA or CRISPR-Cas9 induced rDNA breaks activates ATM signalling. TCOF1 is phosphorylated by ATM and recruits the MRN complex to the nucleolus to partially inhibit RNPI progression. B. ATR activation by TopBP1 recruitment to the nucleolus through a TCOF1 interaction is required for full RNPI shutdown. C. Nucleolar cap formation allows for nuclear repair factors such as BRCA1 to assist in DSB repair. D. Once the DSB is repaired, rDNA transcription can resume.

1.6.3.2 DSB-independent repression of rDNA transcription

In contrast to rDNA DSBs, mild hypoosmotic stress (50% water, 50% media) for short periods of time (0.5-3 hours) does not induce DNA damage but has been demonstrated to shutdown RNPI transcription (Velichko et al., 2019). Of note, this mechanism highlights that the induction of R-loops in the nucleoli are important for RNPI transcription inhibition. In this study, the authors show the accumulation of RPA bound ssDNA from R-loops on the rDNA provides the signal for ATR activation and recruitment to the nucleoli through ATRIP-

TopBP1-TCOF1. Phosphorylation of H2AX by ATR amplifies this DDR signalling by generating a positive feedback loop involving mediator of DNA damage checkpoint 1 (MDC1) and the MRN complex (Lou et al., 2006). Subsequently, ATM is activated either by direct ATR phosphorylation or through the MRN complex to shut down RNPI transcription which results in further phosphorylation of H2AX acting in a feedback loop for full ATM activation. However, although the authors propose that ATM inhibits RNPI transcription through the known mechanisms of ATM dependent RNPII inhibition, the exact mechanism of ATM dependent RNPI shutdown in response to hypoosmotic stress is unclear (**Figure 1.6.3.1.2**) (Shanbhag et al., 2010).

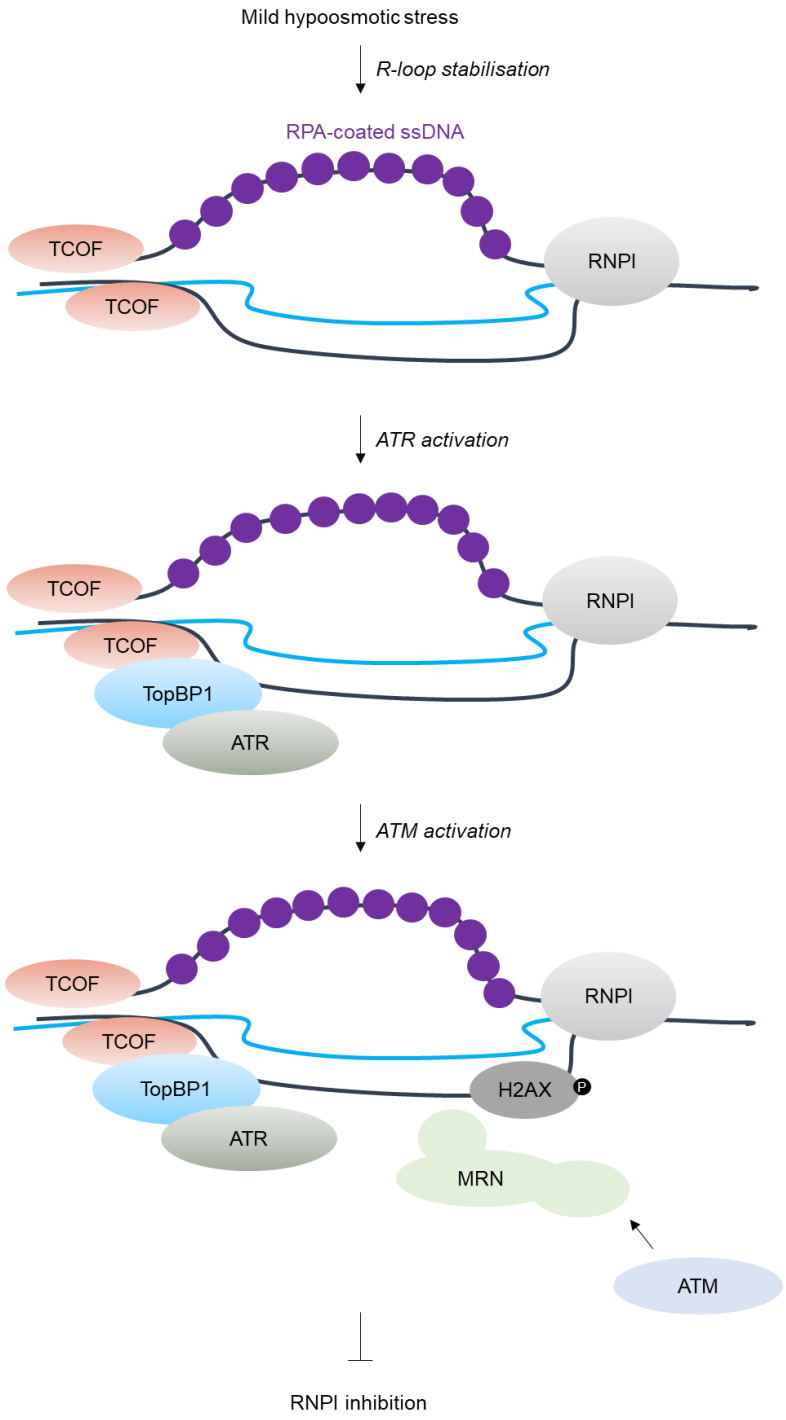


Figure 1.6.3.2. 1. Schematic of the mechanism of mild hypoosmotic stress induced R-loop stabilisation to block RNPI.
Treatment of cells with hypoosmotic conditions (50% water, 50% media) results in the stabilisation of rDNA R-loops. The ssDNA coated with phosphorylated RPA leads to ATRIP and TopBP1 recruitment mediated by TCOF1 resulting in ATR activation. ATM is subsequently activated either through direct phosphorylation by ATR or by recruitment of the MRN complex, resulting in phosphorylation of downstream target H2AX which acts as a feedback loop for full ATM activation and RNPI repression.

An alternative mechanism of RNPI shutdown has been reported in response to harsher hypoosmotic stress (70% water, 30% DMEM, 4 hours). This study demonstrated that the upregulation of a RNPII-transcribed long non-coding RNA known as "promoter and pre-rRNA antisense" (PAPAS) results in the inhibition of RNPI (Zhao et al., 2018). PAPAS which is transcribed in the antisense direction to the 47S coding region by RNPII, recruits the chromatin remodelling complex CHD4/NuRD to the nucleoli to disrupt RNPI progression. Interestingly, PAPAS was not significantly upregulated in milder hypoosmotic stress (Velichko et al., 2019). Therefore, two independent mechanisms exist in response to hypoosmotic stress, the first involving ATR/ATM induction and R-loop formation to initially block RNPI for the first hours of hypoosmotic stress, and the second involving upregulation of PAPAS to sustain RNPI transcriptional repression.

In general, the mechanism of RNPI shutdown in response to stress relies on both ATM and ATR. There are several putative ATM targets that could be phosphorylated to inhibit rDNA transcription, for example, TTF1 or the RNPI subunit RPA34. Patients with ataxia telangiectasia demonstrate high levels of rDNA mutations compared with normal patient cells, which implicates the importance of ATM in the control of rRNA synthesis (Stults et al., 2009). It is likely that cells that fail to activate DDR kinases and shut down RNPI could result in genome instability.

1.6.4 How are R-loops linked to RNPI

In response to stress, R-loops have been implicated in the control of RNPI. For example, as mentioned in section **1.5.3**, R-loops have been shown to form on the rDNA in response to hypoosmotic stress to block RNPI in an ATM/ATR dependent manner (Velichko et al., 2019). Additionally, the sequence of the rDNA repeat has a high GC content which confers a high propensity to form R-loops. There are many factors that regulate R-loops that also act at the rDNA chromatin. For example, R-loops have been shown to form on the rDNA due to a loss

of Top1 (El Hage et al., 2010). Additionally, Shen *et al*., demonstrated that RNase H1 and Top1 localise to the nucleolus to supress RNPI related R-loops (Shen et al., 2017). These studies highlight the importance of nucleolar enzymatic factors such helicases and topoisomerases in preserving the integrity of the highly transcribed rDNA region of the genome.

The yeast homologue of SETX, a RNA/DNA helicase, Sen1p, is required for efficient termination of RNPI (Kawauchi et al., 2008). The combined action of the XRN2 yeast homologue, Rnt1p, and Sen1p uses a mechanism similar to that of RNPII transcriptional termination to degrade the RNPI nascent transcript which promotes termination in the downstream rDNA spacer sequence. The fact that Sen1p acts at the rDNA chromatin would strongly suggest that its activity involves the resolution of R-loops, although this was not discussed in their study (Kawauchi et al., 2008).

Supportive of the role of Sen1p for efficient transcriptional termination of RNPI in yeast, a direct role for RNPII and SETX in the nucleolus has recently been described to drive ribosome biogenesis through the formation of R-loops on the rDNA IGS region in humans (Abraham et al., 2020). Although RNPII has been shown to be enriched at the IGS rDNA in yeast, the existence of RNPII in humans in nucleoli and its role in ribosome biogenesis is unclear (Kobayashi and Ganley, 2005). Abraham et al., demonstrated that phosphorylated serine 2 and 5 of the CTD of RNPII occupies the nucleoli, specifically the IGS, to induce antisense intergenic non-coding RNAs (asincRNAs) which reanneal to the template rDNA to form R-loops on the IGS (**Figure 1.6.4.1A**) (Abraham et al., 2020). When RNPII-dependent R-loops form on the IGS, RNPI loading onto the IGS is blocked, resulting in increased RNPI at the 47S coding region of the rDNA to synthesise the 47S. This study highlighted a role for SETX in the formation of R-loops on the IGS, where it is postulated to form a complex with RNPII near the start and end of the IGS which induces R-loop formation, the accumulation of which

provides a barrier or shield to prevent RNPI loading on these regions. Pharmacological inhibition of RNPII resulted in decreased nucleolar R-loop levels and an increase in sense intergenic non-coding RNA (sincRNA) which are transcribed by RNPI and are necessary to disrupt rRNA synthesis and processing (**Figure 1.6.4.1B**). In the same study, these sincRNA were found to be highly expressed in primary cancer cell lines from Ewing sarcoma patients and important for nucleolar disruption, which suggests that sincRNA and nucleolar disruption may be used as a biomarker for certain cancers which may exhibit greater sensitivity to treatment with RNPII inhibitors. Although the authors briefly discuss that sincRNA are likely to be induced in response to stress such as heat shock, they did not implicate this mechanism in response other physiologically relevant stresses like hypoxia.

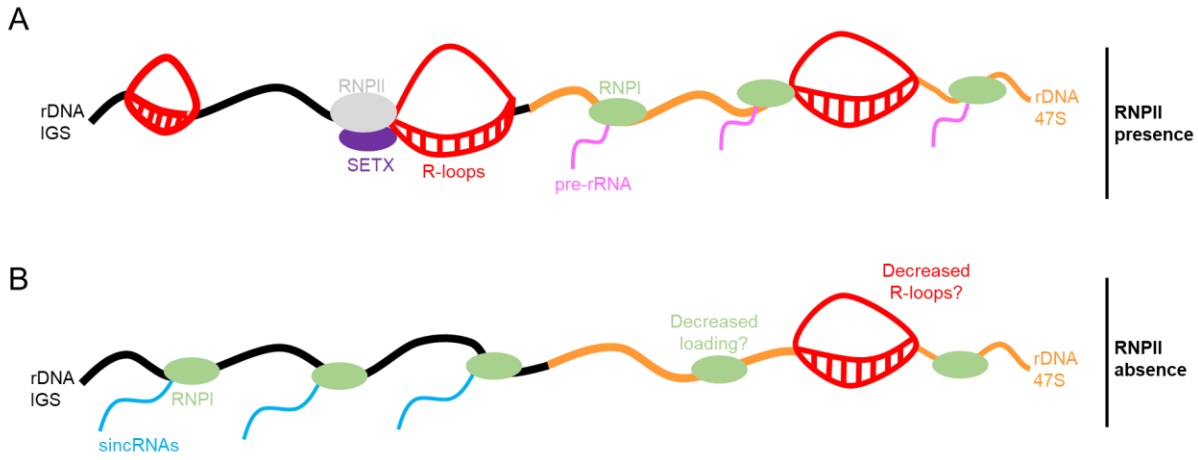


Figure 1.6.4. 1. RNPII drives ribosome biogenesis through R-loop formation.
Active RNPII localised to IGS regions with SETX promotes the formation of shielding R-loops on the IGS to prevent RNPI loading to these regions, which allows RNPI to mainly occupy the 47S coding rDNA to synthesise the 47S (A). Upon RNPII inhibition, RNPI occupies the IGS to induce sincRNA which abrogate the production of pre-rRNA and rRNA processing, presumably by decreased loading of RNPI on the 47S coding region of the rDNA (B).

1.7 RNPI in hypoxia

A report demonstrated that RNPI is repressed in response to long periods (>22 hours) of mild hypoxia (1% O_2) (Mekhail et al., 2006). This mechanism has been shown to be due to the acidic conditions that accompany hypoxic conditions in an unbuffered system. The acidic conditions

associated with chronic hypoxia disrupt the UBF interaction with the rDNA resulting in impaired RNPI initiation. To our knowledge, RNPI transcription has not been studied in more acute periods of hypoxia. A more recent study that measured the *de novo* transcription of mRNA as well as rRNA demonstrated that total cellular rRNA was modestly reduced (30% decrease) after long period (16 hours) of hypoxia (1% O_2). This decrease in cellular rRNA in hypoxia was not due to reduced rDNA transcription, which did not differ significantly but was attributed to increased degradation of rRNA (Tiana et al., 2020).

The current literature suggests that both ATM and ATR are required for RNPI shutdown in response to DNA damage. Given that the major DDR kinases ATM and ATR are active in hypoxia, it is plausible that these kinases also impact RNPI activity despite the lack of associated DNA damage. Similarly, the UPR is upregulated in hypoxia and the literature suggests that the PERK/EIF2α branch of the UPR represses rDNA transcription (DuRose et al., 2009; Koumenis et al., 2002). Therefore, given that the UPR is active in hypoxic conditions, rDNA transcription may be impaired through PERK activity.

Notably, the importance of R-loops in the regulation of RNPI transcription has been highlighted in recent studies, although this was not addressed in a physiologically relevant conditions such as hypoxia (Abraham et al., 2020; Velichko et al., 2019). Given the link between heterochromatin formation and R-loops in multiple studies, the upregulation of heterochromatin marks such as H3K9me3 in hypoxia may suggest that R-loops accumulate. Moreover, the interplay of R-loops in the control of RNPI in hypoxia will be addressed in our study.

1.8 Aims of this study

The current state of hypoxic biology has focused on understanding specific gene induction e.g. the HIF response in hypoxia. Much less is understood about gene-repression in hypoxia and

there is relatively less known about the mechanisms that regulate transcriptional repression. Therefore, the aim of this study was to characterise the global transcriptional response to hypoxia, with focus on the mechanisms of rDNA transcriptional repression. I aim to address whether the DDR or UPR plays a role in the transcriptional repression of rDNA in hypoxia. Of note, I will focus on the role of R-loops in response to hypoxia and characterise their functionality in the control of RNPI, with the goal of elucidating a novel mechanism of transcriptional regulation in hypoxia.

Chapter 2

Materials and Methods

2.1 Cell lines and Reagents

Cells were grown in Dulbecco's Modified Eagle's Medium (DMEM) (Sigma Aldrich) with 10% fetal bovine serum (FBS) (Sigma Aldrich), in a standard humidified incubator at 37°C and 5% CO_2. Cells were passaged with trypsin-ethylenediaminetetraacetic acid (EDTA) solution (Sigma Aldrich) at 80-90% confluency every few days. RKO (human colorectal cancer cells, American Type Culture Collection (ATCC)), HCT116 WT and p53 null (human colorectal cancer cells, a gift from Prof Bert Vogelstein), MRC5 (human lung fibroblast cells, a gift from Prof Geoff Higgins), A549 (lung carcinoma, ATCC), HCT116$^{ATR/-flox}$ (Bencokova et al., 2009) and HCT116 HIF1$\alpha^{-/-}$ (human colorectal cancer cells, (Dang et al., 2006)). GFP-RNase H1 was a gift from Dr Natalia Gromak (The University of Oxford).

2.2 Freezing and thawing cells

Cell monolayers were washed with 1X phosphate buffer solution (PBS), trypsinised and resuspended in 1 ml of freezing medium (10% DMSO, 90% FBS). Cells were frozen at -80°C for 24 hours before long term storage in liquid nitrogen. Cells were thawed from liquid nitrogen by incubating in a water bath at 37°C for 5-10 minutes. The thawed cell suspension was transferred to a 15 ml falcon tube and made up to 10 ml with DMEM + 10% FBS. Cells were centrifuged at 5000 X g for 5 minutes. The supernatant was aspirated and cells were resuspended in DMEM + 10% FBS. Cells were left to regain exponential growth for at least 3 days before use.

2.3 Mycoplasma test

Cells were checked regularly for *Mycoplasma* using the HEK-Blue™ Detection kit (Invivogen). Briefly, the HEK-Blue™ detection reagent was resuspended and HEK-Blue™

SEAP-cells were added as a positive control. Other cell lines were scraped in antibiotic-free media and boiled at 100°C for 10 minutes. These were transferred to a multi-well plate and incubated with the HEK-Blue^{TM} reagent for 24 hours at 37°C. A purple/blue colour change indicated *Mycoplasma* positivity.

2.4 Hypoxia

Hypoxia treatments were carried out in a Bactronez-2 or Bactron II anaerobic chamber (Shell labs) for experiments at <0.1% O_2 or a Don Whitley Scientific H35 anaerobic chamber for experiments at 2% O_2. For experiments at <0.1% O_2 cells were plated on glass dishes. Cells were harvested inside the chamber with equilibrated solutions. The oxygen tension in the chambers was periodically tested either by using the OxyLite probe (Oxford Optronix) or using the anaerobic paper indicator (BR0055B, OXOID).

2.5 Short interfering RNA (siRNA) transfection

Cells were transfected using Dharmafect-1 Transfection Reagent (Horizon Discovery) as recommended in the manufacturer's protocol. Briefly, the siRNA was incubated in FBS- and antibiotic-free DMEM separately from the Dharmafect-1 Transfection reagent in FBS- and antibiotic-free DMEM for 5 minutes at RT. The siRNA mixture was then mixed with the transfection reagent mixture and incubated at RT for 20 minutes at RT. The siRNA transfection mixture was then diluted in antibiotic-free DMEM to a final concentration of 50 nM and added to the plates containing cells. Cells were incubated for 18 hours in a standard humidified incubator at 37°C and the media was replaced with fresh antibiotic-free media. The cells were left for 24 hours at 37°C. siRNA sequences can be found in **Table 2.1**.

Table 2. 1. siRNA sequences

siRNA name	Sequence
sip53	GUAAUCUACUGGGACGGAA
siPERK	CCAAUGGGAUAGUGACGAA, GGUAGGAUCUGAUGAAUUU, GCAAUUAGCCUUAAGUUGU, AAAUUUGGCUGAAAGAUGA
siSETX	CCAAUUGCUCCUUUCAGGUGUUUGA

2.6 Bacterial transformation

DH5α competent cells were taken from -80°C and gently mixed with approximately 100 ng of plasmid DNA in a microcentrifuge tube on ice for 10-20 minutes. The mixture was heat shocked at 42°C in a water bath for 45 seconds. The tube was then placed on ice for 2 minutes. 300 µl of pre-warmed SOC medium (Sigma Aldrich) was added to the mixture for 30 minutes at 37°C. 50 µl of the mixture was plated onto agar plates and the plates were incubated upside down overnight at 37°C. The following day, a single colony was taken into a 50 ml falcon containing 3 ml of Luria broth (LB) supplemented with antibiotic and incubated for 10 hours at 37°C with gentle rotation in a standard bacterial incubator to make a starter culture. The starter culture was propagated into 250 ml LB supplemented with antibiotic in Erlenmeyer flasks and incubated overnight at 37°C. The bacterial cultures were centrifuged at 6000 X g. The pellets were stored long term at -80°C or purified the same day.

2.7 Plasmid purification

The plasmids were purified using a MaxiPrep Plasmid Purification kit (Qiagen). Briefly, the pellets were lysed in buffer P1, followed by addition of buffer P2 and mixed by inverting vigorously 4-6 times and incubation for 5 minutes at RT. Chilled buffer P3 was added and

inverted 4-6 times followed by incubation for 5 minutes on ice. Tubes were centrifuged at 15,000 X g for 10 minutes at RT. The mixture was added to a buffer QBT-equilibrated QIAGEN-tip 20 and was left to enter the resin by gravity flow. The QIAGEN-tip was washed with buffer QC and eluted with buffer QF. The DNA was precipitated by the addition of isopropanol and centrifuged at 15,000 X g for 30 minutes. The pellet was washed with 70% ethanol and centrifuged at 15,000 X g for 10 minutes. The pellet was left to air-dry at room temperature (RT) and resuspended in diethyl pyrocarbonate (DEPC)-H_2O.

2.8 DNA Plasmid transfection

Cells were plated at 40-50% confluency and left overnight to adhere. For a 6 cm^2 dish, 200 µl jetPRIME® Buffer and 2 µg of DNA were added to an Eppendorf and vortexed thoroughly for 3 seconds. 5 µl jetPRIME® reagent was added to the DNA/buffer mixture and vortexed for 10 seconds. The transfection mixture was left for 10 minutes at RT. Cells were transfected by the addition of the transfection mixture in a drop-wise manner directly into the media. Plates were gently rocked back and forth. 18-20 hours post-transfection, the media was replaced with fresh media.

2.9 5'ethynyl uridine (EU) staining

5'ethynyl uridine (EU) (0.5 mM) (Jena Bioscience) was added to cells grown on glass 18 x 18 mm coverslips for 1 hour before fixing with 4% PFA for 10 minutes at RT. Cover slips were permeabilised with 0.5% Triton-PBS and blocked in 2% BSA-PBS for 20 minutes at RT. The cover slips were incubated at RT with a copper catalysed conjugation reaction to a fluorescent azide for 30 minutes using the Click-iT Alexa Fluor 647 labelling kit (Thermofisher). Coverslips were washed with 1X PBS and mounted on glass slides (VWR) using ProLong™ Gold Anti-fade DAPI mounting medium (Thermofisher). Nuclear EU signal was quantified using a DAPI-gated macro. Cells were visualised on a LSM710 or a LSM780 confocal microscope (Carl Zeiss Microscopy Ltd).

2.10 RNA preparation

Cells were scraped and collected in TRIzol™ (Invitrogen/Life Technologies) reagent. 250 µl of chloroform was added and vortexed to an emulsion for 10 seconds. Samples were centrifuged at 16,000 X g for 10 minutes at 4°C. The top aqueous layer containing the RNA was carefully transferred to another Eppendorf. Equal amounts of isopropanol (Fisher) was added and 1 µl of glycogen (Roche) was added. Samples were centrifuged at 16,000 X g for 10 minutes at 4°C. The pellet was washed with 70% ethanol. Samples were centrifuged at 16,000 X g for 10 minutes at 4°C. The pellet was left to dry at RT and resuspended in DEPC-H_2O. RNA purity and concentration was determined using a Nanodrop meter by measuring the absorbance at 260 nm. An A260 nm/A280 nm ratio of 1.9-2.1 indicated that RNA was pure.

2.11 Complementary DNA (cDNA) synthesis

RNA was DNase 1 treated prior to cDNA synthesis at 37°C for 1 hour using 2 units of DNase 1 (New England Biolabs) per 10 µg RNA. The enzyme was then deactivated by adding 1 µl of 0.5 M ethylenediaminetetraacetic acid (EDTA) at 75°C for 5 minutes. The Verso Mastermix was prepared according to the manufacturer's protocol using the Verso cDNA synthesis kit (Thermo Scientific) and was added to 1 µg of RNA. The following conditions were used for reverse transcription (RT) into cDNA - 42°C for 60 minutes, 95°C for 2 minutes, 4°C constant.

2.12 Quantitative PCR (qPCR)

The cDNA was diluted in DEPC-H_2O to 1:50 before it was used for qPCR experiments. Quantitative real time PCR (qPCR) was performed using the following reaction mix in a total volume of 20 µl plus 5 µl of diluted cDNA.

Reaction Mix SYBR® Green PCR Master Mix (Applied Biosystems) 12.5 µl per reaction
Primer Forward 2.5 µl per reaction (100 nM final concentration)
Primer Reverse 2.5 µl per reaction (100 nM final concentration)
DEPC-treated H_2O 2.5 µl per reaction

qPCR was performed using SYBR Green PCR Master Mix kit (Applied Biosystems) in a Step One^{TM} Real-Time PCR thermocycler with v2.0.5 software (Applied Biosystems). RNA fold change was calculated using a $2^{-\Delta\Delta Ct}$ method in relation to the *18S* reference gene. All primer sequences are available in **Table 2.2**. PCR conditions used were as follows: 20 seconds at 50°C, 15 minutes at 95°C then 40 cycles of 15 seconds at 95°C, 30 seconds at 60°C, 30 seconds at 72°C, and finally a melt curve stage of 15 seconds at 95°C, 1 minutes at 60°C, 30 seconds at 95°C and 15 seconds at 60°C.

Table 2. 2. Primer sequences

Primer	Sequence
18S rRNA Forward	TAGAGGGACAAGTGGCGTTC
18S rRNA Reverse	CGGACATCTAAGGGCATCAC
Primer set 1 Forward	ACCTGTCGTCGGAGAGGTTG
Primer set 1 Reverse	GTCACCGTGAGGCCAGAG
Primer set 2 Forward	AACGGTGGTGTGTCGTT
Primer set 2 Reverse	TCTCACTCAAACCGCCT
Primer set 3 Forward	CCGCGCTCTACCTTACCTACCT
Primer set 3 Reverse	GCATGGCTTAATCTTTGAGACAAG
PNRC1F	TATGCTGGGGCAAAGTTTA
PNRC1R	AAGTGTACTGCCATCAGCTC
CHOP Forward	GGAGCATCAGTCCCCCACTT
CHOP Reverse	TGTGGGATTGAGGGTCACA
SETX Forward	CTTCATCCTCGGACATTTGAG
SETX Reverse	TTAATAATGGCACCACGCTTC
RNase H1 Forward	CCTGTACTTACTGGTGTGGA
RNase H1 Reverse	CCGTGTGAAAGACGCATCTG
RNase H2B Forward	GCATCTTGTTGCTGAAACTTC
RNase H2B Reverse	TCCTTGTCAGTGGAAGCTTG
PIF1 Forward	CGAGCCTAGCACAGAAGCC
PIF1 Reverse	CCCAGGATTCGCTTTAGCAG
AQR Forward	GGCGGCATTAGCTGAAACTG
AQR Reverse	CAGCTGTAAGCCCATCCACA
DHX9 Forward	GCCAATTTCTGGCCAAAGCA
DHX9 Reverse	CGAGGCTCAATGGGGAGTTT
RTEL1 Forward	GGACTTGGTCAAGAGCGGAA
RTEL1 Reverse	AGTCAGGTCAAAGGATGCCG

2.13 PAPAS detection using PCR

Synthesis of cDNA was performed with Verso (Thermo Scientific). 1 µg of cellular RNA (TRIzol^{TM} prepared) was used as a template in a 20 µl reaction. For priming of reverse transcription I used 5 pmol of antisense rDNA-sequence coupled to T7-promoter (summarised in **Figure 2.1**). All primer sequences can be found in **Table 2.2**. RT conditions are: 23°C 10 minutes, 50°C 20 minutes, 60°C 10 minutes, 80°C 10 minutes. 2nd strand synthesis and detection by PCR. For subsequent PCR I diluted the reaction 1:5 and use 2-3 µl as template for a 10-15 µl reaction volume using the T7-promoter primers in **Table 2.3**. Conventional end-point PCR is done as a touchdown reaction starting from 65°C to 56°C annealing temperature with a reduction of 1°C after every cycle. At 56°C additional 20 to 25 cycles are performed. Each PCR step (denaturation at 95°C, annealing at 65-56°C and elongation at 72°C) lasts 30 seconds. qPCR was done with constant annealing temperature of 56°C. RNA fold change was calculated using a $2^{-\Delta\Delta Ct}$ method in relation to the *18S* reference gene.

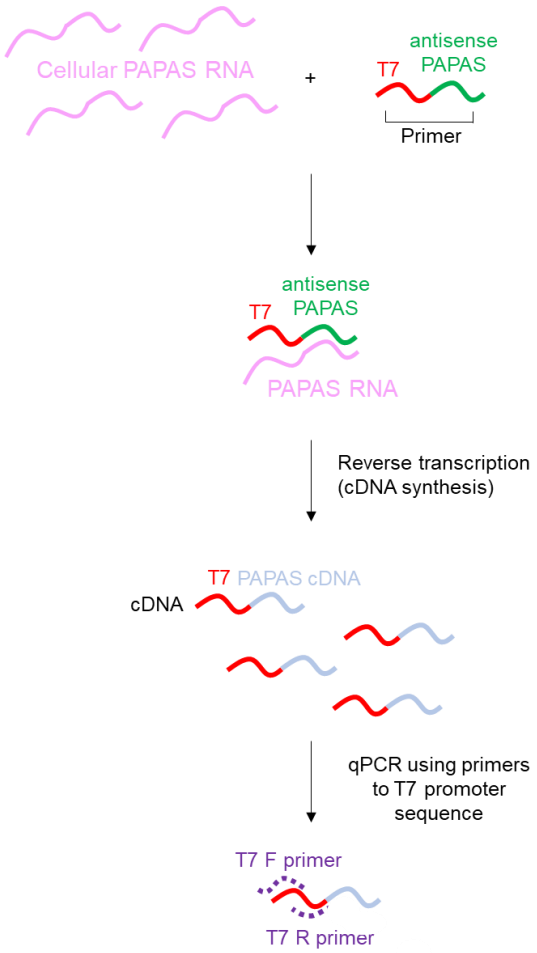


Figure 2.1. Schematic of PAPAS detection experimental procedure.
A primer consisting of T7-promoter sequence (red) coupled with antisense PAPAS encoding DNA sequence (green) was used to prime cellular PAPAS RNA (pink) in HCT116 cells via reverse transcription to produce T7 primed cDNA. The relative levels of T7-primed PAPAS cDNA was detected via qPCR using T7 primers (purple).

Table 2. 3. PAPAS detection primer sequences

Primer	Sequence
T7-promF	TAATACGACTCACTATAGGGAGG
T7-promR	GACGACAGGTCGCCAGAGGA
T7prom-rDNA	TAATACGACTCACTATAGGGAGGGTATATCTTTCGCTCCGAG

2.14 Protein lysate preparation

Cells were washed and scraped with 1X PBS. The sample was collected in an Eppendorf and centrifuged at 5000 X g for 3 minutes. Cells were lysed in UTB (9 M urea, 75 mM Tris-HCl

pH 7.5, 0.15 M β-mercaptoethanol) and briefly sonicated for 10 seconds on, 10 seconds on ice, 10 seconds on using a Diagenode Biorupter. Samples were centrifuged at 16,000 X g for 10 minutes at 4°C to remove insoluble debris. Protein concentration was analysed using a Nanodrop meter and mixed with protein sample buffer (3.3% SDS, 6 M urea, 17 mM Tris-HCl pH 7.5, 0.07 M β-mercaptoethanol, 0.01% bromophenol blue (BPB)) to normalise the protein concentrations between samples. Samples were boiled at 100°C for 5 minutes before loading.

2.15 Western blotting

Protein ladder (Precision plus protein standards, BioRad) (3 µl) was used for the analysis of the molecular weight of the bands. 50 µg of protein was electrophoresed in Mini-Protean TGX 4-20% Tris-HCl gels (BioRad) at 120 V for 1 hour and 15 minutes in Tris-glycine running buffer (25 mM Tris base, 192 mM glycine, 0.1% (w/v) SDS). Gels were transferred to 0.2 µm nitrocellulose membranes Trans-Blot® Turbo Transfer Pack (BioRad) using Trans-Blot® Turbo™ - Transfer System (BioRad). Membranes were blocked in 1:1 ratio of Intercept blocking buffer Tris-Buffered Saline (TBS): TBS (50 mM Tris-HCl, pH 7.6, 150 mM NaCl) for 1 hour at RT and probed with primary antibody diluted in blocking buffer overnight at 4°C on a belly dancer. Membranes were washed for 5 minutes three times the following day in 1X TBS 0.1%-Tween-20 and probed with secondary fluorescent antibodies for 1 hour at RT (LI-COR Biosciences). Antibodies used are listed in **Table 2.4**. Membranes were washed for 5 minutes and another two times with 1X TBS 0.1%-Tween-20 and one 5 minute wash in 1X TBS. Odyssey IR imaging technology (LI-COR Biosciences) was used for imaging.

Table 2.4. Primary antibodies

Name	Cat. number	Host	Company	Applications	Dilutions
53BP1	NB100-904	Rabbit	Novus Biologicals	IF, WB	1:500 (IF), 1:1000 (WB)
Chk1	sc-8408	Mouse	Santa Cruz Biotechnology /	WB	1:1000

			Insight Biotechnology		
Chk1-S317	2344	Rabbit	Cell Signaling	WB	1:1000
C-MYC	5605	Rabbit	Cell Signaling	WB	1:1000
Dicer	3363	Rabbit	Cell Signaling	WB	1:1000
EIF2α	9722S	Rabbit	Cell Signaling	WB	1:1000
EIF2α-s51	3398S	Rabbit	Cell Signaling	WB	1:1000
Fibrillarin	ab4566	Mouse	Abcam	IF, WB	1:500 (IF), 1:1000 (WB)
GRP78	610978	Mouse	BD Biosciences	WB	1:1000
H2AX	07-627	Rabbit	Millipore	WB	1:1000
H3	3638S	Mouse	Cell Signaling	WB	1:1000
H3	ab1791	Rabbit	Abcam	ChIP	1:1000
H3K36me2	2901	Rabbit	Cell Signalling / New England Biolabs	WB	1:1000
H3K4me2	9725	Rabbit	Cell Signalling / New England Biolabs	WB	1:1000
H3K9Ac	9649	Rabbit	Cell Signalling / New England Biolabs	WB	1:1000
H3K9me2	9753	Rabbit	Cell Signalling / New England Biolabs	WB	1:1000
H3K9me2	ab8898	Rabbit	Abcam	ChIP	1:1000
H3K9Me3	9847	Rabbit	Millipore	WB	1:1000
H3-S10	9701	Rabbit	Cell Signalling / New England Biolabs	WB	1:1000
HIF1α	610958	Mouse	Becton Dickinson Biosciences	WB	1:500 (IF)
KAP1	A300-274A	Rabbit	Bethyl/Universal Biologicals Cambridge	WB	1:1000
Nucleolin	ab13541	Mouse	Abcam	IF, WB	1:500 (IF), 1:1000 (WB)
p53	9282	Mouse	Cell Signaling	WB	1:1000
p53-S15	9284	Rabbit	Cell Signaling	WB	1:1000
PERK	3192S	Rabbit	Cell Signaling	WB	1:1000

phospho-KAP1 (Ser824)	4127S	Rabbit	Cell Signalling / New England Biolabs	WB	1:1000
Puromycin	EQ0001	Mouse	Kerafast	WB	1:1000
RNA polymerase II CTD repeat YSPTSPS (phospho S2)	ab5095	Rabbit	Abcam	WB	1:1000
RNA polymerase II CTD repeat YSPTSPS (phospho S5)	ab5131	Rabbit	Abcam	WB	1:1000
RNase H1	sc-365267	Mouse	Santa Cruz	WB	1:200
RPA	2208	Rat	Cell Signalling / New England Biolabs	IF, WB	1:500 (IF), 1:1000 (WB)
RPA-S4/8	Ab87277	Rabbit	Abcam	WB	1:1000
S9.6	ENH001	Mouse	Kerafast	IF	1:1000
ssDNA	MAB3868	Mouse	Milliprore	Slot blot	1 in 5000
TCOF1	HPA038237	Rabbit	Atlas Antibodies	IF, WB	1:500 (IF), 1:1000 (WB)
TopBP1	A300-111A	Mouse	Bethyl/Universal Biologicals Cambridge	IF, WB	1:500 (IF), 1:1000 (WB)
XRN2	11267-1-AP	Rabbit	proteinTech	WB	1:1000
β-actin	sc-69879	Mouse	Santa Cruz Biotechnology / Insight Biotechnology	WB	1:10,000
β-tubulin	ab15568	Rabbit	Abcam	WB	1:1000
γH2AX	05-636	Mouse	Millipore	IF, WB	1:500 (IF), 1:1000 (WB)

Table 2.5. Secondary antibodies

Product Name	Cat. number	Company	Applications	Dilutions

IRDye® 800CW Goat anti-Rabbit IgG	926-32211	LI-COR	WB	1:10,000
IRDye® 800CW Goat anti-Mouse IgG	926-32210	LI-COR	WB	1:10,000
IRDye® 680RD Goat anti-Mouse IgG	926-68070	LI-COR	WB	1:10,000
IRDye® 680RD Goat anti-Rabbit IgG	926-68071	LI-COR	WB	1:10,000
Alexa Fluor 488 F(ab')2 Fragment of Goat Anti-Rabbit	A11070	Life technologies	IF	1:500
Alexa Fluor 647 F(ab')2 Fragment of Goat Anti-Rabbit	A21246	Life technologies	IF	1:500
Alexa Fluor 488 Goat Anti-Mouse IgG (H L)	A11029	Life technologies	IF	1:500
Alexa Fluor 594 Goat Anti-Rabbit IgG (H L)	A11037	Life technologies	IF	1:500

2.16 Puromycin incorporation assay

500,000 cells were plated the day before starting the experiment. Cells were supplemented with 1 µg/ml puromycin for 30 minutes prior to harvesting in UTB buffer. The protein samples were prepared as in **2.14**. The samples were subjected to western blotting as in **2.15** using an anti-puromycin primary antibody (Kerafast) overnight at 4°C (**Table 2.4**).

2.17 Immunofluorescence (IF)

Cells grown on glass 18 x 18 mm coverslips were fixed with methanol or 4% paraformalydehyde (PFA). For PFA, cells were permeabilised with 0.1% Triton X-100. Fixed cells were blocked in 2% bovine serum albumin (BSA) PBS for 1 hour at RT. Primary antibody was made up with 2% BSA PBS and was then incubated overnight at 4°C. The primary antibodies used are listed in **Table 2.4**. Coverslips were washed 3 times in PBS-Tween-20 for a total of 15 minutes. Alexa Fluor secondary antibody (Thermo fisher) dilutions were incubated for 1 hour at RT. Coverslips were then washed 3 times in PBS-Tween-20 for a total of 15 minutes. Coverslips were mounted on glass slides with ProLong™ Gold Anti-fade 4′,6-

diamidino-2-phenylindole (DAPI) mounting medium (Thermofisher) and sealed along the outsides with clear nail-polish (Rimmel London).

2.18 Nucleotide (NTP) measurement

EmbryoMax® Nucleosides were added for 30 minutes prior to experiment (cytidine, 0.0073 mg/ml; guanosine 0.0085 mg/ml; uridine, 0.0073 mg/ml; adenosine, 0.008 mg/ml; thymidine, 0.0024 mg/ml). Cells were lysed with 0.5 ml ice cold 70% methanol and stored at -80°C before analysis. Upon analysis samples were mixed and the centrifuged at 5000 X g. Supernatant was dried down in a medium heated centrifugal evaporator (40°C). Samples were reconstituted with 100 µl 25% methanol/water and spun to remove any resulting precipitate (10 min, 4°C, 13000 X g). High performance liquid chromatography (HPLC) was carried out on a Waters e2695 separations module with a Waters 2996 photodiode array detector to detect the eluted compound. Samples were eluted on a ACE 3 µm, 125 x 3.0 mm column (Hichrom) maintained at 40°C. Samples were eluted in A: 10 mM potassium dihydrogen orthophosphate, 10 mM tertbutylammonium hydroxide, 10% methanol, B: 50 mM potassium dihydrogen orthophosphate, 6 mM tertbutylammonium hydroxide, 30% methanol, with a flow rate of 0.4 ml/min and a linear gradient of 25-75% B in 21 minute and a 26 minute run time, peaks were measured at 258 nm and compared to authentic standards.

2.19 R-loop detection by S9.6 immunofluorescence

Cells plated on 18 x 18 mm coverslips were fixed in 100% methanol at 4°C for 10 mins as previously described (Cristini et al., 2018). Coverslips were washed three times in PBS. Coverslips were dipped briefly in diethyl pyrocarbonate (DEPC)-H_2O. RNase H treatment was performed according to the manufacturers protocol (New England Biolabs) for 36 hours. The cells were then washed in PBS, blocked in 2% BSA overnight. Coverslips were dipped briefly in DEPC-H_2O. Primary antibodies (S9.6 (Kerafast) and nucleolin (Abcam)) were added and incubated at 4°C overnight. Primary antibodies used are listed in **Table 2.4** The coverslips were

washed three times in PBS for 15 minutes total and incubated with Alexa Fluor secondary antibody (Thermofisher) for 1 hour at RT. Coverslips were washed three times with PBS for 15 minutes total. Coverslips were mounted with ProLong^{TM} Gold Anti-fade DAPI mounting medium (Thermofisher) and visualized on a Zeiss 780 confocal microscope.

2.20 RNA gel electrophoresis

An equal number of cells were plated the day before the experiment. Cells were harvested in TRIzol and RNA was isolated using isopropanol precipitation as in section **2.10**. All solutions were made with DEPC-H_2O. An equal volume of sample (approximately 1 µg of total RNA) was resolved at 90 V for 20 minutes on a 1% TAE (40 mM Tris-HCl, 20 mM acetate,1 mM EDTA) agarose gel stained with SYBR^{TM} Safe DNA stain (Thermofisher). RNA was visualised using an ultraviolet (UV) transilluminator.

2.21 Poly-nucleotide Kinase (PNK) radio-end labelling probe preparation

6.5 µl of DEPC-H_2O, 1 µl of 10 µM DNA probe, 1 µl of 10X PNK buffer (NEB), 1 µl of y-^{32}P-dATP (6000 µCi/mmol) (Perkin Elmer) and 1 µl PNK (New England Biolabs) were added in that order to an Eppendorf and incubated at 37°C for 1 hour. G-25 Sephadex columns (GE Lifesciences) were prepared by vortexing so that the resin was suspended. The columns were centrifuged at 4000 X g for 2 minutes. The reaction was diluted with 40 µl H_2O. The reaction was purified by addition to the column and centrifuged at 4000 X g for 4 minutes.

2.22 Northern blotting

2-3 µg of total RNA was glyoxal treated by addition of 6.5 µl glyoxal, 0.6 µl 1 M Na_2PO_4 pH 7 and 16 µl DMSO followed by incubated at 50°C for 1 hour. The samples were left to cool on ice and diluted with 2X RNA loading buffer (50% formamide, 0.025% BPB, 0.025% xylene cyanol, 5 mM EDTA, 20% glycerol). The samples were resolved at 70 V for 4 hours on a 1% Na_2PO_4 pH 7 agarose gel in an Owl EasyCast B2 electrophoresis gel tank (Thermo Scientific).

Agarose gels were transferred onto positively charged nylon membranes (GE Lifesciences) by capillarity overnight in 20X saline sodium citrate (SCC). Membranes were UV crosslinked (0.12 J/m^2) and stained with methylene blue (MB) (0.04% MB in 0.5 M sodium acetate). Membranes were prehybridised in Church Buffer (0.36 M Na_2HPO_4, 0.14 M NaH_2PO_4, 1 mM EDTA, 7% SDS) at 65°C for 1 hour with agitation. The ^{32}P-labelled oligonucleotide probe was incubated with the membrane overnight in a heated oven with agitation at 65°C. Probe sequences are available in **Table 2.6**. The membranes were washed with northern wash buffer (2x SSC, 0.5% SDS) for 20 minutes total and exposed on an x-ray film (GE Healthcare) in a cassette and developed. X-ray films were left at -80°C for a few days before developing to improve signal.

Table 2. 6. Northern blot probes

Probe name	Sequence
Northern N1	CGGAGGCCCAACCTCTCCGACGACAGGTCGCCAGAGGACAGCGTGTCAGC
Northern N2	CGGTACCCCCAAGGCACGCCTCTCAGATCGCTAGAGAAGGCTTTTCTC
Northern N3	CTCTCTTTCCCTCTCCGTCTTCCGGCGGCGGCGCCGCCCTCCCCGTCT
Northern N4	AGCGCGGACACCACCCCACAGGCGCCCGGGGGTTCC

2.23 DNA purification using columns

Samples were purified using a Qiagen DNA Purification Kit (Qiagen). Briefly, 2 X sample volume of buffer PB was added to sample. The mixture was added to purification columns. Columns were centrifuged at 13,000 X g for 1 minute at RT and the effluent was discarded. The columns were washed with wash buffer PE and centrifuged at 13,000 X g for 1 minute at RT. The DNA bound to the column was eluted with 100 µl buffer EB and centrifuged at 13,000 X g for 1 minute at RT. DNA was stored at 4°C or -20°C for long term storage.

2.24 DNA/RNA immunoprecipitation (DRIP)

DRIPs were carried out as described in (Cristini et al., 2018; Cristini et al., 2019). Isolated cell nuclei were lysed in nuclear lysis buffer (50 mM Tris-HCl pH 8.0, 5 mM EDTA, 1% SDS) and digested for 3 hours at 55°C with 3 µl 10 mg/ml proteinase K (Sigma Aldrich Aldrich). Genomic DNA was precipitated and resuspended in IP dilution buffer (16.7 mM Tris-HCl pH 8.0, 1.2 mM EDTA, 167 mM NaCl, 0.01% SDS, 1.1% Triton X-100). DNA was sonicated on high power (Diagenode Bioruptor) and precleared with salmon sperm DNA blocked protein A agarose beads. RNase H treatment was used as described by the manufacturer (M0297; New England Biolabs) for 2.5 hours at 37°C. Equal concentrations of genomic DNA were incubated with S9.6 antibody (Kerafast) or no antibody control overnight at 4°C on a rotating wheel. Salmon sperm DNA blocked protein A agarose beads were used to pull down the immunoprecipitated complexes for 1 hour at 4°C. The beads were washed for 5 minutes each at 4°C on a rotating wheel in wash buffer A (20 mM Tris-HCl pH 8.0, 2 mM EDTA, 150 mM NaCl, 0.1 % SDS, 1% Triton X-100), wash buffer B (20 mM Tris-HCl pH 8.0, 2 mM EDTA, 500 mM NaCl, 0.1% SDS, 1% Triton X-100), wash buffer C (10 mM Tris-HCl pH 8.0, 1 mM EDTA, 250 mM LiCl, 1% sodium deoxycholate (DOC), 1% IGEPAL®) and twice with wash buffer D (10 mM Tris-HCl pH 8.0, 1 mM EDTA). The DNA was then eluted with elution buffer (100 mM $NaHCO_3$, 1% SDS) at RT for 30 minutes on a rotating wheel and treated with 1.1 µl 10 mg/ml proteinase K (Thermofisher) in digestion buffer (0.4M Tris-HCl pH 6.5, 0.1M EDTA) for 2 hours at 45°C. DNA purification was carried out as in **2.22**. The amount of immunoprecipitated material at a particular gene region was calculated as the percentage of input after subtracting the background signal (no antibody control). The values were then normalised to the normoxic untreated condition of the promoter primer. Primer sequences are available in **Table 2.7**.

Table 2. 7. DRIP primer sequences

DRIP primer name	Sequence
D1 Forward	GGTATATCTTTCGCTCCGAGTC
D1 Reverse	ACAGGTCGCCAGAGGACAG
D2 Forward	TGGCGCTAAACCATTCGTAG
D2 Reverse	GTCGAGGGCTGACTTTCAATAG
D3 Forward	CGTTTGCAGACCGAAACAGT
D3 Reverse	ACAAAAAGCAGCAGCGGAAG

2.25 Slot blot assay for R-loop detection

The slot blot assay to determine R-loops was adapted from a previously described method (Schwab et al., 2015). Cells were harvested in lysis buffer (100 mM Tris-HCl pH 8.5, 5 mM EDTA, 0.2% SDS, and 100 mM NaCl containing 0.5 mg/ml proteinase K) and incubated in a 55 °C heated shaker overnight. Genomic DNA was extracted with isopropanol, washed in 70% ethanol, air-dried and re-suspended in TE buffer. Genomic DNA was treated with RNase A (Thermofisher), and using a slot blot apparatus (Bio-Rad), equal amounts of samples were blotted onto a positively charged nylon transfer membrane (GE Healthcare). Where indicated, samples were treated with RNase H1 (NEB) overnight prior to slot blotting. The ssDNA blot was denatured for 10 minutes at RT (0.4 M NaOH and 0.6 M NaCl) and neutralised for 10 minutes at RT (1.5 M NaCl and 0.5 M Tris pH 7.4). Blots were UV crosslinked (0.12 J/m^2), blocked then incubated in S9.6 (Kerafast) or ssDNA (Millipore) antibodies overnight at 4°C (listed in **Table 2.4**). Blots were probed with Alexa Fluor secondary antibody and developed using the Odyssey Infrared imaging system.

2.26 Chromatin immunoprecipitation (ChIP)

Cells were fixed with 1% formaldehyde and quenched with 125 mM glycine. Cells were lysed with SDS lysis buffer (0.5% SDS, 10 mM EDTA, 50 mM Tris-HCl pH 8.1). Samples were sonicated for 30 cycles of 15 seconds on, 15 seconds off at 4°C on a Bioruptor (Diagenode). Samples were centrifuged at 16,000 X g for 10 minutes and the supernatant was transferred to

a new tube. Chromatin was precleared for an hour at RT on a rotating wheel with protein A agarose beads (Millipore) and 100 µg of DNA was immunoprecipitated with 3 µg of antibody overnight at 4°C on a rotating wheel. The immune-antigen complexes were pulled down with agarose beads and washed with a series of buffers – low salt wash buffer (0.1% SDS, 1% Triton X-100, 2 mM EDTA, 20 mM Tris-HCl pH 8.1, 150 mM NaCl), high salt wash (0.1% SDS, 1% Triton X-100, 2 mM EDTA, 20 mM Tris-HCl pH 8.1, 500 mM NaCl), LiCl wash buffer (1% IGEPAL®, 10 mM Tris-HCl pH 8.1, 250 mM LiCl, 1 mM EDTA, 1% DOC), TE wash buffer (10 mM Tris-HCl pH 8.0, 1 mM EDTA). DNA was eluted from beads using elution buffer (0.1 M $NaHCO_3$, 1% SDS). DNA was eluted (100 mM $NaHCO_3$, 1% SDS) overnight at 65°C with agitation and treated with 4 µl of proteinase K (10 mg/ml) in digestion buffer (0.4 M Tris-HCl pH 6.5, 0.1 M EDTA) for 1 hour at 45°C with agitation. DNA purification was carried out as in **2.23** and qPCR was carried out using the primers in **Table 2.7**. The amount of immunoprecipitated material at a particular gene region was calculated as the percentage of input after subtracting the background signal (no antibody control).

2.27 Statistical analysis

The Student's t-test was used when comparing two means. One-way analysis of variance (ANOVA) was used to compare several means. Two-way ANOVA was used to determine statistical significance in a dataset that is affected by two factors. * = p = <0.05 ** = p = <0.01, *** = p = <0.001, **** = p = <0.0001. Errors bars represent mean ± standard error of the mean (SEM). Statistical analysis was carried out using GraphPad Prism 8 Software.

Chapter 3

The effect of hypoxia on the rDNA transcription response

3.1 Introduction

Hypoxia induces several biological responses including upregulation of HIF1, p53 signalling and induction of the DDR (Graeber et al., 1994; Olcina et al., 2013; Wang and Semenza, 1993). Although these mechanisms have been well characterised, transcriptional repression in hypoxia is not understood. There are several studies that have identified RNPII-related gene repression (Cavadas et al., 2016; Denko et al., 2003; Nakamura et al., 2008; Tiana et al., 2020). However, characterisation of the response of RNPI to hypoxia is lacking. The nascent product of RNPI transcription, the 47S, is initially cleaved at sites A' in the 5'ETS region and at 02 in the 3'ETS region before further cleavage and processing of the transcript occurs to generate the mature 18, 28 and 5.8S (**Figure 1.6.1.1**). A recent study showed that 47S levels are unaffected in mild hypoxia (1% O_2) (Tiana et al., 2020). It is unclear whether transcription of rRNA is affected in more severe hypoxia (<0.1% O_2) in which there is concomitant activation of the DDR (Olcina et al., 2013).

In this chapter, I will investigate the global transcriptional response in radiobiological hypoxia, focusing on the transcriptional response of the most abundant and highly transcribed RNA group, rRNA.

3.2 Hypoxia induces the DDR

The DDR has been shown to be active in hypoxic conditions in the absence of detectable DNA damage (Bencokova et al., 2009; Olcina et al., 2013). I demonstrate in HCT116 cells that there is an induction of KAP1-S824, p53-S15 and H2AX-S139 (known as γH2AX) indicating that ATM signalling is active within 1 hour of exposure to <0.1% O_2 (**Figure 3.2A**). I demonstrate that there is no detectable DSBs in <0.1% O_2 using the 53BP1 foci assay. As expected,

treatment with ionising radiation (IR) lead to a significant increase in 53BP1 foci (**Figure 3.2B**).

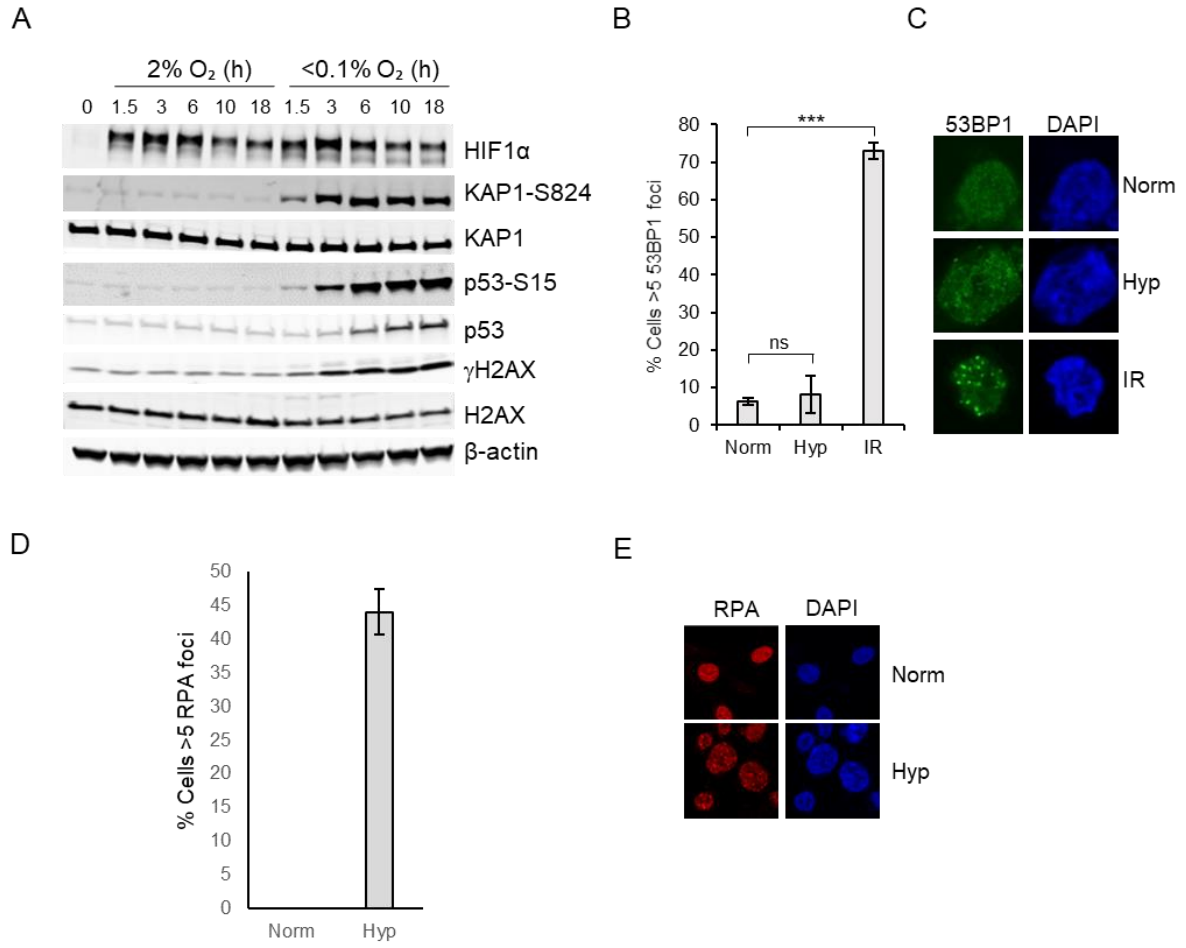


Figure 3.2. The DDR is activated in an oxygen dependent manner.
HCT116 cells in 21, 2 or <0.1% O_2 were subjected to western blot analysis for markers of DDR signalling (A). HCT116 cells with more than five 53BP1 foci were counted and expressed as a percentage of total cells. Norm, 21%; Hyp, <0.1% O_2 (6 hours); IR, ionising radiation (1 h post 5 Gray (Gy)) (B). Representative images of 53BP1 foci and nuclear DAPI staining from B (C). HCT116 cells with more than 5 RPA foci were counted and expressed as a percentage of total cells. n=2. Data provided by Shaliny Ramachandran (D). Representative images of RPA foci in <0.1% O_2 (6 hours) (E). One-way ANOVA was used to calculate statistical significance. Data are displayed ± standard error of the mean (SEM) *** = p = <0.001, ns = not significant.

In addition, hypoxic cells have been reported to exhibit replication stress (Olcina et al., 2013). To demonstrate this, we measured RPA foci in <0.1% O_2. The levels of RPA foci increased significantly in response to 6 hours of <0.1% O_2 (**Figure 3.2D, E**). Taken together these data

demonstrate that there is activation of DDR signalling in hypoxia in a background of replication stress, in the absence of detectable DSBs.

3.3 Hypoxia leads to global transcriptional repression in cancer cells

Hypoxia has been reported to lead to global repression of RNA synthesis after 24 hours at <0.1% O_2 (Johnson et al., 2008). I carried out an EU incorporation assay in HCT116 cells to measure global levels of nascent transcription. Cells in 21 and 2% O_2 incorporated similar levels of EU. However, after 6 hours at <0.1% O_2 there was a significant reduction of around 50% nuclear EU intensity (**Figure 3.3A, B**). As expected, 5,6-dichloro-1-beta-D-ribofuranosylbenzimidazole (DRB), a transcriptional inhibitor, lead to a significant decrease in EU incorporation. Importantly, EU incorporation appeared similar in all cells i.e. not restricted to a subset of the population suggesting that the repression of transcription is not cell cycle dependent. To verify that transcriptional repression was not restricted to this cancer cell line I carried out EU incorporation in a different cancer cell line. Again, I found that transcription was repressed in 6 hours of <0.1% O_2 in RKO cells (**Figure 3.3C**). Together these data demonstrate that the global transcriptional repression and therefore transcriptional stress occurs in an oxygen dependent manner in cancer cells.

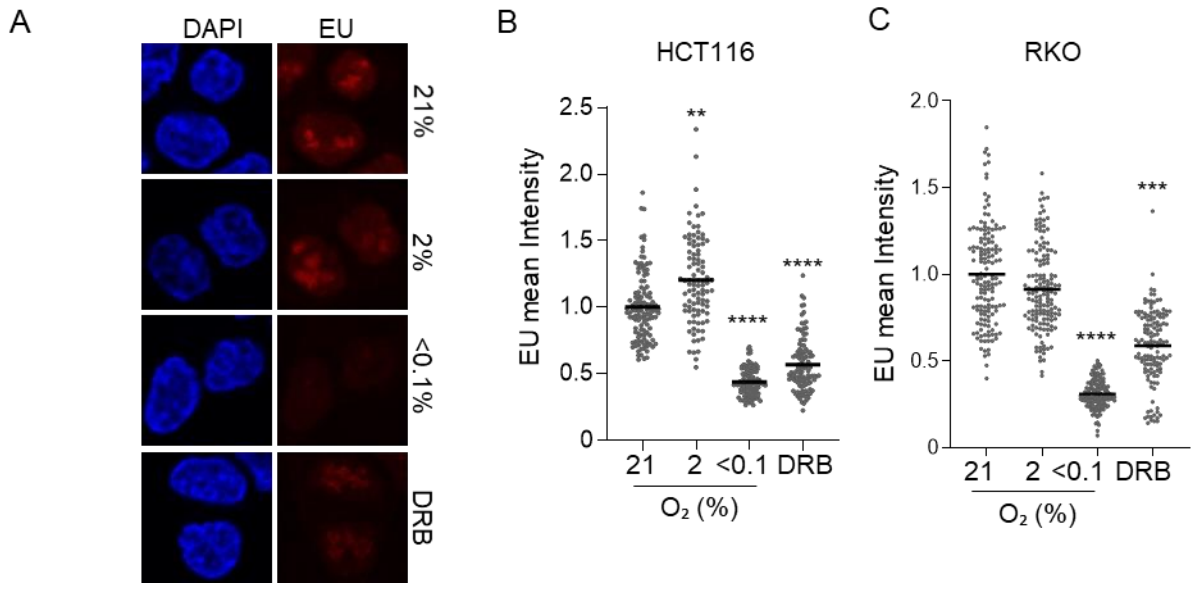


Figure 3.3. Transcription is repressed in an oxygen dependent manner in cancer cells. HCT116 cells in 6 hours of 21%, 2% or <0.1% O_2 were treated with EU (0.5 mM). DRB (100 µM, 6 hours) was used as a positive control for transcriptional repression (A). Nascent transcription in the nucleus was quantified in HCT116 cells (B). Nascent transcription in the nucleus was quantified in RKO cells (C). One-way ANOVA was used to calculate statistical significance. Data from three separate experiments (n=3) are displayed. ** = p = <0.01, *** = p = <0.001, **** = p = <0.0001.

3.4 Transcriptional repression in hypoxia occurs in non-cancer cells

To investigate whether this transcriptional repression was restricted to cancer cell lines, I carried out an EU incorporation assay in a non-cancer cell line, MRC5 lung fibroblasts. As previously, EU incorporation in the MRC5 cell line was significantly reduced in <0.1% O_2 whereas the levels of EU remained similar between 21 and 2% O_2. As expected, treatment of MRC5 cells with DRB significantly reduced EU incorporation (**Figure 3.4A, B**). These data show that hypoxic transcriptional repression occurs in a cell line independent manner.

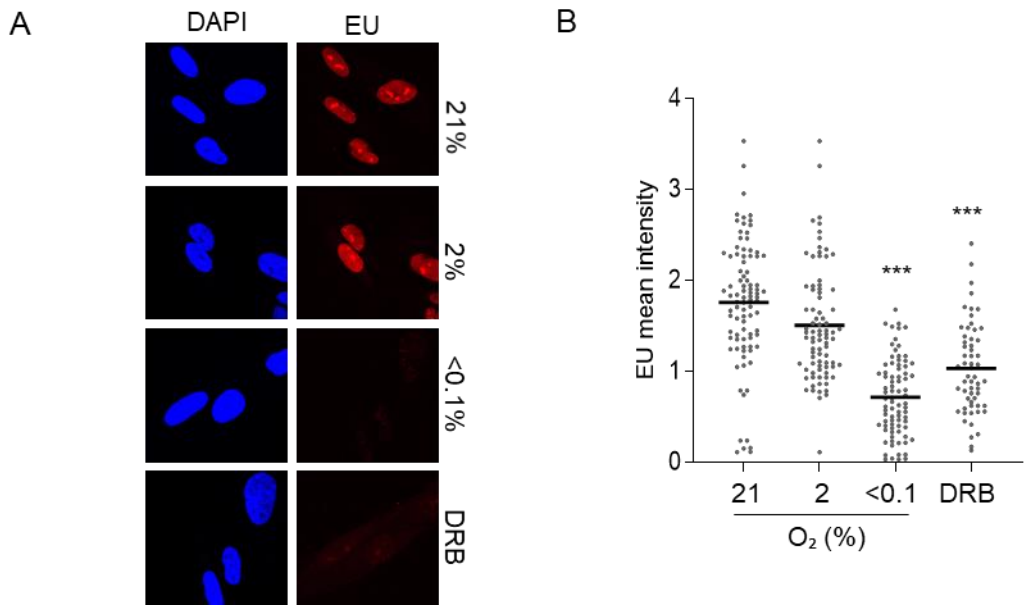


Figure 3.4. Transcriptional repression occurs in non-cancer cells in hypoxia.
MRC5 cells in 21%, 2% or <0.1% O_2 for 6 hours were incubated with EU (0.5 mM, 6 hours). DRB (100 µM, 6 hours) was used a positive control. Nascent transcription was visualised by microscopy (A). Quantification of EU intensity from images in A (B). One-way ANOVA was used to calculate statistical significance. Data from three separate experiments (n=3) are displayed. ** = p = <0.01, *** = p = <0.001.

3.5 Global transcriptional repression in hypoxia occurs in a HIF1α-independent manner

As HIF1α is stable and active in hypoxic conditions, I considered that HIF1α could affect transcriptional repression in <0.1% O_2. Therefore, I determined EU incorporation in HCT116 *HIF1α*$^{+/+}$ and *HIF1α*$^{-/-}$ cells in hypoxia. HIF1α knockout in HCT116 cells were confirmed by western blot (**Figure 3.5A**). As expected, EU incorporation decreased significantly in <0.1% O_2 in HCT116 *HIF1α*$^{+/+}$ cells. Cells lacking HIF1α showed no difference in transcriptional repression in <0.1% O_2 suggesting that HIF1α does not contribute to global transcriptional repression in <0.1% O_2 (**Figure 3.5B**). This finding is not surprising as HIF1α is active at 2% O_2 where transcriptional repression does not occur. Interestingly, cells that lack HIF1α demonstrated higher levels of basal transcription than HCT116 *HIF1α*$^{+/+}$.

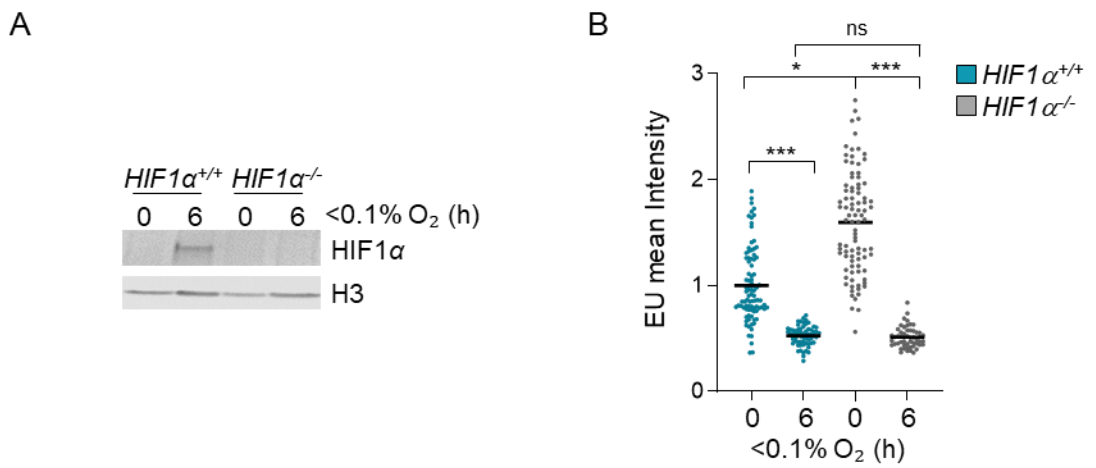


Figure 3.5. Transcriptional repression in hypoxia occurs in a HIF1α-independent manner.
HCT116 *HIF1α*$^{+/+}$ and *HIF1α*$^{-/-}$ cells were incubated in 6 hours (h) of <0.1% O_2 and subjected to western blot for HIF1α protein levels. H3 was used as a loading control (A). HCT116 *HIF1α*$^{+/+}$ and *HIF1α*$^{-/-}$ cells were incubated with EU (1 hour, 0.5 mM) in 6 hours of <0.1% O_2 and EU intensity was quantified (B). One-way ANOVA was used to calculate statistical significance. Data from three separate experiments (n=3) are displayed ± standard error of the mean (SEM) * = p = <0.05, ** = p = <0.01, *** = p = <0.001, ns = not significant.

3.6 Global transcriptional repression in hypoxia occurs independently of p53

Next, I considered p53 as a likely candidate for mediating transcriptional repression in hypoxia as p53 is stabilised and active in these conditions. I carried out EU incorporation in <0.1% O_2 in HCT116 *p53*$^{+/+}$ and HCT116 *p53*$^{-/-}$ cells. HCT116 *p53*$^{-/-}$ cells were confirmed for p53 knockout by western blot (**Figure 3.6A**). There was no change in the transcriptional repression in HCT116 *p53*$^{-/-}$ versus HCT116 *p53*$^{+/+}$ indicating that p53 does not play a role in global transcriptional repression in hypoxia (**Figure 3.6B**). To further confirm the p53 independence of transcriptional repression, I used an siRNA against p53 to reduce total p53 levels. I confirmed siRNA knockdown by western blot for p53 in <0.1% O_2 (**Figure 3.6C**). Global levels of transcription were slightly reduced in p53 siRNA-treated cells which suggests that p53 may be necessary to maintain basal levels of EU incorporation. In agreement with the genetic knockout of *p53*, EU incorporation in p53 knockdown cells demonstrated similar levels of transcriptional repression in 6 hours of <0.1% O_2 (**Figure 3.6D**).

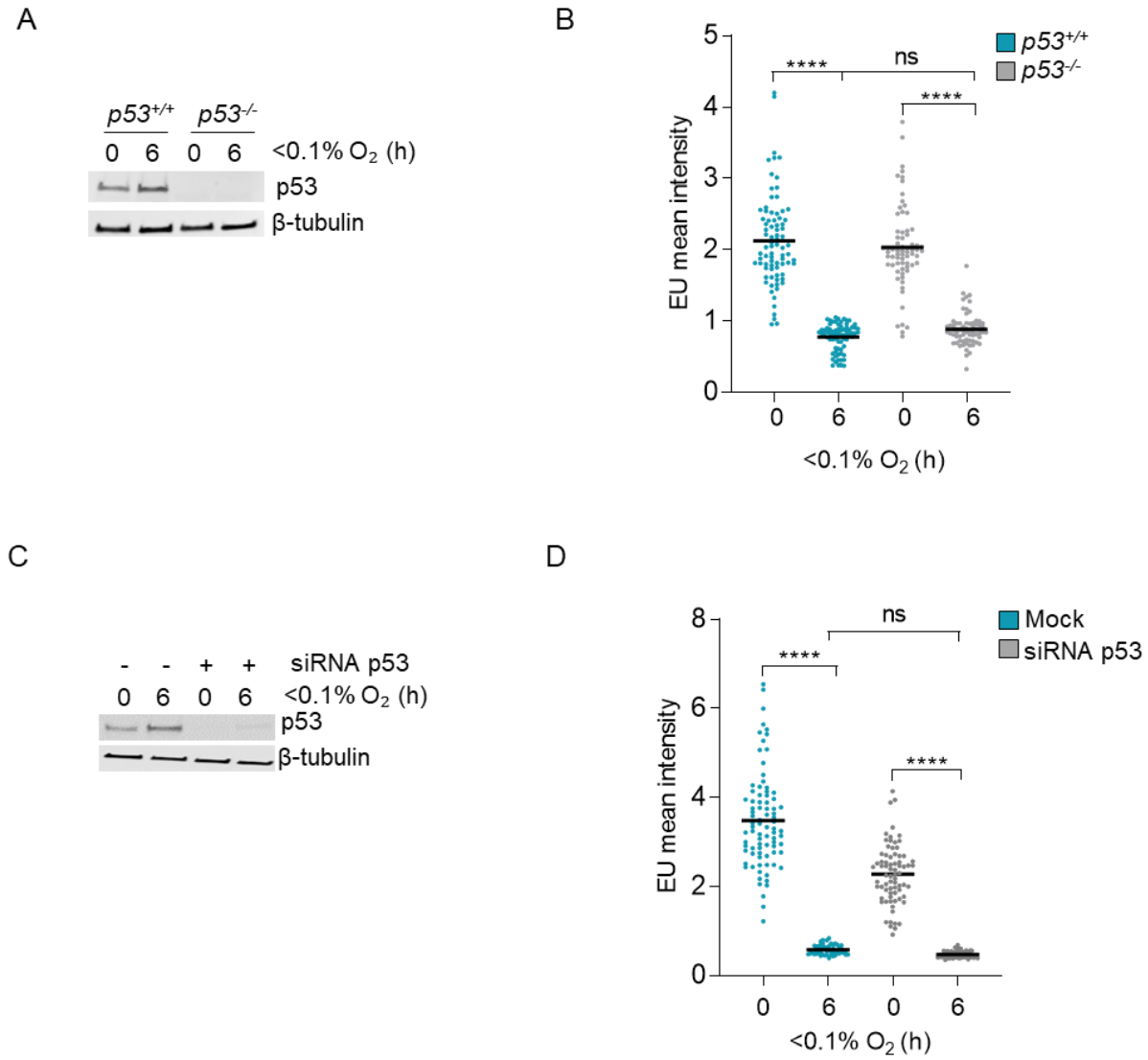


Figure 3.6. Transcriptional repression in hypoxia occurs in a p53-independent manner. HCT116 *p53*$^{-/-}$ cells were incubated in 6 hours of <0.1% O_2 and subjected to western blot for p53 protein levels. H3 was used as a loading control (A). HCT116 *p53*$^{-/-}$ cells were incubated with EU (1 hour, 0.5 mM) in 6 hours of <0.1% O_2 and EU intensity of was quantified (B). HCT116 cells treated with siRNA against p53 in 6 hours of <0.1% O_2 were subjected to western blot (C). EU incorporation of HCT116 cells treated with siRNA against p53 (D). One-way ANOVA was used to calculate statistical significance. Data from three separate experiments (n=3) are displayed ± standard error of the mean (SEM) **** = p = <0.0001, ns = not significant.

3.7 Transcription of ribosomal RNA is repressed in an oxygen dependent manner in hypoxia

Although EU incorporation gives a global measure of RNA synthesis, I noticed that the brightest areas of EU stained cells which correspond to the site of ribosomal RNA transcription, the nucleolus, were notably reduced in <0.1% O_2. The nascent product of RNPI transcription, the 47S, is initially cleaved at sites A' in the 5'ETS region (**Figure 3.7A**). I designed primer set 1 to specifically detect 47S levels indicative of rDNA transcription, shown in green in (**Figure 3.7A**). To determine what happens to rDNA transcription in hypoxia I first performed qPCR using primer set 1. HCT116 cells in <0.1% O_2 demonstrated significant repression of 47S levels, but not at 2% O_2 (**Figure 3.7B**). 47S production was significantly repressed in 6 hours of <0.1% O_2. As expected, 47S levels were reduced upon treatment with RNPI inhibitors, actinomycin D and CX5461. These data suggest that rDNA transcription is repressed in an oxygen dependent manner. To validate these findings, I carried out northern blotting using probe N1 which binds to the same region as primer set 1. In agreement with the qPCR data using primer set 1, the northern blot showed a reduction in transcription of the 47S in <0.1% O_2 (**Figure 3.7C**). Again, as expected, treatment of CX5461 leads to a reduction in 47S levels. Interestingly, the rDNA transcriptional repression exhibited in hypoxia was restored upon 1 hour of reoxygenation to normoxic levels. Together, these data suggest that transcription of rDNA is likely to be repressed in a background of replication stress and DDR activation in hypoxia.

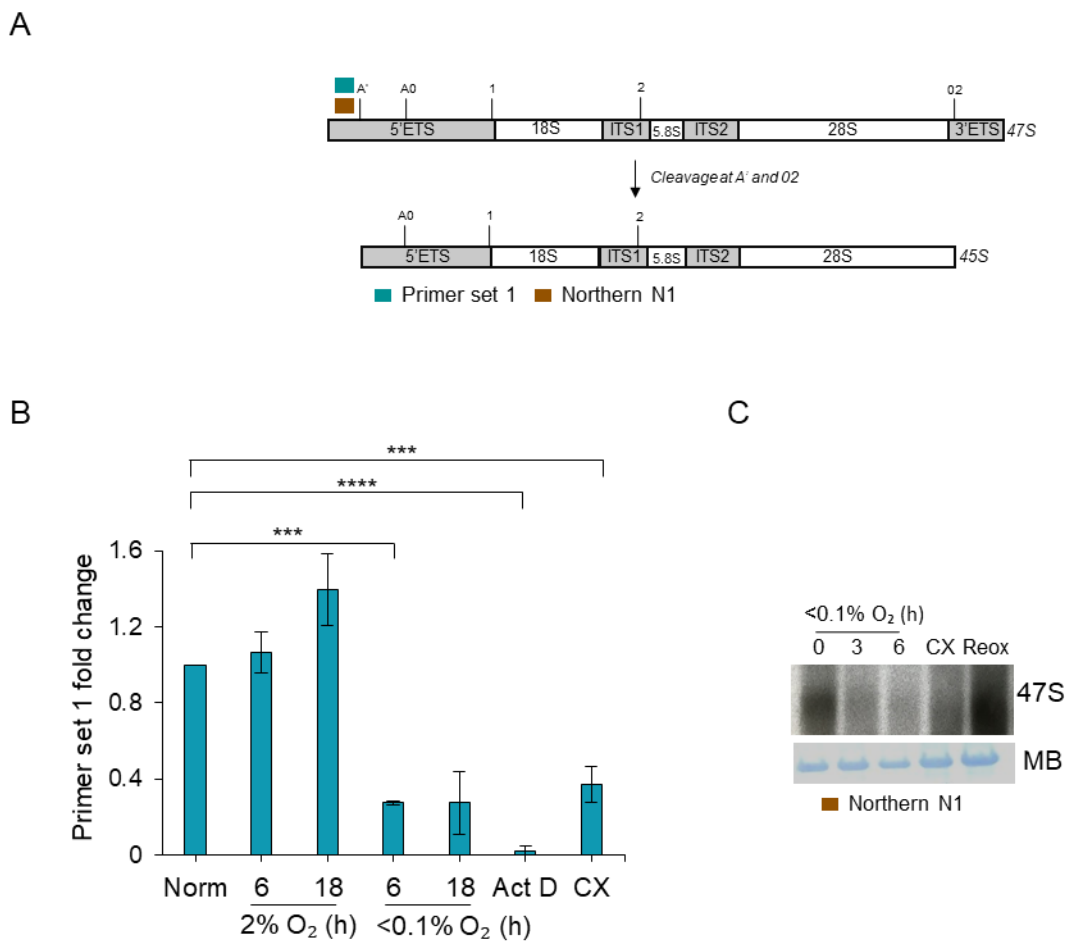


Figure 3.7. Transcription of rDNA is repressed in an oxygen dependent manner.
A schematic of the product of RNPI transcription, the 47S. The 47S is initially cleaved at A' and 02 on the 5'ETS and 3'ETS, respectively. Then, cleavage at A0 on the 5'ETS occurs. Processing of the pre-rRNA is necessary for the proper maturation of the 18S, 5.8S and 28S rRNA (Sloan et al., 2014). Primer and northern probe positions used in this study are indicated (A). qPCR analysis using primer set 1 in HCT116 cells in 21% (Norm), 2% or <0.1% O_2. Actinomycin D (40 nM, 6 hours) and CX5461 (100 nM, 6 hours) were used as inhibitors of rDNA transcription (B). One-way ANOVA was used to calculate statistical significance. Data from three separate experiments (n=3) are displayed ± standard error of the mean (SEM) *** = p = <0.001, **** = p = <0.0001. Northern blot analysis of HCT116 cells using northern probe N1 to detect rDNA transcription (C).

3.8 rDNA transcription is repressed rapidly in hypoxia

Having determined the oxygen dependency of rDNA transcriptional repression, I next sought to investigate the kinetics of this repression. To test this, 47S levels were measured in HCT116 cells in a time course in <0.1% O_2. The levels of 47S were reduced at 1.5 hours of <0.1% O_2

and were sustained at a similar level until 18 hours (**Figure 3.8**). The fast kinetics of this repression suggests that rDNA transcription is actively shut down as opposed to the depletion of energy resources or acidosis (Mekhail et al., 2006).

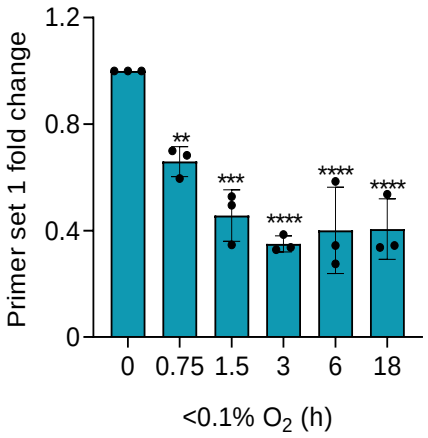


Figure 3.8. Transcription of rDNA is repressed rapidly in hypoxia.
HCT116 cells in <0.1% O_2 were subjected to qPCR analysis using primer set 1. One-way ANOVA was used to calculate statistical significance. Data from three separate experiments (n=3) are displayed ± standard error of the mean (SEM) ** = p = <0.01, *** = p = <0.001, **** = p = <0.0001.

3.9 Total levels of 18S and 28S rRNA are maintained in hypoxia

As the levels of pre-rRNA were reduced significantly in hypoxia, I hypothesised that reduced rDNA transcription would affect the levels of the 28S and 18S mature rRNA. To investigate this, HCT116 cells were incubated in <0.1% O_2 and an equal amount of RNA was run on an agarose gel stained with SYBR Safe™ (experimental design shown schematically in **Figure 3.9A**). The levels of 28S and 18S were then visualised as they are the most abundant cellular rRNA species. The levels of 28S and 18S were maintained up to 24 hours of <0.1% O_2 (**Figure 3.9B, C**). Surprisingly, the levels of 28S and 18S did not decrease until 32 hours of hypoxia. Interestingly, a faint upper band appeared at 32 hours of <0.1% O_2 which may correspond to an unprocessed rRNA population and will be investigated further. These data suggest that the half-lives of the 18 and 28S ensure that even though transcription of the rDNA decreases

rapidly in response to hypoxia (<1 hour) the mature 18 and 28S persist significantly longer. As the 18S levels did not change up to 24 hours in hypoxia, I used the 18S as a qPCR control in all experiments within this time frame.

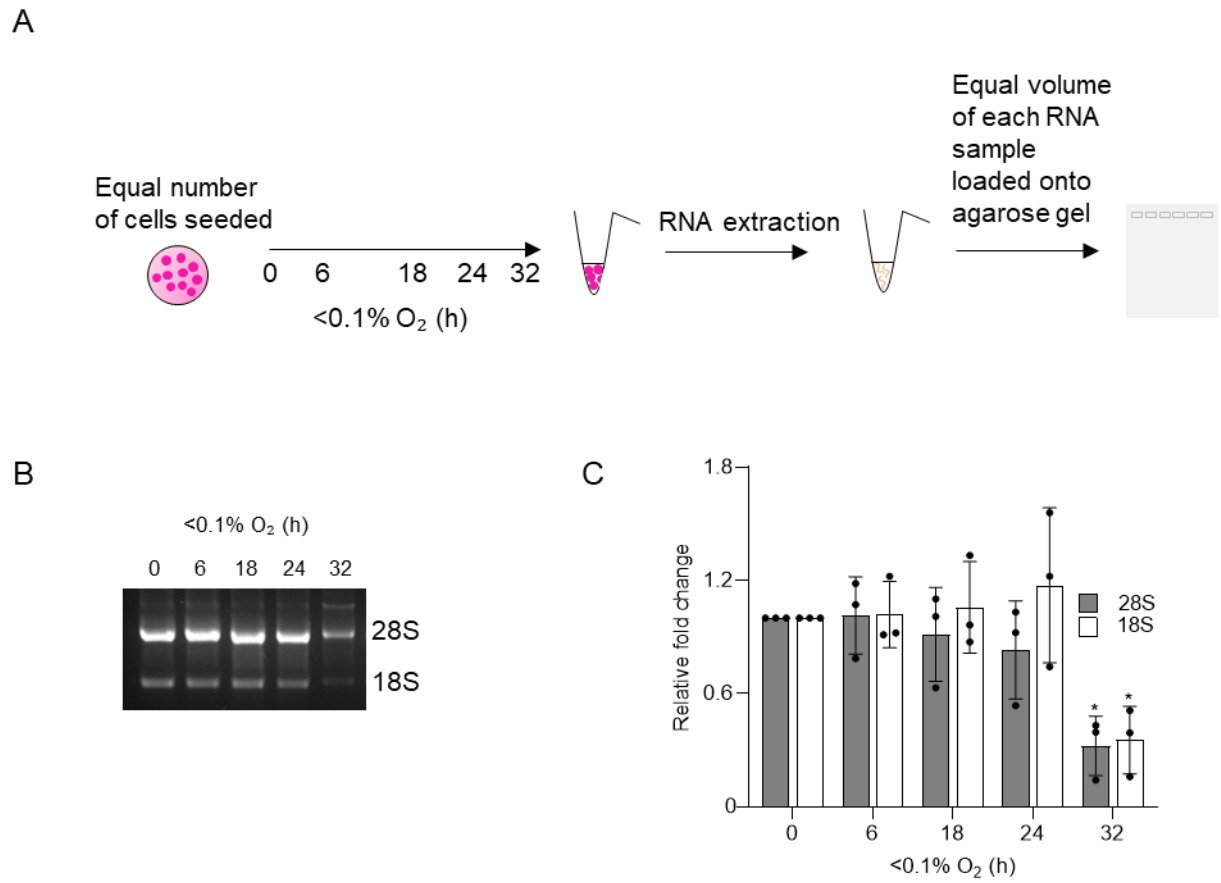


Figure 3.9. The levels of 18S and 28S are maintained in hypoxia.
Schematic of experimental design of total RNA gel electrophoresis (A). HCT116 RNA was resolved in <0.1% O_2. 28S and 18S are indicated (B). Quantification of RNA in A (C). One-way ANOVA was used to calculate statistical significance. Data from three separate experiments (n=3) are displayed ± standard error of the mean (SEM) * = p = <0.05.

3.10 Protein synthesis is repressed in hypoxia

Protein translation has been shown to be repressed in hypoxia (Koritzinsky et al., 2006). Protein translation has been shown to be downregulated by activation of the UPR in hypoxic conditions (Koumenis et al., 2002). However, the sustained levels of 18S and 28S in hypoxia suggested that protein translation can persist for prolonged periods in hypoxia. To measure global

translation, I carried out a puromycin incorporation assay in hypoxia. HCT116 cells treated with puromycin and hypoxia showed around a 30% loss of translation at 6 hours of <0.1% O_2, which was further decreased to 25% at 24 hours (**Figure 3.10A, B**). As expected, HCT116 cells treated with cycloheximide demonstrated a significant reduction in translation. These data demonstrate that protein translational repression may occur in a delayed kinetic to rDNA transcriptional repression. The initial decrease in protein translation observed is likely to occur through an EIF2α-dependent manner through PERK activation of the UPR (Koritzinsky et al., 2006). Although the 18S and 28S are repressed significantly in a similar kinetic to the repression of protein translation in 24 hours of hypoxia, the prolonged repression of protein translation is likely to occur through concomitant activation of the UPR-induced mechanism of translational control such as EIF4F disruption through 4E-BP and 4E-T activation and inhibition of the mTOR kinase (Connolly et al., 2006; Koritzinsky et al., 2006).

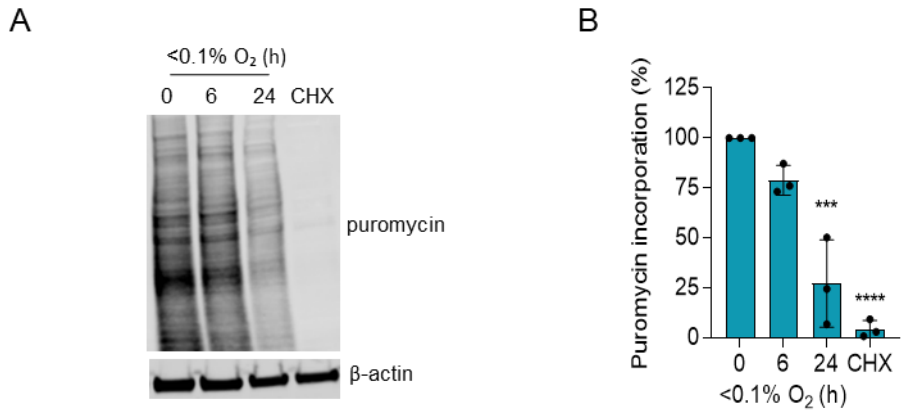


Figure 3.10. Protein translation is reduced significantly in prolonged hypoxia.
Puromycin incorporation assay to assess global translation was carried out in HCT116 cells in <0.1% O_2. Cyclohexamide (CHX) (100 µM, 1 h) was used to block protein translation (A). Quantification of puromycin levels in A (B). One-way ANOVA was used to calculate statistical significance. Data from three separate experiments (n=3) are displayed ± standard error of the mean (SEM) *** = p = <0.001, **** = p = <0.0001.

3.11 Hypoxia leads to an rRNA processing defect at A0 on the 5'ETS

Having observed the appearance of a faint upper band in **Figure 3.9B**, I investigated the processing of rRNA in hypoxia. I designed primers to the 47S to detect the specific stages of pre-rRNA processing. The next cleavage step after A' occurs at A0 on the 5'ETS. Using primer set 2 in purple (shown schematically on **Figure 3.11A**) which detects between A' and A0, I carried out qPCR in HCT116 cells to evaluate rRNA processing. Surprisingly, the levels of primer set 2 did not change over time in hypoxia indicating that processing does not occur at A0 in hypoxia. In contrast, treatment with CX5461 significantly reduced the levels of the primer set 2 products indicating that the cleavage and processing of the 47S at A0 still occurs when RNPI is inhibited pharmacologically (**Figure 3.11B**). Furthermore, the levels of primer set 3 in gold which detects between the sites of A0 and 1 on the 5'ETS also did not change in hypoxia (**Figure 3.11C**).

The processing defect identified by qPCR at A0 was confirmed by northern blotting which demonstrated an accumulation of the probe N2 product shown in pink in hypoxia (**Figure 3.11D**). In agreement with the qPCR data, treatment with CX5461 reduced the levels of the probe N2 product. 1 hour of reoxygenation to normoxia partially restored processing at site A0 indicating that the rRNA processing defect is quickly rescued when oxygen is restored. Together, these data suggest that RNPI transcription is decoupled from pre-rRNA processing in hypoxia, a concept that is supported by a study that reports decoupling of pre-rRNA processing from RNPI transcription upon processing inhibition by flavopirodol treatment in cells (Burger et al., 2013). Abrogation of cleavage at site A0 on the 5'ETS results in the accumulation of intermediate pre-rRNA species.

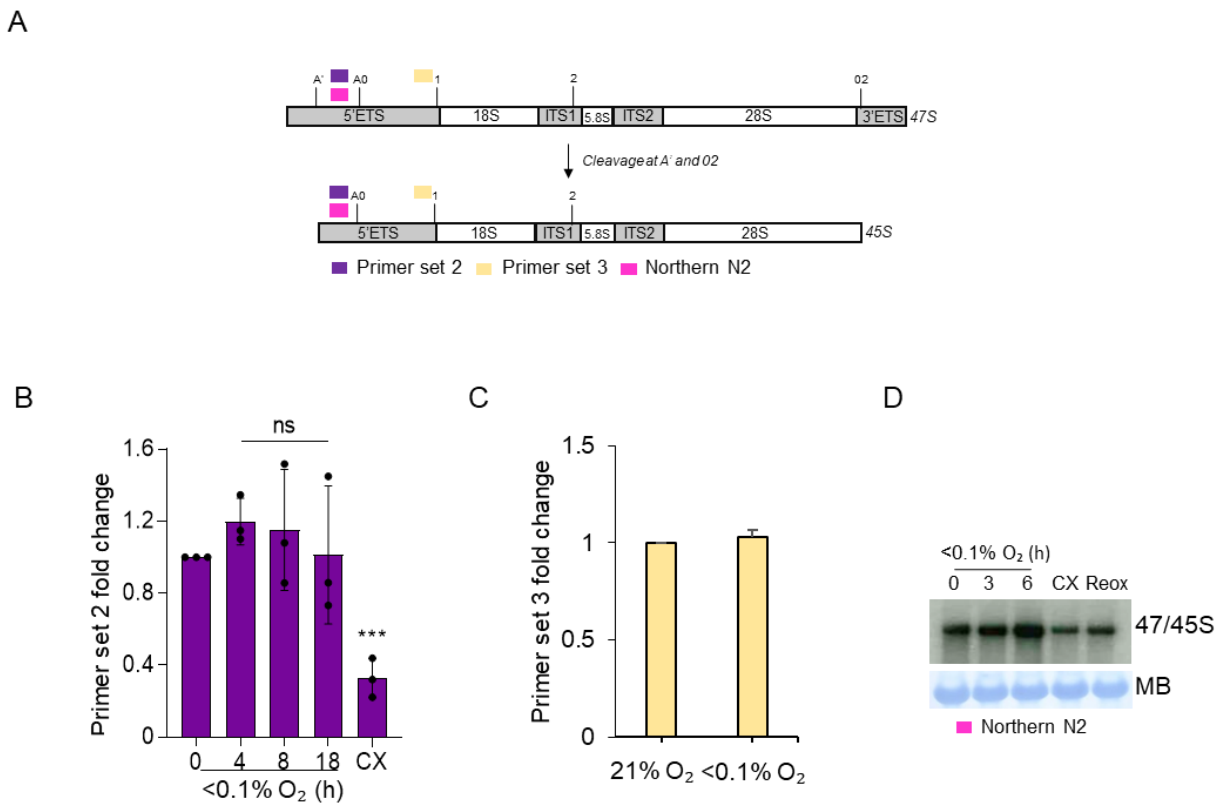


Figure 3.11. Processing at the A0 site of the 5'ETS pre-rRNA occurs aberrantly in hypoxia.
Schematic of primer and northern probe positions (A). qPCR of primer set 2 (purple) in HCT116 cells in <0.1% O_2. CX, CX5461 (100 nM, 6 hours) was used as an inhibitor of RNPI (B). qPCR of primer set 3 (gold) in HCT116 cells in <0.1% O_2. Student's t-test was used to calculate statistical significance (C). Northern blot analysis using northern probe N1 (pink) in <0.1% O_2 and reoxygenation to 21% O_2 (3 h hypoxia + 1 h reoxygenation). Methylene blue (MB) (D). Northern blot using probe N2 (pink) (E). (A-D) One-way ANOVA was used to calculate statistical significance unless otherwise specified. Data from three separate experiments (n=3) are displayed ± standard error of the mean (SEM) *** = p = <0.001, ns = not significant.

3.12 Downstream processing of pre-rRNA is on the ITS1 and ITS2 region in hypoxia

Having determined that processing on the 5'ETS occurs abnormally in hypoxia, I hypothesised that downstream processing of pre-rRNA was also affected. To investigate this, I carried out northern blotting in HCT116 cells using probe N3 (orange) and N4 (black) which indicate processing on the ITS1 and ITS2, respectively (shown schematically on **Figure 3.12A**). In agreement with the previous northern blot using probe N2, the levels of the N3 and N4 probe product accumulated in <0.1% O_2 indicating that processing at the ITS1 and ITS2 does not

occur in hypoxic conditions. As observed with probe N2, reoxygenation to normoxic levels partially restored the processing with the products of probes N3 and N4. As expected, treatment with CX5461 reduced the levels of N3 and N4 products which suggests that processing at these regions occurs when RNPI is pharmacologically inhibited (**Figure 3.12B, C**). These data suggest that the processing defect exhibited at A0 is accompanied by downstream defects in pre-rRNA processing on the ITS1 and ITS2.

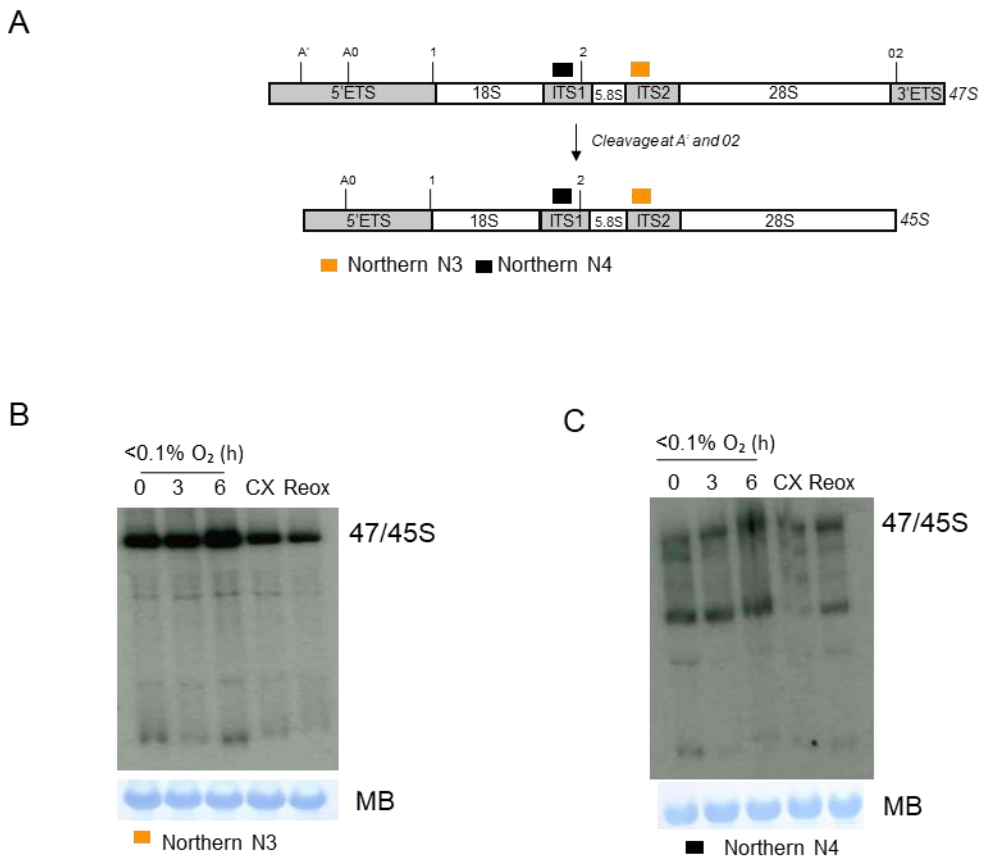


Figure 3.12. Processing at the ITS1 and ITS2 region of pre-rRNA occurs aberrantly in hypoxia.
Schematic of northern probe positioning for ITS2 (orange) and ITS1 (black) (A). Northern blot of ITS2 and ITS1 using probes N3 and N4 in HCT116 cells in <0.1% O_2 and reoxygenation (Reox) to 21% O_2 (3 h hypoxia + 1 h reoxygenation). CX, CX5461 (100 nM, 6 hours); MB, methylene blue (B, C). Representative images are shown of 3 independent experiments.

3.13 snoRNA expression is maintained in hypoxia

Cleavage and processing of the 5'ETS is brought about through the hybridisation of small guide RNA known as small nucleolar RNA (snoRNA) with the nascent pre-rRNA and recruitment of the small nucleolar ribonucleotide protein (snoRNP) complex to catalyse cleavage. I postulated that the loss of one or more snoRNA may affect pre-rRNA processing in hypoxia. Therefore, I determined the expression of a panel of snoRNAs reported to be involved in 5'ETS processing (Kass et al., 1990). The levels of U3, U6, U14, U16, U22 did not change significantly in 6 hours of <0.1% O_2 in HCT116 cells which suggests that the loss of snoRNAs is not the reason for the processing defect (**Figure 3.13**). However, although the levels of snoRNA expression did not differ significantly in hypoxia, it is possible that they were not present in the correct compartment of the nucleolus, which could in turn affect processing of the pre-rRNA.

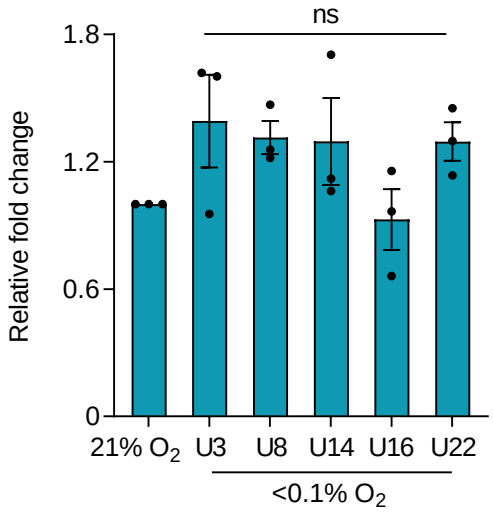


Figure 3.13. SnoRNA expression panel in hypoxia.
qPCR of snoRNA in HCT116 cells in 6 hours of <0.1% O_2. One-way ANOVA was used to calculate statistical significance. Data from three separate experiments (n=3) are displayed ± standard error of the mean (SEM). ns = not significant.

3.14 PNRC1 is upregulated in an oxygen-dependent manner

A previous report demonstrated that proline-rich nuclear receptor coactivator 1 (PNRC1) is required for rRNA maturation (Gaviraghi et al., 2018). Briefly, PNRC1 recruits the DCP2/DCP1α decapping complex to the nucleolus. The methylguanine caps on the snoRNAs are removed by the decapping complex which results in impaired snoRNA function and improper pre-rRNA processing. Importantly, the overexpression of PNRC1 did not result in a reduction in snoRNA levels, as observed upon PNRC1 overexpression in previous studies (Gaviraghi et al., 2018). As I previously demonstrated that the levels of U3 and U8 snoRNA did not change in hypoxic conditions, I hypothesised that PNRC1 upregulation could disrupt rRNA processing in hypoxia. Therefore, I examined the expression of PNRC1 in hypoxic conditions. Our preliminary data demonstrates that PNRC1 was upregulated in HCT116 cells in 6 hours of <0.1%, but not in 2% O_2 which suggests PNRC1 upregulation occurs in an oxygen-dependent manner (**Figure 3.14A**). Interestingly, PNRC1 mRNA expression continued to rise up to 16 hours of <0.1% O_2. I investigated if PNRC1 upregulation was cell line-specific by measuring PNRC1 mRNA levels in additional cell lines, RKO and A549 cells after 6 hours of <0.1% O_2 (**Figure 3.14B, C**). The levels of PNRC1 were significantly upregulated (7-fold) in hypoxia which suggests that PNRC1 is upregulated in a cell-line-independent manner. These preliminary data suggest that PNRC1 upregulation in hypoxia may block pre-rRNA processing.

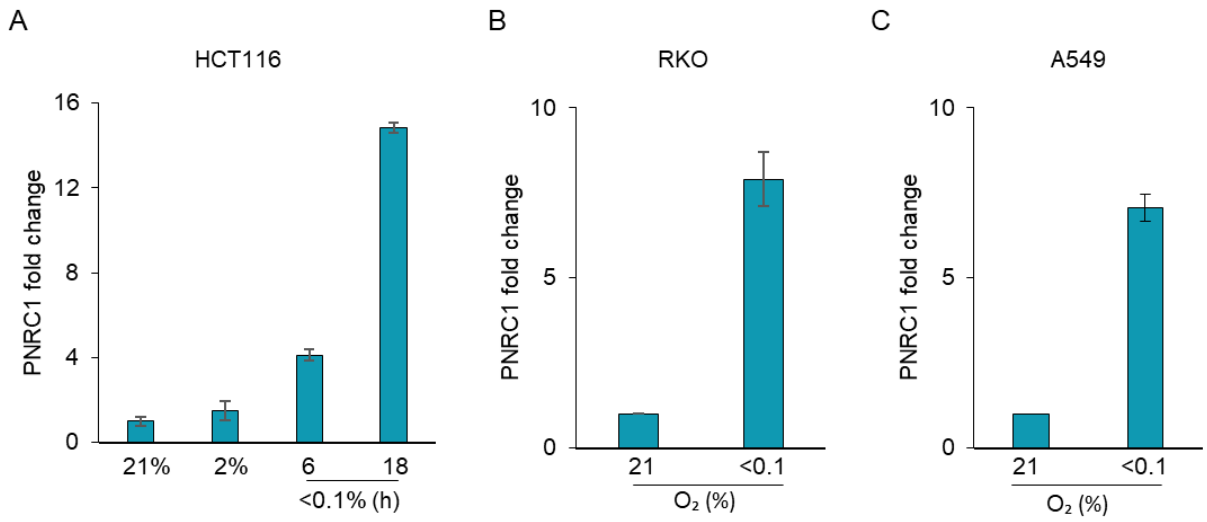


Figure 3.14. PNRC1 mRNA is upregulated in hypoxic conditions.
qPCR analysis in HCT116 cells of PNRC1 mRNA levels in 6 hours of 2% O_2 and 6 or 18 hours of <0.1% O_2 (A). PNRC1 mRNA levels in 6 hours of <0.1% O_2 in RKO cells (B). PNRC1 mRNA levels in 6 hours of <0.1% O_2 in A549 cells (C) n=2.

3.15 Discussion

In this chapter, I demonstrate that global transcription is repressed in an oxygen-dependent manner, and that this hypoxic repression occurs in both cancer and non-cancer cell lines. I showed that global repression of transcription occurs independently of HIF1α which is unsurprising given that HIF1α is active at 2% O_2 as well as <0.1% O_2. I also show that transcriptional repression occurs in a p53-independent manner in hypoxia. Specifically, I have demonstrated that rDNA transcription is likely to be repressed rapidly within 1.5 hours of hypoxia suggesting that shutdown of RNPI transcription involves an active mechanism in contrast to those described previously in prolonged periods of mild hypoxia (22 hours of 1% O_2) (Mekhail et al., 2006). However, I have not directly measured rDNA transcription and therefore cannot be completely sure that transcription of rDNA is repressed. Further studies utilising native elongating transcription-seq (NET-seq) using a RNPI subunit antibody or RNPI subunit ChIP would strengthen the hypothesis that rDNA transcription is repressed in hypoxia (Turowski et al., 2020). The levels of 18S and 28S in hypoxia were maintained in

hypoxia, suggesting that the half-lives of the mature rRNA ensure that 18S and 28S steady state levels remain long enough to sustain protein translation for longer periods in hypoxia. Accordingly, I found that protein translational repression occurred in prolonged hypoxia probably through the activation of the UPR.

I describe for the first time, to our knowledge, that a processing defect of the rRNA occurs in hypoxia. I demonstrate that pharmacological inhibition of RNPI with CX5461 results in cleavage at A0 and degradation of pre-rRNA. These data suggest that cleavage at the site A0 occurs upon RNPI shutdown. In contrast, hypoxic inhibition of RNPI leads to a processing defect at A0. In support of this, pharmacological inhibition of RNPI results in cleavage and degradation in the ITS1 and ITS2 region, whereas upon hypoxic inhibition of RNPI, abrogation of cleavage and degradation of ITS1 and ITS2 results in the build-up of pre-rRNA intermediates.

An abrogation of cleavage at the A0 site on the 5'ETS results in the build-up of an intermediate rRNA species, the 45S, which presumably impacts the downstream sequence of processing of the cleavage sites on the ITS1 and ITS2 that would normally occur upon RNPI inhibition. It is unclear why this processing defect happens in hypoxia. I found that a factor that has been reported to inhibit rRNA processing, PNRC1, was significantly upregulated in <0.1% O_2. The contribution of PNRC1 to the processing defect in hypoxia is yet to be determined. The processing defect is rapidly rescued upon reoxygenation indicating that the cell accumulates intermediate species of rRNA under hypoxic stress so that when reoxygenation occurs the cell can quickly start assembling ribosomes to sustain protein synthesis and ultimately cellular functions.

In summary, the data suggests that RNPI is likely to be repressed in hypoxia and that processing of pre-rRNA occurs aberrantly, which ultimately impact protein synthesis. The rapid inhibition

of RNPI in hypoxia that I observed may occur to prevent replication-transcription collisions on the rDNA and ultimately genome stability. I will discuss the potential mechanisms that support rDNA transcriptional repression in hypoxia in the following chapters.

Chapter 4

Mechanisms of rDNA transcriptional repression

4.1 Introduction

I determined that rDNA transcription was repressed in an oxygen dependent manner in hypoxia (Chapter 3). rDNA transcription is a highly dynamic process regulated by many mechanisms. The substrate of rDNA transcription are NTPs which can be made *de novo*. Nucleotide imbalance has been shown to impact DNA replication in hypoxia (Foskolou et al., 2017). It is unclear whether nucleotide imbalance in hypoxia affects rDNA transcription in hypoxia and will be investigated further in this chapter.

The response of rDNA transcription upon an rDNA DSB has been studied in detail by using the rDNA homing endonuclease I-PPo1 or CRISPR-Cas9 targeted DSB technology. The mechanism of DSB-dependent transcriptional repression of rDNA involves the activation of ATM which phosphorylates TCOF1 in the nucleolus. TCOF1 then recruits TopBP1 which is required for ATR activation and full transcriptional repression. ATM activation has also been implicated in the transcriptional repression of rDNA in mild hypoosmotic stress (Velichko et al., 2019). R-loop formation in response to hypoosmotic stress leads to exposed ssDNA which is coated by RPA. Activation of the ATR kinase through TCOF1 mediated TopBP1 recruitment to the nucleoli results in the shutdown of RNPI transcription. ATM is then activated in a

positive feedback loop through phosphorylation of H2AX. More severe hypoosmotic stress leads to rDNA transcriptional repression mediated through PAPAS, a lncRNA transcribed in the antisense direction to the 47S coding region of the rDNA, the induction of which recruits the chromatin remodelling complex CHD4/NuRD to the rDNA promoter which affects methylation of H4K20 (H4K20me3) and reduces rDNA transcription (Bierhoff et al., 2014; Zhao et al., 2016). Furthermore, p53 has been implicated in the repression of rDNA in hypoxia (Zhai and Comai, 2000). p53 directly interferes with interaction between SL1 and UBF to form the initiation complex, impairing the basal productive transcription machinery on the rDNA promoter. Given that ATM and ATR and downstream target p53 are active in hypoxic conditions, it is possible that DDR signalling plays a role in the transcriptional repression of rDNA in hypoxia.

RNPII activity is regulated via the phosphorylation status of the CTD. Phosphorylation of serine 2 and 5 on the CTD indicate engaged RNPII status, either in elongation or initiation phases of the transcriptional cycle. Studies have demonstrated that RNPII phosphorylation of the CTD on serine 2 and 5 is diminished in long periods of mild hypoxia (>22 hours, 1% O_2), however it is currently unknown what happens in shorter periods of hypoxia.

Activation of the UPR with thapsigargin and tunicamycin has been shown to repress rDNA transcription through activation of PERK and phosphorylation of EIF2α which abrogates RRN3 recruitment to the rDNA promoter (DuRose et al., 2009). It is not known if the UPR plays a role in the transcriptional repression in hypoxia and therefore warrants further investigation.

4.2 Nucleotide levels are reduced in hypoxia

Maintaining NTP levels is crucial for sustaining basal levels of transcription (Gaal et al., 1997). I measured NTP levels in hypoxia and found that adenosine triphosphate (ATP), cytidine

triphosphate (CTP), guanosine triphosphate (GTP) and uridine triphosphate (UTP) were significantly reduced by 50% in 1.5 hours of <0.1% O_2 and remained low for 4 hours (**Figure 4.2**). These data suggest that a reduction in nucleotide levels occur rapidly in hypoxia.

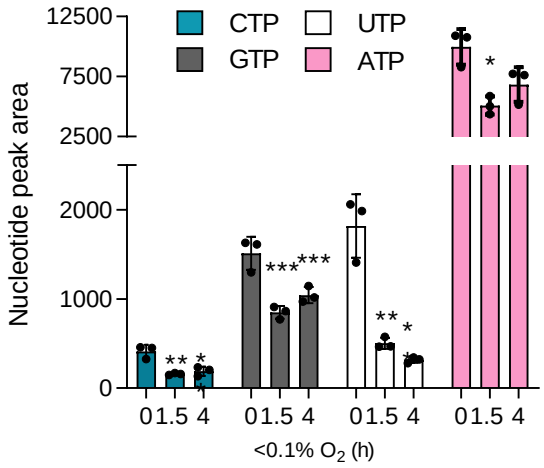


Figure 4.2. NTP levels are reduced in hypoxia.
NTP levels were measured in <0.1% O_2 in HCT116 cells. CTP, UTP, GTP and ATP are shown. One-way ANOVA was used to calculate statistical significance. Data from three separate experiments (n=3) are shown ± standard error of the mean (SEM) * = p = <0.05, ** = p = <0.01, *** = p = <0.001.

4.3 Nucleotide supplementation does not affect rRNA transcription in hypoxia

To investigate whether a lack of NTPs could affect rDNA transcription in hypoxia I supplemented hypoxic cells with the nucleosides. The nucleosides were used because they lack phosphate groups which would impair entry to the cell. Using this approach, the nucleoside passes through the cell membrane and is then phosphorylated. The levels of UTP, CTP and ATP in hypoxia were restored to normoxic levels upon nucleoside supplementation (**Figure 4.3A**). However, the levels of GTP were not restored upon nucleoside supplementation which led us to hypothesise than guanosine was either not entering the cell or not being phosphorylated once inside the cell. However, the levels of intracellular levels of GDP were restored upon nucleoside supplementation in hypoxia, which demonstrates that guanosine

entered the cell and became phosphorylated (**Figure 4.3B**). Interestingly, I saw an increase in GDP levels after 1.5 hours of <0.1% O_2. The apparent reduction in the levels of GTP with nucleoside supplementation in hypoxia could be due to a high consumption of GTP in HCT116 cells which have a KRAS hypermutation which requires GTP as a substrate (Shirasawa et al., 1993). The levels of rDNA transcription were not rescued through addition of nucleosides in hypoxia which suggests that insufficient NTPs is unlikely to cause the initial transcriptional repression (**Figure 4.3C**).

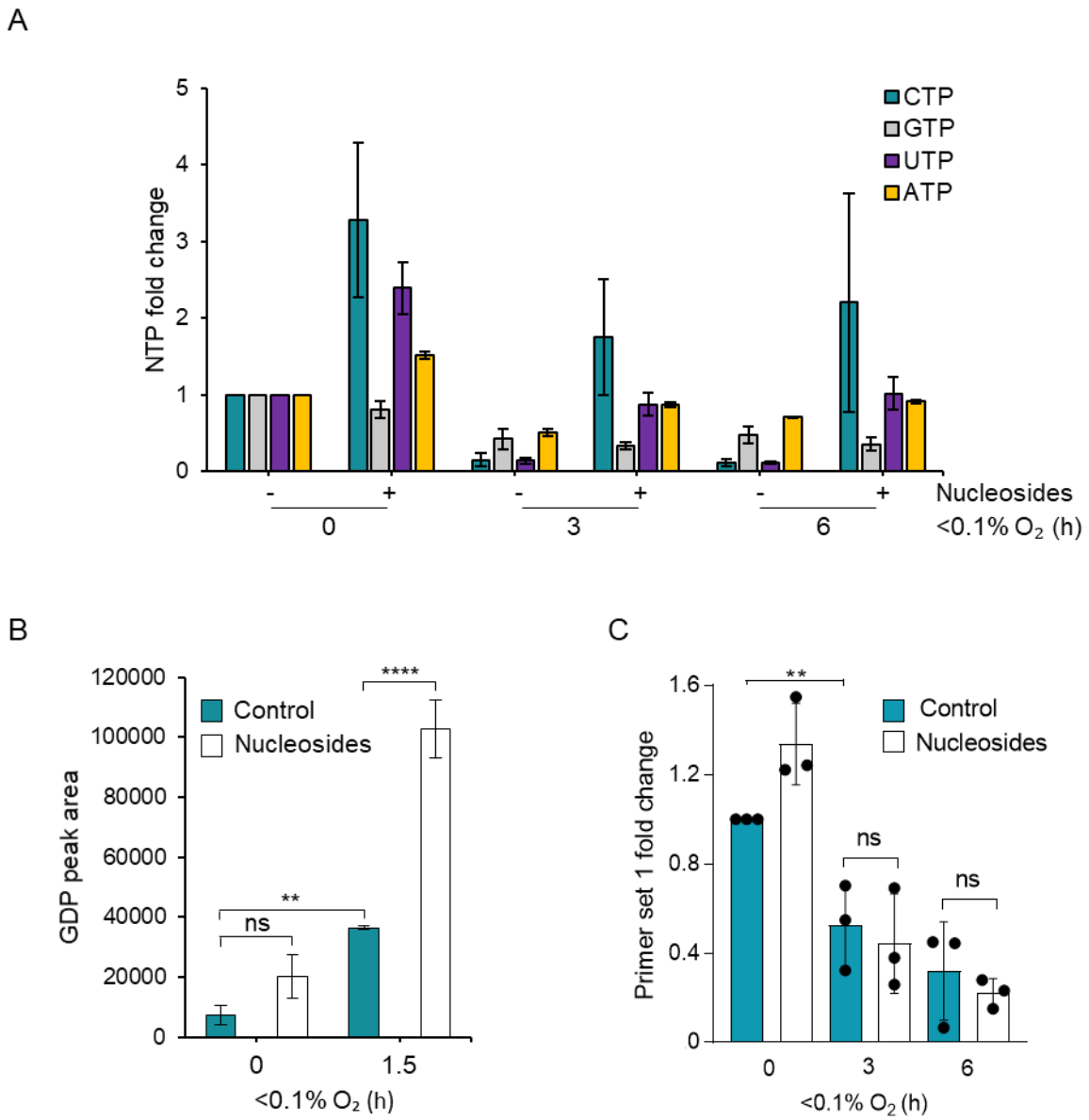


Figure 4.3. Nucleoside supplementation in hypoxia restores NTP levels.
The NTP levels in HCT116 cells were measured in <0.1% O_2 at the times indicated after the addition of nucleosides (3 or 6 hours) (A). GDP levels were measured in HCT116 cells after the addition of nucleosides in 1.5 hours of <0.1% O_2 (B). HCT116 cells were analysed by qPCR using primer set 1 in <0.1% O_2 supplemented with nucleosides (C). Two-way ANOVA was used to calculate statistical significance. Data from three separate experiments (n=3) are displayed ± standard error of the mean (SEM) ** = p = <0.01, **** = p = <0.0001, ns = not significant.

4.4 POLR1A and POLR1B subunits are repressed at the mRNA level in prolonged hypoxia

The RNPI complex consists of 11 subunits, 6 of which are shared between RNPI and RNPII, and 5 of which are specific to RNPI. As a preliminary investigation to check for the stability of the RNPI subunits, I investigated the mRNA levels in hypoxia by qPCR. I chose to measure the levels of POLR1A and POLR1B because they are subunits essential for the catalytic/enzymatic function of the RNPI complex. The levels of POLR1A and POLR1B were not significantly repressed in hypoxia until 18 hours of <0.1% O_2 which demonstrate that POLR1A and POLR1B expression remains stable for long periods in hypoxia (**Figure 4.4A, B**).

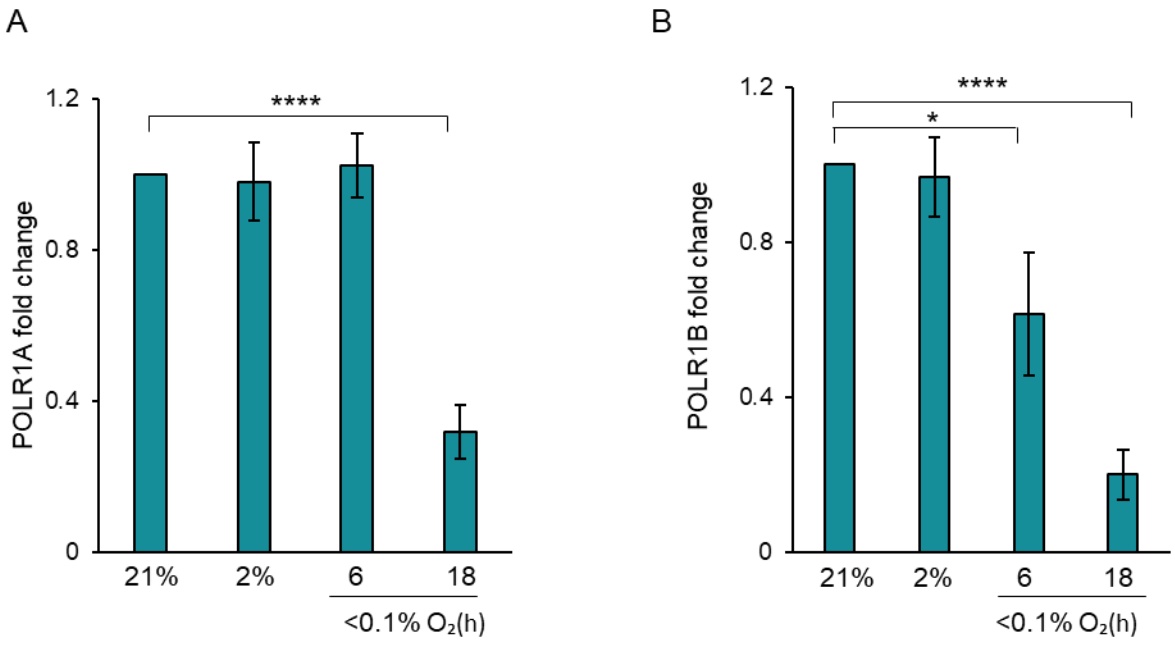


Figure 4.4. POLR1A and POLR1B mRNA are repressed after prolonged hypoxia. qPCR analysis of POLR1A and POLR1B in RKO cells in 6 hours of 2% and 6 or 18 hours of <0.1% O_2. One-way ANOVA was used to calculate statistical significance. Data from three separate experiments (n=3) are displayed ± standard error of the mean (SEM) * = p = <0.05, **** = p = <0.0001.

4.5 The expression of RNPI associated factors

A more likely hypothesis is that the loss of one or more reported RNPI associated proteins could impact rDNA transcription in hypoxia. Therefore, to investigate this I carried out western blotting for a panel of known RNPI associated factors UBF1, nucleolin, fibrillarin, C-MYC and dicer. The expression of UBF1, nucleolin, fibrillarin and dicer remained stable in periods (>6 hours) of hypoxia (**Figure 4.5A**). Previous studies have identified that C-MYC is repressed in hypoxic conditions through HIF1α dependent mechanisms (Koshiji et al., 2004; Zhang et al., 2007). Interestingly, I found that the levels of C-MYC were decreased in 6 hours of hypoxia, however the kinetics of this repression did not match the repression of rDNA transcription in hypoxia (**Figure 4.5B**). Therefore, these data suggest that the loss of C-MYC is unlikely to contribute to rDNA transcriptional repression in hypoxia.

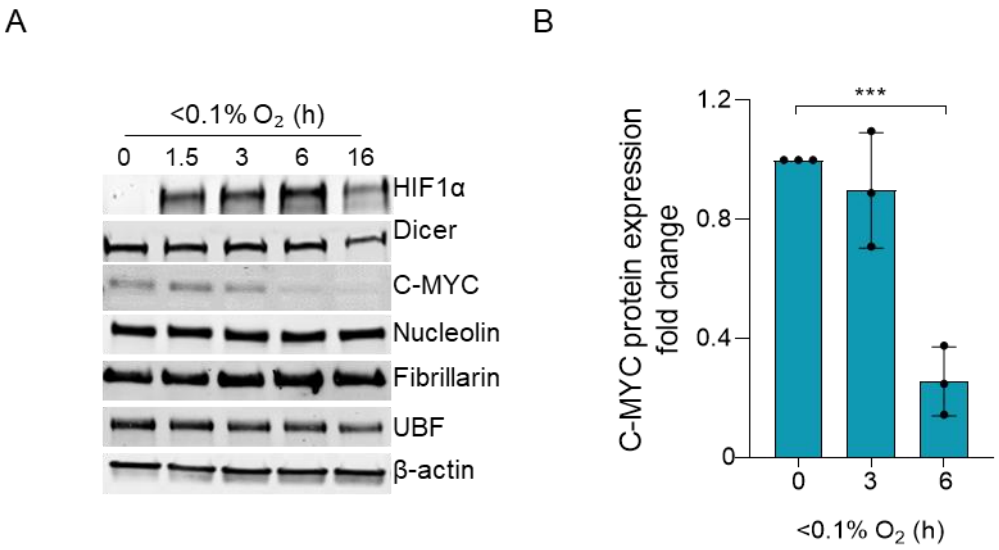


Figure 4.5. RNPI-associated factors expression in hypoxia.
HCT116 cells in <0.1% O_2 were analysed by western blot for RNPI-associated factors. Representative images are shown of three independent experiments. (A). Quantification of C-MYC expression in HCT116 cells in <0.1% O_2 from 3 independent experiments (B). Data provided by Shaliny Ramachandran.

4.6 Fibrillarin and nucleolin change localisation in prolonged periods of hypoxia

Although the expression of nucleolin and fibrillarin did not change significantly, their localisation could impact RNPI transcription in hypoxia. Specifically, the localisation of fibrillarin into nucleolar caps has been shown to be important to shut down rDNA transcription in response to DNA damage (van Sluis and McStay, 2015). Therefore, I investigated the localisation of fibrillarin in hypoxia. Fibrillarin reorganisation was observed in the nucleolus but only at prolonged periods of hypoxia (>18 hours) (**Figure 4.6A**). Nucleolin formed spheres indicative of sustained transcriptional silencing in prolonged periods of hypoxia (**Figure 4.6B**). These data suggest that rDNA transcriptional repression precedes nucleolar organisation in hypoxia.

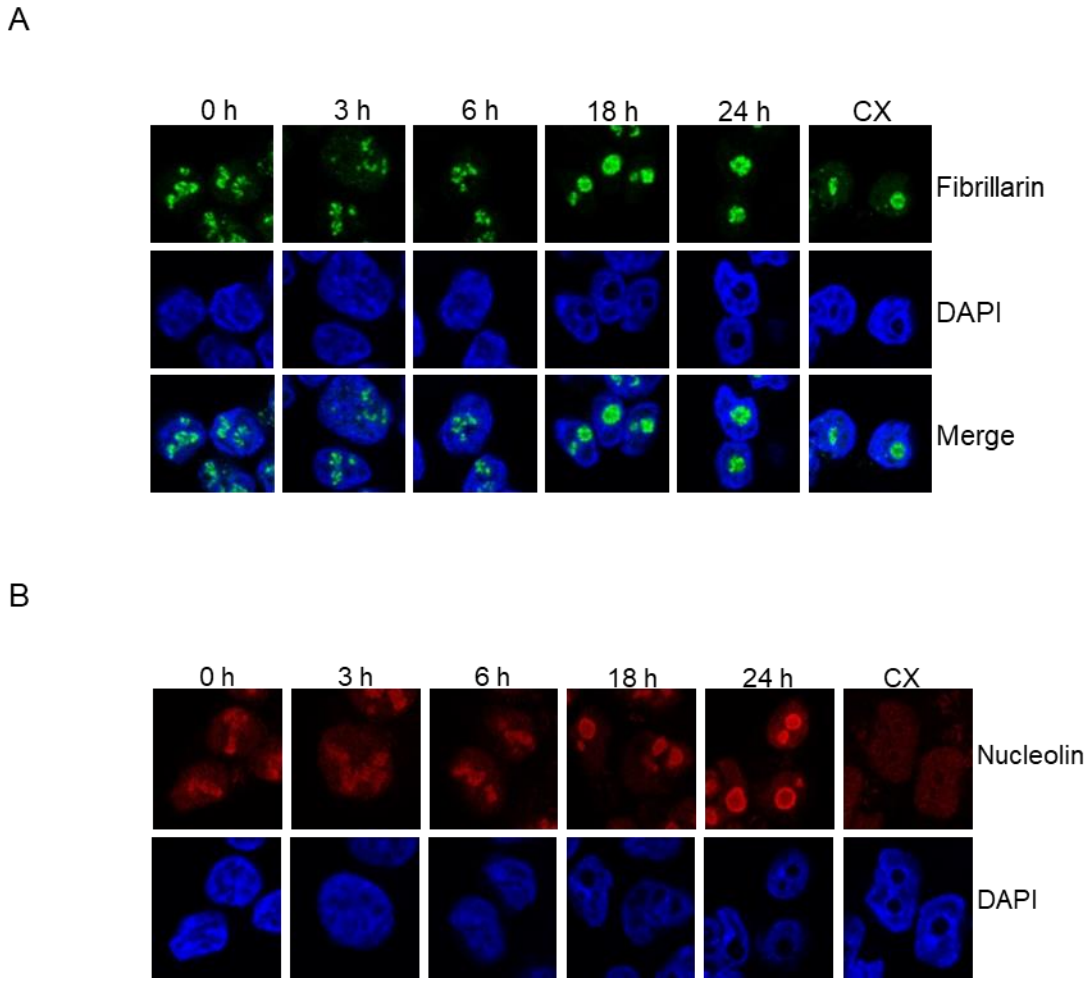
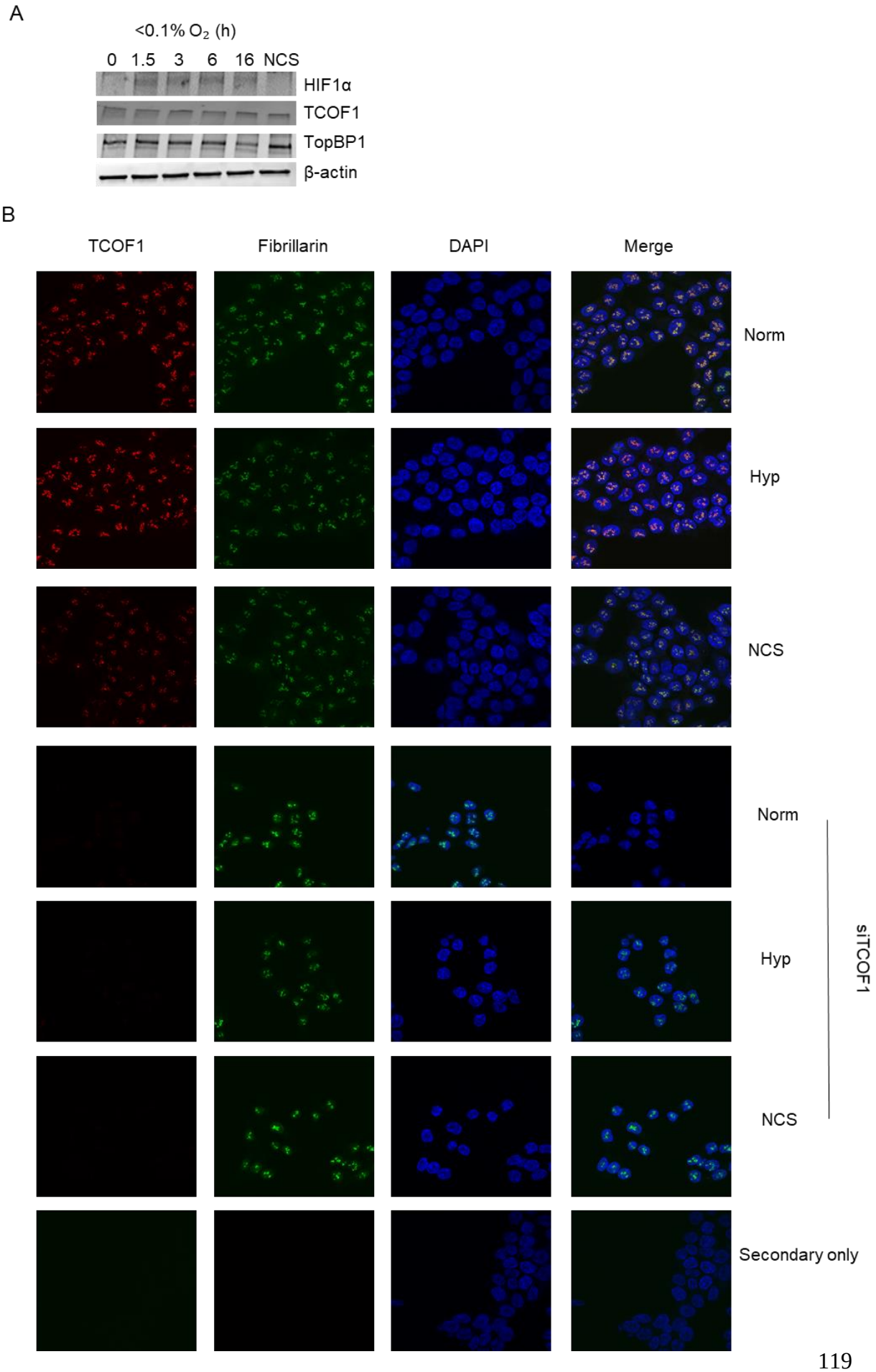


Figure 4.6. The nucleolus undergoes nucleolar reorganisation in hypoxia.
HCT116 cells in <0.1% O_2 were assessed for fibrillarin localisation by immunofluorescence. CX5461 (100 nM, 6 hours) was used as a RNPI inhibitor (A). HCT116 cells in <0.1% O_2 were assessed for nucleolin localisation by immunofluorescence (B). Representative images are shown of three independent experiments. Data provided by Shaliny Ramachandran.

4.7 TCOF1 is not involved in rDNA repression in hypoxia

TCOF1 has shown to be important for the shutdown of rDNA transcription in response to DNA damage (Larsen et al., 2014; Mooser et al., 2020). As many DDR proteins are repressed in hypoxia, I considered that TCOF1 expression could be lost in hypoxia. Western blot analysis of TCOF1 demonstrated that TCOF1 protein levels remained unchanged in hypoxia indicating that TCOF1 protein was not reduced in the time frame of the hypoxic rDNA transcriptional repression. (**Figure 4.7A**). Furthermore, TopBP1 levels were not reduced until long periods in

hypoxia which suggests that a lack of TopBP1 is not responsible for rDNA transcriptional repression in hypoxia. To determine the localisation of TCOF1, I carried out immunofluorescence. The specificity of the antibody signal for immunofluorescence was validated using an siRNA targeting TCOF1 and a secondary only control (**Figure 4.7B**). The cells exposed to hypoxia showed punctate TCOF1 staining, similar to normoxia and as expected, treatment with the DNA damaging agent, neocarzinostatin (NCS) resulted in the fusion of the punctual TCOF1 staining in the nucleolus leading to fewer foci as previously described in response to DNA damage (**Figure 4.7C, D**) (Mooser et al., 2020). To formally rule out TCOF1 dependence of rDNA transcriptional repression in hypoxia, I depleted TCOF1 protein levels by siRNA (**Figure 4.7E**). 47S levels were unaffected by a reduction in TCOF1 levels in hypoxia, suggesting that TCOF1 does not affect the rapid repression of rDNA transcriptional repression in hypoxia (**Figure 4.7F**).


A
<0.1% O2 (h)
0 1.5 3 6 16 NCS
HIF1α
TCOF1
TopBP1
β-actin
B
TCOF1
Fibrillarin
DAPI
Merge
Norm
Hyp
NCS
Norm
Hyp
NCS
siTCOF1
Secondary only

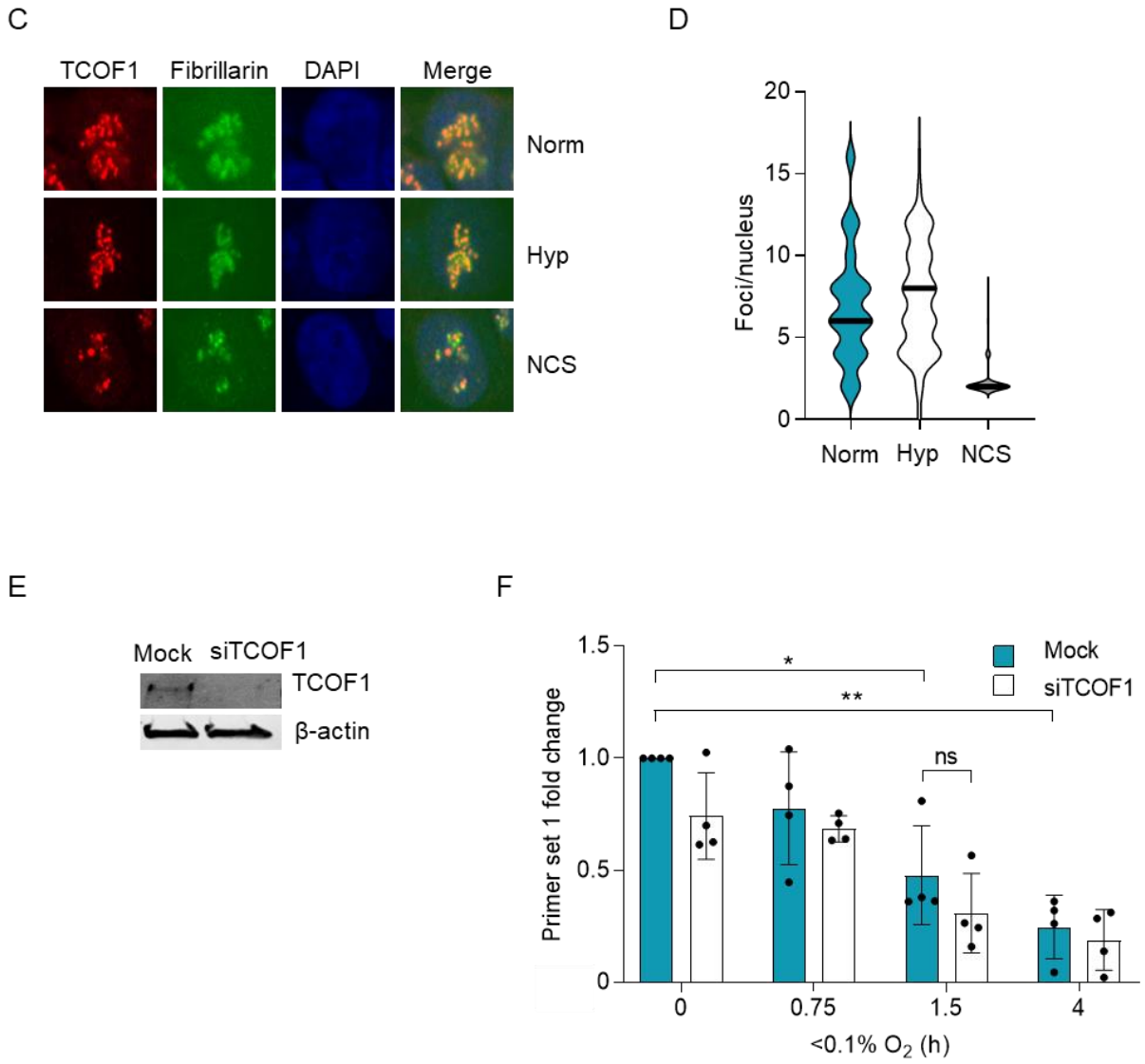


Figure 4.7. TCOF1 is not involved in rDNA transcriptional repression in hypoxia.
HCT116 cells in <0.1% O_2 were assessed for TCOF1 and TopBP1 protein levels by western blot. β-actin was used a loading control (A). HCT116 cells in 1.5 hours <0.1% O_2 were assessed for TCOF1 nucleolar localisation by co-immunofluorescence with fibrillarin. NCS (200 ng/ml, 2 hours) was used as a DNA damage inducing agent. HCT116 cells were treated with mock or siRNA against TCOF1 (siTCOF1) and secondary antibody only was used as a control (B). Representative images of TCOF1 immunofluorescence (C). Violin plot of the quantification of TCOF1 foci/nucleus. A minimum of 100 nuclei were counted. The average mean number of foci is represented by a black bar (D). HCT116 cells were treated with mock or siRNA against TCOF1 (siTCOF1) in 2 hours of <0.1% O_2 and subjected to western blot for TCOF1 (E). qPCR analysis using primer set 1 in HCT116 cells in <0.1% O_2 (F). Two-way ANOVA was used to calculate statistical significance. Data from three separate experiments (n=3) are displayed ± standard error of the mean (SEM) * = p =<0.05, ** = p = <0.01, **** = p = <0.0001, ns = not significant.

4.8 RNA polymerase II CTD levels do not change in acute hypoxia

Previous work has shown that RNA polymerase II (RNPII) activity is repressed in prolonged periods (>22 hours) of <0.1% O_2 (Denko et al., 2003). Therefore, I considered that a loss or inactivity of RNPII may, in turn, affect RNPI activity in hypoxia. To investigate the activity of RNPII in hypoxia, I carried out western blotting for the RNPII CTD phosphorylations at serine 2 and 5 which indicate RNPII activation. As expected, treatment of HCT116 cells with RNPII inhibitors, alpha amanitin and DRB reduced the levels of phospho-serine 2 and 5 on the RNPII CTD. Unexpectedly, the levels of phospho-serine 2 and 5 on the RNPII CTD did not change up to 18 hours in <0.1% O_2 (**Figure 4.8A**). In agreement with a previous report, a reduction in phospho-serine 2 and 5 were observed in >24 hours <0.1% O_2 (**Figure 4.8B**) (Denko et al., 2003). These data suggest that RNPI repression does not occur through a loss of RNPII activity in hypoxia.

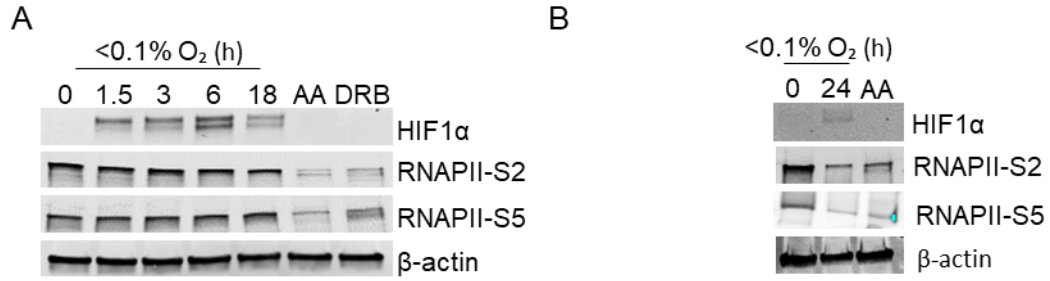


Figure 4.8. RNPII CTD phosphorylation of S2 and S5 levels in hypoxia.
HCT116 cells in <0.1% O_2 were analysed by western blotting for RNPII CTD serine 2 and 5 phosphorylation. Alpha amanitin (AA) and DRB were used as RNPII inhibitors. (A) Western blot analysis of RNPII levels in 24 hours of <0.1% O_2 (B).

4.9 RNA polymerase II inhibitors lead to decreased RNPI activity

Next, I compared the effect of RNPII inhibitors with hypoxia on rDNA transcription. Previous studies have reported that RNPII inhibition can, in turn, impact RNPI transcription (Burger et al., 2013). I used inhibitors of RNPII, alpha amanitin (AA) and DRB, and measured 47S levels using qPCR with primer set 1. The levels of 47S were reduced rapidly in 1.5 hours of <0.1%

O_2. Treatment with AA and DRB significantly reduced 47S levels, however this occurred with delayed kinetics compared to hypoxia which suggests that the initial transcriptional repression of rDNA in hypoxia does not rely on RNPII activity (**Figure 4.9**).

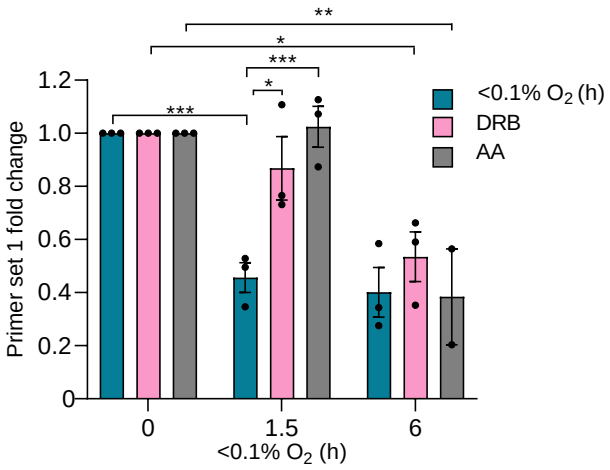


Figure 4.9. RNPII inhibitors decrease RNPI activity.
HCT116 cells treated with AA, DRB and <0.1% O_2 and were analysed by qPCR using primer set 1. One-way ANOVA was used to calculate statistical significance. Data from three separate experiments (n=3) are displayed ± standard error of the mean (SEM) * = p = <0.05, ** = p = <0.01, *** = p = <0.001, **** = p = <0.0001.

4.10 PAPAS expression does not change in hypoxia

rDNA transcriptional silencing in response to hypoosmotic stress has been shown to depend on the expression of a long non-coding RNA called PAPAS ("promoter and pre-rRNA antisense"). Briefly, PAPAS was reported to be transcribed by RNPII antisense to the 47S coding region resulting in the recruitment of the CHD4/NuRD complex to remodel the chromatin and repress rDNA transcription (Zhao et al., 2018). I hypothesised that PAPAS could be upregulated in hypoxia to repress rDNA transcription. To investigate the expression of PAPAS in hypoxia, I performed cDNA synthesis using a primer specific to the PAPAS encoding rDNA sequence coupled to the T7-promoter sequence followed by qPCR as used previously to detect PAPAS expression in response to hypoosmotic stress, which is summarised schematically in **Figure 2.1** (Zhao et al., 2016). The PAPAS sequence was

unsuitable to design optimal qPCR primers. Therefore, by priming the cDNA with T7 sequence and then using the T7 promoter primers for qPCR, I could detect the relative T7-coupled PAPAS levels. This method was necessary as PAPAS is expressed at very low levels and are undetectable by conventional qPCR methods (Zhao et al., 2016). PAPAS levels did not change significantly in response to <0.1% O_2 compared to the normoxic control suggesting that PAPAS is not involved in the shutdown of rDNA transcription in hypoxia (**Figure 4.10**). However, in our hands the conditions reported to induce hypoosmotic stress (70% H_2O, 30% DMEM) did not lead to PAPAS upregulation (Zhao et al., 2016). This lack of positive control means I have to interpret this data with caution and cannot therefore formally rule out the involvement of PAPAS.

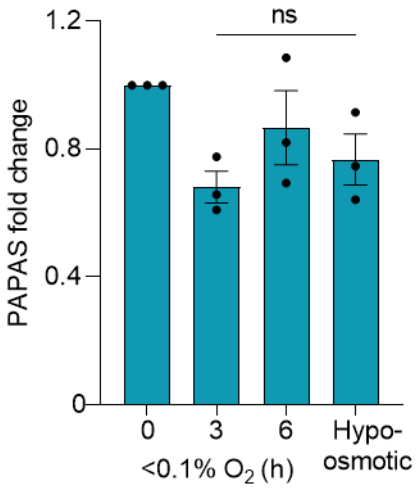


Figure 4.10. PAPAS expression in hypoxia.
HCT116 cells in <0.1% O_2 or hypoosmotic stress (70% H_2O, 30% media, 1 hour) were measured by qPCR for PAPAS expression using the T7 promoter as primers. One-way ANOVA was used to calculate statistical significance. Data from three separate experiments (n=3) are displayed ± standard error of the mean (SEM). ns = not significant.

4.11 Transcriptional repression of rDNA occurs independently of p53

Previous studies have identified p53 as a repressor of transcriptional inhibition (Zhai and Comai, 2000). I considered that the stabilisation and activation of p53 in hypoxic conditions could affect rDNA transcription in hypoxia. Therefore, I employed HCT116 *p53*$^{-/-}$ cells and measured 47S levels by qPCR. The absence of p53 was confirmed by western blot analysis previously (**Figure 3.6A**). In agreement with the EU incorporation data in Chapter 3, I observed rDNA transcriptional repression in <0.1% O_2 in both the p53 wild type and knockout cell lines which suggests hypoxic rDNA transcriptional repression occurs independently of p53 (**Figure 4.11**).

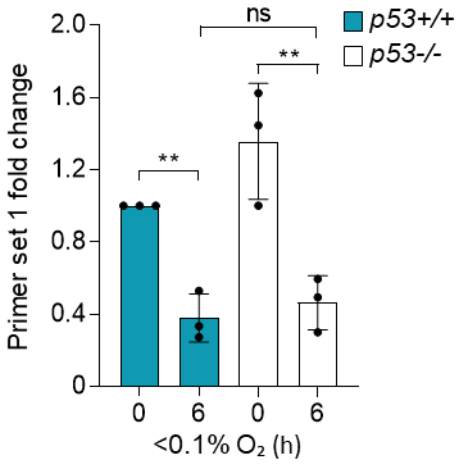


Figure 4.11. rDNA transcriptional repression occurs independently of p53 in hypoxia. HCT116 *p53*$^{+/+}$ and HCT116 *p53*$^{-/-}$ cells in <0.1% O_2 were subjected to qPCR using primer set 1. One-way ANOVA was used to calculate statistical significance. Data from three separate experiments (n=3) are displayed ± standard error of the mean (SEM). ** = p = <0.01, ns = not significant.

4.12 Transcriptional repression of rDNA occurs independently of ATM

ATM has been reported to shutdown rDNA transcription in response to DSBs (Harding et al., 2015; Korsholm et al., 2019; Kruhlak et al., 2007; Mooser et al., 2020). Although DSBs do not accumulate in hypoxia, I postulated that as the DDR is initiated with similar kinetics to the repression of rDNA transcription, ATM could play a role in the repression of rDNA

transcription in hypoxia. The experimental procedure is summarised schematically in **Figure 4.12A**. I used an inhibitor of ATM, KU55933, and confirmed inactivation of ATM signalling by western blotting for KAP1-S824, a downstream target of ATM (**Figure 4.12B**). Treatment with KU55933 did not alleviate transcriptional repression in a time course in <0.1% O_2 which suggests that rDNA silencing in hypoxia does not rely on ATM activity **(Figure 4.12C**). To further validate our findings, I used an alternative inhibitor of ATM, AZD1390, and confirmed inhibition of ATM signalling by western blot for KAP1-S824 (**Figure 4.12D**). In agreement with our previous data using KU55933, treatment with AZD1390 did not rescue transcriptional repression in <0.1% O_2 which supports the ATM-independent mechanism of rDNA transcriptional repression in hypoxia (**Figure 4.12E**).

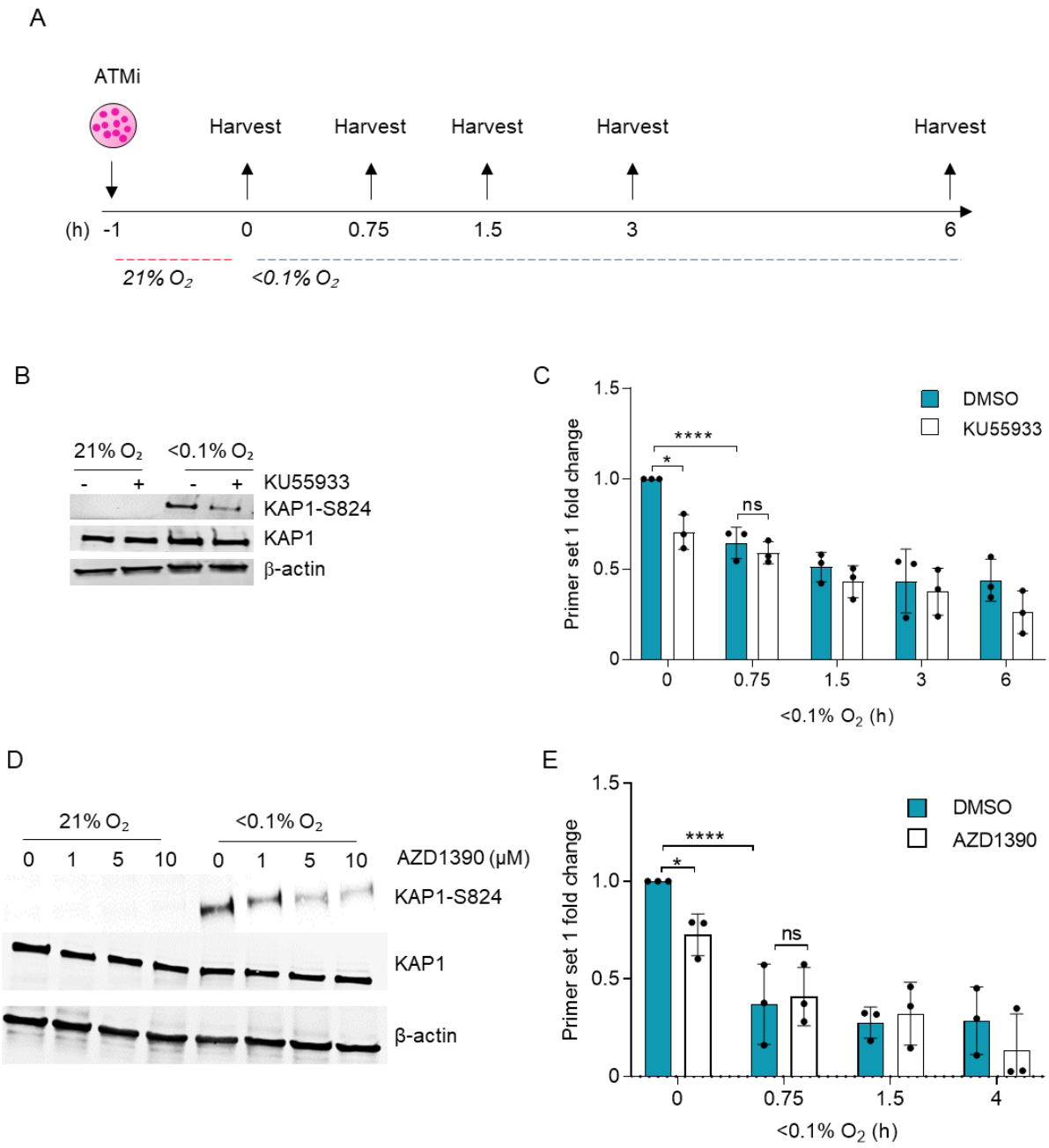


Figure 4.12. rDNA transcriptional repression occurs independently of ATM in hypoxia. Schematic of experimental procedure indicating HCT116 cells in <0.1% O_2 pre-treated with ATM inhibitor (ATMi), KU55933 (1 hour (h) pre-treatment + duration of hypoxia, 10 μM) (A). HCT116 cells in 3 hours <0.1% O_2 treated with KU55933 (1 hour pre-treatment + 3 hours, 10 μM) were subjected to western blot analysis for KAP1-S824, KAP1 and β-actin (B). qPCR analysis of HCT116 cells treated with KU55933 for primer set 1 in <0.1% O_2 (C). HCT116 cells in 2.5 hours<0.1% O_2 treated with AZD1390 (1 hour (h) pre-treatment + duration of hypoxia) were subjected to western blot for KAP1-S824, KAP1 and β-actin (D). HCT116 cells were analysed by qPCR for primer set 1 in <0.1% O_2 treated with AZD1390 (1 hour pre-treatment + 3 hours, 10 μM) (E). Two-way ANOVA was used to calculate statistical significance. Data from three separate experiments (n=3) are displayed ± standard error of the mean (SEM) * = p = <0.05, **** = p = <0.0001, ns = not significant.

4.13 Transcriptional repression of rDNA occurs independently of ATR

Transcriptional repression in response to DSBs has been shown to rely on ATR (Korsholm et al., 2019; Mooser et al., 2020). I hypothesised that activation of ATR in hypoxia may affect rDNA transcription in hypoxia. Therefore, I used an inhibitor of ATR (AZD6738) and measured 47S levels. The experimental design is indicated schematically in **Figure 4.13A**. I confirmed inhibition of ATR signalling by western blot for a downstream target, Chk1-S345 (**Figure 4.13B**). As seen with an ATM inhibitor, treatment of cells with AZD6738 could not rescue transcriptional repression in a time course in <0.1% O_2 (**Figure 4.13C**). These data suggest that the mechanism of rDNA transcriptional shutdown in hypoxia does not rely on ATR. To further validate that ATR is not involved in the transcriptional repression of rDNA in hypoxia, I used the HCT116$^{ATR/-flox}$ cell line containing one intact copy of the *ATR* allele which has significantly reduced levels of endogenous ATR compared to the wild-type cell line (**Figure 4.14D**) (Bencokova et al., 2009). HCT116$^{ATR-/flox}$ cells demonstrated a similar reduction in RNPI transcription to HCT116 wild-type cells in <0.1% O_2 which supports the ATR-independent mechanism of transcriptional repression of rDNA in hypoxia (**Figure 4.14E**).

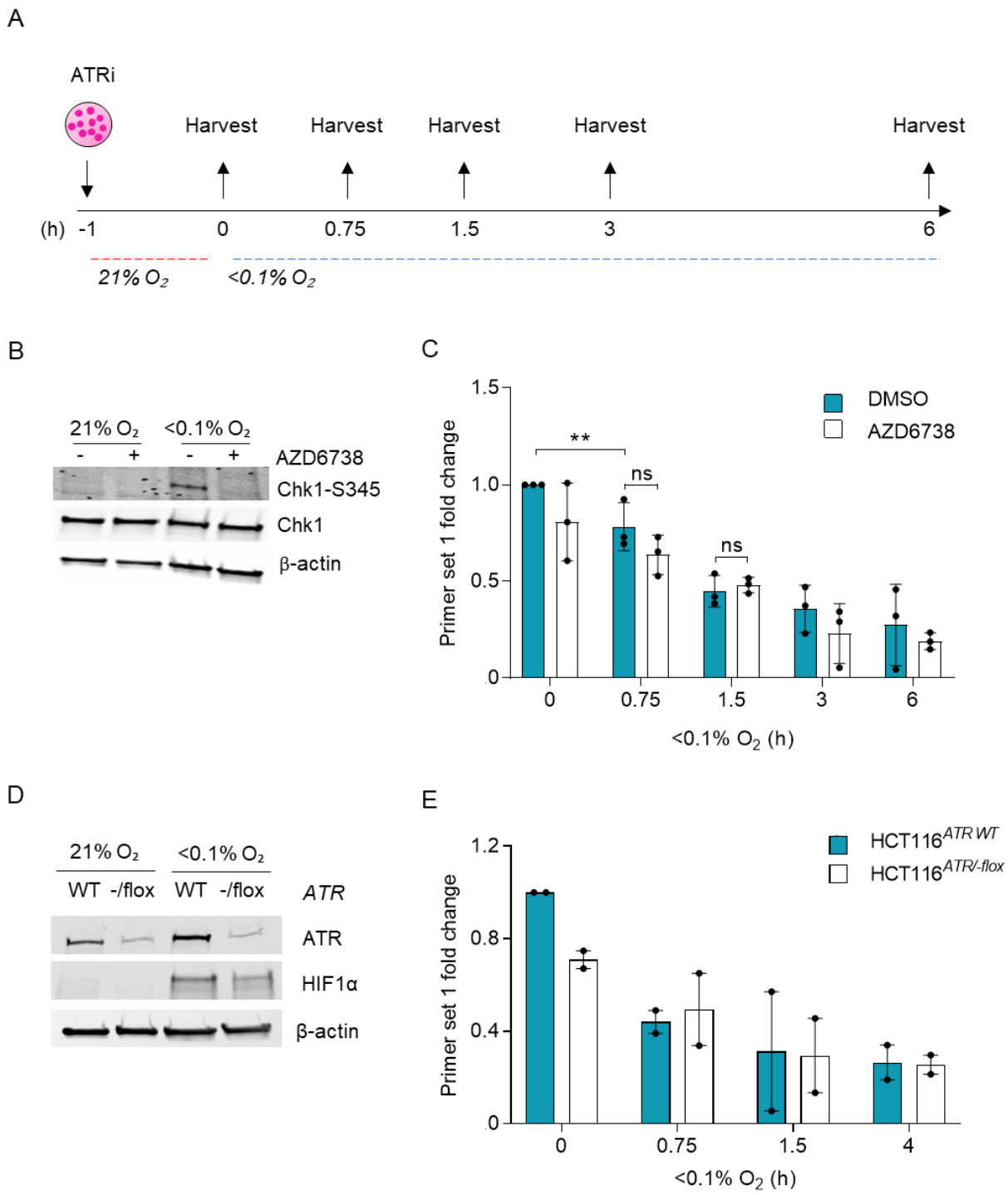


Figure 4.13. rDNA transcriptional repression occurs independently of ATR in hypoxia. Schematic of experimental procedure indicating HCT116 cells in <0.1% O_2 pre-treated with ATR inhibitor (ATRi), AZD6738 (1 hour (h) pre-treatment + duration of hypoxia, 10 μM) (A). HCT116 cells in 6 hours <0.1% O_2 treated with AZD6738 (1 hour pre-treatment + 6 hours, 1 nM) were subjected to western blot analysis for Chk1-S345 (B). qPCR analysis of HCT116 cells treated with AZD6738 for primer set 1 in <0.1% O_2 (C). HCT116$^{ATR\ WT}$ and HCT116$^{ATR/-flox}$ were subjected to western blot to confirm ATR protein levels in 4 h of <0.1% O_2 (D). qPCR for primer set 1 of HCT116$^{ATR\ WT}$ and HCT116$^{ATR/-flox}$ in hypoxia (<0.1% O_2). n=2 (E). Two-way ANOVA was used to calculate statistical significance. Data from three separate

experiments (n=3) are displayed ± standard error of the mean (SEM) ** = p = <0.01, ns = not significant.

4.14 Transcriptional repression of rDNA occurs independently of PERK

Previous studies have shown that pharmacological activation of the UPR with tunicamycin and thapsigargin repress rDNA transcription through activation of EIF2α and PERK (DuRose et al., 2009). As the UPR is active in hypoxic conditions, I hypothesised that UPR activity could repress transcription in hypoxia. To investigate this, I performed PERK knockdown by siRNA in HCT116 cells. I confirmed knockdown of PERK by siRNA by qPCR for mRNA levels of CHOP, a downstream target of PERK, which demonstrated significant reduction with siRNA PERK in <0.1% O_2 (**Figure 4.14A**). The levels of 47S were not rescued upon PERK knockdown in <0.1% O_2 which suggests that the UPR is not involved in the initial repression of rDNA transcription in hypoxia (**Figure 4.14B**). In accordance with the literature, PERK inhibition at longer periods (>6 hours) in hypoxia partially restored transcription which suggests that although PERK is not involved in the initial response, PERK is required for sustained transcriptional repression (**Figure 4.14C**). Supportively, PERK inhibition by siRNA for longer periods (>6 hours) in hypoxia partially restored global transcription which suggests that sustained transcriptional repression relies, in part, on PERK (**Figure 4.14D**).

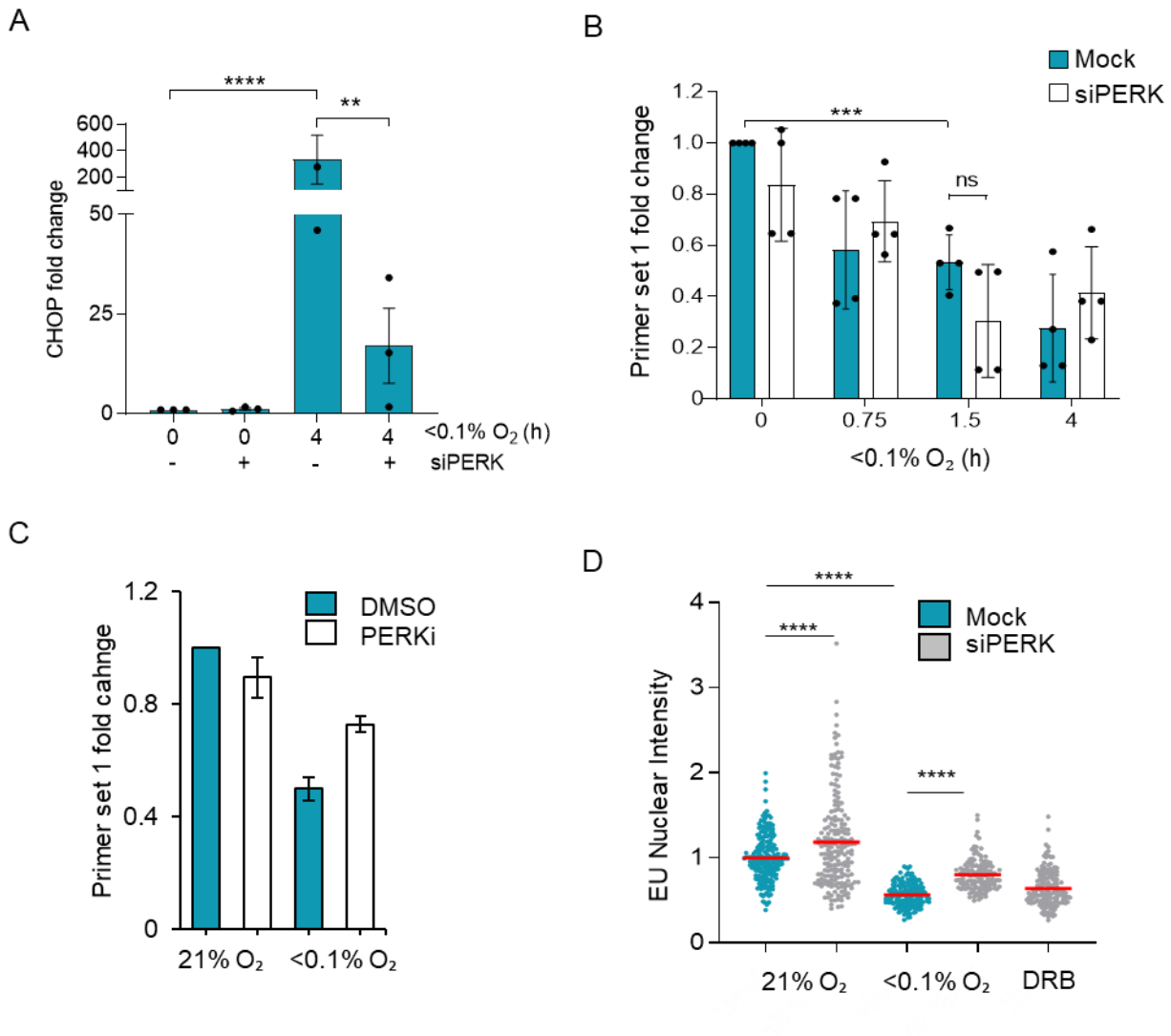


Figure 4.14. Initial rDNA transcriptional repression occurs independently of PERK in hypoxia.

HCT116 cells in 4 hours <0.1% O_2 treated with siRNA against PERK (siPERK) were subjected to qPCR analysis for CHOP (A). qPCR analysis of HCT116 cells treated with siRNA for primer set 1 in <0.1% O_2, n=4 (B). qPCR for primer set 1 in HCT116 cells treated with PERK inhibitor in 6 hours <0.1% O_2. n=1 in triplicate is displayed, error bars represent standard deviation (C). A549 control cells or PERK depleted cells were exposed to 21 or <0.1% O_2 for 6 hours, EU (0.5 mM) was added for the final hour of treatment. DRB was used as the positive control. Cells were fixed, stained and quantified for EU incorporation. Data provided by Shaliny Ramachandran (D). Two-way ANOVA was used to calculate statistical significance. Data from three separate experiments (n=3) are displayed ± standard error of the mean (SEM) * = p = <0.05, ** = p = <0.01, *** = p = <0.001, **** = p = <0.0001, ns = not significant.

4.15 Discussion

Here, I investigated the potential molecular mechanisms for RNPI inhibition in hypoxia. I demonstrate that hypoxia leads to a reduction in NTP levels and that supplementing with nucleosides does not affect transcriptional inhibition in hypoxia. The levels of all NTPs except GTP were restored upon nucleoside addition which may be due to the high turnover or usage of GTP. The reduction in NTP levels may occur through a mechanism involving impairment of function or loss of a metabolic enzyme.

The mechanism of rDNA repression in response to hypoosmotic stress has been shown to be dependent on the expression of PAPAS which recruits chromatin remodelling complex CHD4/NuRD to silence rDNA transcription (Zhao et al., 2018). I demonstrated that PAPAS was not upregulated in hypoxic conditions suggesting a PAPAS-independent mechanism. However, our positive control, hypoosmotic stress, did not result in an induction of PAPAS in our hands which means that I cannot formally exclude PAPAS from the mechanism of rDNA transcriptional repression in hypoxia. I demonstrate RNPI transcriptional repression is unlikely to occur through an RNPII-dependent mechanism. First, RNPII activation marks on the CTD are unaffected until long periods in hypoxia. However, I did not measure the levels of total RNPII in this assay and should treat this result with caution. Secondly, treatment of cells with RNPII inhibitors represses rDNA transcription slower than the hypoxic inhibition of rDNA transcription. These data suggest that a lack of RNPII activity is not responsible for the initial loss of RNPI activity.

The mechanism of transcriptional inhibition in hypoxia differs from that in response to DNA damage (Mooser et al., 2020). First, rDNA transcriptional inhibition does not rely on ATM or ATR activity. This is perhaps surprising given that transcriptional inhibition and activation of a DDR occurs with similar kinetics in hypoxia. However, hypoxic activation of ATM/ATR only occurs in S phase, whereas transcriptional repression occurs in all cell cycle phases

(Bencokova et al., 2009; Olcina et al., 2013). Pre-treatment of 1 hour was used in our experimental design to increase the likelihood that ATM/ATR activity was abolished, however, I have not assayed for ATM/ATR activity at all our times points. It is possible that the residual KAP-S824 signal indicative of ATM activity upon ATMi in hypoxia could affect rDNA transcriptional repression. Our results could be strengthened using cells with a genetic depletion of *ATM* in hypoxia. By using the HCT116$^{ATR-/flox}$ cells I reduced endogenous levels of ATR protein. However, I could not deplete *ATR* levels completely as this would lead to cell death as *ATR* is an essential gene. Furthermore, I did not use a positive control in ATM/ATR experiments, therefore I cannot formally rule out ATM or ATR in the hypoxic mechanism for rDNA transcriptional repression.

The mechanism of transcriptional inhibition in response to DSBs requires the nucleolar localisation of TCOF1/TopBP1 to activate ATR signalling. I demonstrate here that TCOF1 does not fuse puncta in the nucleolus in hypoxia which supports that the mechanism of transcriptional inhibition in hypoxia does not rely on the same mechanisms in response to DSBs and therefore relies on an alternative and novel mechanism to that of other reported stresses (Mooser et al., 2020; Velichko et al., 2019).

Together, these data suggest that there is a distinct mechanism for RNPI transcriptional repression in hypoxia that has not yet been described in the literature. In the following chapter, I focus our studies on the role of R-loops in the repression of rDNA in hypoxia.

Chapter 5

Hypoxia leads to R-loop formation in the nucleolus which impact rDNA transcription

5.1 Introduction

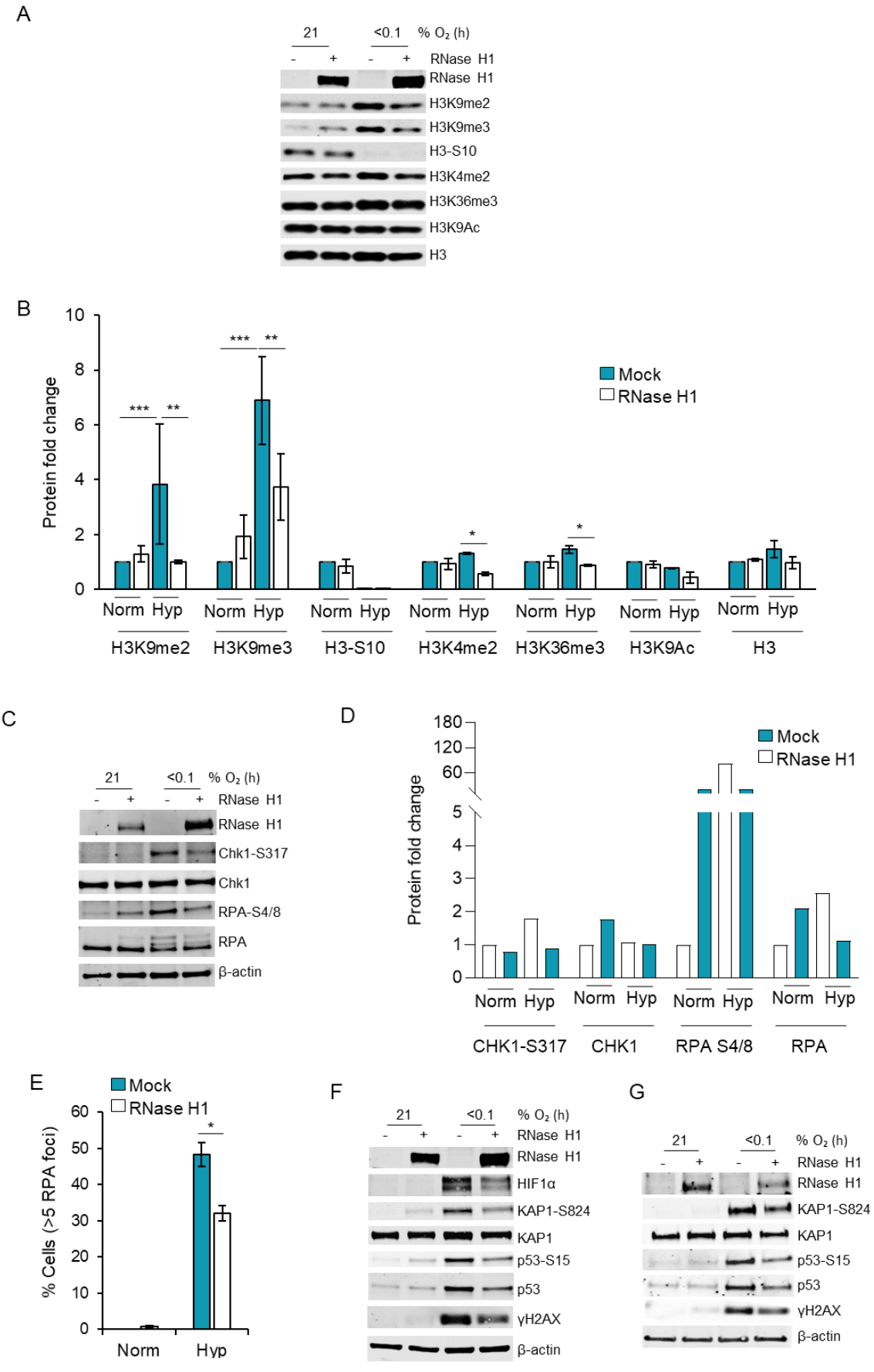
R-loops, or DNA/RNA hybrids are a potential threat to genome stability as discussed in Chapter 1. A number of factors are known to resolve R-loops, for example SETX, whereas the enzyme RNase H1 specifically degrades the RNA component of the R-loop, both of which help regulate basal R-loop levels. Recent work in our laboratory has described the accumulation of R-loops in response to hypoxia (Ramachandran et al., 2020). R-loops are proposed to help recruit chromatin remodelling complexes such as G9a to gene loci to promote transcriptional silencing via the formation of heterochromatin (Skourti-Stathaki et al., 2014). Hypoxia has been demonstrated to lead to increased global levels of heterochromatin, although the role of R-loops in heterochromatin formation has not been investigated.

The hypoxic activation of ATM signalling has been demonstrated to be, in part, due to RS which activates ATR, in the context of a heterochromatic environment. ATM/ATR signalling has been shown to be activated in response to R-loops (Tresini et al., 2015). Therefore, I hypothesise that an accumulation of R-loops in a heterochromatic environment in hypoxia could lead to activation of ATM/ATR signalling.

In the previous chapter, I ruled out several potential mechanisms for the transcriptional repression of rDNA in hypoxia. R-loops have also been demonstrated to block RNPI progression in response to mild hypoosmotic stress (Velichko et al., 2019). Here I will focus on the role of R-loops in the repression of rDNA in hypoxia.

5.2 R-loops impact the biological response to hypoxia

R-loop accumulation has recently been described in hypoxia, although their impact on the hypoxic biological response is unknown (Ramachandran et al., 2020). I first overexpressed RNase H1 which degrades the RNA in an R-loop to determine the impact on the biological response to hypoxia. R-loops can lead to a localised increase in H3K9me2 and to replication stress, both of which are part of the hypoxic response (Groh et al., 2014; Skourti-Stathaki et al., 2014). Overexpression of RNase H1 lead to a decrease in H3K9me2 (3-fold) and H3K9me3 (3-fold) in hypoxia but had no significant impact on the levels of these marks in normoxic conditions (**Figure 5.2A, B**). These data show that heterochromatin formation in hypoxia is dependent on R-loop formation, which possibly by acts as a landing pad for histone methyltransferases recruitment such as G9a (Skourti-Stathaki et al., 2014). As expected, exposure to 6 hours of <0.1% O_2 led to phosphorylation of RPA and Chk1, confirming RS. However, cells overexpressing RNase H1 showed decreased levels of hypoxic RPA and Chk1 phosphorylation, and RPA foci in comparison to the mock treated cells which indicate that R-loops may impede the replication fork resulting in RS (**Figure 5.2C, D, E**). It has been previously shown that RS and a heterochromatic environment lead to an ATM-dependent DDR in hypoxia (Olcina et al., 2013). Overexpression of RNase H1 led to a decrease in ATM signalling, including reduced KAP1-S824, p53-S15 and γH2AX in hypoxia (**Figure 5.F, H**). Decreased ATM-mediated activity in response to RNase H1 overexpression in hypoxia was confirmed in a second cell line in RKO (**Figure 5.2G**). These data suggest that a combination of heterochromatin formation and replication stress that are induced through R-loop formation, lead to ATM activation in hypoxic conditions. Together, these data demonstrate that overexpression of RNase H1 significantly impacts both RS and the DDR in hypoxia (<0.1% O_2) suggesting that R-loops accumulate in hypoxic conditions.


A
21
<0.1
% O2 (h)
- + - +
RNase H1
RNase H1
H3K9me2
H3K9me3
H3-S10
H3K4me2
H3K36me3
H3K9Ac
H3
B
Protein fold change
Mock
RNase H1
Norm Hyp
H3K9me2
H3K9me3
H3-S10
H3K4me2
H3K36me3
H3K9Ac
H3
C
RNase H1
Chk1-S317
Chk1
RPA-S4/8
RPA
β-actin
D
Protein fold change
CHK1-S317
CHK1
RPA S4/8
RPA
E
% Cells (>5 RPA foci)
F
HIF1α
KAP1-S824
KAP1
p53-S15
p53
γH2AX
β-actin
G

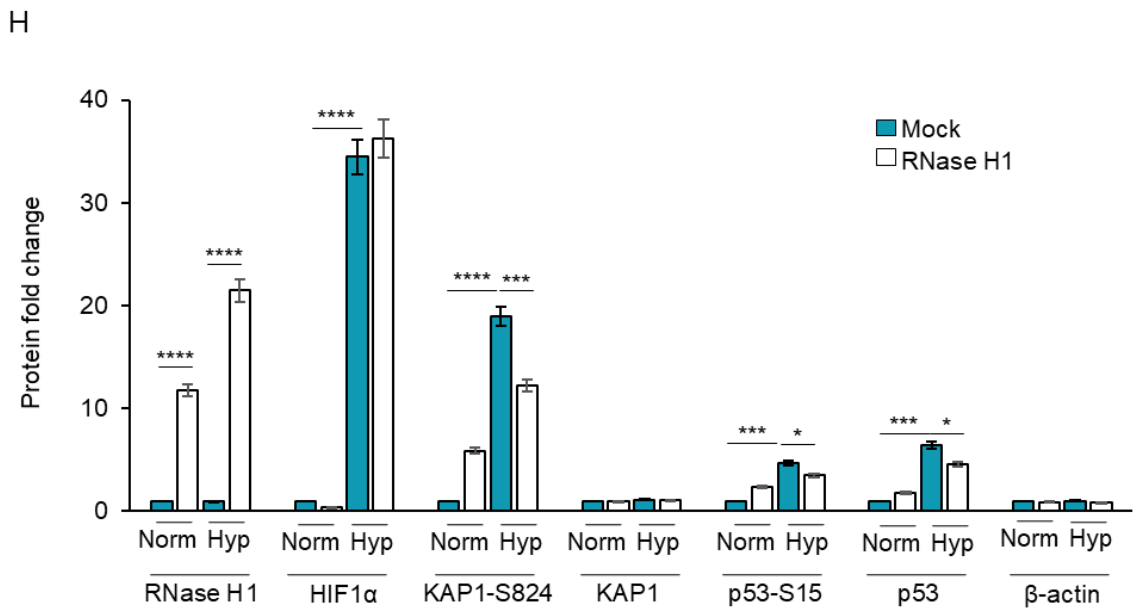


Figure 5.2. RNase H1 overexpression impacts the biological response in hypoxia.
RNase H1 was overexpressed in HCT116 cells in 6 hours of <0.1% O_2 and subjected to western blot for histone modifications. H3 is used as a loading control (A). Quantification of chromatin modification western blots from A. n=2 (B). RNase H1 overexpression was performed as in A and blotted for markers of RS. β-actin was used as a loading control (C). Quantification of replication stress marker western blots from C. n=1 (D). RPA foci were quantified in HCT116 cells with RNase H1 overexpression in 6 hours of <0.1% O_2 (Hyp). Values are plotted as cells with >5 RPA foci. Data from three independent experiments (n=3) are displayed ± standard error of the mean (SEM) (E). RNase H1 overexpression was performed in HCT116 cells in <0.1% O_2 and western blot analysis was carried out for markers of ATM signalling. Images shown are representative of n=2 (F). RNase H1 was overexpressed in RKO cells in 6 hours of <0.1% O_2 and subjected to western blotting for ATM signalling. n=1 (G). Quantification of ATM signalling target western blots from F. n=2 (H). One-way ANOVA was used to calculate statistical significance. * = p = <0.05, ** = p = <0.01, *** = p = <0.001, **** = p = <0.0001. Data generated by Shaliny Ramachandran.

5.3 R-loops accumulate in hypoxic conditions in the nucleolus

The impact of RNase H1 on the biological response to hypoxia strongly suggested that R-loops accumulate in hypoxia. To investigate this, I used the S9.6 antibody to detect R-loops. Supportively, these images revealed that R-loops do accumulate in hypoxic conditions in the entire nucleus, but more noticeably in the nucleolus (**Figure 5.3A, B**). The specificity of the antibody was confirmed by treatment with recombinant RNase H.

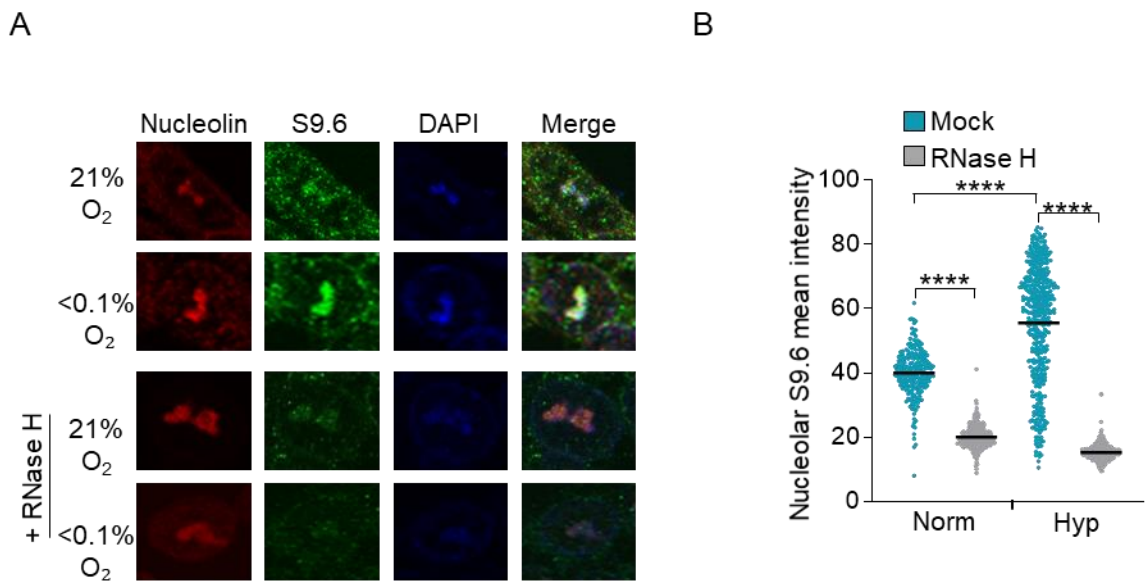


Figure 5.3. R-loops accumulate in the nucleolus in hypoxia.
S9.6 co-immunofluorescence with nucleolin in 1.5 hours of <0.1% O_2 in HCT116 cells. RNase H treatment was used to decrease S9.6 levels. Representative images are shown (A). Quantification of nucleolar S9.6 levels in A (B). Two-way ANOVA was used to calculate statistical significance. Data from three separate experiments (n=3) are displayed ± standard error of the mean (SEM) **** = p = <0.0001.

5.4 Transcription of rDNA can be rescued by RNase H1 overexpression in hypoxia

Having determined that R-loops accumulate and play a role in the biological response to hypoxia, I next sought to determine if R-loops play a role in the repression of rDNA transcription in hypoxia. I overexpressed RNase H1 to reduce the levels of R-loops in hypoxia and measured 47S levels using primer set 1. RNase H1 overexpression was confirmed by western blot, endogenous levels of RNase H1 were not detectable (**Figure 5.4A**). Strikingly, overexpression of RNase H1 lead to around a 20-fold induction of 47S levels at 1.5 hours of <0.1% O_2. rDNA transcription was restored to normoxic levels by 6 hours of <0.1% O_2 (**Figure 5.4B**). These data demonstrate the importance of R-loops in the inhibition of rDNA transcription in hypoxia.

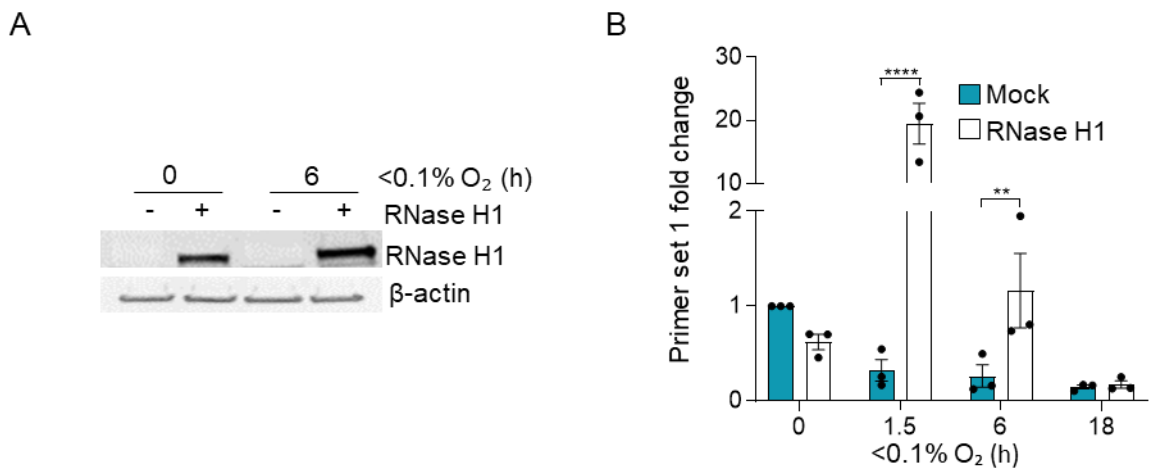


Figure 5.4. RNase H1 overexpression results in higher levels of 47S production in hypoxia. RNase H1 overexpression in 6 hours of <0.1% O_2 was confirmed in HCT116 cells by western blot (A). qPCR using primer set 1 in HCT116 cells overexpressing RNase H1 in <0.1% O_2 (B). Two-way ANOVA was used to calculate statistical significance. Data from three independent experiments (n=3) are displayed ± standard error of the mean (SEM) ** = p = <0.01, **** = p = <0.0001.

5.5 RNase H1 overexpression does not affect pre-rRNA processing in hypoxia

I hypothesised that the R-loop formation in hypoxia may also affect processing of rRNA. To test this, I used measured cleavage at A0 on the 5'ETS by qPCR, as described in Chapter 3. Interestingly, the processing defect at the site of A0 on the 5'ETS still remained upon overexpression of RNase H1 in hypoxia which indicates that the processing defect occurs independently of RNase H1. These data suggest that the processing defect in hypoxia is mechanistically distinct to the repression of rRNA transcription (**Figure 5.5**).

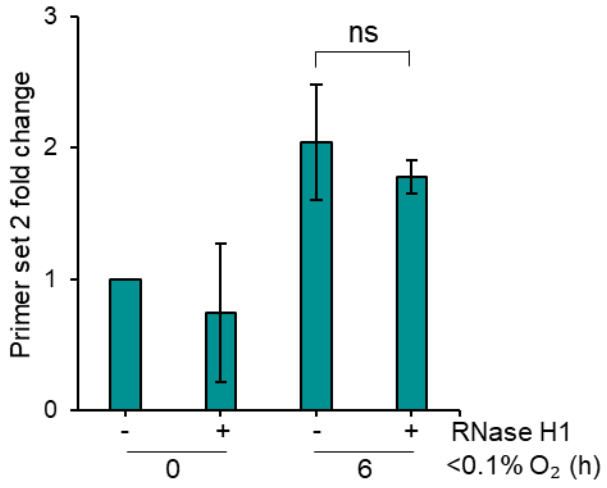


Figure 5.5. RNase H1 overexpression does not affect processing at A0 on the 5'ETS in hypoxia.
qPCR using primer set 2 to measure processing at A0 on the 5'ETS in HCT116 cells overexpressing RNase H1 in 6 hours of <0.1% O_2. Two-way ANOVA was used to calculate statistical significance. Data from three independent experiments (n=3) are displayed ± standard error of the mean (SEM). ns = not significant.

5.6 C-MYC repression is not rescued by RNase H1 overexpression in hypoxia

Our data suggests that R-loops form in hypoxia to block RNPI transcription. A known driver of RNPI transcription, C-MYC, has been shown to be repressed by R-loop formation on the *C-MYC* locus (Yang et al., 2014). This led us to re-consider the role of C-MYC in hypoxia-mediated repression of RNPI and specifically if repression of C-MYC in hypoxia could in part be R-loop dependent. Therefore, I evaluated the expression of C-MYC protein levels in hypoxia with RNase H1 overexpression. The repression of C-MYC could not be rescued with RNase H1 overexpression which suggests that the repression of RNPI transcription in hypoxia is not due to R-loop formation on the *C-MYC* locus (**Figure 5.6**).

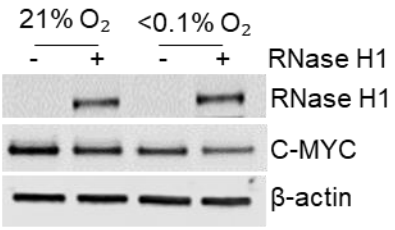


Figure 5.6. RNase H1 overexpression does not rescue C-MYC repression in hypoxia. HCT116 cells upon RNase H1 overexpression were subjected to western blot for C-MYC levels. n=2

5.7 R-loops form on the rDNA in hypoxia

Next, I considered a direct mechanism for RNPI transcriptional inhibition in hypoxia. To investigate this, I measured R-loops on the rDNA by DNA/RNA immunoprecipitation (DRIP). As a positive control, cells were treated with camptothecin (CPT) as this has been demonstrated to increase R-loop formation at the rDNA (Shen et al., 2017). I designed qPCR primers to three regions of the rDNA based on previous reports of the location of stress-induced R-loop accumulation, upstream of the main promoter (D1), in the 28S region (D2) and in the IGS (D3) (**Figure 5.7A**) (Velichko et al., 2019). As predicted from the S9.6 nucleolar immunofluorescence data in Figure **5.3**, a significant increase in R-loops was detected at D1; importantly this signal was sensitive to RNase H1 and also increased in response to CPT. R-loop accumulation could also be detected at the 28S region demonstrating widespread R-loop accumulation across the 47S-coding region (D2). Interestingly, R-loops did not form in the IGS region of the rDNA in hypoxia (D3) indicating that R-loop accumulation in hypoxia on the rDNA does not occur across the entire rDNA repeat and are distinct to those induced by CPT (**Figure 5.7B**). As R-loop formation was restricted to the 47S-coding region of the rDNA, this suggested R-loop formation in hypoxia is a mechanism to physically block and inhibit RNPI progression and therefore the production of rRNA. In support of this hypothesis, the lack of R-

loops at the IGS region suggests that RNPI does not reach the IGS region in hypoxia as RNPI due to barriers in the 47S-coding region.

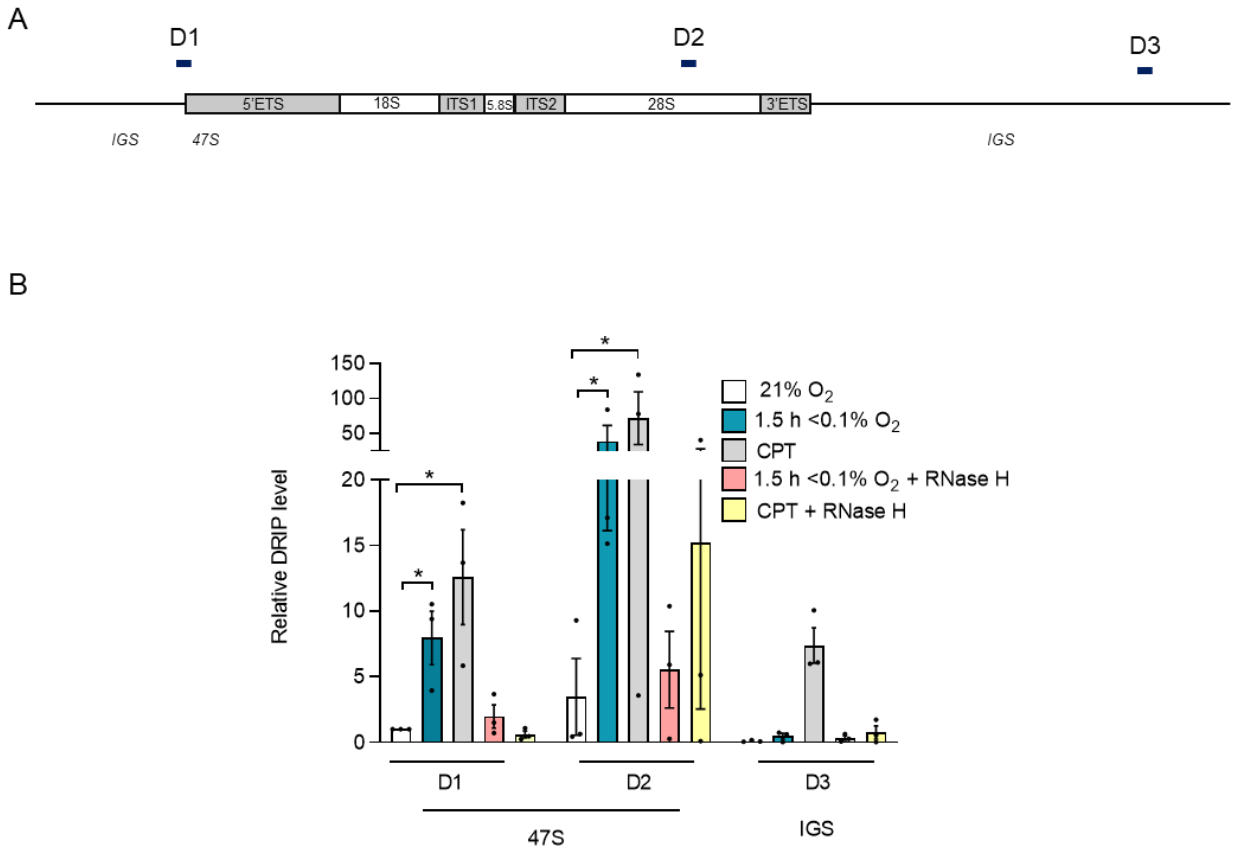


Figure 5.7. R-loops accumulate on the rDNA in hypoxia.
Schematic of DNA/RNA immunoprecipitation (DRIP) amplicon positions on the rDNA. D1 – 5' rDNA promoter. D2 – 3' 28S rRNA region. D3 - IGS (A). DRIP levels in HCT116 cells in 1.5 hours <0.1% O_2. CPT, camptothecin (2 µM, 1 hour) was used a positive control. RNase H was used to decrease DRIP signal. Values were normalised to the normoxic control sample of D1. Student's t-test was used to calculate statistical significance. Data from three independent experiments (n=3) are displayed ± standard error of the mean (SEM) * = p = <0.05, ** = p = <0.01, *** = p = <0.001, **** = p = <0.0001.

5.8 Senataxin knockdown leads to reduced R-loops on the rDNA in hypoxia

Senataxin (SETX) is a putative RNA/DNA helicase that unwinds DNA/RNA hybrids leading to resolution of R-loops (Skourti-Stathaki et al., 2011). Using siRNA to SETX I increased R-loops in hypoxia and determined the rate of loss of RNPI activity. An increase in R-loops by siRNA was determined by slot blot assay (**Figure 5.8A**). SETX knockdown was confirmed by

qPCR for SETX mRNA levels (**Figure 5.8B**). Interestingly, SETX mRNA levels increased in hypoxic conditions (Ramachandran et al., 2020). Intriguingly, cells lacking SETX resulted in reduced R-loops over the 47S coding region in <0.1% O_2 (**Figure 5.8C**). These data suggest that although SETX reduces R-loops on a global level, SETX induces R-loops locally on the rDNA in hypoxia to limit RNPI transcription. Next, we investigated whether other R-loop regulatory factors are affected in hypoxia. In contrast to SETX mRNA, other R-loop factors mRNA levels, most notably PIF1, were repressed in hypoxic conditions (**Figure 5.8D**). These data demonstrate that SETX induction is unique among other known R-loop regulatory factors, supporting its function in R-loop regulation on the rDNA in hypoxia.

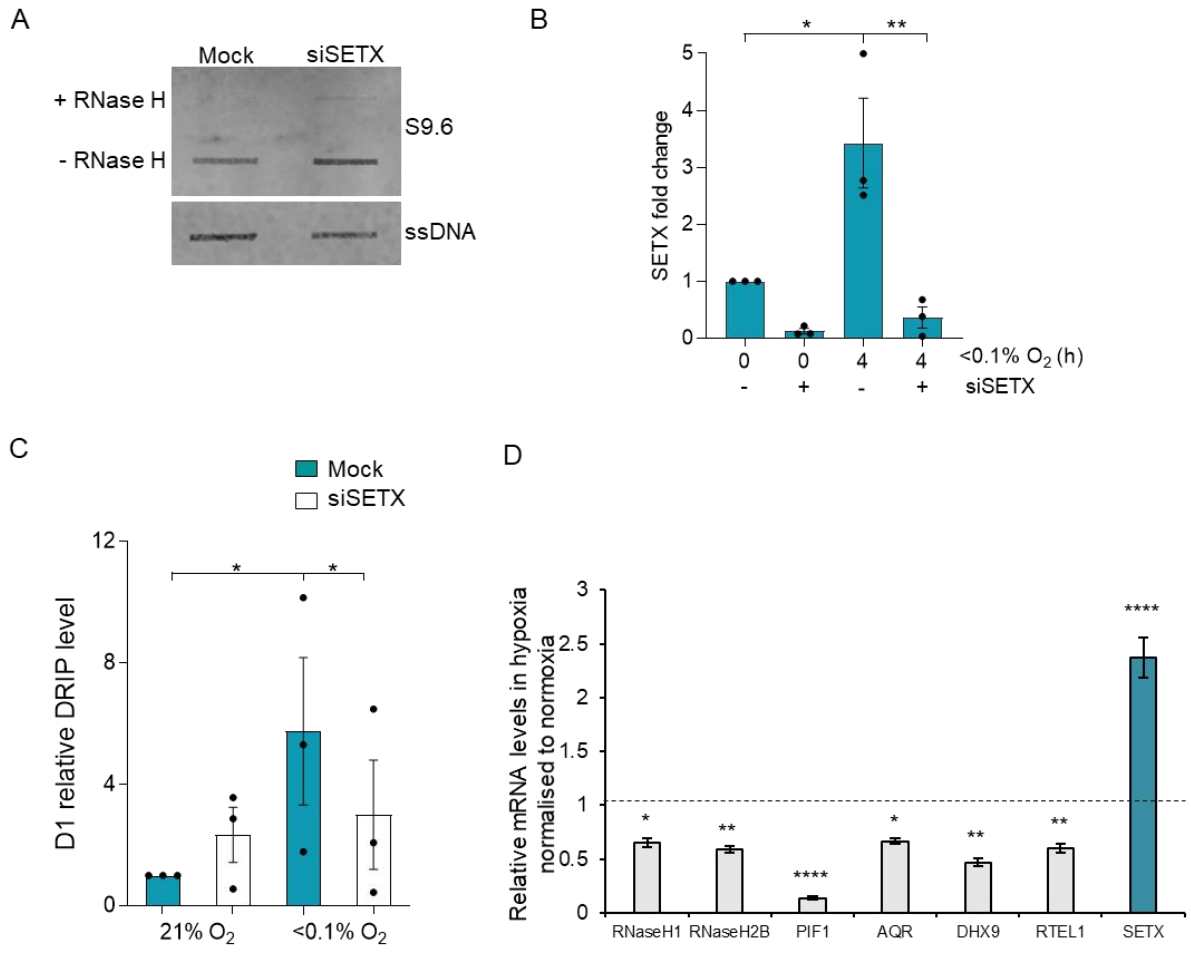


Figure 5.8. Senataxin knockdown in hypoxia leads to reduced R-loops on the rDNA.
Slot blot assay for S9.6 levels in HCT116 cells in normoxia treated with siSETX. ssDNA was used as a loading control. Data provided by Shaliny Ramachandran (A). SETX mRNA levels

were determined by qPCR of HCT116 cells in 4 hours of <0.1% O_2, n=3 (B). D1 DRIP level upon siSETX in 1.5 hours of <0.1% O_2, n=3 (C). mRNA expression panel of R-loop regulatory factors in A549 cells in 6 hours of <0.1% O_2, n=3 Data provided by Shaliny Ramachandran (D). Two-way ANOVA was used to calculate statistical significance. Data are displayed ± standard error of the mean (SEM) * = p = <0.05, ** = p = <0.01, *** = p = <0.001. **** = p = <0.0001

5.9 Heterochromatin forms on the rDNA in hypoxia

R-loop formation has been shown to lead to localised heterochromatin deposition (Groh et al., 2014; Skourti-Stathaki et al., 2014). Hypoxia has been shown to lead to heterochromatin formation (Johnson et al., 2008). Moreover, histone modifications on the rDNA has been reported to epigenetically silence rDNA transcription (Yu et al., 2015). To further investigate the mechanism of RNPI repression in hypoxia, I postulated that a heterochromatic environment could accompany R-loop formation on the rDNA in hypoxia. ChIP for H3K9me3 at the D1 and D2 regions after 1.5 hours at <0.1% O_2 demonstrated an accumulation of H3K9me3 over the 47S coding region of the rDNA suggesting that heterochromatin acts to prevent RNPI transcription in hypoxia (**Figure 5.9**).

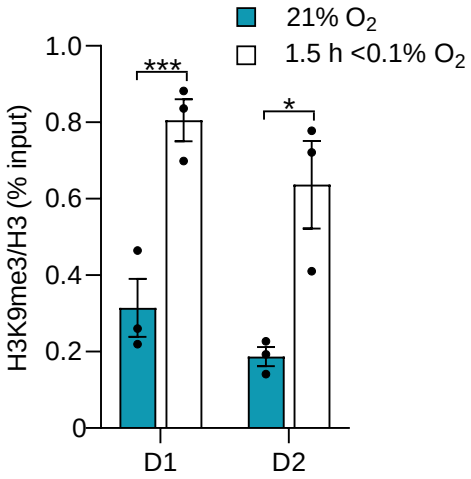


Figure 5.9. Heterochromatin accumulates on the rDNA in hypoxia.
HCT116 cells were subjected to ChIP for H3K9me3/H3 in 1.5 hours of <0.1% O_2 using probes D1 and D2. Values are expressed as % input minus the no antibody control sample value.

Student's t-test was used to calculate statistical significance. Data from three independent experiments (n=3) are displayed ± standard error of the mean (SEM) * = p = <0.05, ** = p = <0.01, *** = p = <0.001.

5.10 Heterochromatin formation on the rDNA is RNase H1-sensitive in hypoxia

I further hypothesised that the H3K9me3 formation on the rDNA may rely on R-loop formation in hypoxia. Supporting this notion, RNase H1 overexpression resulted in a significant reduction of basal levels of H3K9me3 in normoxia on the rDNA suggesting that the mechanism for heterochromatin formation on the rDNA relies on R-loop formation. Most importantly, as predicted from the western blots in **Figure 5.2** which showed a reduction in global heterochromatin marks upon RNase H1 overexpression in <0.1% O_2, H3K9me3 deposition on the rDNA was reduced when RNase H1 was overexpressed in hypoxia indicating that R-loops leads to heterochromatin formation in hypoxic conditions (**Figure 5.10**). In summary, these data demonstrate that R-loops accumulate on the rDNA in hypoxia to block RNPI progression resulting in reduced rDNA transcription and increased heterochromatin.

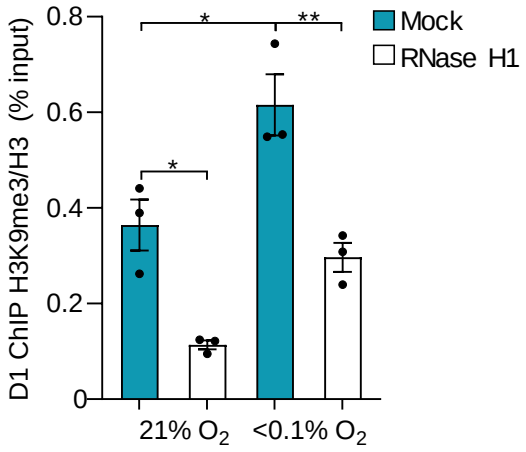


Figure 5.10. Heterochromatin accumulation on the rDNA is RNase H1-sensitive.
HCT116 cells overexpressing RNase H1 were subjected to ChIP for H3K9me3/H3 in 1.5 hours of <0.1% O_2 using probes D1. Values are expressed as % input minus the no antibody control sample value. Student's t-test was used to calculate statistical significance. Data from three independent experiments (n=3) are displayed ± standard error of the mean (SEM) * = p = <0.05, ** = p = <0.01.

5.11 Discussion

In this chapter, in line with previous work from our lab, I demonstrate that R-loops accumulate in hypoxia (Ramachandran et al., 2020). The rapid induction of R-loops in hypoxia may act as a signal of transcriptional stress to the cell, leading to a further cascade of stress-response signalling pathways. R-loops have previously been shown to activate non-canonical ATM signalling through spliceosomal displacement (Tresini et al., 2015). We show that by reducing R-loops through the overexpression of RNase H1 in hypoxia, both the DDR and replication stress responses are alleviated. The reduction in RS in hypoxia upon RNase H1 overexpression could be due to less R-loops forming barriers to replication fork progression (Gan et al., 2011). The combination of reduced replication stress and H3K9me3 in hypoxia would be expected to reduce ATM activation (Olcina et al., 2013). Together, these data highlight transcriptional stress as an additional signal to nucleotide depletion in the induction of ATM/ATR signalling in hypoxia.

Our data demonstrates that in hypoxia, one of the sites of R-loop accumulation is on the 47S coding region of the rDNA which suggests that these R-loops form a barrier to pause rDNA transcription. In support of this, a previous report found that the rDNA loci are a 'hot-spot' for R-loop formation (Nadel et al., 2015). Our data demonstrate that R-loops that accumulate on the 47S coding region are induced in a SETX-dependent manner which may suggest that SETX forms a protective R-loop shield to limit rRNA synthesis. Specifically, the hypoxia-induced barrier to rDNA transcription is accompanied by increased H3K9me3 and therefore a more heterochromatic and transcriptionally silent context. The mechanism of increased H3K9me3 by R-loops has been reported to be due to induction of localized antisense transcription leading to double stranded RNA and recruitment of the RNAi-associated factors, dicer, AGO1 or AGO2 and recruitment of heterochromatic proteins such as the HP1 isoforms (Skourti-Stathaki

et al., 2014). It is possible that heterochromatin formation in hypoxia occurs through mechanisms involving HP1. Further studies into the methyltransferases responsible for H3K9me3 deposition on the rDNA will be a further addition to the mechanism already described here.

Chapter 6

Discussion and conclusions

Characterisation of the transcriptional response to hypoxia is important to understand the molecular mechanisms underpinning the adaptive response to low oxygen tensions. Here I provide an analysis of transcriptional repression in hypoxia.

From my studies, I hypothesise the following working model which is summarised in **Figure 6.1**. I propose that under hypoxic conditions, R-loops form over the 47S coding region of the rDNA in a SETX dependent and heterochromatin linked manner to restrict RNPI activity.

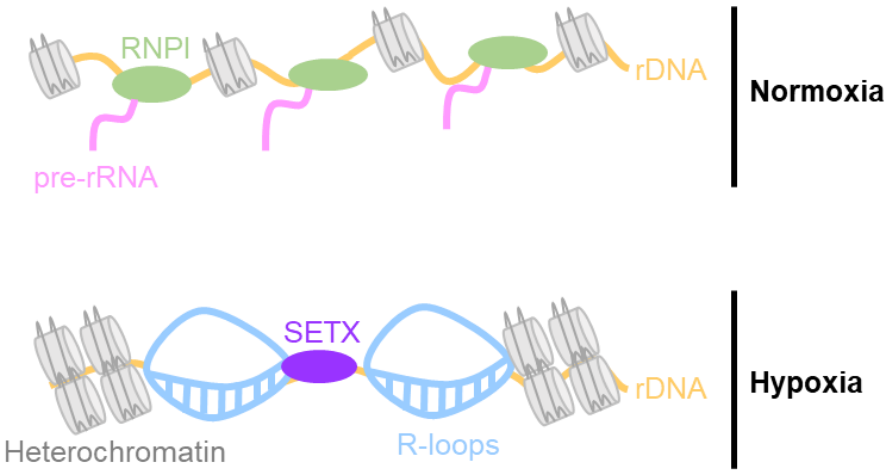


Figure 6.1. Model hypothesis of rDNA transcriptional repression in hypoxia. SETX localisation on the rDNA chromatin induces R-loops over the 47S region of the rDNA and heterochromatin formation blocks RNPI transcription and limits rRNA synthesis.

I demonstrate that the global transcriptional repression known to occur in hypoxic conditions includes the repression of rDNA transcription which rapidly occurs within 1.5 hours in an oxygen dependent manner. The efficient and quick repression of rDNA transcription is likely to be crucial to prevent TRCs and genome instability. To our knowledge, the current literature has shown rDNA transcriptional repression in longer periods of mild hypoxia in acidic

conditions (>22 hours, 1% O_2), whereas our data demonstrates that transcriptional repression occurs in response to short and severe periods of hypoxia. The previous study deduces that rDNA transcriptional repression is due the acidic conditions that accompany prolonged hypoxia which leads to a loss of UBF binding to the rDNA. Whether this mechanism applies to our study remains unknown. This could be addressed by carrying out a UBF ChIP in hypoxia over the rDNA repeat. Furthermore, a study has shown that global RNA synthesis is reduced in hypoxia (<0.01% O_2), which could and is likely to include a reduction in rRNA synthesis (Johnson et al., 2008).

Strikingly, I demonstrate that R-loops significantly increase at the site of rDNA transcription, the nucleolus. These studies have a potential caveat in that the S9.6 antibody that was used to generate our data has been reported to also bind to double stranded RNA (dsRNA). Therefore, this raises the possibility that the S9.6 antibody may not bind solely to R-loops (Hartono et al., 2018). However, to obtain confidence in the antibody, I treated the samples with recombinant RNase H which specially degrades the RNA component of the DNA/RNA hybrid and found the S9.6 signal was reduced upon RNase H treatment. Additionally, future experiments using RNase III treatment, which specifically degrades dsRNA, followed by S9.6 immunofluorescence intensity measurements will confirm the specificity of the signal obtained from the S9.6 antibody. Our data could be strengthened by using an alternative approach such as the V5-tagged RNase H1 catalytically dead mutant protein construct to visualise R-loops in hypoxia (Chen et al., 2017). This construct is a catalytically inactive version of RNase H1 through a mutation at D210N allowing binding and expression of an epitope tag, V5, to R-loops which can be probed for and visualised using an anti-V5-tag antibody.

Importantly, I discovered that the accumulation of R-loops plays a functional role in the regulation of RNPI activity in response to hypoxia. I demonstrated the functional role of R-loops on RNPI activity through RNase H1 overexpression which relieved the initial

transcriptional repression of rDNA in hypoxia. Further studies to validate this finding will require the use of an RNase H1 enzymatically dead mutant as mentioned previous, or by using the three specific mutations (W43A, K59A, K60A) and the D210N mutant version of RNase H1 (WKKD) which inactivates enzymatic and binding abilities to rule out the possibility that RNase H1 overexpression rescuing transcription could be an artefact (Chen et al., 2017). Recently, Abraham et al., developed a novel technology to deplete R-loop levels at specific rDNA loci using RNA-guided RNase H activity (Abraham et al., 2020). This technique allows for site-specific reduction of R-loops, providing greater specificity of the manipulation of R-loop location than using a global overexpression vector of RNase H which could lead to indirect effects. It would be of great interest to implement this technology to study the effects of rDNA R-loops in hypoxia.

Interestingly, I found that depleting SETX reduced the levels of R-loops at the rDNA which suggests that although SETX resolves R-loops elsewhere in the genome, SETX induces the formation of R-loops on the rDNA in hypoxia, leading to transcriptional repression. A recent report demonstrated that SETX forms an R-loop protective shield with RNPII on the rDNA to limit the spurious production of sincRNA on the non-coding IGS regions of the rDNA. I found that there was no accumulation of R-loops on the IGS region in hypoxia so it is unlikely that SETX in hypoxia acts through the same mechanism as in Abraham et al., (Abraham et al., 2020). It is plausible that SETX forms a protective shield with RNPI on the 47S coding region of the rDNA in hypoxia to limit transcription although it is unclear how SETX regulates rDNA associated R-loops and RNPI transcription. A ChIP for SETX on the rDNA in hypoxia would be useful to assess this hypothesis.

Interestingly, many factors associated with R-loop resolution such as PIF1 are repressed in hypoxia at the mRNA level except for SETX which was found to be hypoxia-inducible (Ramachandran et al., 2020). Our data provides a novel role for SETX through the induction

of R-loops on the rDNA in the control of RNPI progression in response to hypoxia. Interestingly, the rescue of RNPI transcription upon RNase H1 was not evident at longer periods of hypoxia (18 hours) which suggest that R-loops are important during the initial phase of hypoxic rDNA transcriptional repression but are not required to sustain transcriptional repression.

I provide data that demonstrates that heterochromatin formation on the rDNA in hypoxia is impaired by RNase H1 overexpression. From these data, our hypothesis is that R-loops are necessary for heterochromatin formation on rDNA, potentially acting as landing pads for the recruitment of methyltransferases to the chromatin which leads to H3K9me3 formation. Further investigation by ChIP into the methyltransferase responsible for H3K9me3 distribution on the rDNA will provide a further insight into the mechanism of rDNA transcriptional repression in hypoxia. The mechanism of increased H3K9me3 by R-loops has been reported to be due to induction of localised antisense transcription leading to double stranded RNA and recruitment of the RNAi-associated factors, dicer, AGO1 or AGO2 and recruitment of heterochromatic proteins such as the HP1 isoforms (Skourti-Stathaki et al., 2014).

Furthermore, RNase H1 overexpression in hypoxic cells impacts the hypoxic biological response through a reduction in DDR signalling. Together, these data suggest that R-loops mediate heterochromatin formation which contributes to ATM/ATR activation in hypoxia. This is of particular interest to the field of hypoxia, as although previous studies have shown that a heterochromatin context with concomitant RS, in part, leads to ATM activation, our knowledge of how ATM is activated was incomplete (Olcina et al., 2013). R-loops have been reported to activate non-canonical ATM signalling to impede spliceosomal assembly and trigger alternative splicing (Tresini et al., 2015).

Therefore, the data presented here provides an additional component, R-loops, to the molecular pathway of DDR activation in hypoxic conditions. It remains unknown whether the R-loops present on the rDNA specifically contribute to global ATM activation, however it is possible that R-loops outside of the nucleolus trigger a DDR, as work from our lab demonstrated that R-loops in the nucleus are upregulated in hypoxia (Ramachandran et al., 2020). Further studies using nucleolar fractionation with western blot analysis or immunofluorescence analysis of ATM/ATR protein targets will help to decipher the contribution of rDNA R-loops to DDR activation. The repair of rDNA DSBs has been shown to rely on the activation of ATM/ATR in the nucleolus and preserving rDNA genome integrity. The activation of ATM/ATR in the nucleolus could be essential to prevent DSBs from occurring on the rDNA in hypoxia.

The question of what triggers R-loops to form in hypoxia is still unknown. It is plausible that the loss or altered cellular localisation of R-loop resolving factors such as BRCA1, which has been shown to be repressed in hypoxia, could lead to R-loop accumulation (Chan et al., 2010). However, BRCA1 repression in hypoxia is unlikely to affect rDNA transcription as the decrease occurs in longer time points. A previous study characterised the R-loop interactome, which has identified several novel R-loop associated nucleolar factors, some of which could be either excluded from the nucleolus or lost in hypoxia (Cristini et al., 2018). Further studies into the nucleolar proteome in hypoxic conditions may assist further investigation into the causative factors in R-loop accumulation. An alternative hypothesis could include the displacement of protein-rRNA interactions through the deposition of H3K9me3 which leads to the accumulation of R-loops. Previous studies have shown that primary ribosomal proteins bind to the nascent rRNA as it emerges from the RNPI complex which helps with folding and stabilisation (Duss et al., 2019). The displacement of ribosomal proteins through a H3K9me3 dependent mechanism in hypoxia may allow for the nascent transcript to anneal to the template DNA and form an R-loop.

Other stress-induced mechanisms of rDNA transcriptional repression involve the DDR kinases ATM and ATR. However, I found that the hypoxia-induced mechanism of rDNA transcriptional repression occurred independently of ATM and ATR and therefore highlight a unique mechanism of stress-induced rDNA transcriptional repression. This is not altogether surprising as ATM and ATR are only reported to be active in S phase in hypoxia, whereas transcriptional repression of rDNA was shown to occur in all cells (Bencokova et al., 2009). Furthermore, the ATM/ATR dependent rDNA transcriptional repression mechanism has been demonstrated in response to DSBs, as opposed to hypoxia where there is no detectable DNA damage (Pires et al., 2010b).

The nucleolar factor TCOF1 has been shown to be important in transcriptional silencing upon DNA DSBs (Mooser et al., 2020). In agreement with an ATM/ATR-independent mechanism of rDNA transcriptional repression, I demonstrated that TCOF1/TopBP1 is not involved in the hypoxic repression of rDNA. These findings suggest that the hypoxic shutdown of RNPI relies on a unique and novel mechanism that is distinct from that of DSBs or hypoosmotic stress.

Previous studies have identified DNA-PK and PARP1 in the inhibition of rRNA synthesis in response to DNA damage (Calkins et al., 2013). Although I have not addressed the role of these repair factors in the repression of rDNA transcription in our studies, there is certainly precedent to investigate the dependency of DNA-PK and PARP1 in hypoxic transcriptional inhibition. DNA-PK is reported to be active in mild hypoxia (0.1-1% O_2) so there is a strong likelihood of similar DNA-PK activation in more severe hypoxic conditions that I have used although further investigation into the kinetics of its activation i.e. if DNA-PK is active by 1.5 hours <0.1% O_2 then it may represent a potential candidate for rDNA transcriptional repression in hypoxia. (Bouquet et al., 2011).

Although our data show that the DDR kinases were not involved in the initial rDNA transcriptional repression, our preliminary results suggest a partial restoration of rDNA transcription in hypoxia in the absence of PERK at later time points. Previous studies have implicated the UPR in regulating the transcription of rDNA in response to pharmacological inducing agents thapsigargin and tunicamycin (DuRose et al., 2009). The partial rescue of transcription at later time points in hypoxia suggest that although the UPR does not play a role in the initial repression of rDNA in hypoxia, activation of the UPR is required to maintain low levels of rDNA transcription. The mechanism by which PERK elicits transcriptional repression in hypoxia is unknown but it is likely to act through a previously reported mechanism by which EIF2α inactivates the RNPI initiation factor, RRN3, thereby limiting rRNA synthesis (DuRose et al., 2009).

I hypothesised that insufficient nucleotide levels could impact RNPI transcription in hypoxia. I investigated this first through the observation that nucleotide levels were depleted quickly in hypoxia, and second through the supplementation of additional nucleosides into hypoxic cells. Although I were unable to restore rDNA transcription upon nucleoside supplementation in hypoxia, I must treat the nucleotide independent mechanism of rDNA transcriptional repression result with caution for the following reason. I was unable to restore the basal levels of cellular GTP upon addition of nucleosides which may be explained, but not formally proven, by the high level of GTP consumption. HCT116 cells have a *KRAS* mutation, leading to elevated activity of KRAS which require GTP as a substrate (Shirasawa et al., 1993). Given that GDP levels were restored upon nucleoside addition in hypoxia, it is unlikely that there was a problem with the cells ability to take up the nucleoside.

Additionally, I have identified a problem with the processing of rRNA, which to our knowledge has not been described before in hypoxia. The correct processing of the 47S which liberates the mature rRNA is essential to fuel the process of protein translation. Global protein

translation is repressed in hypoxia through a number of mechanisms. From our findings, it is likely that inhibition of rRNA processing in hypoxia impacts the formation of pre-ribosomes which subsequently compromises the translational ability. The revolution of cryo-electron microscopy (cryo-EM) has allowed for the study of sub-cellular processes including the formation of half-assembled pre-ribosome intermediates in the emergence of global architecture of the ribosomal subunits (Zhou et al., 2019). Defects in nucleolar factors are known to impact the organisation of the pre-ribosome leading to aberrant protein translation (Tafforeau et al., 2013). Therefore, the impact of pre-rRNA processing on the formation of pre-ribosomes in hypoxia would be interesting for further studies.

Specifically, we demonstrated that there is a processing defect at site A0 on the 5'ETS in hypoxic conditions by qPCR and northern blotting techniques. Depletion of exosome components such as RRP6 and DIS3 have been shown to lead to aberrant cleavage at A0 on the 5'ETS (Kobylecki et al., 2018). This processing defect at site A0 is likely to have an impact on downstream cleavage and processing at subsequent sites on the 5'ETS as well as the ITS1 and ITS2 of the pre-rRNA. Indeed, I demonstrate that cleavage on the ITS1 and ITS2 are also abrogated in hypoxia. I demonstrated that the processing of pre-rRNA is restored upon reoxygenation. Although it remains unclear why this processing defect occurs in response to hypoxia, these data may suggest that pre-rRNA intermediates build up in hypoxia, in part, to limit mature rRNA so that when oxygen is restored, the cell can utilise the reservoir of pre-rRNA intermediates in the assembly ribosomes.

Tumours undergo periods of hypoxia and reoxygenation due to fluctuations in blood flow in the abnormal vasculature. Here, I demonstrate that in response to a physiologically relevant oxygen tension, RNPI activity is quickly shutdown and rapidly restored upon reoxygenation. As oxygen levels are dynamic and fluctuate in a tumour, it is likely that RNPI undergoes pausing, stalling and restart frequently, which may lead to TRCs and pose a threat to genome

stability. Given that RNPI activity is affected in an oxygen dependent manner, the rDNA mutation rate in hypoxic tumours is likely to be high. Further study into the link between oxygen and rDNA transcription will provide more understanding of the hypoxic adaptive response and highlight novel avenues of treatment. A selective inhibitor of RNPI, CX5461, has been shown to be highly effective in the treatment of solid and haematological cancers in pre-clinical studies. However, resistance to the drug eventually reduces its efficacy in solid tumours. A phase I clinical trial testing the efficacy of CX5461 in local, recurrent and metastatic breast cancer is currently ongoing (NCT02719977). Our study may inform the use of CX5461 in solid tumours in breast cancer which are often hypoxic and therefore may be prone to deregulated RNPI activity.

Some important questions of the mechanisms of nucleolar control in hypoxia have arisen from my work. The nucleolus is known to form through a phenomenon of the coexistence of two thermodynamically equilibrium phases with the same cationic composition called phase separation. The importance of phase separation in the nucleolus was recently highlighted although this study did not touch on physiologically relevant conditions such as hypoxia (Abraham et al., 2020). How physiologically-relevant oxygen levels impact phase separation is currently unknown. I have observed that nucleoli in cells exposed to hypoxia show a clear change in morphology, becoming increasingly spherical with time. This suggests that nucleolar structure is responsive to oxygen levels and raises the question of how hypoxia impacts phase separation. Future studies will investigate the changes to the protein composition of the subcellular compartments of the nucleolus in response to stress signals such as hypoxia. Specifically, investigation into the quantitative changes to the protein composition of the sub-cellular nucleolar compartments will shed light on the nucleolar dynamics in response to hypoxia.

References

Abraham, K.J., Khosraviani, N., Chan, J.N.Y., Gorthi, A., Samman, A., Zhao, D.Y., Wang, M., Bokros, M., Vidya, E., Ostrowski, L.A., *et al.* (2020). Nucleolar RNA polymerase II drives ribosome biogenesis. Nature *585*, 298–302.

Alexandrov, L.B., Nik-Zainal, S., Wedge, D.C., Campbell, P.J., and Stratton, M.R. (2013). Deciphering signatures of mutational processes operative in human cancer. Cell Rep *3*, 246-259.

Andersen, J.S., Lyon, C.E., Fox, A.H., Leung, A.K., Lam, Y.W., Steen, H., Mann, M., and Lamond, A.I. (2002). Directed proteomic analysis of the human nucleolus. Curr Biol *12*, 1-11.

Appelhoff, R.J., Tian, Y.M., Raval, R.R., Turley, H., Harris, A.L., Pugh, C.W., Ratcliffe, P.J., and Gleadle, J.M. (2004). Differential function of the prolyl hydroxylases PHD1, PHD2, and PHD3 in the regulation of hypoxia-inducible factor. J Biol Chem *279*, 38458-38465.

Arabi, A., Wu, S., Ridderstrale, K., Bierhoff, H., Shiue, C., Fatyol, K., Fahlen, S., Hydbring, P., Soderberg, O., Grummt, I., *et al.* (2005). c-Myc associates with ribosomal DNA and activates RNA polymerase I transcription. Nat Cell Biol *7*, 303-310.

Bakkenist, C.J., and Kastan, M.B. (2003). DNA damage activates ATM through intermolecular autophosphorylation and dimer dissociation. Nature *421*, 499-506.

Baluk, P., Hashizume, H., and McDonald, D.M. (2005). Cellular abnormalities of blood vessels as targets in cancer. Curr Opin Genet Dev *15*, 102-111.

Barna, M., Pusic, A., Zollo, O., Costa, M., Kondrashov, N., Rego, E., Rao, P.H., and Ruggero, D. (2008). Suppression of Myc oncogenic activity by ribosomal protein haploinsufficiency. Nature *456*, 971-975.

Bass, T.E., Luzwick, J.W., Kavanaugh, G., Carroll, C., Dungrawala, H., Glick, G.G., Feldkamp, M.D., Putney, R., Chazin, W.J., and Cortez, D. (2016). ETAA1 acts at stalled replication forks to maintain genome integrity. Nat Cell Biol *18*, 1185-1195.

Batie, M., Frost, J., Frost, M., Wilson, J.W., Schofield, P., and Rocha, S. (2019). Hypoxia induces rapid changes to histone methylation and reprograms chromatin. Science *363*, 1222-1226.

Batrakou, D.G., Muller, C.A., Wilson, R.H.C., and Nieduszynski, C.A. (2020). DNA copy-number measurement of genome replication dynamics by high-throughput sequencing: the sort-seq, sync-seq and MFA-seq family. Nat Protoc *15*, 1255-1284.

Bencokova, Z., Kaufmann, M.R., Pires, I.M., Lecane, P.S., Giaccia, A.J., and Hammond, E.M. (2009). ATM activation and signaling under hypoxic conditions. Mol Cell Biol *29*, 526-537.

Bernstein, E., Caudy, A.A., Hammond, S.M., and Hannon, G.J. (2001). Role for a bidentate ribonuclease in the initiation step of RNA interference. Nature *409*, 363-366.

Bertolotti, A., Zhang, Y., Hendershot, L.M., Harding, H.P., and Ron, D. (2000). Dynamic interaction of BiP and ER stress transducers in the unfolded-protein response. Nat Cell Biol *2*, 326-332.

Beyer, S., Kristensen, M.M., Jensen, K.S., Johansen, J.V., and Staller, P. (2008). The histone demethylases JMJD1A and JMJD2B are transcriptional targets of hypoxia-inducible factor HIF. J Biol Chem *283*, 36542-36552.

Bierhoff, H., Dammert, M.A., Brocks, D., Dambacher, S., Schotta, G., and Grummt, I. (2014). Quiescence-induced LncRNAs trigger H4K20 trimethylation and transcriptional silencing. Mol Cell *54*, 675-682.

Bindra, R.S., Gibson, S.L., Meng, A., Westermark, U., Jasin, M., Pierce, A.J., Bristow, R.G., Classon, M.K., and Glazer, P.M. (2005). Hypoxia-induced down-regulation of BRCA1 expression by E2Fs. Cancer Res *65*, 11597-11604.

Bindra, R.S., and Glazer, P.M. (2007). Repression of RAD51 gene expression by E2F4/p130 complexes in hypoxia. Oncogene *26*, 2048-2057.

Blobel, G., and Potter, V.R. (1967). Studies on free and membrane-bound ribosomes in rat liver. I. Distribution as related to total cellular RNA. J Mol Biol *26*, 279-292.

Boguslawski, S.J., Smith, D.E., Michalak, M.A., Mickelson, K.E., Yehle, C.O., Patterson, W.L., and Carrico, R.J. (1986). Characterization of monoclonal antibody to DNA.RNA and its application to immunodetection of hybrids. J Immunol Methods *89*, 123-130.

Bouquet, F., Ousset, M., Biard, D., Fallone, F., Dauvillier, S., Frit, P., Salles, B., and Muller, C. (2011). A DNA-dependent stress response involving DNA-PK occurs in hypoxic cells and contributes to cellular adaptation to hypoxia. J Cell Sci *124*, 1943-1951.

Brady, C.A., Jiang, D., Mello, S.S., Johnson, T.M., Jarvis, L.A., Kozak, M.M., Kenzelmann Broz, D., Basak, S., Park, E.J., McLaughlin, M.E., *et al.* (2011). Distinct p53 transcriptional programs dictate acute DNA-damage responses and tumor suppression. Cell *145*, 571-583.

Brill, S.J., DiNardo, S., Voelkel-Meiman, K., and Sternglanz, R. (1987). Need for DNA topoisomerase activity as a swivel for DNA replication for transcription of ribosomal RNA. Nature *326*, 414-416.

Brown, E.J., Albers, M.W., Shin, T.B., Ichikawa, K., Keith, C.T., Lane, W.S., and Schreiber, S.L. (1994). A mammalian protein targeted by G1-arresting rapamycin-receptor complex. Nature *369*, 756-758.

Brown, J.M. (1979). Evidence for acutely hypoxic cells in mouse tumours, and a possible mechanism of reoxygenation. Br J Radiol *52*, 650-656.

Bryan, T.M., Englezou, A., Gupta, J., Bacchetti, S., and Reddel, R.R. (1995). Telomere elongation in immortal human cells without detectable telomerase activity. EMBO J *14*, 4240-4248.

Burger, K., Muhl, B., Rohrmoser, M., Coordes, B., Heidemann, M., Kellner, M., Gruber-Eber, A., Heissmeyer, V., Strasser, K., and Eick, D. (2013). Cyclin-dependent kinase 9 links RNA polymerase II transcription to processing of ribosomal RNA. J Biol Chem *288*, 21173-21183.

Bursac, S., Brdovcak, M.C., Pfannkuchen, M., Orsolic, I., Golomb, L., Zhu, Y., Katz, C., Daftuar, L., Grabusic, K., Vukelic, I., *et al.* (2012). Mutual protection of ribosomal proteins L5 and L11 from degradation is essential for p53 activation upon ribosomal biogenesis stress. Proc Natl Acad Sci U S A *109*, 20467-20472.

Buttgereit, F., and Brand, M.D. (1995). A hierarchy of ATP-consuming processes in mammalian cells. Biochem J *312 (Pt 1)*, 163-167.

Cairns, R.A., and Hill, R.P. (2004). Acute hypoxia enhances spontaneous lymph node metastasis in an orthotopic murine model of human cervical carcinoma. Cancer Res *64*, 2054-2061.

Calfon, M., Zeng, H., Urano, F., Till, J.H., Hubbard, S.R., Harding, H.P., Clark, S.G., and Ron, D. (2002). IRE1 couples endoplasmic reticulum load to secretory capacity by processing the XBP-1 mRNA. Nature *415*, 92-96.

Calkins, A.S., Iglehart, J.D., and Lazaro, J.B. (2013). DNA damage-induced inhibition of rRNA synthesis by DNA-PK and PARP-1. Nucleic Acids Res *41*, 7378-7386.

Canman, C.E., Lim, D.S., Cimprich, K.A., Taya, Y., Tamai, K., Sakaguchi, K., Appella, E., Kastan, M.B., and Siliciano, J.D. (1998). Activation of the ATM kinase by ionizing radiation and phosphorylation of p53. Science *281*, 1677-1679.

Cancer Research UK. (2018). Retrieved 9th September 2020, from https://www.cancerresearchuk.org/health-professional/cancer-statistics-for-the-uk#heading-One

Cardenas-Navia, L.I., Mace, D., Richardson, R.A., Wilson, D.F., Shan, S., and Dewhirst, M.W. (2008). The pervasive presence of fluctuating oxygenation in tumors. Cancer Res *68*, 5812-5819.

Carreau, A., El Hafny-Rahbi, B., Matejuk, A., Grillon, C., and Kieda, C. (2011). Why is the partial oxygen pressure of human tissues a crucial parameter? Small molecules and hypoxia. J Cell Mol Med *15*, 1239-1253.

Cavadas, M.A., Mesnieres, M., Crifo, B., Manresa, M.C., Selfridge, A.C., Keogh, C.E., Fabian, Z., Scholz, C.C., Nolan, K.A., Rocha, L.M., *et al.* (2016). REST is a hypoxia-responsive transcriptional repressor. Sci Rep *6*, 31355.

Chan, N., Ali, M., McCallum, G.P., Kumareswaran, R., Koritzinsky, M., Wouters, B.G., Wells, P.G., Gallinger, S., and Bristow, R.G. (2014). Hypoxia provokes base excision repair changes

and a repair-deficient, mutator phenotype in colorectal cancer cells. Mol Cancer Res *12*, 1407-1415.

Chan, N., Koritzinsky, M., Zhao, H., Bindra, R., Glazer, P.M., Powell, S., Belmaaza, A., Wouters, B., and Bristow, R.G. (2008). Chronic hypoxia decreases synthesis of homologous recombination proteins to offset chemoresistance and radioresistance. Cancer Res *68*, 605-614.

Chan, N., Pires, I.M., Bencokova, Z., Coackley, C., Luoto, K.R., Bhogal, N., Lakshman, M., Gottipati, P., Oliver, F.J., Helleday, T., *et al.* (2010). Contextual synthetic lethality of cancer cell kill based on the tumor microenvironment. Cancer Res *70*, 8045-8054.

Chaplin, D.J., Durand, R.E., and Olive, P.L. (1986). Acute hypoxia in tumors: implications for modifiers of radiation effects. Int J Radiat Oncol Biol Phys *12*, 1279-1282.

Chen, H., Yan, Y., Davidson, T.L., Shinkai, Y., and Costa, M. (2006). Hypoxic stress induces dimethylated histone H3 lysine 9 through histone methyltransferase G9a in mammalian cells. Cancer Res *66*, 9009-9016.

Chen, L., Chen, J.Y., Huang, Y.J., Gu, Y., Qiu, J., Qian, H., Shao, C., Zhang, X., Hu, J., Li, H., *et al.* (2018). The Augmented R-Loop Is a Unifying Mechanism for Myelodysplastic Syndromes Induced by High-Risk Splicing Factor Mutations. Mol Cell *69*, 412-425 e416.

Chen, L., Chen, J.Y., Zhang, X., Gu, Y., Xiao, R., Shao, C., Tang, P., Qian, H., Luo, D., Li, H., *et al.* (2017). R-ChIP Using Inactive RNase H Reveals Dynamic Coupling of R-loops with Transcriptional Pausing at Gene Promoters. Mol Cell *68*, 745-757 e745.

Chen, P.B., Chen, H.V., Acharya, D., Rando, O.J., and Fazzio, T.G. (2015). R loops regulate promoter-proximal chromatin architecture and cellular differentiation. Nat Struct Mol Biol *22*, 999-1007.

Connolly, E., Braunstein, S., Formenti, S., and Schneider, R.J. (2006). Hypoxia inhibits protein synthesis through a 4E-BP1 and elongation factor 2 kinase pathway controlled by mTOR and uncoupled in breast cancer cells. Mol Cell Biol *26*, 3955-3965.

Coquelle, A., Toledo, F., Stern, S., Bieth, A., and Debatisse, M. (1998). A new role for hypoxia in tumor progression: induction of fragile site triggering genomic rearrangements and formation of complex DMs and HSRs. Mol Cell *2*, 259-265.

Couture, J.F., Collazo, E., Ortiz-Tello, P.A., Brunzelle, J.S., and Trievel, R.C. (2007). Specificity and mechanism of JMJD2A, a trimethyllysine-specific histone demethylase. Nat Struct Mol Biol *14*, 689-695.

Cox, J.S., Shamu, C.E., and Walter, P. (1993). Transcriptional induction of genes encoding endoplasmic reticulum resident proteins requires a transmembrane protein kinase. Cell *73*, 1197-1206.

Cristini, A., Groh, M., Kristiansen, M.S., and Gromak, N. (2018). RNA/DNA Hybrid Interactome Identifies DXH9 as a Molecular Player in Transcriptional Termination and R-Loop-Associated DNA Damage. Cell Rep *23*, 1891-1905.

Cristini, A., Ricci, G., Britton, S., Salimbeni, S., Huang, S.N., Marinello, J., Calsou, P., Pommier, Y., Favre, G., Capranico, G., *et al.* (2019). Dual Processing of R-Loops and Topoisomerase I Induces Transcription-Dependent DNA Double-Strand Breaks. Cell Rep *28*, 3167-3181 e3166.

Dang, D.T., Chen, F., Gardner, L.B., Cummins, J.M., Rago, C., Bunz, F., Kantsevoy, S.V., and Dang, L.H. (2006). Hypoxia-inducible factor-1alpha promotes nonhypoxia-mediated proliferation in colon cancer cells and xenografts. Cancer Res *66*, 1684-1936.

Deniaud, A., Sharaf el dein, O., Maillier, E., Poncet, D., Kroemer, G., Lemaire, C., and Brenner, C. (2008). Endoplasmic reticulum stress induces calcium-dependent permeability transition, mitochondrial outer membrane permeabilization and apoptosis. Oncogene *27*, 285-299.

Denko, N., Wernke-Dollries, K., Johnson, A.B., Hammond, E., Chiang, C.M., and Barton, M.C. (2003). Hypoxia actively represses transcription by inducing negative cofactor 2 (Dr1/DrAP1) and blocking preinitiation complex assembly. J Biol Chem *278*, 5744-5749.

Dewhirst, M.W. (2009). Relationships between cycling hypoxia, HIF-1, angiogenesis and oxidative stress. Radiat Res *172*, 653-665.

Diesch, J., Bywater, M.J., Sanij, E., Cameron, D.P., Schierding, W., Brajanovski, N., Son, J., Sornkom, J., Hein, N., Evers, M., *et al.* (2019). Changes in long-range rDNA-genomic interactions associate with altered RNA polymerase II gene programs during malignant transformation. Commun Biol *2*, 39.

Donahue, B.A., Yin, S., Taylor, J.S., Reines, D., and Hanawalt, P.C. (1994). Transcript cleavage by RNA polymerase II arrested by a cyclobutane pyrimidine dimer in the DNA template. Proc Natl Acad Sci U S A *91*, 8502-8506.

Dudas, J., Schartinger, V.H., Romani, A., Schweigl, G., Kordsmeyer, K., Marta, P.I., Url, C., Kral, F., and Riechelmann, H. (2014). Cell cycle association and hypoxia regulation of excision repair cross complementation group 1 protein (ERCC1) in tumor cells of head and neck cancer. Tumour Biol *35*, 7807-7819.

Duriez, B., Chilaka, S., Bercher, J.F., Hercul, E., and Prioleau, M.N. (2019). Replication dynamics of individual loci in single living cells reveal changes in the degree of replication stochasticity through S phase. Nucleic Acids Res *47*, 5155-5169.

DuRose, J.B., Scheuner, D., Kaufman, R.J., Rothblum, L.I., and Niwa, M. (2009). Phosphorylation of eukaryotic translation initiation factor 2alpha coordinates rRNA transcription and translation inhibition during endoplasmic reticulum stress. Mol Cell Biol *29*, 4295-4307.

Duss, O., Stepanyuk, G.A., Puglisi, J.D., and Williamson, J.R. (2019). Transient Protein-RNA Interactions Guide Nascent Ribosomal RNA Folding. Cell *179*, 1357-1369 e1316.

Edwards, S.J., Gladwin, A.J., and Dixon, M.J. (1997). The mutational spectrum in Treacher Collins syndrome reveals a predominance of mutations that create a premature-termination codon. Am J Hum Genet *60*, 515-524.

El Hage, A., French, S.L., Beyer, A.L., and Tollervey, D. (2010). Loss of Topoisomerase I leads to R-loop-mediated transcriptional blocks during ribosomal RNA synthesis. Genes Dev *24*, 1546-1558.

Erlacher, M.D., Lang, K., Wotzel, B., Rieder, R., Micura, R., and Polacek, N. (2006). Efficient ribosomal peptidyl transfer critically relies on the presence of the ribose 2'-OH at A2451 of 23S rRNA. J Am Chem Soc *128*, 4453-4459.

Ernens, I., Goodfellow, S.J., Innes, F., Kenneth, N.S., Derblay, L.E., White, R.J., and Scott, P.H. (2006). Hypoxic stress suppresses RNA polymerase III recruitment and tRNA gene transcription in cardiomyocytes. Nucleic Acids Res *34*, 286-294.

Evers, R., Smid, A., Rudloff, U., Lottspeich, F., and Grummt, I. (1995). Different domains of the murine RNA polymerase I-specific termination factor mTTF-I serve distinct functions in transcription termination. EMBO J *14*, 1248-1256.

Falaleeva, M., Pages, A., Matuszek, Z., Hidmi, S., Agranat-Tamir, L., Korotkov, K., Nevo, Y., Eyras, E., Sperling, R., and Stamm, S. (2016). Dual function of C/D box small nucleolar RNAs in rRNA modification and alternative pre-mRNA splicing. Proc Natl Acad Sci U S A *113*, E1625-1634.

Fanale, D., Bazan, V., Caruso, S., Castiglia, M., Bronte, G., Rolfo, C., Cicero, G., and Russo, A. (2013). Hypoxia and human genome stability: downregulation of BRCA2 expression in breast cancer cell lines. Biomed Res Int *2013*, 746858.

Foskolou, I.P., Jorgensen, C., Leszczynska, K.B., Olcina, M.M., Tarhonskaya, H., Haisma, B., D'Angiolella, V., Myers, W.K., Domene, C., Flashman, E., *et al.* (2017). Ribonucleotide Reductase Requires Subunit Switching in Hypoxia to Maintain DNA Replication. Mol Cell *66*, 206-220 e209.

Gaal, T., Bartlett, M.S., Ross, W., Turnbough, C.L., Jr., and Gourse, R.L. (1997). Transcription regulation by initiating NTP concentration: rRNA synthesis in bacteria. Science *278*, 2092-2097.

Galardi, S., Fatica, A., Bachi, A., Scaloni, A., Presutti, C., and Bozzoni, I. (2002). Purified box C/D snoRNPs are able to reproduce site-specific 2'-O-methylation of target RNA in vitro. Mol Cell Biol *22*, 6663-6668.

Gan, W., Guan, Z., Liu, J., Gui, T., Shen, K., Manley, J.L., and Li, X. (2011). R-loop-mediated genomic instability is caused by impairment of replication fork progression. Genes Dev *25*, 2041-2056.

Garcia-Pichardo, D., Canas, J.C., Garcia-Rubio, M.L., Gomez-Gonzalez, B., Rondon, A.G., and Aguilera, A. (2017). Histone Mutants Separate R Loop Formation from Genome Instability Induction. Mol Cell *66*, 597-609 e595.

Garcia-Rubio, M.L., Perez-Calero, C., Barroso, S.I., Tumini, E., Herrera-Moyano, E., Rosado, I.V., and Aguilera, A. (2015). The Fanconi Anemia Pathway Protects Genome Integrity from R-loops. PLoS Genet *11*, e1005674.

Gardner, L.B. (2008). Hypoxic inhibition of nonsense-mediated RNA decay regulates gene expression and the integrated stress response. Mol Cell Biol *28*, 3729-3741.

Gaviraghi, M., Vivori, C., Pareja Sanchez, Y., Invernizzi, F., Cattaneo, A., Santoliquido, B.M., Frenquelli, M., Segalla, S., Bachi, A., Doglioni, C., *et al.* (2018). Tumor suppressor PNRC1 blocks rRNA maturation by recruiting the decapping complex to the nucleolus. EMBO J *37*.

Gjerset, R.A., and Bandyopadhyay, K. (2006). Regulation of p14ARF through subnuclear compartmentalization. Cell Cycle *5*, 686-690.

Gomez-Schiavon, M., and Buchler, N.E. (2019). Epigenetic switching as a strategy for quick adaptation while attenuating biochemical noise. PLoS Comput Biol *15*, e1007364.

Goodfellow, S.J., and Zomerdijk, J.C. (2013). Basic mechanisms in RNA polymerase I transcription of the ribosomal RNA genes. Subcell Biochem *61*, 211-236.

Gordon, J., Pillon, M.C., and Stanley, R.E. (2019). Nol9 Is a Spatial Regulator for the Human ITS2 Pre-rRNA Endonuclease-Kinase Complex. J Mol Biol *431*, 3771-3786.

Graeber, T.G., Peterson, J.F., Tsai, M., Monica, K., Fornace, A.J., Jr., and Giaccia, A.J. (1994). Hypoxia induces accumulation of p53 protein, but activation of a G1-phase checkpoint by low-oxygen conditions is independent of p53 status. Mol Cell Biol *14*, 6264-6277.

Groh, M., Lufino, M.M., Wade-Martins, R., and Gromak, N. (2014). R-loops associated with triplet repeat expansions promote gene silencing in Friedreich ataxia and fragile X syndrome. PLoS Genet *10*, e1004318.

Grummt, I., Rosenbauer, H., Niedermeyer, I., Maier, U., and Ohrlein, A. (1986). A repeated 18 bp sequence motif in the mouse rDNA spacer mediates binding of a nuclear factor and transcription termination. Cell *45*, 837-846.

Guo, Z., Kozlov, S., Lavin, M.F., Person, M.D., and Paull, T.T. (2010). ATM activation by oxidative stress. Science *330*, 517-521.

Haahr, P., Hoffmann, S., Tollenaere, M.A., Ho, T., Toledo, L.I., Mann, M., Bekker-Jensen, S., Raschle, M., and Mailand, N. (2016). Activation of the ATR kinase by the RPA-binding protein ETAA1. Nat Cell Biol *18*, 1196-1207.

Hammond, E.M., Denko, N.C., Dorie, M.J., Abraham, R.T., and Giaccia, A.J. (2002). Hypoxia links ATR and p53 through replication arrest. Mol Cell Biol *22*, 1834-1843.

Hammond, E.M., Dorie, M.J., and Giaccia, A.J. (2003). ATR/ATM targets are phosphorylated by ATR in response to hypoxia and ATM in response to reoxygenation. J Biol Chem *278*, 12207-12213.

Hammond, E.M., Dorie, M.J., and Giaccia, A.J. (2004). Inhibition of ATR leads to increased sensitivity to hypoxia/reoxygenation. Cancer Res *64*, 6556-6562.

Hammond, E.M., and Giaccia, A.J. (2004). The role of ATM and ATR in the cellular response to hypoxia and re-oxygenation. DNA Repair (Amst) *3*, 1117-1122.

Hammond, E.M., and Giaccia, A.J. (2006). Hypoxia-inducible factor-1 and p53: friends, acquaintances, or strangers? Clin Cancer Res *12*, 5007-5009.

Hamperl, S., Bocek, M.J., Saldivar, J.C., Swigut, T., and Cimprich, K.A. (2017). Transcription-Replication Conflict Orientation Modulates R-Loop Levels and Activates Distinct DNA Damage Responses. Cell *170*, 774-786 e719.

Han, D., Williams, E., and Cadenas, E. (2001). Mitochondrial respiratory chain-dependent generation of superoxide anion and its release into the intermembrane space. Biochem J *353*, 411-416.

Hanahan, D., and Weinberg, R.A. (2000). The hallmarks of cancer. Cell *100*, 57-70.

Hanahan, D., and Weinberg, R.A. (2011). Hallmarks of cancer: the next generation. Cell *144*, 646-674.

Hancock, R.L., Masson, N., Dunne, K., Flashman, E., and Kawamura, A. (2017). The Activity of JmjC Histone Lysine Demethylase KDM4A is Highly Sensitive to Oxygen Concentrations. ACS Chem Biol *12*, 1011-1019.

Harding, S.M., Boiarsky, J.A., and Greenberg, R.A. (2015). ATM Dependent Silencing Links Nucleolar Chromatin Reorganization to DNA Damage Recognition. Cell Rep *13*, 251-259.

Hartono, S.R., Malapert, A., Legros, P., Bernard, P., Chedin, F., and Vanoosthuyse, V. (2018). The Affinity of the S9.6 Antibody for Double-Stranded RNAs Impacts the Accurate Mapping of R-Loops in Fission Yeast. J Mol Biol *430*, 272-284.

Hatchi, E., Skourti-Stathaki, K., Ventz, S., Pinello, L., Yen, A., Kamieniarz-Gdula, K., Dimitrov, S., Pathania, S., McKinney, K.M., Eaton, M.L., *et al.* (2015). BRCA1 recruitment to transcriptional pause sites is required for R-loop-driven DNA damage repair. Mol Cell *57*, 636-647.

Hayflick, L. (1965). The Limited in Vitro Lifetime of Human Diploid Cell Strains. Exp Cell Res *37*, 614-636.

Heiss, N.S., Knight, S.W., Vulliamy, T.J., Klauck, S.M., Wiemann, S., Mason, P.J., Poustka, A., and Dokal, I. (1998). X-linked dyskeratosis congenita is caused by mutations in a highly conserved gene with putative nucleolar functions. Nat Genet *19*, 32-38.

Henras, A.K., Plisson-Chastang, C., O'Donohue, M.F., Chakraborty, A., and Gleizes, P.E. (2015). An overview of pre-ribosomal RNA processing in eukaryotes. Wiley Interdiscip Rev RNA *6*, 225-242.

Ho, J.J., Metcalf, J.L., Yan, M.S., Turgeon, P.J., Wang, J.J., Chalsev, M., Petruzziello-Pellegrini, T.N., Tsui, A.K., He, J.Z., Dhamko, H., *et al.* (2012). Functional importance of Dicer protein in the adaptive cellular response to hypoxia. J Biol Chem *287*, 29003-29020.

Hodroj, D., Recolin, B., Serhal, K., Martinez, S., Tsanov, N., Abou Merhi, R., and Maiorano, D. (2017). An ATR-dependent function for the Ddx19 RNA helicase in nuclear R-loop metabolism. EMBO J *36*, 1182-1198.

Holz, M.K., Ballif, B.A., Gygi, S.P., and Blenis, J. (2005). mTOR and S6K1 mediate assembly of the translation preinitiation complex through dynamic protein interchange and ordered phosphorylation events. Cell *123*, 569-580.

Huang, F.T., Yu, K., Balter, B.B., Selsing, E., Oruc, Z., Khamlichi, A.A., Hsieh, C.L., and Lieber, M.R. (2007). Sequence dependence of chromosomal R-loops at the immunoglobulin heavy-chain Smu class switch region. Mol Cell Biol *27*, 5921-5932.

Ide, S., Miyazaki, T., Maki, H., and Kobayashi, T. (2010). Abundance of ribosomal RNA gene copies maintains genome integrity. Science *327*, 693-696.

Ito, A., Koshikawa, N., Mochizuki, S., Omura, K., and Takenaga, K. (2006). Hypoxia-inducible factor-1 mediates the expression of DNA polymerase iota in human tumor cells. Biochem Biophys Res Commun *351*, 306-311.

Iyer-Bierhoff, A., Krogh, N., Tessarz, P., Ruppert, T., Nielsen, H., and Grummt, I. (2018). SIRT7-Dependent Deacetylation of Fibrillarin Controls Histone H2A Methylation and rRNA Synthesis during the Cell Cycle. Cell Rep *25*, 2946-2954 e2945.

Jahanban-Esfahlan, R., de la Guardia, M., Ahmadi, D., and Yousefi, B. (2018). Modulating tumor hypoxia by nanomedicine for effective cancer therapy. J Cell Physiol *233*, 2019-2031.

Jansa, P., and Grummt, I. (1999). Mechanism of transcription termination: PTRF interacts with the largest subunit of RNA polymerase I and dissociates paused transcription complexes from yeast and mouse. Mol Gen Genet *262*, 508-514.

Johnson, A.B., Denko, N., and Barton, M.C. (2008). Hypoxia induces a novel signature of chromatin modifications and global repression of transcription. Mutat Res *640*, 174-179.

Johnson, L.F., Levis, R., Abelson, H.T., Green, H., and Penman, S. (1976). Changes in RNA in relation to growth of the fibroblast. IV. Alterations in theproduction and processing of mRNA and rRNA in resting and growing cells. J Cell Biol *71*, 933-938.

Jongen, J.M.J., van der Waals, L.M., Trumpi, K., Laoukili, J., Peters, N.A., Schenning-van Schelven, S.J., Govaert, K.M., Borel Rinkes, I.H.M., and Kranenburg, O. (2017). Downregulation of DNA repair proteins and increased DNA damage in hypoxic colon cancer cells is a therapeutically exploitable vulnerability. Oncotarget *8*, 86296-86311.

Kass, S., Craig, N., and Sollner-Webb, B. (1987). Primary processing of mammalian rRNA involves two adjacent cleavages and is not species specific. Mol Cell Biol *7*, 2891-2898.

Kass, S., Tyc, K., Steitz, J.A., and Sollner-Webb, B. (1990). The U3 small nucleolar ribonucleoprotein functions in the first step of preribosomal RNA processing. Cell *60*, 897-908.

Kawauchi, J., Mischo, H., Braglia, P., Rondon, A., and Proudfoot, N.J. (2008). Budding yeast RNA polymerases I and II employ parallel mechanisms of transcriptional termination. Genes Dev *22*, 1082-1092.

Kimura, H., Braun, R.D., Ong, E.T., Hsu, R., Secomb, T.W., Papahadjopoulos, D., Hong, K., and Dewhirst, M.W. (1996). Fluctuations in red cell flux in tumor microvessels can lead to transient hypoxia and reoxygenation in tumor parenchyma. Cancer Res *56*, 5522-5528.

Knocke, T.H., Weitmann, H.D., Feldmann, H.J., Selzer, E., and Potter, R. (1999). Intratumoral pO2-measurements as predictive assay in the treatment of carcinoma of the uterine cervix. Radiother Oncol *53*, 99-104.

Kobayashi, T., and Ganley, A.R. (2005). Recombination regulation by transcription-induced cohesin dissociation in rDNA repeats. Science *309*, 1581-1584.

Kobylecki, K., Drazkowska, K., Kulinski, T.M., Dziembowski, A., and Tomecki, R. (2018). Elimination of 01/A'-A0 pre-rRNA processing by-product in human cells involves cooperative action of two nuclear exosome-associated nucleases: RRP6 and DIS3. RNA *24*, 1677-1692.

Kohanski, M.A., Dwyer, D.J., Wierzbowski, J., Cottarel, G., and Collins, J.J. (2008). Mistranslation of membrane proteins and two-component system activation trigger antibiotic-mediated cell death. Cell *135*, 679-690.

Koritzinsky, M., Levitin, F., van den Beucken, T., Rumantir, R.A., Harding, N.J., Chu, K.C., Boutros, P.C., Braakman, I., and Wouters, B.G. (2013). Two phases of disulfide bond formation have differing requirements for oxygen. J Cell Biol *203*, 615-627.

Koritzinsky, M., Magagnin, M.G., van den Beucken, T., Seigneuric, R., Savelkouls, K., Dostie, J., Pyronnet, S., Kaufman, R.J., Weppler, S.A., Voncken, J.W., *et al.* (2006). Gene expression during acute and prolonged hypoxia is regulated by distinct mechanisms of translational control. EMBO J *25*, 1114-1125.

Koritzinsky, M., Wouters, B.G., Amellem, O., and Pettersen, E.O. (2001). Cell cycle progression and radiation survival following prolonged hypoxia and re-oxygenation. Int J Radiat Biol *77*, 319-328.

Korsholm, L.M., Gal, Z., Lin, L., Quevedo, O., Ahmad, D.A., Dulina, E., Luo, Y., Bartek, J., and Larsen, D.H. (2019). Double-strand breaks in ribosomal RNA genes activate a distinct signaling and chromatin response to facilitate nucleolar restructuring and repair. Nucleic Acids Res *47*, 8019-8035.

Koshiji, M., Kageyama, Y., Pete, E.A., Horikawa, I., Barrett, J.C., and Huang, L.E. (2004). HIF-1alpha induces cell cycle arrest by functionally counteracting Myc. EMBO J *23*, 1949-1956.

Kotsantis, P., Silva, L.M., Irmscher, S., Jones, R.M., Folkes, L., Gromak, N., and Petermann, E. (2016). Increased global transcription activity as a mechanism of replication stress in cancer. Nat Commun *7*, 13087.

Koumenis, C., Naczki, C., Koritzinsky, M., Rastani, S., Diehl, A., Sonenberg, N., Koromilas, A., and Wouters, B.G. (2002). Regulation of protein synthesis by hypoxia via activation of the endoplasmic reticulum kinase PERK and phosphorylation of the translation initiation factor eIF2alpha. Mol Cell Biol *22*, 7405-7416.

Krieg, A.J., Rankin, E.B., Chan, D., Razorenova, O., Fernandez, S., and Giaccia, A.J. (2010). Regulation of the histone demethylase JMJD1A by hypoxia-inducible factor 1 alpha enhances hypoxic gene expression and tumor growth. Mol Cell Biol *30*, 344-353.

Kruhlak, M., Crouch, E.E., Orlov, M., Montano, C., Gorski, S.A., Nussenzweig, A., Misteli, T., Phair, R.D., and Casellas, R. (2007). The ATM repair pathway inhibits RNA polymerase I transcription in response to chromosome breaks. Nature *447*, 730-734.

Lang, K.S., Hall, A.N., Merrikh, C.N., Ragheb, M., Tabakh, H., Pollock, A.J., Woodward, J.J., Dreifus, J.E., and Merrikh, H. (2017). Replication-Transcription Conflicts Generate R-Loops that Orchestrate Bacterial Stress Survival and Pathogenesis. Cell *170*, 787-799 e718.

Langhendries, J.L., Nicolas, E., Doumont, G., Goldman, S., and Lafontaine, D.L. (2016). The human box C/D snoRNAs U3 and U8 are required for pre-rRNA processing and tumorigenesis. Oncotarget *7*, 59519-59534.

Larsen, D.H., Hari, F., Clapperton, J.A., Gwerder, M., Gutsche, K., Altmeyer, M., Jungmichel, S., Toledo, L.I., Fink, D., Rask, M.B., *et al.* (2014). The NBS1-Treacle complex controls ribosomal RNA transcription in response to DNA damage. Nat Cell Biol *16*, 792-803.

Lazdins, I.B., Delannoy, M., and Sollner-Webb, B. (1997). Analysis of nucleolar transcription and processing domains and pre-rRNA movements by in situ hybridization. Chromosoma *105*, 481-495.

Lee, K., Tirasophon, W., Shen, X., Michalak, M., Prywes, R., Okada, T., Yoshida, H., Mori, K., and Kaufman, R.J. (2002). IRE1-mediated unconventional mRNA splicing and S2P-mediated ATF6 cleavage merge to regulate XBP1 in signaling the unfolded protein response. Genes Dev *16*, 452-466.

Lemacon, D., Jackson, J., Quinet, A., Brickner, J.R., Li, S., Yazinski, S., You, Z., Ira, G., Zou, L., Mosammaparast, N., *et al.* (2017). MRE11 and EXO1 nucleases degrade reversed forks and elicit MUS81-dependent fork rescue in BRCA2-deficient cells. Nat Commun *8*, 860.

Leszczynska, K.B., Dobrynin, G., Leslie, R.E., Ient, J., Boumelha, A.J., Senra, J.M., Hawkins, M.A., Maughan, T., Mukherjee, S., and Hammond, E.M. (2016a). Preclinical testing of an Atr inhibitor demonstrates improved response to standard therapies for esophageal cancer. Radiother Oncol *121*, 232-238.

Leszczynska, K.B., Gottgens, E.L., Biasoli, D., Olcina, M.M., Ient, J., Anbalagan, S., Bernhardt, S., Giaccia, A.J., and Hammond, E.M. (2016b). Mechanisms and consequences of ATMIN repression in hypoxic conditions: roles for p53 and HIF-1. Sci Rep *6*, 21698.

Levine, M., and Manley, J.L. (1989). Transcriptional repression of eukaryotic promoters. Cell *59*, 405-408.

Levy, A.P., Levy, N.S., and Goldberg, M.A. (1996). Post-transcriptional regulation of vascular endothelial growth factor by hypoxia. J Biol Chem *271*, 2746-2753.

Lin, C., Yang, L., Tanasa, B., Hutt, K., Ju, B.G., Ohgi, K., Zhang, J., Rose, D.W., Fu, X.D., Glass, C.K., *et al.* (2009). Nuclear receptor-induced chromosomal proximity and DNA breaks underlie specific translocations in cancer. Cell *139*, 1069-1083.

Lindstrom, M.S., Jurada, D., Bursac, S., Orsolic, I., Bartek, J., and Volarevic, S. (2018). Nucleolus as an emerging hub in maintenance of genome stability and cancer pathogenesis. Oncogene *37*, 2351-2366.

Liu, J., Carmell, M.A., Rivas, F.V., Marsden, C.G., Thomson, J.M., Song, J.J., Hammond, S.M., Joshua-Tor, L., and Hannon, G.J. (2004). Argonaute2 is the catalytic engine of mammalian RNAi. Science *305*, 1437-1441.

Liu, W., Shen, S.M., Zhao, X.Y., and Chen, G.Q. (2012a). Targeted genes and interacting proteins of hypoxia inducible factor-1. Int J Biochem Mol Biol *3*, 165-178.

Liu, Y., Bernauer, A.M., Yingling, C.M., and Belinsky, S.A. (2012b). HIF1alpha regulated expression of XPA contributes to cisplatin resistance in lung cancer. Carcinogenesis *33*, 1187-1192.

Lohrum, M.A., Ludwig, R.L., Kubbutat, M.H., Hanlon, M., and Vousden, K.H. (2003). Regulation of HDM2 activity by the ribosomal protein L11. Cancer Cell *3*, 577-587.

Lopez de Mesa, R., Lopez de Cerain Salsamendi, A., Ariznabarreta, L.S., Calasanz Abinzano, M.J., and Patino-Garcia, A. (2002). Measurement and analysis of the chemotherapy-induced genetic instability in pediatric cancer patients. Mutagenesis *17*, 171-175.

Lou, Z., Minter-Dykhouse, K., Franco, S., Gostissa, M., Rivera, M.A., Celeste, A., Manis, J.P., van Deursen, J., Nussenzweig, A., Paull, T.T., *et al.* (2006). MDC1 maintains genomic stability by participating in the amplification of ATM-dependent DNA damage signals. Mol Cell *21*, 187-200.

Lu, Y., Chu, A., Turker, M.S., and Glazer, P.M. (2011). Hypoxia-induced epigenetic regulation and silencing of the BRCA1 promoter. Mol Cell Biol *31*, 3339-3350.

Madan, E., Gogna, R., and Pati, U. (2012). p53 Ser15 phosphorylation disrupts the p53-RPA70 complex and induces RPA70-mediated DNA repair in hypoxia. Biochem J *443*, 811-820.

Marabitti, V., Lillo, G., Malacaria, E., Palermo, V., Sanchez, M., Pichierri, P., and Franchitto, A. (2019). ATM pathway activation limits R-loop-associated genomic instability in Werner syndrome cells. Nucleic Acids Res *47*, 3485-3502.

Marechal, V., Elenbaas, B., Piette, J., Nicolas, J.C., and Levine, A.J. (1994). The ribosomal L5 protein is associated with mdm-2 and mdm-2-p53 complexes. Mol Cell Biol *14*, 7414-7420.

Masse, E., Phoenix, P., and Drolet, M. (1997). DNA topoisomerases regulate R-loop formation during transcription of the rrnB operon in Escherichia coli. J Biol Chem *272*, 12816-12823.

Matos, D.A., Zhang, J.M., Ouyang, J., Nguyen, H.D., Genois, M.M., and Zou, L. (2020). ATR Protects the Genome against R Loops through a MUS81-Triggered Feedback Loop. Mol Cell *77*, 514-527 e514.

Matsuoka, S., Ballif, B.A., Smogorzewska, A., McDonald, E.R., 3rd, Hurov, K.E., Luo, J., Bakalarski, C.E., Zhao, Z., Solimini, N., Lerenthal, Y., *et al.* (2007). ATM and ATR substrate analysis reveals extensive protein networks responsive to DNA damage. Science *316*, 1160-1166.

Matsushima, H., Yonemura, K., Ohishi, K., and Hishida, A. (1998). The role of oxygen free radicals in cisplatin-induced acute renal failure in rats. J Lab Clin Med *131*, 518-526.

Maxwell, P.H., Wiesener, M.S., Chang, G.W., Clifford, S.C., Vaux, E.C., Cockman, M.E., Wykoff, C.C., Pugh, C.W., Maher, E.R., and Ratcliffe, P.J. (1999). The tumour suppressor protein VHL targets hypoxia-inducible factors for oxygen-dependent proteolysis. Nature *399*, 271-275.

Mayer, C., Zhao, J., Yuan, X., and Grummt, I. (2004). mTOR-dependent activation of the transcription factor TIF-IA links rRNA synthesis to nutrient availability. Genes Dev *18*, 423-434.

Mekhail, K., Rivero-Lopez, L., Khacho, M., and Lee, S. (2006). Restriction of rRNA synthesis by VHL maintains energy equilibrium under hypoxia. Cell Cycle *5*, 2401-2413.

Meng, A.X., Jalali, F., Cuddihy, A., Chan, N., Bindra, R.S., Glazer, P.M., and Bristow, R.G. (2005). Hypoxia down-regulates DNA double strand break repair gene expression in prostate cancer cells. Radiother Oncol *76*, 168-176.

Mihaylova, V.T., Bindra, R.S., Yuan, J., Campisi, D., Narayanan, L., Jensen, R., Giordano, F., Johnson, R.S., Rockwell, S., and Glazer, P.M. (2003). Decreased expression of the DNA mismatch repair gene Mlh1 under hypoxic stress in mammalian cells. Mol Cell Biol *23*, 3265-3273.

Momand, J., Zambetti, G.P., Olson, D.C., George, D., and Levine, A.J. (1992). The mdm-2 oncogene product forms a complex with the p53 protein and inhibits p53-mediated transactivation. Cell *69*, 1237-1245.

Mooser, C., Symeonidou, I.E., Leimbacher, P.A., Ribeiro, A., Shorrocks, A.K., Jungmichel, S., Larsen, S.C., Knechtle, K., Jasrotia, A., Zurbriggen, D., *et al.* (2020). Treacle controls the nucleolar response to rDNA breaks via TOPBP1 recruitment and ATR activation. Nat Commun *11*, 123.

Nadanaka, S., Okada, T., Yoshida, H., and Mori, K. (2007). Role of disulfide bridges formed in the luminal domain of ATF6 in sensing endoplasmic reticulum stress. Mol Cell Biol *27*, 1027-1043.

Nadel, J., Athanasiadou, R., Lemetre, C., Wijetunga, N.A., P, O.B., Sato, H., Zhang, Z., Jeddeloh, J., Montagna, C., Golden, A., *et al.* (2015). RNA:DNA hybrids in the human genome have distinctive nucleotide characteristics, chromatin composition, and transcriptional relationships. Epigenetics Chromatin *8*, 46.

Nagy, J.A., Chang, S.H., Shih, S.C., Dvorak, A.M., and Dvorak, H.F. (2010). Heterogeneity of the tumor vasculature. Semin Thromb Hemost *36*, 321-331.

Nakamura, H., Tanimoto, K., Hiyama, K., Yunokawa, M., Kawamoto, T., Kato, Y., Yoshiga, K., Poellinger, L., Hiyama, E., and Nishiyama, M. (2008). Human mismatch repair gene, MLH1, is transcriptionally repressed by the hypoxia-inducible transcription factors, DEC1 and DEC2. Oncogene *27*, 4200-4209.

Nelson, D.A., Tan, T.T., Rabson, A.B., Anderson, D., Degenhardt, K., and White, E. (2004). Hypoxia and defective apoptosis drive genomic instability and tumorigenesis. Genes Dev *18*, 2095-2107.

Nordsmark, M., Bentzen, S.M., Rudat, V., Brizel, D., Lartigau, E., Stadler, P., Becker, A., Adam, M., Molls, M., Dunst, J., *et al.* (2005). Prognostic value of tumor oxygenation in 397 head and neck tumors after primary radiation therapy. An international multi-center study. Radiother Oncol *77*, 18-24.

O'Sullivan, A.C., Sullivan, G.J., and McStay, B. (2002). UBF binding in vivo is not restricted to regulatory sequences within the vertebrate ribosomal DNA repeat. Mol Cell Biol *22*, 657-668.

Olcina, M.M., Foskolou, I.P., Anbalagan, S., Senra, J.M., Pires, I.M., Jiang, Y., Ryan, A.J., and Hammond, E.M. (2013). Replication stress and chromatin context link ATM activation to a role in DNA replication. Mol Cell *52*, 758-766.

Papp-Szabo, E., Josephy, P.D., and Coomber, B.L. (2005). Microenvironmental influences on mutagenesis in mammary epithelial cells. Int J Cancer *116*, 679-685.

Paredes, S., and Maggert, K.A. (2009). Ribosomal DNA contributes to global chromatin regulation. Proc Natl Acad Sci U S A *106*, 17829-17834.

Pengue, G., and Lania, L. (1996). Kruppel-associated box-mediated repression of RNA polymerase II promoters is influenced by the arrangement of basal promoter elements. Proc Natl Acad Sci U S A *93*, 1015-1020.

Pires, I.M., Bencokova, Z., McGurk, C., and Hammond, E.M. (2010a). Exposure to acute hypoxia induces a transient DNA damage response which includes Chk1 and TLK1. Cell Cycle *9*, 2502-2507.

Pires, I.M., Bencokova, Z., Milani, M., Folkes, L.K., Li, J.L., Stratford, M.R., Harris, A.L., and Hammond, E.M. (2010b). Effects of acute versus chronic hypoxia on DNA damage responses and genomic instability. Cancer Res *70*, 925-935.

Pires, I.M., Olcina, M.M., Anbalagan, S., Pollard, J.R., Reaper, P.M., Charlton, P.A., McKenna, W.G., and Hammond, E.M. (2012). Targeting radiation-resistant hypoxic tumour cells through ATR inhibition. Br J Cancer *107*, 291-299.

Pollard, P.J., Loenarz, C., Mole, D.R., McDonough, M.A., Gleadle, J.M., Schofield, C.J., and Ratcliffe, P.J. (2008). Regulation of Jumonji-domain-containing histone demethylases by hypoxia-inducible factor (HIF)-1alpha. Biochem J *416*, 387-394.

Preti, M., O'Donohue, M.F., Montel-Lehry, N., Bortolin-Cavaille, M.L., Choesmel, V., and Gleizes, P.E. (2013). Gradual processing of the ITS1 from the nucleolus to the cytoplasm during synthesis of the human 18S rRNA. Nucleic Acids Res *41*, 4709-4723.

Prieto, J.L., and McStay, B. (2007). Recruitment of factors linking transcription and processing of pre-rRNA to NOR chromatin is UBF-dependent and occurs independent of transcription in human cells. Genes Dev *21*, 2041-2054.

Promonet, A., Padioleau, I., Liu, Y., Sanz, L., Biernacka, A., Schmitz, A.L., Skrzypczak, M., Sarrazin, A., Mettling, C., Rowicka, M., *et al.* (2020). Topoisomerase 1 prevents replication stress at R-loop-enriched transcription termination sites. Nat Commun *11*, 3940.

Ramachandran, S., Ma, T., Ng, N., Foskolou, I.P., Hwang, M.-S., Victori, P., Cheng, W.-C., Buffa, F.M., Leszczynska, K.B., Gromak, N., *et al.* (2020). Hypoxia-induced SETX links replication stress with the unfolded protein response. bioRxiv.

Ren, Y., Hao, P., Dutta, B., Cheow, E.S., Sim, K.H., Gan, C.S., Lim, S.K., and Sze, S.K. (2013). Hypoxia modulates A431 cellular pathways association to tumor radioresistance and enhanced migration revealed by comprehensive proteomic and functional studies. Mol Cell Proteomics *12*, 485-498.

Reynolds, T.Y., Rockwell, S., and Glazer, P.M. (1996). Genetic instability induced by the tumor microenvironment. Cancer Res *56*, 5754-5757.

Rezvani, H.R., Mahfouf, W., Ali, N., Chemin, C., Ged, C., Kim, A.L., de Verneuil, H., Taieb, A., Bickers, D.R., and Mazurier, F. (2010). Hypoxia-inducible factor-1alpha regulates the expression of nucleotide excision repair proteins in keratinocytes. Nucleic Acids Res *38*, 797-809.

Ribeiro de Almeida, C., Dhir, S., Dhir, A., Moghaddam, A.E., Sattentau, Q., Meinhart, A., and Proudfoot, N.J. (2018). RNA Helicase DDX1 Converts RNA G-Quadruplex Structures into R-Loops to Promote IgH Class Switch Recombination. Mol Cell *70*, 650-662 e658.

Robledo, S., Idol, R.A., Crimmins, D.L., Ladenson, J.H., Mason, P.J., and Bessler, M. (2008). The role of human ribosomal proteins in the maturation of rRNA and ribosome production. RNA *14*, 1918-1929.

Rodier, F., Coppe, J.P., Patil, C.K., Hoeijmakers, W.A., Munoz, D.P., Raza, S.R., Freund, A., Campeau, E., Davalos, A.R., and Campisi, J. (2009). Persistent DNA damage signalling triggers senescence-associated inflammatory cytokine secretion. Nat Cell Biol *11*, 973-979.

Romero-Ramirez, L., Cao, H., Nelson, D., Hammond, E., Lee, A.H., Yoshida, H., Mori, K., Glimcher, L.H., Denko, N.C., Giaccia, A.J., *et al.* (2004). XBP1 is essential for survival under hypoxic conditions and is required for tumor growth. Cancer Res *64*, 5943-5947.

Safronova, O.S., Nakahama, K., and Morita, I. (2014). Acute hypoxia affects P-TEFb through HDAC3 and HEXIM1-dependent mechanism to promote gene-specific transcriptional repression. Nucleic Acids Res *42*, 8954-8969.

Santoro, R., and Grummt, I. (2005). Epigenetic mechanism of rRNA gene silencing: temporal order of NoRC-mediated histone modification, chromatin remodeling, and DNA methylation. Mol Cell Biol *25*, 2539-2546.

Sanz, L.A., Hartono, S.R., Lim, Y.W., Steyaert, S., Rajpurkar, A., Ginno, P.A., Xu, X., and Chedin, F. (2016). Prevalent, Dynamic, and Conserved R-Loop Structures Associate with Specific Epigenomic Signatures in Mammals. Mol Cell *63*, 167-178.

Saponaro, M., Kantidakis, T., Mitter, R., Kelly, G.P., Heron, M., Williams, H., Soding, J., Stewart, A., and Svejstrup, J.Q. (2014). RECQL5 controls transcript elongation and suppresses genome instability associated with transcription stress. Cell *157*, 1037-1049.

Savitsky, K., Bar-Shira, A., Gilad, S., Rotman, G., Ziv, Y., Vanagaite, L., Tagle, D.A., Smith, S., Uziel, T., Sfez, S., *et al.* (1995). A single ataxia telangiectasia gene with a product similar to PI-3 kinase. Science *268*, 1749-1753.

Scherl, A., Coute, Y., Deon, C., Calle, A., Kindbeiter, K., Sanchez, J.C., Greco, A., Hochstrasser, D., and Diaz, J.J. (2002). Functional proteomic analysis of human nucleolus. Mol Biol Cell *13*, 4100-4109.

Schwab, R.A., Nieminuszczy, J., Shah, F., Langton, J., Lopez Martinez, D., Liang, C.C., Cohn, M.A., Gibbons, R.J., Deans, A.J., and Niedzwiedz, W. (2015). The Fanconi Anemia Pathway Maintains Genome Stability by Coordinating Replication and Transcription. Mol Cell *60*, 351-361.

Shanbhag, N.M., Rafalska-Metcalf, I.U., Balane-Bolivar, C., Janicki, S.M., and Greenberg, R.A. (2010). ATM-dependent chromatin changes silence transcription in cis to DNA double-strand breaks. Cell *141*, 970-981.

Shav-Tal, Y., Blechman, J., Darzacq, X., Montagna, C., Dye, B.T., Patton, J.G., Singer, R.H., and Zipori, D. (2005). Dynamic sorting of nuclear components into distinct nucleolar caps during transcriptional inhibition. Mol Biol Cell *16*, 2395-2413.

Shen, W., Sun, H., De Hoyos, C.L., Bailey, J.K., Liang, X.H., and Crooke, S.T. (2017). Dynamic nucleoplasmic and nucleolar localization of mammalian RNase H1 in response to RNAP I transcriptional R-loops. Nucleic Acids Res *45*, 10672-10692.

Shimizu, N., Ooka, M., Takagi, T., Takeda, S., and Hirota, K. (2015). Distinct DNA Damage Spectra Induced by Ionizing Radiation in Normoxic and Hypoxic Cells. Radiat Res *184*, 442-448.

Shirasawa, S., Furuse, M., Yokoyama, N., and Sasazuki, T. (1993). Altered growth of human colon cancer cell lines disrupted at activated Ki-ras. Science *260*, 85-88.

Shivji, M.K.K., Renaudin, X., Williams, C.H., and Venkitaraman, A.R. (2018). BRCA2 Regulates Transcription Elongation by RNA Polymerase II to Prevent R-Loop Accumulation. Cell Rep *22*, 1031-1039.

Siebenwirth, C., Greubel, C., Drexler, G.A., Reindl, J., Walsh, D.W.M., Schwarz, B., Sammer, M., Baur, I., Pospiech, H., Schmid, T.E., *et al.* (2019). Local inhibition of rRNA transcription without nucleolar segregation after targeted ion irradiation of the nucleolus. J Cell Sci *132*.

Sinkkonen, L., Hugenschmidt, T., Filipowicz, W., and Svoboda, P. (2010). Dicer is associated with ribosomal DNA chromatin in mammalian cells. PLoS One *5*, e12175.

Skourti-Stathaki, K., Kamieniarz-Gdula, K., and Proudfoot, N.J. (2014). R-loops induce repressive chromatin marks over mammalian gene terminators. Nature *516*, 436-439.

Skourti-Stathaki, K., Proudfoot, N.J., and Gromak, N. (2011). Human senataxin resolves RNA/DNA hybrids formed at transcriptional pause sites to promote Xrn2-dependent termination. Mol Cell *42*, 794-805.

Sloan, K.E., Bohnsack, M.T., Schneider, C., and Watkins, N.J. (2014). The roles of SSU processome components and surveillance factors in the initial processing of human ribosomal RNA. RNA *20*, 540-550.

Sloan, K.E., Mattijssen, S., Lebaron, S., Tollervey, D., Pruijn, G.J., and Watkins, N.J. (2013). Both endonucleolytic and exonucleolytic cleavage mediate ITS1 removal during human ribosomal RNA processing. J Cell Biol *200*, 577-588.

Sokka, M., Rilla, K., Miinalainen, I., Pospiech, H., and Syvaoja, J.E. (2015). High levels of TopBP1 induce ATR-dependent shut-down of rRNA transcription and nucleolar segregation. Nucleic Acids Res *43*, 4975-4989.

Sollier, J., Stork, C.T., Garcia-Rubio, M.L., Paulsen, R.D., Aguilera, A., and Cimprich, K.A. (2014). Transcription-coupled nucleotide excision repair factors promote R-loop-induced genome instability. Mol Cell *56*, 777-785.

Stein, H., and Hausen, P. (1969). Enzyme from calf thymus degrading the RNA moiety of DNA-RNA Hybrids: effect on DNA-dependent RNA polymerase. Science *166*, 393-395.

Stenstrom, L., Mahdessian, D., Gnann, C., Cesnik, A.J., Ouyang, W., Leonetti, M.D., Uhlen, M., Cuylen-Haering, S., Thul, P.J., and Lundberg, E. (2020). Mapping the nucleolar proteome reveals a spatiotemporal organization related to intrinsic protein disorder. Mol Syst Biol *16*, e9469.

Stults, D.M., Killen, M.W., Williamson, E.P., Hourigan, J.S., Vargas, H.D., Arnold, S.M., Moscow, J.A., and Pierce, A.J. (2009). Human rRNA gene clusters are recombinational hotspots in cancer. Cancer Res *69*, 9096-9104.

Sugasawa, K., Ng, J.M., Masutani, C., Iwai, S., van der Spek, P.J., Eker, A.P., Hanaoka, F., Bootsma, D., and Hoeijmakers, J.H. (1998). Xeroderma pigmentosum group C protein complex is the initiator of global genome nucleotide excision repair. Mol Cell *2*, 223-232.

Tafforeau, L., Zorbas, C., Langhendries, J.L., Mullineux, S.T., Stamatopoulou, V., Mullier, R., Wacheul, L., and Lafontaine, D.L. (2013). The complexity of human ribosome biogenesis revealed by systematic nucleolar screening of Pre-rRNA processing factors. Mol Cell *51*, 539-551.

Takeshima, H., Yamashita, S., Shimazu, T., Niwa, T., and Ushijima, T. (2009). The presence of RNA polymerase II, active or stalled, predicts epigenetic fate of promoter CpG islands. Genome Res *19*, 1974-1982.

Tausendschon, M., Dehne, N., and Brune, B. (2011). Hypoxia causes epigenetic gene regulation in macrophages by attenuating Jumonji histone demethylase activity. Cytokine *53*, 256-262.

Tessarz, P., Santos-Rosa, H., Robson, S.C., Sylvestersen, K.B., Nelson, C.J., Nielsen, M.L., and Kouzarides, T. (2014). Glutamine methylation in histone H2A is an RNA-polymerase-I-dedicated modification. Nature *505*, 564-568.

Thomas, M., White, R.L., and Davis, R.W. (1976). Hybridization of RNA to double-stranded DNA: formation of R-loops. Proc Natl Acad Sci U S A *73*, 2294-2298.

Thomlinson, R.H., and Gray, L.H. (1955). The histological structure of some human lung cancers and the possible implications for radiotherapy. Br J Cancer *9*, 539-549.

Tiana, M., Acosta-Iborra, B., Hernandez-Sierra, R., Galiana-Ribote, C., Fernandez-Moreno, M.A., Jimenez, B., and Del Peso, L. (2020). Metabolic labelling of RNA uncovers the contribution of transcription and decay rates on hypoxia-induced changes in RNA levels. RNA.

Tomasetti, C., and Vogelstein, B. (2015). Cancer etiology. Variation in cancer risk among tissues can be explained by the number of stem cell divisions. Science *347*, 78-81.

Tresini, M., Warmerdam, D.O., Kolovos, P., Snijder, L., Vrouwe, M.G., Demmers, J.A., van, I.W.F., Grosveld, F.G., Medema, R.H., Hoeijmakers, J.H., *et al.* (2015). The core spliceosome as target and effector of non-canonical ATM signalling. Nature *523*, 53-58.

Tsukada, Y., Fang, J., Erdjument-Bromage, H., Warren, M.E., Borchers, C.H., Tempst, P., and Zhang, Y. (2006). Histone demethylation by a family of JmjC domain-containing proteins. Nature *439*, 811-816.

Turowski, T.W., Petfalski, E., Goddard, B.D., French, S.L., Helwak, A., and Tollervey, D. (2020). Nascent Transcript Folding Plays a Major Role in Determining RNA Polymerase Elongation Rates. Mol Cell *79*, 488-503 e411.

Tycowski, K.T., Shu, M.D., and Steitz, J.A. (1994). Requirement for intron-encoded U22 small nucleolar RNA in 18S ribosomal RNA maturation. Science *266*, 1558-1561.

van den Beucken, T., Koch, E., Chu, K., Rupaimoole, R., Prickaerts, P., Adriaens, M., Voncken, J.W., Harris, A.L., Buffa, F.M., Haider, S., *et al.* (2014). Hypoxia promotes stem cell phenotypes and poor prognosis through epigenetic regulation of DICER. Nat Commun *5*, 5203.

van Sluis, M., and McStay, B. (2015). A localized nucleolar DNA damage response facilitates recruitment of the homology-directed repair machinery independent of cell cycle stage. Genes Dev *29*, 1151-1163.

Velichko, A.K., Petrova, N.V., Luzhin, A.V., Strelkova, O.S., Ovsyannikova, N., Kireev, II, Petrova, N.V., Razin, S.V., and Kantidze, O.L. (2019). Hypoosmotic stress induces R loop formation in nucleoli and ATR/ATM-dependent silencing of nucleolar transcription. Nucleic Acids Res *47*, 6811-6825.

Villunger, A., Michalak, E.M., Coultas, L., Mullauer, F., Bock, G., Ausserlechner, M.J., Adams, J.M., and Strasser, A. (2003). p53- and drug-induced apoptotic responses mediated by BH3-only proteins puma and noxa. Science *302*, 1036-1038.

Wahba, L., Costantino, L., Tan, F.J., Zimmer, A., and Koshland, D. (2016). S1-DRIP-seq identifies high expression and polyA tracts as major contributors to R-loop formation. Genes Dev *30*, 1327-1338.

Wang, G.L., Jiang, B.H., Rue, E.A., and Semenza, G.L. (1995). Hypoxia-inducible factor 1 is a basic-helix-loop-helix-PAS heterodimer regulated by cellular O2 tension. Proc Natl Acad Sci U S A *92*, 5510-5514.

Wang, G.L., and Semenza, G.L. (1993). General involvement of hypoxia-inducible factor 1 in transcriptional response to hypoxia. Proc Natl Acad Sci U S A *90*, 4304-4308.

Wang, M., and Pestov, D.G. (2011). 5'-end surveillance by Xrn2 acts as a shared mechanism for mammalian pre-rRNA maturation and decay. Nucleic Acids Res *39*, 1811-1822.

Wang, P., Li, J., Tao, J., and Sha, B. (2018). The luminal domain of the ER stress sensor protein PERK binds misfolded proteins and thereby triggers PERK oligomerization. J Biol Chem *293*, 4110-4121.

Wasmuth, E.V., and Lima, C.D. (2012). Exo- and endoribonucleolytic activities of yeast cytoplasmic and nuclear RNA exosomes are dependent on the noncatalytic core and central channel. Mol Cell *48*, 133-144.

Wellinger, R.E., Prado, F., and Aguilera, A. (2006). Replication fork progression is impaired by transcription in hyperrecombinant yeast cells lacking a functional THO complex. Mol Cell Biol *26*, 3327-3334.

Wittner, M., Hamperl, S., Stockl, U., Seufert, W., Tschochner, H., Milkereit, P., and Griesenbeck, J. (2011). Establishment and maintenance of alternative chromatin states at a multicopy gene locus. Cell *145*, 543-554.

Wong, J.M., and Collins, K. (2006). Telomerase RNA level limits telomere maintenance in X-linked dyskeratosis congenita. Genes Dev *20*, 2848-2858.

Wong, W.J., Qiu, B., Nakazawa, M.S., Qing, G., and Simon, M.C. (2013). MYC degradation under low O2 tension promotes survival by evading hypoxia-induced cell death. Mol Cell Biol *33*, 3494-3504.

Xu, B., Li, H., Perry, J.M., Singh, V.P., Unruh, J., Yu, Z., Zakari, M., McDowell, W., Li, L., and Gerton, J.L. (2017). Ribosomal DNA copy number loss and sequence variation in cancer. PLoS Genet *13*, e1006771.

Yang, Y., McBride, K.M., Hensley, S., Lu, Y., Chedin, F., and Bedford, M.T. (2014). Arginine methylation facilitates the recruitment of TOP3B to chromatin to prevent R loop accumulation. Mol Cell *53*, 484-497.

Young, S.D., Marshall, R.S., and Hill, R.P. (1988). Hypoxia induces DNA overreplication and enhances metastatic potential of murine tumor cells. Proc Natl Acad Sci U S A *85*, 9533-9537.

Yu, F., Shen, X., Fan, L., and Yu, Z. (2015). Analysis of histone modifications at human ribosomal DNA in liver cancer cell. Sci Rep *5*, 18100.

Yuan, J., Narayanan, L., Rockwell, S., and Glazer, P.M. (2000). Diminished DNA repair and elevated mutagenesis in mammalian cells exposed to hypoxia and low pH. Cancer Res *60*, 4372-4376.

Yuce, O., and West, S.C. (2013). Senataxin, defective in the neurodegenerative disorder ataxia with oculomotor apraxia 2, lies at the interface of transcription and the DNA damage response. Mol Cell Biol *33*, 406-417.

Zellweger, R., Dalcher, D., Mutreja, K., Berti, M., Schmid, J.A., Herrador, R., Vindigni, A., and Lopes, M. (2015). Rad51-mediated replication fork reversal is a global response to genotoxic treatments in human cells. J Cell Biol *208*, 563-579.

Zentner, G.E., Saiakhova, A., Manaenkov, P., Adams, M.D., and Scacheri, P.C. (2011). Integrative genomic analysis of human ribosomal DNA. Nucleic Acids Res *39*, 4949-4960.

Zhai, W., and Comai, L. (2000). Repression of RNA polymerase I transcription by the tumor suppressor p53. Mol Cell Biol *20*, 5930-5938.

Zhang, H., Gao, P., Fukuda, R., Kumar, G., Krishnamachary, B., Zeller, K.I., Dang, C.V., and Semenza, G.L. (2007). HIF-1 inhibits mitochondrial biogenesis and cellular respiration in VHL-deficient renal cell carcinoma by repression of C-MYC activity. Cancer Cell *11*, 407-420.

Zhao, Z., Dammert, M.A., Grummt, I., and Bierhoff, H. (2016). lncRNA-Induced Nucleosome Repositioning Reinforces Transcriptional Repression of rRNA Genes upon Hypotonic Stress. Cell Rep *14*, 1876-1882.

Zhao, Z., Senturk, N., Song, C., and Grummt, I. (2018). lncRNA PAPAS tethered to the rDNA enhancer recruits hypophosphorylated CHD4/NuRD to repress rRNA synthesis at elevated temperatures. Genes Dev *32*, 836-848.

Zhou, D., Zhu, X., Zheng, S., Tan, D., Dong, M.Q., and Ye, K. (2019). Cryo-EM structure of an early precursor of large ribosomal subunit reveals a half-assembled intermediate. Protein Cell *10*, 120-130.

Zhou, X., Sun, H., Chen, H., Zavadil, J., Kluz, T., Arita, A., and Costa, M. (2010). Hypoxia induces trimethylated H3 lysine 4 by inhibition of JARID1A demethylase. Cancer Res *70*, 4214-4221.

Zhu, Y., McAvoy, S., Kuhn, R., and Smith, D.I. (2006). RORA, a large common fragile site gene, is involved in cellular stress response. Oncogene *25*, 2901-2908.

Appendix

8.1 Copyright details

Relevant to Figure 1.1

License Number	4856560560000
License date	Jun 26, 2020
Licensed Content Publisher	Elsevier
Licensed Content Publication	Cell
Licensed Content Title	Hallmarks of Cancer: The Next Generation
Licensed Content Author	Douglas Hanahan, Robert A. Weinberg
Licensed Content Date	Mar 4, 2011
Licensed Content Volume	144
Licensed Content Issue	5
Licensed Content Pages	29
Start Page	646
End Page	674
Type of Use	reuse in a thesis/dissertation
Portion	figures/tables/illustrations
Number of figures/tables/illustrations	1
Format	both print and electronic
Are you the author of this Elsevier article?	No
Will you be translating?	No
Title	Investigating the response of rRNA to hypoxia
Institution name	University of Oxford
Expected presentation date	Jan 2021
Portions	Figure 6, Therapeutic Targeting of the Hallmarks of Cancer
Requestor Location	Miss. Natalie Ng United Kingdom Attn: University of Oxford
Publisher Tax ID	GB 494 6272 12
Total	0.00 GBP

Relevant to Publications from Thesis

License Number	4946040588109
License date	Nov 11, 2020
Licensed Content Publisher	John Wiley and Sons
Licensed Content Publication	FEBS Journal
Licensed Content Title	Challenges to DNA replication in hypoxic conditions

Licensed Content Date	Jan 12, 2018
Licensed Content Pages	1
Type of use	Dissertation/Thesis
Requestor type	Author of this Wiley article
Format	Print and electronic
Portion	Full article
Will you be translating?	No
Title	Investigating the response of rRNA to hypoxia
Institution name	University of Oxford
Expected presentation date	Jan 2021
Requestor Location	Miss. Natalie Ng Wychwood Cottage Chipping Norton, Oxfordshire OX73DF United Kingdom Attn: University of Oxford
Publisher Tax ID	EU826007151
Total	0.00 GBP

8.2 Publications from this thesis

1) Hypoxia-induced R-loop accumulation blocks RNA polymerase I mediated transcription **Natalie Ng**, Shaliny Ramachandran, Lisa Folkes, Timothy C. Humphrey, Nicholas C. Denko and Ester M. Hammond (Manuscript in review)

2) Hypoxia-induced SETX links replication stress with the unfolded protein response Shaliny Ramachandran, Tiffany Ma, **Natalie Ng**, Iosifina P. Foskolou, Ming-Shih Hwang, Pedro Victori, Wei-Chen Cheng, Francesca M. Buffa, Katarzyna B. Leszczynska, Natalia Gromak and Ester M. Hammond. bioRxiv 2020 (Manuscript in preparation for submission)

3) Challenges to DNA replication in hypoxic conditions
Natalie Ng, Karin Purshouse, Iosifina P. Foskolou, Monica M. Olcina and Ester M. Hammond. *285*, 1563–1571 FEBS letters 2018 (Reprinted with permission from John Wiley and Sons with FEBS Letters)

8.3 Awards and Prizes

MRC Doctoral Training Partnership Supplementary Funding Award
MRC DPhil studentship
Trinity College Graduate Award 2017 & 2020
Travel grant from Don Whitley Scientific

8.4 Presentations

Oncology Departmental Seminar Series – 2019 (Oral Presentation) 'Investigating the transcriptional response of rRNA to hypoxia'

Department of Oncology Annual Student Symposium – 2018 (Oral Presentation)
EMBO Transcription and Genome Maintenance – Mainz, Germany 2018 (Poster)
Oxford Institute for Radiation Oncology Conference (OIRO) – 2017 (Poster)
Oxford-MRC DTP annual symposium – 2017 (Poster)
Association for Radiation Research – 2017 (Poster)

bioRxiv preprint doi: https://doi.org/10.1101/2020.05.24.113548; this version posted May 26, 2020. The copyright holder for this preprint (which was not certified by peer review) is the author/funder. All rights reserved. No reuse allowed without permission.

Hypoxia-induced SETX links replication stress with the unfolded protein response

Shaliny Ramachandran[1], Tiffany Ma[1], Natalie Ng[1], Iosifina P. Foskolou[1], Ming-Shih Hwang[1], Pedro Victori[1], Wei-Chen Cheng[1], Francesca M. Buffa[1], Katarzyna B. Leszczynska[1*], Natalia Gromak[2], and Ester M. Hammond[1$]

[1] Oxford Institute for Radiation Oncology, Department of Oncology, University of Oxford, Oxford, UK. [2] Sir William Dunn School of Pathology, University of Oxford, Oxford, United Kingdom

*current address - Laboratory of Molecular Neurobiology, Neurobiology Center, Nencki Institute of Experimental Biology, Polish Academy of Sciences, Warsaw, Poland.

[$]corresponding author

ester.hammond@oncology.ox.ac.uk

ORCID – 0000-0002-2335-3146

Other ORCIDs

KBL - 0000-0002-3504-1553

NG - 0000-0002-4158-3586

NN - 0000-0003-0099-5557

PV - 0000-0001-6321-5584

FMB - 0000-0003-0409-406X

KEYWORDS: Hypoxia, Replication stress, UPR, SETX, R-loops, RNA/DNA hybrids

bioRxiv preprint doi: https://doi.org/10.1101/2020.05.24.113548; this version posted May 26, 2020. The copyright holder for this preprint (which was not certified by peer review) is the author/funder. All rights reserved. No reuse allowed without permission.

ABSTRACT

The levels of hypoxia associated with resistance to radiotherapy significantly impact cancer patient prognosis. These levels of hypoxia initiate a unique transcriptional response with the rapid activation of numerous transcription factors in a background of global repression of transcription. Here, we show that the biological response to radiobiological hypoxia includes the induction of the DNA/RNA helicase SETX. In the absence of hypoxia-induced SETX, R-loop levels increase, DNA damage accumulates, and DNA replication rates decrease. SETX plays a key role in protecting cells from DNA damage induced during transcription in hypoxia. Importantly, we show that the mechanism of SETX induction is reliant on the PERK/ATF4 arm of the unfolded protein response. These data not only highlight the unique cellular response to radiobiological hypoxia, which includes both a replication stress dependent DNA damage response and an unfolded protein response but uncover a novel link between these two distinct pathways.

bioRxiv preprint doi: https://doi.org/10.1101/2020.05.24.113548; this version posted May 26, 2020. The copyright holder for this preprint (which was not certified by peer review) is the author/funder. All rights reserved. No reuse allowed without permission.

INTRODUCTION

The microenvironment of the majority of solid tumours is characterised by regions of low oxygen (hypoxia), which result from abnormal vasculature and increased oxygen demand. Tumour hypoxia plays a pivotal role in tumourigenesis, and has been associated with increased aggressiveness, metastasis, resistance to radiation therapy, and poor patient prognosis [1]. The level of hypoxia associated with radiation resistance, radiobiological hypoxia (<0.13% O_2), is characterised by a rapid induction of replication stress, which is defined as the slowing or stalling of replication forks. We have attributed hypoxia-induced replication stress to decreased nucleotide availability [2-4]. Previously, we demonstrated that hypoxia-induced replication stress leads to the induction of an ATR- and ATM-dependent DNA damage response (DDR). However, hypoxia-induced replication stress is insufficient to induce ATM-mediated signalling and increased levels of heterochromatic histone marks, most notably H3K9me3 are also required [5-7]. Importantly, both hypoxia-induced ATR and ATM activity occur in the absence of detectable DNA damage [8].

R-loops are 3–stranded nucleic acid structures which are linked to transcription and can contribute to replication stress [9]. R-loops are comprised of an RNA/DNA hybrid and a displaced single-stranded DNA (ssDNA). R-loops form within the genome at actively transcribed genes preferentially occurring at gene promoters and terminators, but also in response to the loss of RNA biogenesis factors, and at sites of head-on transcription-replication collisions [10-13]. R-loops regulate gene expression but can also lead to genome instability, which is particularly apparent in cells with deficiencies in R-loop processing and binding factors, including for example BRCA1 [14-18]. Many different factors including RNase H enzymes, RNA/DNA helicases, topoisomerases, and mRNA biogenesis/processing factors are involved in the processing and resolution of R-loops [19,20]. The hypoxic environment is known to significantly change the transcriptional network of the cell, suggesting that there may also be an impact on R-loop formation and resolution [21,22]. DNA repair pathways, including critical components such as BRCA1 and Rad51, have been shown to be repressed through a variety of mechanisms in response to hypoxia [23-25]. In contrast, a number of transcriptional pathways are induced in radiobiological hypoxia including the hypoxia-inducible factors (HIF1-3),

bioRxiv preprint doi: https://doi.org/10.1101/2020.05.24.113548; this version posted May 26, 2020. The copyright holder for this preprint (which was not certified by peer review) is the author/funder. All rights reserved. No reuse allowed without permission.

p53 and those initiated by the unfolded protein response (UPR) [26-28]. The UPR is an ER stress response pathway that leads to global translation inhibition while upregulating selective genes including those involved in protein folding, redox homeostasis and protein degradation [29]. In contrast to the DDR, which is activated by ssDNA in hypoxia, the UPR is activated by misfolded proteins.

Senataxin (SETX) is a putative RNA/DNA helicase that can facilitate transcription termination and gene transcription of a subset of genes [12,30-33]. The yeast homolog of SETX, Sen1, was shown to be involved in transcription-coupled repair and protect cells from transcription-associated recombination [34-36]. In addition, Sen1 has been shown to act at the replication fork and facilitate replication at highly transcribed genes [37]. SETX has also been linked to R-loops at transcription-replication collisions and to participate in the antiviral response [36,38]. Mutations in SETX have been associated with two neurodegenerative diseases, ataxia with oculomotor apraxia type 2 (AOA2) and amyotrophic lateral sclerosis type 4 (ALS4) [39,40].

The role of R-loops and factors involved in R-loop processing including RNA/DNA helicases have not been investigated in response to hypoxia. We show that in radiobiological hypoxia, in the context of transcriptional and replication stress, R-loops increase. The majority of factors associated with R-loops were repressed with the notable exception of SETX, which was specifically induced in radiobiological hypoxia, prompting us to focus on the role of SETX in hypoxia. We found that the loss of SETX lead to an accumulation of R-loops, and that hypoxia-induced SETX protected cells from replication stress, transcription dependent DNA damage and apoptosis. Most importantly, hypoxia-induced SETX was dependent on the PERK branch of the UPR, providing the first evidence of a link between the UPR and replication stress in hypoxia.

RESULTS

SETX is induced in an oxygen-dependent manner

Exposure to hypoxia (<0.1% O_2) led to the rapid accumulation of RPA foci and pan-nuclear γH2AX in the absence of 53BP1 foci. Importantly, the cells that had pan-nuclear γH2AX also had RPA foci

bioRxiv preprint doi: https://doi.org/10.1101/2020.05.24.113548; this version posted May 26, 2020. The copyright holder for this preprint (which was not certified by peer review) is the author/funder. All rights reserved. No reuse allowed without permission.

which indicates a replication stress-dependent DDR despite the absence of detectable DNA damage (Figure 1A, B, S1A). The cellular response to radiobiological hypoxia included the rapid repression of global transcription rates as shown by quantification of 5-ethynyluridine (5'EU) incorporation (Figure 1C, D, S1B). In these same conditions (<0.1% O_2), the transcript levels of a number of R-loop processing factors including RNase H1, RNase H2B, PIF1, DHX9, RTEL1 and AQR, were significantly repressed. In contrast, SETX mRNA was upregulated in hypoxia (<0.1% O_2) (Figure 1E) and this was evident in a number of cell lines (Figure S1C-E). SETX has not previously been shown to be stress-responsive at the transcriptional level. SETX protein levels were also upregulated in hypoxia in various cell lines including RKO, A549 and HCT116 (Figure 1F-H). To determine oxygen dependency, we compared expression levels in <0.1% O_2 to 2% O_2 and found that SETX was specifically induced at <0.1% O_2 (Figure 1I). To investigate whether this oxygen dependent expression of SETX was evident in cancer patients, we used The Cancer Genome Atlas (TCGA) datasets for colorectal and lung cancers. Here, we compared SETX expression with both, a validated hypoxia signature and with a group of genes that we have previously shown are induced at <0.1% O_2 but not 2% O_2 [26,41]. As we saw no indication of SETX induction in 2% O_2, we were not surprised to find that SETX expression did not correlate with a hypoxia signature (Figure S1F). However, in agreement with the SETX induction at <0.1% O_2, SETX expression showed a positive correlation in the three datasets used with the group of p53-target genes specifically induced at <0.1% O_2 (Figure 1J). Therefore, it seems likely that SETX expression is increased in patient samples from tumours with radiobiological levels of hypoxia, lending further support to our novel finding that SETX is induced in an oxygen-dependent manner.

SETX alleviates R-loops and replication stress in hypoxia

To determine the impact of loss of SETX in hypoxia on R-loops, we used the S9.6 antibody, which specifically recognises RNA/DNA hybrids. R-loop levels increased in hypoxia in A549 and RKO cells and this increase was ablated when the cells were treated with RNase H, an endonuclease that degrades the RNA component of R-loops (Figure 2A, B and S2A). SETX depletion led to an increase in the levels of R-loops in both normoxia and hypoxia, and again, this increase was ablated with

bioRxiv preprint doi: https://doi.org/10.1101/2020.05.24.113548; this version posted May 26, 2020. The copyright holder for this preprint (which was not certified by peer review) is the author/funder. All rights reserved. No reuse allowed without permission.

RNase H treatment (Figure 2C and S2B-F). R-loops can contribute to replication stress, so we asked if SETX had a role to play in replication in hypoxia. Depletion of SETX led to a significant increase in stalled replication forks in normoxic conditions (Figure 2D). However, no changes were detected in hypoxic conditions, likely because hypoxia alone induced high levels of stalled forks (Figure 2E). SETX depletion decreased replication rates in both normoxia and hypoxia, however, this was more significant in the hypoxic conditions (Figure 2F and S2G, H).

SETX protects hypoxic cells from transcription associated DNA damage and apoptosis

SETX has been suggested to affect RNA polymerase II (Pol II) binding at certain genes and to facilitate transcriptional termination of a number of genes [12,32,42]. Under normoxic conditions SETX-knock-down lead to a significant decrease in 5'EU incorporation suggesting that SETX plays a role in global transcription. In hypoxia where transcription is repressed, there was a modest, further decrease in 5'EU incorporation upon SETX depletion (Figure 3A and S3A). A previous study identified changes in the expression of 36 genes in response to SETX depletion, and 60 genes changing in a SETX-dependent manner in response to viral infection [38]. We carried out RNA-sequencing (RNA-seq) and found that SETX depletion only affected a small subset of genes (17 increasing and 48 decreasing) in normoxia, and of these genes, 5 were previously identified as regulated in a SETX-dependent manner. In contrast, SETX depletion had a much higher impact in hypoxia causing 341 genes to increase and 256 genes to decrease in expression (Figure 3B). These results were validated by RT-qPCR (Figure S3B). We investigated whether the differentially expressed genes shared any common features by gene ontology analysis and found that approximately 20% of genes upregulated in SETX depleted hypoxic cells were involved in rRNA processing, nucleolus and ribosome biogenesis (Figure S3C). We also investigated whether the differentially expressed genes shared any other common features. Hypoxia-induced genes that had increased expression in SETX depleted cells had a slightly shorter gene length compared to the hypoxia-induced genes that were unaffected or had decreased expression upon SETX depletion (Figure S4A). There was no evidence for the genes differentially expressed upon SETX depletion that are also hypoxia inducible or repressive, having similar number of exons, number of G4 quadruple structures or GC percent (Figure S4B-D).

bioRxiv preprint doi: https://doi.org/10.1101/2020.05.24.113548; this version posted May 26, 2020. The copyright holder for this preprint (which was not certified by peer review) is the author/funder. All rights reserved. No reuse allowed without permission.

Given that unresolved R-loops have been associated with DNA damage, we asked whether depleting SETX would lead to DNA damage in hypoxia. As expected, there was no increase in DNA damage in hypoxia but upon SETX depletion there was a significant increase in DNA damage as determined by the increase in cells with 53BP1 foci (Figure 3C and S5A). To test whether the DNA damage observed in the SETX depleted hypoxic cells was linked to transcription we treated cells with dichloro-beta-D-ribofuranosylbenzimidazole (DRB), which inhibits Pol II-mediated transcription. DRB rescued the DNA damage observed in the SETX depleted hypoxic cells suggesting that the damage observed in SETX depleted hypoxic cells was transcription dependent (Figure 3C). We confirmed that DRB did not rescue DNA damage non-specifically by demonstrating that DRB did not rescue Adriamycin-induced DNA damage (Figure S5B). It should be noted that by inhibiting transcription, DRB led to a decrease in R-loop levels, suggesting that SETX may be protecting the hypoxic cells from co-transcriptional R-loop associated DNA damage (Figure S5C-E). The damage observed in SETX-depleted hypoxic cells is independent of cell cycle occurring in both S-phase and non-S-phase cells, supporting the hypothesis that the damage could be the result of transcription dependent R-loops (Figure S5F, G). DNA damage, if unrepaired, can lead to increased apoptosis and reduced survival. In hypoxia, SETX depletion led to decreased colony survival when compared to control cells, suggesting that SETX function contributes to hypoxic cell viability (Figure 3D). SETX depletion also led to a significant increase in apoptosis compared to the control cells specifically in hypoxia and again, this was found to be transcription dependent as the addition of DRB rescued the apoptosis induced by SETX loss (Figure 3E, F). Taken together, SETX protects hypoxic cells from transcription linked DNA damage and apoptosis.

SETX upregulation is dependent on the UPR

To investigate the mechanism of SETX induction in hypoxia, A549 cells were used as these showed the most robust transcriptional induction of SETX in hypoxia. SETX mRNA induction occurred at <0.1% O_2, and multiple candidate transcription factors are active at this oxygen level, including HIF, p53 and those involved in the UPR (ATF3, ATF4, ATF5 and CHOP) (Figure S6A, B). Given that SETX was not induced at 2% O_2 where HIF is active, and SETX expression did not correlate with a

bioRxiv preprint doi: https://doi.org/10.1101/2020.05.24.113548; this version posted May 26, 2020. The copyright holder for this preprint (which was not certified by peer review) is the author/funder. All rights reserved. No reuse allowed without permission.

hypoxia signature, it seemed unlikely that SETX induction was dependent on HIF. However, to formally test this, we depleted HIF1α and asked whether this affected SETX induction in hypoxia. As expected SETX induction in hypoxia was not affected by HIF1α siRNA in contrast to the control gene VEGF, confirming that SETX is not induced by HIF1α in hypoxia (Figure S6C, D). Next, we found that SETX induction in hypoxia was not affected by p53 siRNA when compared to control cells, suggesting that p53 signalling does not contribute to SETX induction in hypoxia (Figure 4A, S6E). In support of this conclusion, we and others have found no evidence of a functional p53 response element in the SETX promoter [43]. Next, we investigated whether SETX induction could be linked to the UPR. Predicted binding sites were identified for the UPR transcription factor ATF4 in the GeneHancer identifier GH09J132349 corresponding to the SETX promoter region. We depleted ATF4 using siRNA and demonstrated that ATF4 is responsible for the induction of SETX in hypoxia (Figure 4B, S7A). The transcript levels of the ATF4 target CHOP were tested in parallel to confirm ATF4 knock-down (Figure S7B). Chromatin immunoprecipitation qPCR was used to confirm that ATF4 is responsible for SETX induction in hypoxia. ATF4 was enriched at the SETX promoter specifically in hypoxia (Figure 4C). ATF4 enrichment at the CHOP gene was used as a positive control (Figure S7C). To further investigate whether SETX is a UPR target, we exposed cells to a range of stresses including tunicamycin and thapsigargin, both of which are known to induce the UPR, and found that both led to a significant increase in SETX mRNA similar to the induction observed in hypoxia (<0.1% O_2) (Figure 4D, S7D). Consistent with this, SETX was found to be upregulated in a RNA sequencing dataset upon tunicamycin addition although this was not specifically reported [44]. As expected, we also demonstrated that SETX expression was not induced with hypoxia mimetics desferrioxamine (DFO) and 2% O_2, which lead to HIF stabilisation (Figure 4D, S7E). Importantly, hydroxyurea did not affect SETX transcript levels demonstrating that hypoxia-mediated induction of SETX is UPR dependent and distinct from replication stress (Figure 4D). Thapsigargin and tunicamycin induced SETX but did not lead to replication stress as observed by an absence of RPA phosphorylation (Figure 4E, S7F).

bioRxiv preprint doi: https://doi.org/10.1101/2020.05.24.113548; this version posted May 26, 2020. The copyright holder for this preprint (which was not certified by peer review) is the author/funder. All rights reserved. No reuse allowed without permission.

As signalling to ATF4 in hypoxia is primarily mediated by the protein kinase R (PKR)-like endoplasmic reticulum kinase (PERK), we hypothesised that SETX induction in hypoxia would also be PERK dependent [45,46]. Depleting PERK abrogated the hypoxia-mediated induction of SETX (Figure 4F, S7G). To further validate our finding, we used a PERK inhibitor GSK2606414 (PERKi). Pre-treating cells with PERKi led to a significant decrease in SETX mRNA levels in hypoxia as compared to the control cells (Figure 4G, S7H). We also verified that pre-treating cells with PERKi abrogated SETX induction observed upon thapsigargin treatment, again demonstrating that SETX induction during the UPR is downstream of PERK (Figure S7I, J).

The UPR is linked with replication stress in hypoxia

Since SETX depletion led to an increase in R-loops, we hypothesised that PERK depletion would have a similar effect. Both, siRNA mediated PERK depletion and pharmacological inhibition of PERK led to an increase in R-loop levels in hypoxia suggesting that, like SETX, PERK signalling negatively regulates R-loops in hypoxia (Figure 5A and S8A, B). PERK depletion or inhibition also partially rescued the global transcriptional repression observed in hypoxia (Figure 5B, S8C). As SETX depletion led to an increase in transcription dependent DNA damage, we asked whether PERK inhibition showed a similar effect. Akin to SETX depletion, PERK inhibition led to an accumulation of DNA damage which was more significant under hypoxic conditions and dependent on transcription (Figure 5C). Additionally, both PERK inhibition and depletion led to increased DDR signalling in hypoxia, specifically increased phosphorylation of p53 and RPA (Figure 5D). PERK inhibition was confirmed by the absence in the electrophoretic mobility shift of PERK on western blot (Figure 5D). Increased RPA phosphorylation with PERK inhibition would indicate a possible increase in replication stress. The percentage of cells experiencing replication stress in hypoxia did not change with PERK depletion, which is expected since hypoxic cells in S phase of cell cycle have replication stress due to the lack of dNTPs (Figure S8D). However, there was an observable increase in the number of RPA foci per cell upon PERK depletion or inhibition in hypoxia suggesting that hypoxic cells with PERK depletion or inhibition may have increased replication stress (Figure 5E, F and S8E). Finally, we tested whether PERK inhibition led to increased replication stress in hypoxia by DNA

bioRxiv preprint doi: https://doi.org/10.1101/2020.05.24.113548; this version posted May 26, 2020. The copyright holder for this preprint (which was not certified by peer review) is the author/funder. All rights reserved. No reuse allowed without permission.

fibre assay. Inhibition of PERK led to decreased replication rates in both normoxia and hypoxia, suggesting that PERK signalling acts to alleviate replication stress (Figure 5G). Taken together, our data suggests that in radiobiological hypoxia, the PERK branch of the UPR signals through SETX and potentially other unidentified factors to reduce R-loops, replication stress, DNA damage and apoptosis (Figure 5H).

DISCUSSION

Our study demonstrates that in radiobiological hypoxia R-loops accumulate and the RNA/DNA helicase SETX is induced. Hypoxia-induced SETX alleviates replication stress and protects hypoxic cells from transcription-associated DNA damage and apoptosis. Importantly, SETX induction was dependent on the PERK branch of the UPR, the first evidence of a link between the UPR and the replication stress dependent DDR in hypoxia. Furthermore, PERK inhibition increased R loops and replication stress in hypoxia, uncovering an entirely novel aspect of PERK function in hypoxia.

Although this is the first link between the UPR and replication stress in hypoxia, a previous report showed that in response to a short exposure (1 hour) of thapsigargin or DTT, PERK inhibits replication fork progression, and origin firing through a Claspin/Chk1 pathway [47]. In contrast, we found that PERK signalling supports replication fork progression in hypoxia, suggesting that chemically induced UPR signalling may have different outcomes to the hypoxia induced UPR [48]. Alternatively, PERK signalling in response to short periods of the UPR activation may differ from extended UPR-mediated signalling.

While the DDR and UPR are both active in radiobiological hypoxia, the DDR is restricted to S phase cells [5]. Here, we show for the first time that SETX is responsive to the UPR. The PERK dependency of SETX induction ensures that cells in all phases of the cell cycle increase SETX levels in radiobiological hypoxia, which may be important for protecting cells from co-transcriptional R-loops which are prone to DNA damage in all phases of the cell cycle.

bioRxiv preprint doi: https://doi.org/10.1101/2020.05.24.113548; this version posted May 26, 2020. The copyright holder for this preprint (which was not certified by peer review) is the author/funder. All rights reserved. No reuse allowed without permission.

Previous reports have demonstrated that an accumulation of R-loops can lead to an increase in DNA damage. However, radiobiological hypoxia does not lead to an accumulation of DNA damage even after extended periods of time, suggesting that the hypoxia-induced R-loops are distinct to those induced by other genotoxic stresses such as camptothecin and G-quadruplex ligands [49,50]. One mechanism by which R-loops lead to DNA damage involves the nucleotide excision repair (NER) DNA repair pathway [51-53]. DNA repair pathways including NER are repressed in hypoxia, which potentially could protect hypoxic cells from R-loop dependent DNA damage particularly after chronic exposures of hypoxia where repression of repair is more evident [54,55]. We have shown that depleting SETX in hypoxia leads to an increase in DNA damage. The damage in SETX depleted hypoxic cells is transcription dependent and cell cycle independent, supporting the hypothesis that the role of hypoxia induced SETX is to resolve the co-transcriptional R-loops that are prone to DNA damage and therefore reduce genomic instability.

SETX has been suggested as a potential tumour suppressor from a screen using exome and transcriptome sequencing [56]. Additionally, akin to characterised tumour suppressors, SETX expression was down-regulated in a number of cancers compared to normal tissue controls [40]. However, AOA2 patients do not present with increased cancer susceptibility. While SETX loss can lead to genome instability, it is possible redundancy with other R-loop resolution mechanisms protect genome stability. In this study, SETX depletion increased R-loops, replication stress, DNA damage and apoptosis in hypoxia suggesting that SETX may promote hypoxic tumour growth, and hence be a potential therapeutic target. It is possible that in the hypoxic microenvironment in which multiple pathways including DNA repair and potentially R-loop resolution factors are repressed, loss of SETX function would not be readily compensated by other mechanisms.

Given that our study showed that inhibiting PERK led to increased R-loops, DNA damage and replication stress in hypoxia, PERK could therefore be a potential therapeutic target. Targeting PERK in cancer has been controversial as PERK has demonstrated both tumour promoting and suppressive activities depending on the type of cancer and intensity of stress [57]. However, in hypoxia, PERK supports tumour survival and growth, therefore suggesting PERK as a potential therapeutic target

bioRxiv preprint doi: https://doi.org/10.1101/2020.05.24.113548; this version posted May 26, 2020. The copyright holder for this preprint (which was not certified by peer review) is the author/funder. All rights reserved. No reuse allowed without permission.

specifically for hypoxic tumours [58,59]. Since PERK inhibition also increased replication stress in hypoxic conditions, we postulate that using PERK inhibitors in conjunction with replication stress inducers such as ATR inhibitors may be beneficial in solid tumours.

ACKNOWLEDGEMENTS

Thank you to Monica Olcina and Kienan Savage for helpful comments on the manuscript. SR, KBL, PV and MH were supported by a CRUK grant C5255/A23755 (awarded to EMH). NN was supported by an MRC studentship (MC_ST_U16007). IPF was supported by CRUK Oxford Centre Prize DPhil Studentship C38302/A12981. NG was supported by a Royal Society University Research fellowship. W-CC was funded by CRUK grant 23969 (awarded to FMB).

AUTHOR CONTRIBUTIONS

SR designed, conducted and interpreted the experiments and wrote the paper, TM, NN, IPF and MH conducted experiments, PV, W-CC, and FMB carried out the RNA-seq bioinformatics, KBL performed the TCGA analysis and advised on experiments, NG advised on the project, EMH conceived the project, designed and interpreted experiments and wrote the paper. All authors commented on the manuscript.

METHODS

Cell lines and reagents

RKO, HCT116 and A549 (ATCC) were grown in DMEM supplemented with 10% FBS and cultured in humidified incubators at 37 °C and 5% CO_2. Cells were routinely tested for mycoplasma and found to be negative. For plasmid transfections, JetPrime (Polyplus transfection) was used. siRNA transfections were performed using Dharma-FECT-1 (Thermo Fisher Scientific), sequences are available in the SI. siSETX-A siRNA was used for Figures 2D-F, 3B and Supplementary Figures 2D-

bioRxiv preprint doi: https://doi.org/10.1101/2020.05.24.113548; this version posted May 26, 2020. The copyright holder for this preprint (which was not certified by peer review) is the author/funder. All rights reserved. No reuse allowed without permission.

G, 3, 4, 5A, G. siSETX-B siRNA was used for Figures 2C, 3A, 3C-F and Supplementary Figures 2B, C and 5F. AllStars negative control siRNA (Qiagen) and ON-TARGETplus non-targeting pool (Dharmacon) were used as control siRNA. Drugs used were neocarzinostatin (NCS), DRB, Hydroxyurea, DFO, Adriamycin (Sigma), tunicamycin and thapsigargin (MP Biomedicals), and PERK inhibitor GSK2606414 (Calbiochem). Irradiations were performed using a Gamma Service GSR D1 Cs137 irradiator.

Hypoxia Treatment

Bactron II and BactronEZ anaerobic chambers (Shel Lab) were used for <0.1% O_2. An M35 hypoxia work station (Don Whitley Ltd) was used for 2% O_2. All experiments at <0.1% O_2 were plated in glass dishes, except for colony survival assays, which were plated in 6 well plates. All hypoxic treatments were harvested within the chamber using equilibrated buffers. Oxygen tensions were confirmed with the Oxylite probe (Oxford Optronix).

Immunoblotting

Cells were harvested in UTB lysis buffer (9 M Urea, 75 mM Tris-HCl pH 7.5, 0.15 M β-mercaptoethanol). Blots were visualised using the Odyssey Infrared imaging system. Antibodies used were SETX, KAP1 (Bethyl); GRP78, HIF1α, (BD Biosciences); ATM-S1981, ATM (Abcam); RPA, KAP1-S824, p53-S15 (Cell Signaling); p53, β-actin, RNase H1 (Santa Cruz); and γH2AX, H2AX (Millipore).

RT-qPCR

RNA was extracted using TRI reagent (Sigma), treated with DNase I (NEB) and cDNA prepared using the Verso cDNA synthesis kit (Thermo Scientific). SYBR Green PCR master mix (Applied Biosystems) and 7500 FAST Real-Time PCR machine (Applied Biosystems) were used. The ΔΔCt method was used to determine relative mRNA fold change with 18S as the reference gene. Primer sequences can be found in Table S1.

Chromatin immunoprecipitation (ChIP) - qPCR

bioRxiv preprint doi: https://doi.org/10.1101/2020.05.24.113548; this version posted May 26, 2020. The copyright holder for this preprint (which was not certified by peer review) is the author/funder. All rights reserved. No reuse allowed without permission.

Treated cells were fixed with 1% formaldehyde and quenched in 125 mM glycine. Cells were lysed with SDS lysis buffer (0.5% SDS, 10 mM EDTA, 50 mM tris pH 8.1). After sonication with Diagenode Bioruptor, samples were precleared with protein A agarose beads and subsequently incubated with ATF4 antibody (Cell Signaling) overnight. Antibody-antigen complexes were then pulled down with agarose beads and washed with the following buffers – low salt wash buffer (0.1% SDS, 1% Triton X-100, 2 mM EDTA, 20 mM Tris pH 8.1, 150 mM NaCl), high salt wash (0.1% SDS, 1% Triton X-100, 2 mM EDTA, 20 mM Tris pH 8.1, 500 mM NaCl), LiCl wash buffer (1% Igepal, 10 mM Tris pH 8.1, 250 mM LiCl, 1 mM EDTA, 1% sodium deoxycholate), TE wash buffer (10 mM Tris pH 8.0, 1 mM EDTA). DNA was eluted with 0.1M NaHCO3 and 1% SDS, cross-linking reversed and treated with proteinase K. DNA was purified with Qiagen PCR purification kits and qPCR was carried out using the following primers: SETX For: CTCAGGTGTCTCAGCGGATG, SETX Rev: CGCATTGTTCGCAAGACCTA, CHOP For: AAGAGGCTCACGACCGACTA and CHOP Rev: ATGATGCAATGTTTGGCAAC. The amount of immunoprecipitated material was calculated as the fold enrichment over IgG control.

Immunofluorescence and confocal microscopy

Cells were fixed in 4% (w/v) paraformaldehyde in PBS, permeabilised in 1% Triton-X-100 in PBS and blocked with 2% (w/v) BSA in 0.1% Tween-20 in PBS. Primary antibodies 53BP1 (Novus Biologicals), RPA (Cell Signaling), cleaved caspase 3 (Cell Signaling) and BrdU (BD Biosciences) were used. For BrdU staining, cells were exposed to BrdU (20 μM) for the final 1 hour in normxoia and 6 hours in hypoxia, after permeabilization cells were denatured in 2 N HCl for 30 min at 37°C, and blocked with 4% (w/v) BSA in 0.05% Tween-20 in PBS before incubation with the antibody. For 5'EU staining, cells were incubated with 5'ethynyluridine (EU) (0.5 mM) (Jena Bioscience) and Click-iT Alexa Fluor 647 labelling kit (Thermofisher) was used to measure nascent transcription. For EdU staining, cells were incubated with EdU (10 μM) and Click-iT Alexa Fluor 647 labelling kit (Thermofisher) was used to measure replication. S9.6 staining protocol was as previously described [10]. Coverslips were treated with RNase A (Fermentas) for 1 hour at 37°C and where indicated with RNase H (NEB) for 24 hours at 37°C prior to blocking. Coverslips were then incubated with 1:100

bioRxiv preprint doi: https://doi.org/10.1101/2020.05.24.113548; this version posted May 26, 2020. The copyright holder for this preprint (which was not certified by peer review) is the author/funder. All rights reserved. No reuse allowed without permission.

diluted S9.6 antibody (Kerafast) for 36 hours at 4°C. Cells were mounted and the entire nucleus imaged using LSM780 or LSM710 confocal microscope (Carl Zeiss Microscopy Ltd). The 5'EU and S9.6 mean nuclear intensity signal was determined using ImageJ plugin/algorithm kindly provided by Dr Kienan Savage, Queen's University Belfast [60]. A minimum of 100 cells were included per treatment.

RNA-seq

RNA was extracted using TRI reagent (Sigma) and treated with DNase I (NEB). The samples were purified using the RNeasy MinElute Clean-up kit (Qiagen) and purity confirmed using a Bioanalyzer. The mRNA fraction was selected for reverse transcription to cDNA. The cDNA generated was end-repaired, A-tailed and adapter-ligated. cDNA libraries were size selected, multiplexed, tested for quality and subjected to paired end sequencing in one lane of a flow cell.

RNA-seq differential expression analysis

The analyses were run through an established RNA-seq pipeline by the Buffa lab. The technical adapters in the pair-end raw reads were trimmed out by trimmomatic-0.32 and the clear reads were aligned to human genome version GRCh38 release 82 using tophat v2.0.13. The mapped reads from each gene were counted and normalised to fragments per kilobase of transcript per million (FPKM) using Cuffdiff-2.2.1. Fragments from PCR duplication were removed by Picard 1.124. The significance of fold changes of genes among samples were estimated by nonparametric method Rank Product 3.3, a package in R [61-66].

Correlation of SETX expression with TCGA RNA-seq data

RNA-seq data (RNA Seq V2 RSEM) for 382 colorectal adenocarcinoma tumours, 501 lung squamous cell carcinomas and 517 lung adenocarcinomas were downloaded from the TCGA project (accessed through cBioportal: http://www.cbioportal.org/ on the 12th April 2017). To examine *SETX* expression against hypoxia, a validated hypoxia metagene signature was used [41]. To examine *SETX* expression against tumour-associated, hypoxia-induced p53-activity (referred to as hypoxic p53 targets in the figure), raw data for each sequenced gene were rescaled to set the median equal to

bioRxiv preprint doi: https://doi.org/10.1101/2020.05.24.113548; this version posted May 26, 2020. The copyright holder for this preprint (which was not certified by peer review) is the author/funder. All rights reserved. No reuse allowed without permission.

1, and hypoxic p53 targets were determined by quantifying the median expression of 6 p53 target genes associated with hypoxia-induced p53 activity (encoding *BTG2, CYFIP2, INPP5D, KANK3, PHLDA3* and *SULF2*) [26].

DNA fibre analysis

DNA fibre assays were carried out as described [67]. For normoxic (21% O_2) treatments, cells were pulse-labelled with CldU (25 mM) for 20 min, washed once with fresh media, followed by the second label IdU (250 mM) for 20 min. For hypoxic (<0.1% O_2) treatments, cells were incubated in hypoxia for 3 hours before being pulse-labelled with CldU (25 mM) for 2 hours, washed once with fresh media, then followed by IdU (250 mM) for 1 hour. Cells were mounted (Invitrogen) and imaged using LSM780 confocal microscope (Carl Zeiss Microscopy Ltd). Replication rates were calculated as V_{IdU} (kb/min) = [(x * 0.132 μm) * 2.59 kb / μm] / t (min), where x = length of IdU.

Statistical analysis

Statistical tests were performed using GraphPad Prism software (GraphPad Software Inc.) and include one-way ANOVA, two-way ANOVA, 2-tailed Student's *t* test and Mann-Whitney U tests. ns = non-significant, * = $p \leq 0.05$, ** = $p \leq 0.01$, *** = $p \leq 0.001$, **** = $p \leq 0.0001$.

FIGURE LEGENDS

Figure 1. **SETX is induced in an oxygen dependent manner**

A. RKO cells were exposed to <0.1% O_2 for 0, 3, 6 and 18 hours or to NCS (200 ng/μL) for 6 hours. Cells were fixed and stained for γH2AX, RPA and 53BP1. A representative plot (of 2 independent) experiments is shown.

B. Representative images from A.

C. RKO cells were exposed to <0.1% O_2 for 0, 6 and 18 hours with 5'EU (0.5 mM) added for the final 6 hours. Representative of 3 independent experiments.

bioRxiv preprint doi: https://doi.org/10.1101/2020.05.24.113548; this version posted May 26, 2020. The copyright holder for this preprint (which was not certified by peer review) is the author/funder. All rights reserved. No reuse allowed without permission.

D. Representative images from C.

E. RKO cells were exposed to <0.1% O_2 for 6 hours followed by RT-qPCR for the mRNAs indicated relative to the normoxic control. The dashed line indicates normoxic expression levels.

F. RKO cells were treated for 0, 3, 6 and 18 hours of <0.1% O_2. The levels of SETX, HIF1α and RPA are shown. β-actin is the loading control.

G. A549 cells were treated for 0, 3, 6 and 18 hours of <0.1% O_2. The levels of SETX, HIF1α and p53 are shown. β-actin is the loading control.

H. HCT116 cells at 0, 4, 8 and 12 hours of treatment with <0.1% O_2. The levels of SETX, HIF1α, p53 and the loading control β-actin, are shown.

I. A549 cells were exposed to hypoxia, 2% O_2 or <0.1% O_2 for the times indicated and the relative mRNA levels of SETX determined.

J. To examine *SETX* expression against tumour-associated hypoxia-induced p53-activity (referred to as hypoxia-induced p53 targets), raw data for each sequenced gene were rescaled to set the median equal to 1, and hypoxic p53 targets were determined by quantifying the median expression of 6 p53 target genes associated with hypoxia-induced p53 activity (encoding *BTG2, CYFIP2, INPP5D, KANK3, PHLDA3* and *SULF2*) [26]. Correlations and statistical significance were determined by calculating Spearman's rho rank correlation coefficient (r) and two-tailed *P* value using Hmisc package in RStudio.

(A-I) Data from three independent experiments (n=3), mean ± standard error of the mean (SEM) are displayed unless otherwise indicated.

Figure 2. **SETX alleviates R-loops levels and replication stress in hypoxia**

A. A549 cells were exposed to 21% O_2 or <0.1% O_2 for 12 hours, fixed and stained with the S9.6 antibody and DAPI. Where indicated, coverslips were treated with RNase H prior to staining.

bioRxiv preprint doi: https://doi.org/10.1101/2020.05.24.113548; this version posted May 26, 2020. The copyright holder for this preprint (which was not certified by peer review) is the author/funder. All rights reserved. No reuse allowed without permission.

B. Representative images from A. Dashed white line indicates nuclear outline based on DAPI stain that was used to measure the nuclear S9.6 intensity.

C. A549 cells that were either mock transfected (grey) or transfected with SETX siRNA (green), were exposed to 21% O_2 or <0.1% O_2 for 12 hours. Cells were fixed and stained with the S9.6 antibody and DAPI. Where indicated, coverslips were treated with RNase H prior to staining. n=1

D. RKO cells transfected with control siRNA (grey) or SETX siRNA (green), were subjected to DNA fibre assays at 21% O_2 (Normoxia) and the different types of replication structures were quantified.

E. RKO cells transfected with control siRNA or SETX siRNA, were subjected to DNA fibre assays at <0.1% O_2 (Hypoxia) and the different types of replication structures were quantified.

F. Replication rates, as determined by IdU incorporation rates, of RKO cells transfected with control siRNA versus SETX siRNA exposed to 21% O_2 (Norm) or <0.1% O_2 (Hyp) for 6 hours.

(A-F) Data from three independent experiments (n=3), mean ± SEM are displayed unless otherwise indicated.

Figure 3. **SETX protects hypoxic cells from transcription associated DNA damage and apoptosis**

A. RKO control cells or SETX depleted cells were exposed to 21% and <0.1% O_2 for 6 hours in the presence of 5'EU. Cells were fixed, stained and quantified for 5'EU (0.5 mM) incorporation.

B. RNA-seq results comparing RKO cells treated with control siRNA or SETX-siRNA in 21% O_2 (Norm, grey) and <0.1% O_2 (Hyp). Genes with decreased expression upon SETX depletion in hypoxia shown in red, and genes with increased expression upon SETX depletion in hypoxia shown in blue. RNA-seq was carried out in 3 biological replicates (n=3).

C. Percentage of cells displaying 53BP1 foci (>5 per nucleus) in RKO cells with either mock treatment or SETX siRNA. Cells were exposed to 21% O_2 (Norm), 6 hours of <0.1% O_2 (Hyp) or pre-treated with DRB (100 μM) followed by 6 hours of <0.1% O_2 (Hyp + DRB).

bioRxiv preprint doi: https://doi.org/10.1101/2020.05.24.113548; this version posted May 26, 2020. The copyright holder for this preprint (which was not certified by peer review) is the author/funder. All rights reserved. No reuse allowed without permission.

D. Colony survival of A549 cells with either mock treatment or SETX siRNA after 0 and 18 hours of hypoxia (Hyp) (<0.1% O_2) treatment.

E. A549 cells were treated with SETX siRNA or mock and exposed to 21% O_2 (Norm) or <0.1% O_2 (Hyp) for 24 hours. The percentage of cells undergoing apoptosis as determined by DAPI staining is shown.

F. A549 cells were mock treated or treated with SETX siRNA and exposed to 21% O_2 (Norm), <0.1% O_2 (Hyp) for 24 hours or pre-treated with DRB (100 μM) followed by 24 hours of <0.1% O_2 (Hyp + DRB). The percentage of cells positive for cleaved caspase 3 is shown. Representative images of a normal and apoptotic cell are included.

(A-F) Data from three independent experiments (n=3), mean ± SEM are displayed unless otherwise indicated.

Figure 4. **SETX upregulation is dependent on the PERK branch of the UPR**

A. A549 cells were treated with either control siRNA or p53 siRNA and exposed to 21% O_2 (Norm) or <0.1% O_2 (Hyp) for 6 hours. SETX mRNA levels were determined by RT-qPCR.

B. A549 cells were treated with either control siRNA or ATF4 siRNA and exposed to 21% O_2 (Norm) or <0.1% O_2 (Hyp) for 16 hours. SETX mRNA levels were determined by RT-qPCR.

C. A549 cells were exposed to 21% O_2 (Norm) or <0.1% O_2 (Hyp) for 4 hours, and ChIP-qPCR experiments were performed to determine fold enrichment of ATF4 at the SETX promoter relative to IgG control.

D. SETX mRNA levels in non-treated A549 cells (N), cells exposed to irradiation (5 Gy) followed by a 1 hour recovery, Hu (1 mM), DFO (100 μM), hypoxia (2% O_2 or < 0.1% O_2), tunicamycin (Tuni, 5 μg/mL) or thapsigargin (Thaps, 2 μM) for 16 hours.

bioRxiv preprint doi: https://doi.org/10.1101/2020.05.24.113548; this version posted May 26, 2020. The copyright holder for this preprint (which was not certified by peer review) is the author/funder. All rights reserved. No reuse allowed without permission.

E. A549 cells were exposed to Thaps (2 μM) or Tuni (5 μg/mL) for the times indicated, or to Hu (2 mM, 8 h) followed by western blotting.

F. A549 cells were treated with either control siRNA or PERK siRNA and exposed to 21% O_2 (Norm) or <0.1% O_2 (Hyp) for 16 hours. SETX mRNA levels were determined by RT-qPCR. n=4

G. A549 cells were treated with either DMSO or PERKi (10 μM) and exposed to 21% O_2 (Norm) or <0.1% O_2 (Hyp) for 6 hours. SETX mRNA levels were determined by RT-qPCR. n=4

(A-G) Data from three independent experiments (n=3), mean ± SEM are displayed unless otherwise indicated.

Figure 5. **The UPR is linked with replication stress in hypoxia**

A. A549 cells that were either mock transfected (grey) or transfected with PERK siRNA (green), were exposed to 21% O_2 or <0.1% O_2 for 6 hours. Cells were fixed and stained with the S9.6 antibody and DAPI. Where indicated, coverslips were treated with RNase H (RNH) prior to staining.

B. A549 control cells or PERK depleted cells were exposed to 21% and <0.1% O_2 for 6 hours, 5'EU (0.5 mM) was added for the final hour of treatment. DRB was used as the positive control. Cells were fixed, stained and quantified for 5'EU incorporation.

C. The percentage of cells displaying 53BP1 foci (>5 per nucleus) as determined by immunofluorescence, in A549 cells exposed to 21% O_2 (Norm) or 6 hours of <0.1% O_2 (Hyp). Cells were pre-treated with DMSO, PERKi (10 μM), or DRB (100 μM) and PERKi (10 μM) (PERKi + DRB). n=3

D. A549 cells were treated with DMSO or PERKi (10 μM) and exposed to normoxia or hypoxia (<0.1% O_2) for 6 hours followed by western blotting as indicated.

bioRxiv preprint doi: https://doi.org/10.1101/2020.05.24.113548; this version posted May 26, 2020. The copyright holder for this preprint (which was not certified by peer review) is the author/funder. All rights reserved. No reuse allowed without permission.

E. A549 cells with either mock treatment or PERK siRNA were exposed to hypoxia (<0.1% O_2) for 6 hours, cells were fixed and stained for RPA by immunofluorescence assays. The number of RPA foci per cell was quantified.

F. Representative images from E.

G. Replication rates, as determined by IdU incorporation rates, of A549 cells treated with DMSO or PERKi (10 μM) and exposed to 21% O_2 (Norm) or <0.1% O_2 (Hyp) for 6 hours. Over 90 fibres were measured for each normoxic sample and over 150 fibres for each hypoxic sample, n=1.

H. Hypoxia leads to the activation of the UPR and replication stress. In addition to a shortage of nucleotides, R-loops accumulate in hypoxia and contribute to replication stress. The PERK branch of the UPR signals through ATF4 to increase SETX expression in hypoxia. Hypoxia-induced SETX reduces R-loop accumulation and subsequent replication stress-mediated signalling.

(A-G) Data from two independent experiments (n=2), mean ± SEM are displayed unless otherwise indicated.

REFERENCES

1 Hammond, E. M. *et al.* The meaning, measurement and modification of hypoxia in the laboratory and the clinic. *Clinical oncology (Royal College of Radiologists (Great Britain))* **26**, 277-288, doi:10.1016/j.clon.2014.02.002 (2014).
2 Foskolou, I. P. *et al.* Ribonucleotide Reductase Requires Subunit Switching in Hypoxia to Maintain DNA Replication. *Molecular cell* **66**, 206-220.e209, doi:10.1016/j.molcel.2017.03.005 (2017).
3 Pires, I. M. *et al.* Effects of acute versus chronic hypoxia on DNA damage responses and genomic instability. *Cancer research* **70**, 925-935, doi:10.1158/0008-5472.can-09-2715 (2010).
4 Ng, N., Purshouse, K., Foskolou, I. P., Olcina, M. M. & Hammond, E. M. Challenges to DNA replication in hypoxic conditions. *The FEBS journal* **285**, 1563-1571, doi:10.1111/febs.14377 (2018).
5 Olcina, M. M. *et al.* Replication stress and chromatin context link ATM activation to a role in DNA replication. *Molecular cell* **52**, 758-766, doi:10.1016/j.molcel.2013.10.019 (2013).
6 Dobrynin, G. *et al.* KDM4A regulates HIF-1 levels through H3K9me3. *Scientific reports* **7**, 11094, doi:10.1038/s41598-017-11658-3 (2017).
7 Olcina, M. M. *et al.* H3K9me3 facilitates hypoxia-induced p53-dependent apoptosis through repression of APAK. *Oncogene* **35**, 793-799, doi:10.1038/onc.2015.134 (2016).
8 Bencokova, Z. *et al.* ATM activation and signaling under hypoxic conditions. *Molecular and cellular biology* **29**, 526-537, doi:10.1128/mcb.01301-08 (2009).
9 Zeman, M. K. & Cimprich, K. A. Causes and consequences of replication stress. *Nature cell biology* **16**, 2-9, doi:10.1038/ncb2897 (2014).

bioRxiv preprint doi: https://doi.org/10.1101/2020.05.24.113548; this version posted May 26, 2020. The copyright holder for this preprint (which was not certified by peer review) is the author/funder. All rights reserved. No reuse allowed without permission.

10 Hamperl, S., Bocek, M. J., Saldivar, J. C., Swigut, T. & Cimprich, K. A. Transcription-Replication Conflict Orientation Modulates R-Loop Levels and Activates Distinct DNA Damage Responses. *Cell* **170**, 774-786.e719, doi:10.1016/j.cell.2017.07.043 (2017).

11 Santos-Pereira, J. M. & Aguilera, A. R loops: new modulators of genome dynamics and function. *Nature reviews. Genetics* **16**, 583-597, doi:10.1038/nrg3961 (2015).

12 Skourti-Stathaki, K., Proudfoot, N. J. & Gromak, N. Human senataxin resolves RNA/DNA hybrids formed at transcriptional pause sites to promote Xrn2-dependent termination. *Molecular cell* **42**, 794-805, doi:10.1016/j.molcel.2011.04.026 (2011).

13 Sollier, J. & Cimprich, K. A. Breaking bad: R-loops and genome integrity. *Trends in cell biology* **25**, 514-522, doi:10.1016/j.tcb.2015.05.003 (2015).

14 Li, X. & Manley, J. L. Inactivation of the SR protein splicing factor ASF/SF2 results in genomic instability. *Cell* **122**, 365-378, doi:10.1016/j.cell.2005.06.008 (2005).

15 Wahba, L., Amon, J. D., Koshland, D. & Vuica-Ross, M. RNase H and multiple RNA biogenesis factors cooperate to prevent RNA:DNA hybrids from generating genome instability. *Molecular cell* **44**, 978-988, doi:10.1016/j.molcel.2011.10.017 (2011).

16 Huertas, P. & Aguilera, A. Cotranscriptionally formed DNA:RNA hybrids mediate transcription elongation impairment and transcription-associated recombination. *Molecular cell* **12**, 711-721 (2003).

17 Hamperl, S. & Cimprich, K. A. The contribution of co-transcriptional RNA:DNA hybrid structures to DNA damage and genome instability. *DNA repair* **19**, 84-94, doi:10.1016/j.dnarep.2014.03.023 (2014).

18 Hatchi, E. *et al.* BRCA1 recruitment to transcriptional pause sites is required for R-loop-driven DNA damage repair. *Molecular cell* **57**, 636-647, doi:10.1016/j.molcel.2015.01.011 (2015).

19 Skourti-Stathaki, K., Kamieniarz-Gdula, K. & Proudfoot, N. J. R-loops induce repressive chromatin marks over mammalian gene terminators. *Nature* **516**, 436-439, doi:10.1038/nature13787 (2014).

20 Aguilera, A. & Garcia-Muse, T. R loops: from transcription byproducts to threats to genome stability. *Molecular cell* **46**, 115-124, doi:10.1016/j.molcel.2012.04.009 (2012).

21 Johnson, A. B., Denko, N. & Barton, M. C. Hypoxia induces a novel signature of chromatin modifications and global repression of transcription. *Mutation research* **640**, 174-179, doi:10.1016/j.mrfmmm.2008.01.001 (2008).

22 Denko, N. *et al.* Hypoxia actively represses transcription by inducing negative cofactor 2 (Dr1/DrAP1) and blocking preinitiation complex assembly. *The Journal of biological chemistry* **278**, 5744-5749, doi:10.1074/jbc.M212534200 (2003).

23 Scanlon, S. E. & Glazer, P. M. Multifaceted control of DNA repair pathways by the hypoxic tumor microenvironment. *DNA repair* **32**, 180-189, doi:10.1016/j.dnarep.2015.04.030 (2015).

24 Chan, N. *et al.* Contextual synthetic lethality of cancer cell kill based on the tumor microenvironment. *Cancer research* **70**, 8045-8054, doi:10.1158/0008-5472.can-10-2352 (2010).

25 Leszczynska, K. B. *et al.* Mechanisms and consequences of ATMIN repression in hypoxic conditions: roles for p53 and HIF-1. *Scientific reports* **6**, 21698, doi:10.1038/srep21698 (2016).

26 Leszczynska, K. B. *et al.* Hypoxia-induced p53 modulates both apoptosis and radiosensitivity via AKT. *The Journal of clinical investigation* **125**, 2385-2398, doi:10.1172/jci80402 (2015).

27 Rzymski, T. *et al.* Regulation of autophagy by ATF4 in response to severe hypoxia. *Oncogene* **29**, 4424-4435, doi:10.1038/onc.2010.191 (2010).

28 Koumenis, C. *et al.* Regulation of protein synthesis by hypoxia via activation of the endoplasmic reticulum kinase PERK and phosphorylation of the translation initiation factor eIF2alpha. *Molecular and cellular biology* **22**, 7405-7416 (2002).

29 Koumenis, C. & Wouters, B. G. "Translating" tumor hypoxia: unfolded protein response (UPR)-dependent and UPR-independent pathways. *Molecular cancer research : MCR* **4**, 423-436, doi:10.1158/1541-7786.Mcr-06-0150 (2006).

bioRxiv preprint doi: https://doi.org/10.1101/2020.05.24.113548; this version posted May 26, 2020. The copyright holder for this preprint (which was not certified by peer review) is the author/funder. All rights reserved. No reuse allowed without permission.

30 Martin-Tumasz, S. & Brow, D. A. Saccharomyces cerevisiae Sen1 Helicase Domain Exhibits 5'- to 3'-Helicase Activity with a Preference for Translocation on DNA Rather than RNA. *The Journal of biological chemistry* **290**, 22880-22889, doi:10.1074/jbc.M115.674002 (2015).

31 Kim, H. D., Choe, J. & Seo, Y. S. The sen1(+) gene of Schizosaccharomyces pombe, a homologue of budding yeast SEN1, encodes an RNA and DNA helicase. *Biochemistry* **38**, 14697-14710 (1999).

32 Suraweera, A. *et al.* Functional role for senataxin, defective in ataxia oculomotor apraxia type 2, in transcriptional regulation. *Human molecular genetics* **18**, 3384-3396, doi:10.1093/hmg/ddp278 (2009).

33 Fogel, B. L. *et al.* Mutation of senataxin alters disease-specific transcriptional networks in patients with ataxia with oculomotor apraxia type 2. *Human molecular genetics* **23**, 4758-4769, doi:10.1093/hmg/ddu190 (2014).

34 Mischo, H. E. *et al.* Yeast Sen1 helicase protects the genome from transcription-associated instability. *Molecular cell* **41**, 21-32, doi:10.1016/j.molcel.2010.12.007 (2011).

35 Li, W., Selvam, K., Rahman, S. A. & Li, S. Sen1, the yeast homolog of human senataxin, plays a more direct role than Rad26 in transcription coupled DNA repair. *Nucleic acids research* **44**, 6794-6802, doi:10.1093/nar/gkw428 (2016).

36 Yuce, O. & West, S. C. Senataxin, defective in the neurodegenerative disorder ataxia with oculomotor apraxia 2, lies at the interface of transcription and the DNA damage response. *Molecular and cellular biology* **33**, 406-417, doi:10.1128/mcb.01195-12 (2013).

37 Alzu, A. *et al.* Senataxin associates with replication forks to protect fork integrity across RNA-polymerase-II-transcribed genes. *Cell* **151**, 835-846, doi:10.1016/j.cell.2012.09.041 (2012).

38 Miller, M. S. *et al.* Senataxin suppresses the antiviral transcriptional response and controls viral biogenesis. *Nature immunology* **16**, 485-494, doi:10.1038/ni.3132 (2015).

39 Bennett, C. L. & La Spada, A. R. Unwinding the role of senataxin in neurodegeneration. *Discovery medicine* **19**, 127-136 (2015).

40 Groh, M., Albulescu, L. O., Cristini, A. & Gromak, N. Senataxin: Genome Guardian at the Interface of Transcription and Neurodegeneration. *Journal of molecular biology* **429**, 3181-3195, doi:10.1016/j.jmb.2016.10.021 (2017).

41 Buffa, F. M., Harris, A. L., West, C. M. & Miller, C. J. Large meta-analysis of multiple cancers reveals a common, compact and highly prognostic hypoxia metagene. *British journal of cancer* **102**, 428-435, doi:10.1038/sj.bjc.6605450 (2010).

42 Steinmetz, E. J. *et al.* Genome-wide distribution of yeast RNA polymerase II and its control by Sen1 helicase. *Molecular cell* **24**, 735-746, doi:10.1016/j.molcel.2006.10.023 (2006).

43 Tebaldi, T. *et al.* Whole-genome cartography of p53 response elements ranked on transactivation potential. *BMC genomics* **16**, 464, doi:10.1186/s12864-015-1643-9 (2015).

44 Luhr, M. *et al.* The kinase PERK and the transcription factor ATF4 play distinct and essential roles in autophagy resulting from tunicamycin-induced ER stress. *The Journal of biological chemistry* **294**, 8197-8217, doi:10.1074/jbc.RA118.002829 (2019).

45 Rzymski, T. & Harris, A. L. The unfolded protein response and integrated stress response to anoxia. *Clinical cancer research : an official journal of the American Association for Cancer Research* **13**, 2537-2540, doi:10.1158/1078-0432.ccr-06-2126 (2007).

46 Cojocari, D. *et al.* New small molecule inhibitors of UPR activation demonstrate that PERK, but not IRE1alpha signaling is essential for promoting adaptation and survival to hypoxia. *Radiotherapy and oncology : journal of the European Society for Therapeutic Radiology and Oncology* **108**, 541-547, doi:10.1016/j.radonc.2013.06.005 (2013).

47 Cabrera, E. *et al.* PERK inhibits DNA replication during the Unfolded Protein Response via Claspin and Chk1. *Oncogene* **36**, 678-686, doi:10.1038/onc.2016.239 (2017).

48 Bergmann, T. J. & Molinari, M. Three branches to rule them all? UPR signalling in response to chemically versus misfolded proteins-induced ER stress. *Biol Cell* **110**, 197-204, doi:10.1111/boc.201800029 (2018).

49 De Magis, A. *et al.* DNA damage and genome instability by G-quadruplex ligands are mediated by R loops in human cancer cells. *Proceedings of the National Academy of Sciences of the United States of America* **116**, 816-825, doi:10.1073/pnas.1810409116 (2019).

bioRxiv preprint doi: https://doi.org/10.1101/2020.05.24.113548; this version posted May 26, 2020. The copyright holder for this preprint (which was not certified by peer review) is the author/funder. All rights reserved. No reuse allowed without permission.

50 Sordet, O. *et al.* Ataxia telangiectasia mutated activation by transcription- and topoisomerase I-induced DNA double-strand breaks. *EMBO reports* **10**, 887-893, doi:10.1038/embor.2009.97 (2009).

51 Sollier, J. *et al.* Transcription-coupled nucleotide excision repair factors promote R-loop-induced genome instability. *Molecular cell* **56**, 777-785, doi:10.1016/j.molcel.2014.10.020 (2014).

52 Brustel, J., Kozik, Z., Gromak, N., Savic, V. & Sweet, S. M. M. Large XPF-dependent deletions following misrepair of a DNA double strand break are prevented by the RNA:DNA helicase Senataxin. *Scientific reports* **8**, 3850, doi:10.1038/s41598-018-21806-y (2018).

53 Cristini, A. *et al.* Dual Processing of R-Loops and Topoisomerase I Induces Transcription-Dependent DNA Double-Strand Breaks. *Cell reports* **28**, 3167-3181.e3166, doi:10.1016/j.celrep.2019.08.041 (2019).

54 Yuan, J., Narayanan, L., Rockwell, S. & Glazer, P. M. Diminished DNA repair and elevated mutagenesis in mammalian cells exposed to hypoxia and low pH. *Cancer research* **60**, 4372-4376 (2000).

55 Bindra, R. S., Crosby, M. E. & Glazer, P. M. Regulation of DNA repair in hypoxic cancer cells. *Cancer Metastasis Rev* **26**, 249-260, doi:10.1007/s10555-007-9061-3 (2007).

56 Zhao, Q. *et al.* Systematic detection of putative tumor suppressor genes through the combined use of exome and transcriptome sequencing. *Genome Biol* **11**, R114, doi:10.1186/gb-2010-11-11-r114 (2010).

57 Ojha, R. & Amaravadi, R. K. Targeting the unfolded protein response in cancer. *Pharmacol Res* **120**, 258-266, doi:10.1016/j.phrs.2017.04.003 (2017).

58 Fels, D. R. & Koumenis, C. The PERK/eIF2alpha/ATF4 module of the UPR in hypoxia resistance and tumor growth. *Cancer Biol Ther* **5**, 723-728, doi:10.4161/cbt.5.7.2967 (2006).

59 Feldman, D. E., Chauhan, V. & Koong, A. C. The unfolded protein response: a novel component of the hypoxic stress response in tumors. *Molecular cancer research : MCR* **3**, 597-605, doi:10.1158/1541-7786.Mcr-05-0221 (2005).

60 Vohhodina, J. *et al.* The RNA processing factors THRAP3 and BCLAF1 promote the DNA damage response through selective mRNA splicing and nuclear export. *Nucleic acids research* **45**, 12816-12833, doi:10.1093/nar/gkx1046 (2017).

61 Andrews, S. *FastQC: a quality control tool for high throughput sequence data.*, <http://www.bioinformatics.babraham.ac.uk/projects/fastqc/ Key: citeulike:11583827> (2010).

62 Bolger, A. M., Lohse, M. & Usadel, B. Trimmomatic: a flexible trimmer for Illumina sequence data. *Bioinformatics (Oxford, England)* **30**, 2114-2120, doi:10.1093/bioinformatics/btu170 (2014).

63 Langmead, B. & Salzberg, S. L. Fast gapped-read alignment with Bowtie 2. *Nature methods* **9**, 357-359, doi:10.1038/nmeth.1923 (2012).

64 Trapnell, C., Pachter, L. & Salzberg, S. L. TopHat: discovering splice junctions with RNA-Seq. *Bioinformatics (Oxford, England)* **25**, 1105-1111, doi:10.1093/bioinformatics/btp120 (2009).

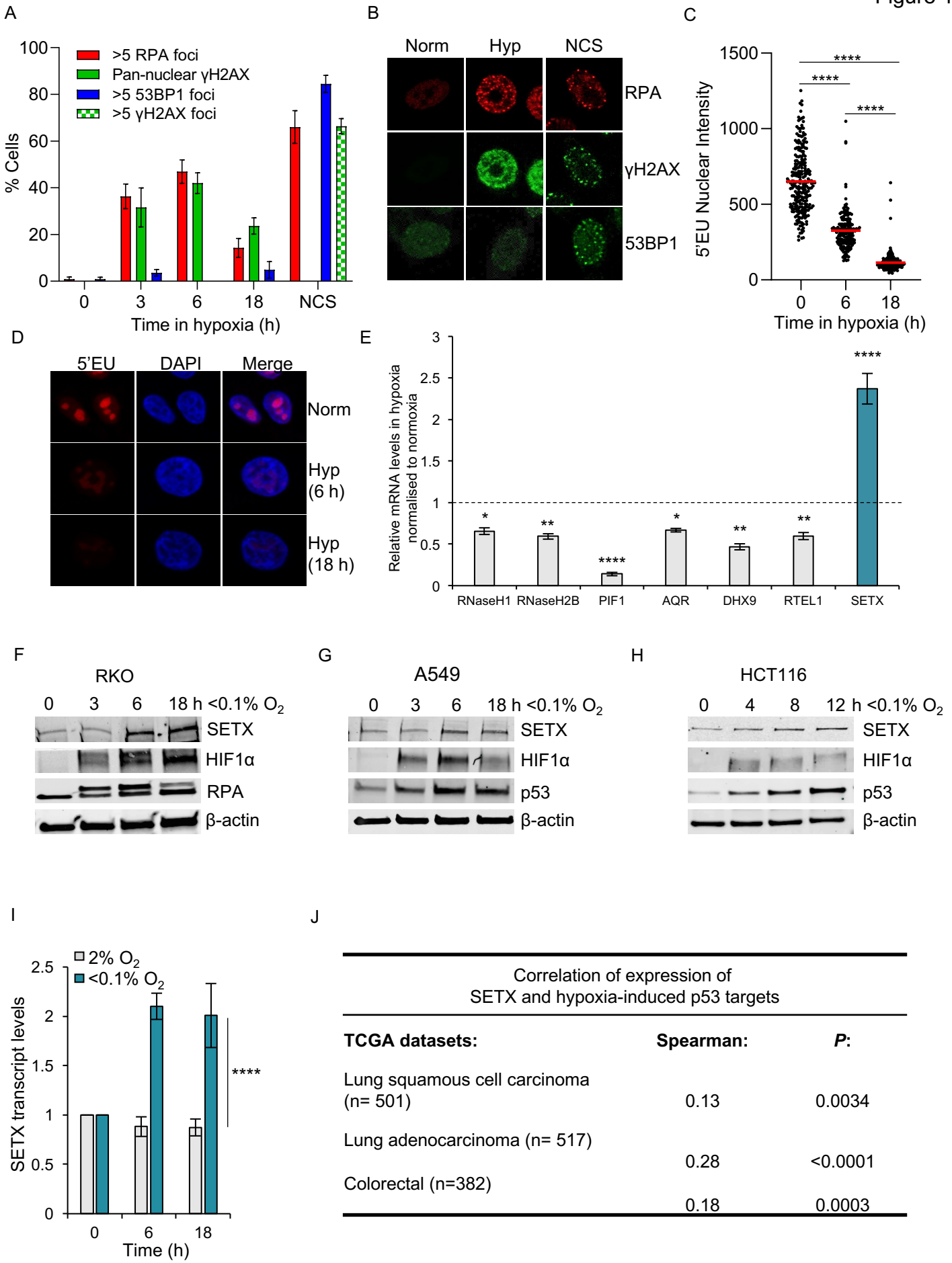
65 Trapnell, C. *Cufflinks and Cuffdiff Documentation, v6, Open Module on GenePattern Public Server.*, <http://www.broadinstitute.org/cancer/software/genepattern/modules/docs/Cufflinks.cuffdiff/6.> (2013).

66 Breitling, R., Armengaud, P., Amtmann, A. & Herzyk, P. Rank products: a simple, yet powerful, new method to detect differentially regulated genes in replicated microarray experiments. *FEBS letters* **573**, 83-92, doi:10.1016/j.febslet.2004.07.055 (2004).

67 Foskolou, I. P., Biasoli, D., Olcina, M. M. & Hammond, E. M. Measuring DNA Replication in Hypoxic Conditions. *Advances in experimental medicine and biology* **899**, 11-25, doi:10.1007/978-3-319-26666-4_2 (2016).

bioRxiv preprint doi: https://doi.org/10.1101/2020.05.24.113548; this version posted May 26, 2020. The copyright holder for this preprint (which was not certified by peer review) is the author/funder. All rights reserved. No reuse allowed without permission.

Figure 1



J

Correlation of expression of SETX and hypoxia-induced p53 targets		
TCGA datasets:	**Spearman:**	***P*:**
Lung squamous cell carcinoma (n= 501)	0.13	0.0034
Lung adenocarcinoma (n= 517)	0.28	<0.0001
Colorectal (n=382)	0.18	0.0003

Figure 2

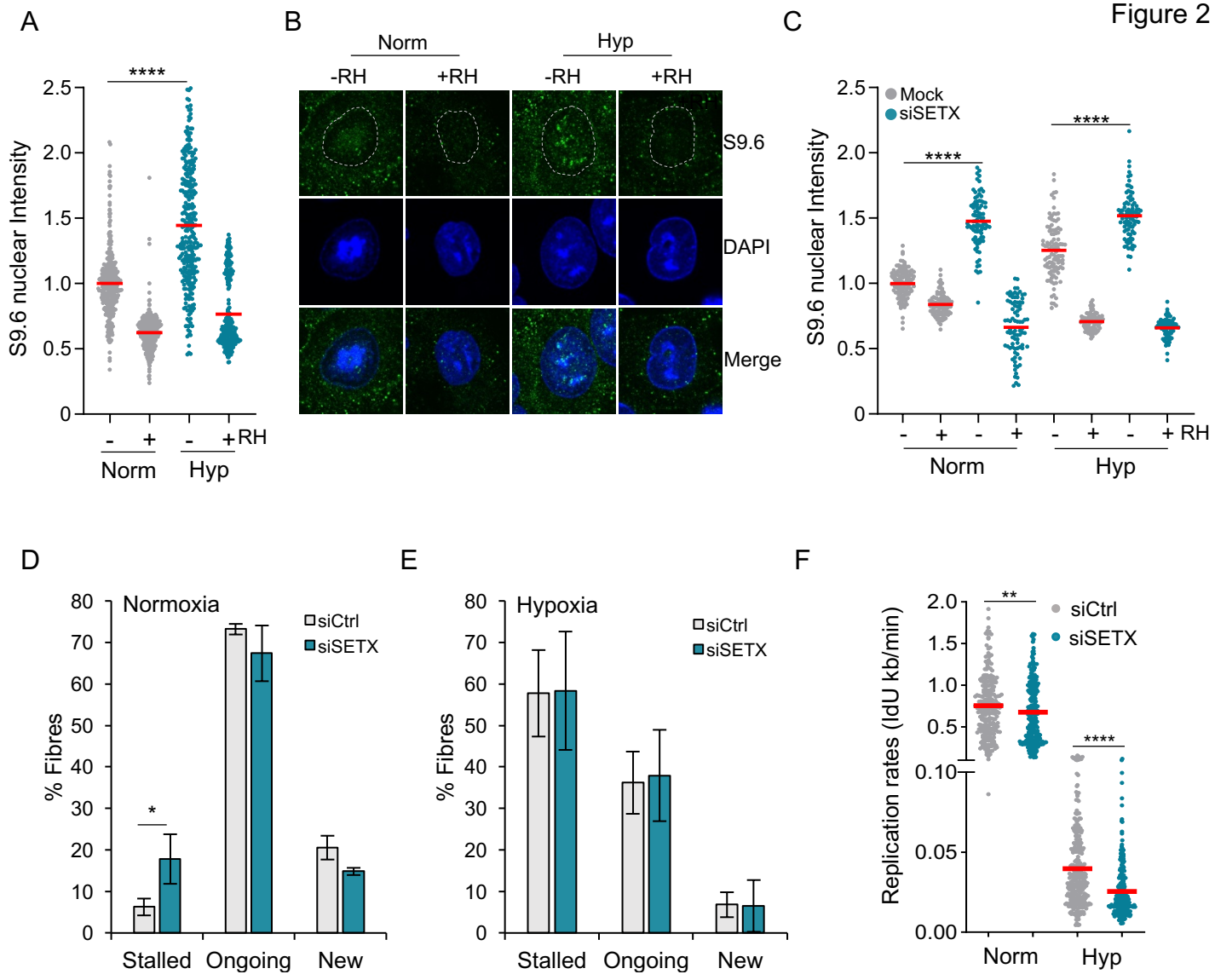
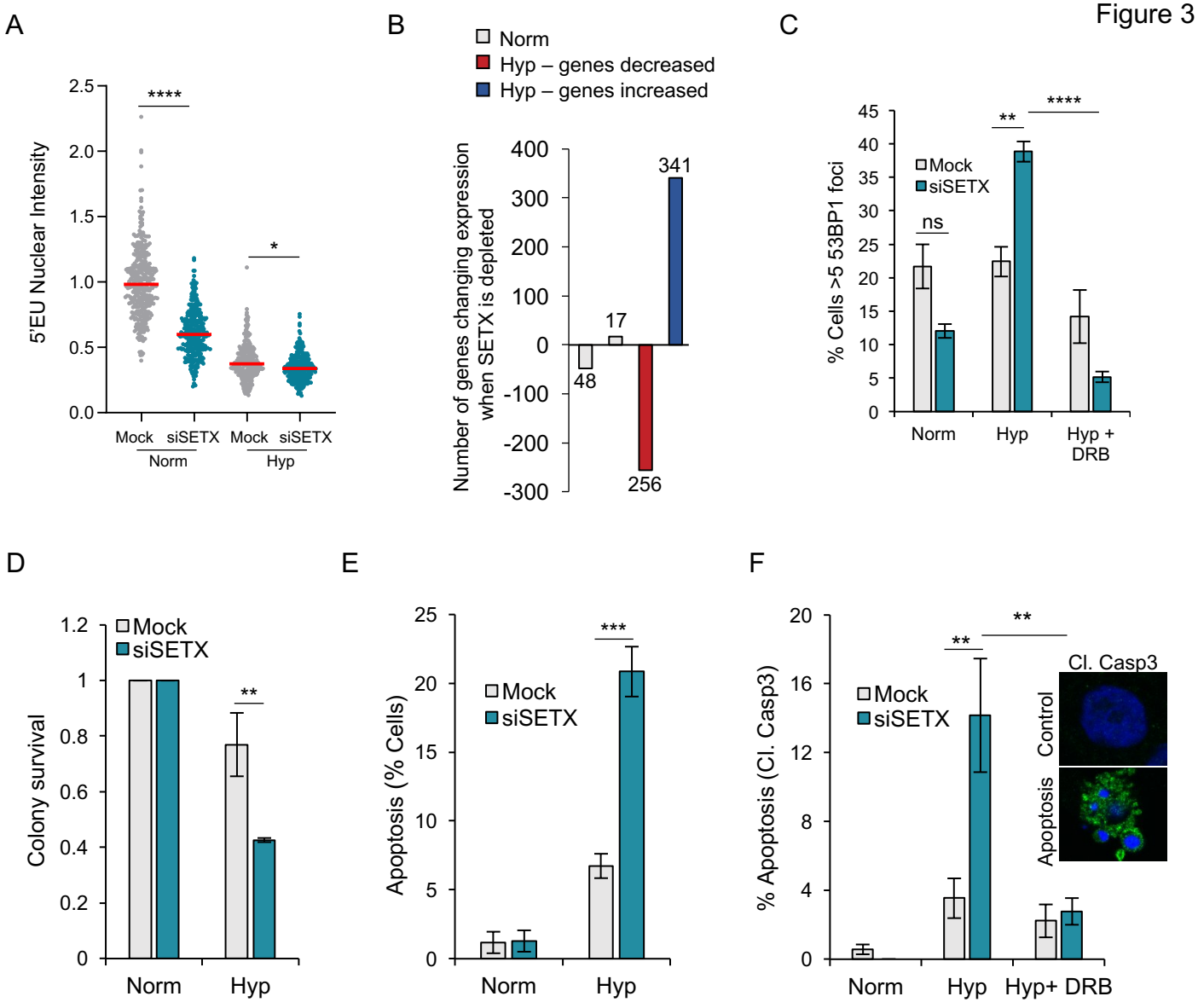
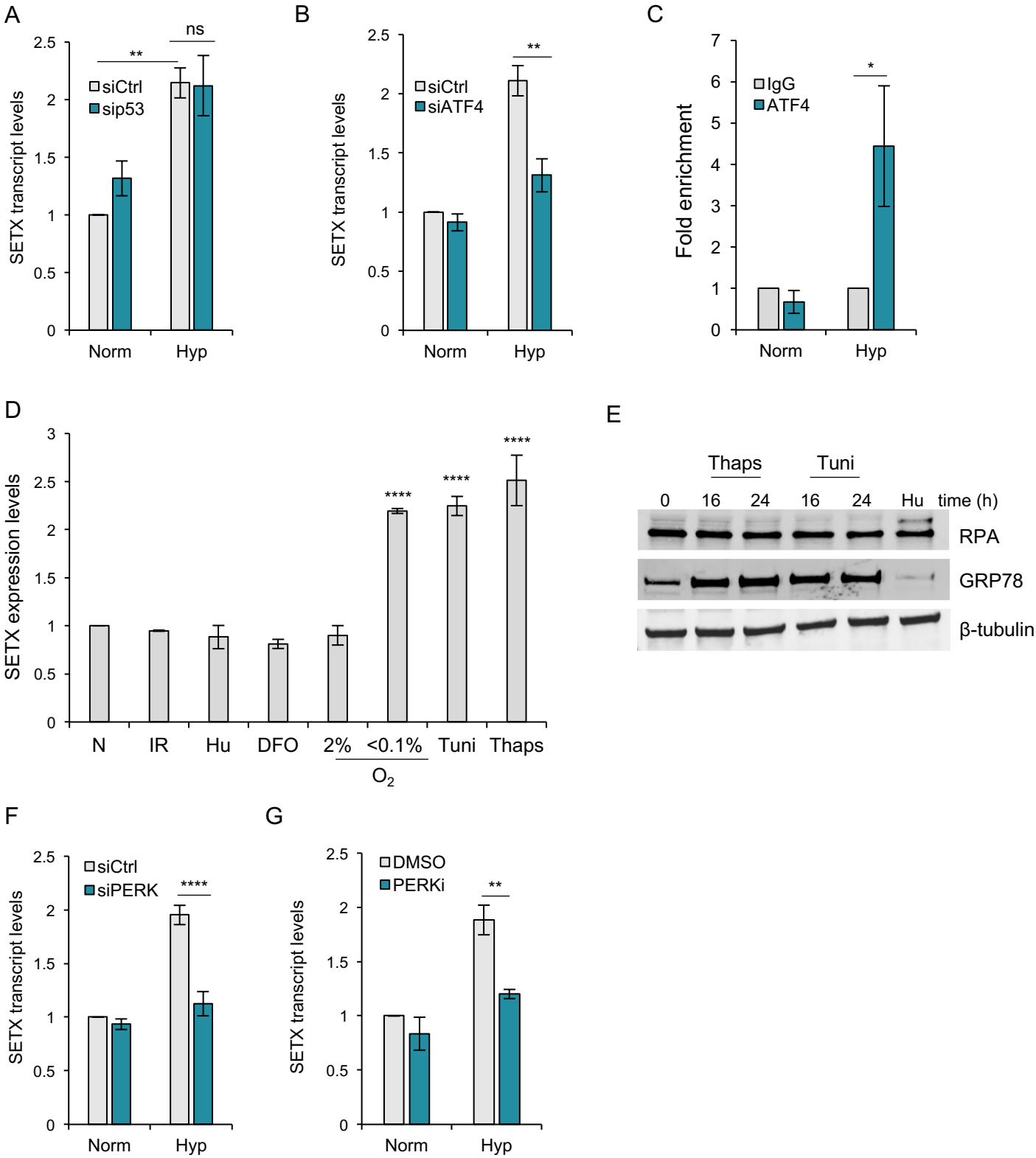
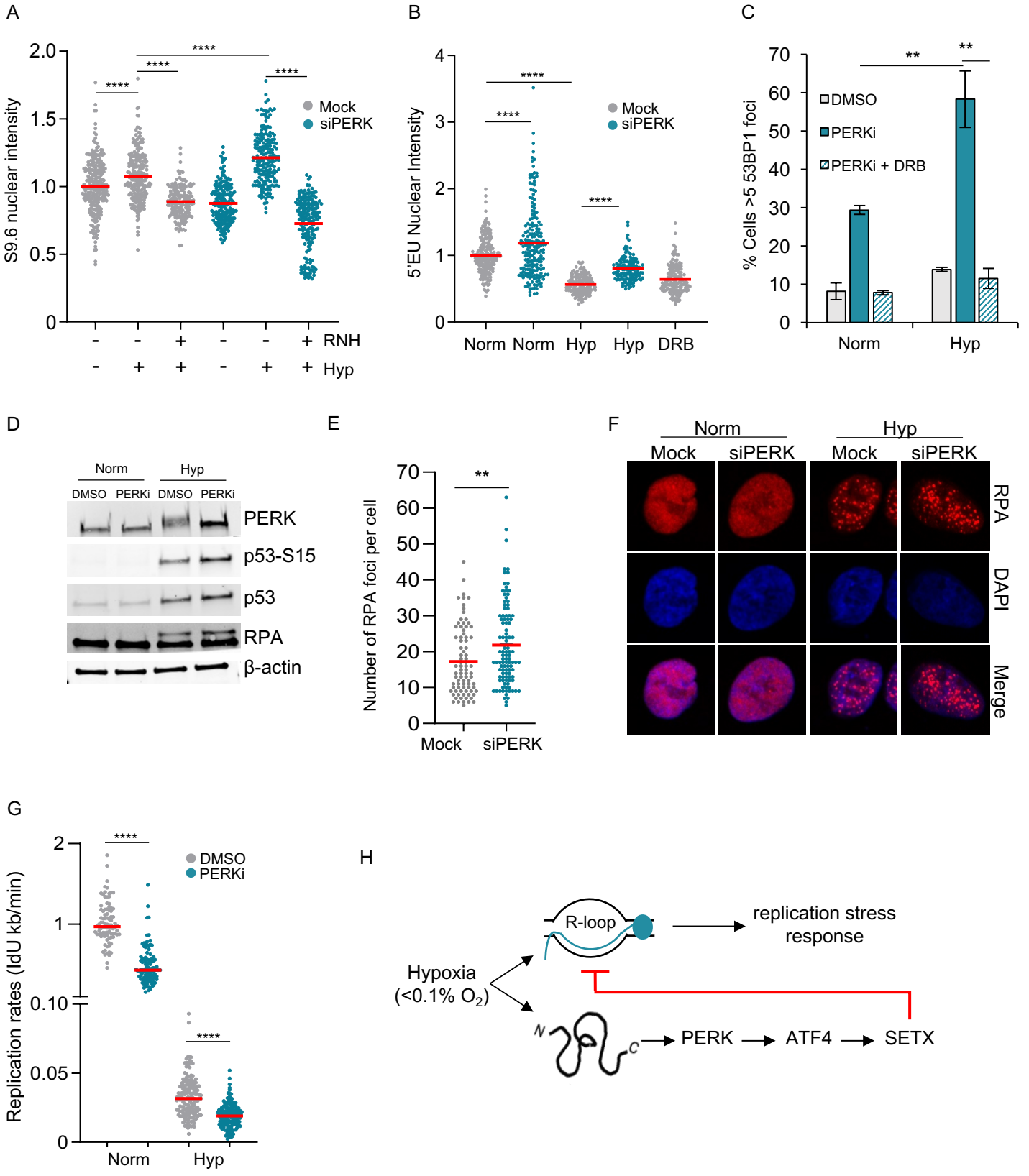

A
S9.6 nuclear Intensity
****
Norm
Hyp
B
Norm
Hyp
-RH
+RH
S9.6
DAPI
Merge
C
Mock
siSETX
S9.6 nuclear Intensity
****
Norm
Hyp
D
Normoxia
siCtrl
siSETX
% Fibres
Stalled
Ongoing
New
E
Hypoxia
F
Replication rates (IdU kb/min)
**
Norm
Hyp

Figure 3


A
5'EU Nuclear Intensity
2.5
2.0
1.5
1.0
0.5
0.0
****
*
Mock
siSETX
Mock
siSETX
Norm
Hyp
B
Norm
Hyp – genes decreased
Hyp – genes increased
Number of genes changing expression when SETX is depleted
400
300
200
100
0
-100
-200
-300
341
17
48
256
C
% Cells >5 53BP1 foci
45
40
35
30
25
20
15
10
5
0
**
****
ns
Mock
siSETX
Norm
Hyp
Hyp + DRB
D
Colony survival
1.2
1
0.8
0.6
0.4
0.2
0
Mock
siSETX
**
Norm
Hyp
E
Apoptosis (% Cells)
25
20
15
10
5
0
***
Mock
siSETX
Norm
Hyp
F
% Apoptosis (Cl. Casp3)
20
16
12
8
4
0
**
**
Mock
siSETX
Cl. Casp3
Control
Apoptosis
Norm
Hyp
Hyp+ DRB


A
SETX transcript levels
siCtrl
sip53
**
ns
Norm
Hyp
B
SETX transcript levels
siCtrl
siATF4
**
Norm
Hyp
C
Fold enrichment
IgG
ATF4
*
Norm
Hyp
D
SETX expression levels
****
****
****
N
IR
Hu
DFO
2%
<0.1%
O2
Tuni
Thaps
E
Thaps
Tuni
0
16
24
16
24
Hu
time (h)
RPA
GRP78
β-tubulin
F
SETX transcript levels
siCtrl
siPERK
****
Norm
Hyp
G
SETX transcript levels
DMSO
PERKi
**
Norm
Hyp


A
S9.6 nuclear intensity
Mock
siPERK
RNH
Hyp
B
5'EU Nuclear Intensity
Norm Norm Hyp Hyp DRB
C
% Cells >5 53BP1 foci
DMSO
PERKi
PERKi + DRB
Norm
Hyp
D
Norm
Hyp
DMSO PERKi DMSO PERKi
PERK
p53-S15
p53
RPA
β-actin
E
Number of RPA foci per cell
Mock
siPERK
F
Norm
Hyp
Mock siPERK Mock siPERK
RPA
DAPI
Merge
G
Replication rates (IdU kb/min)
DMSO
PERKi
Norm
Hyp
H
Hypoxia
(<0.1% O2)
R-loop
replication stress
response
N
C
PERK
ATF4
SETX

The FEBS Journal

FEBS PRESS science publishing by scientists

STATE-OF-THE-ART REVIEW

Challenges to DNA replication in hypoxic conditions

Natalie Ng[1], Karin Purshouse[1], Iosifina P. Foskolou[1], Monica M. Olcina[2] and Ester M. Hammond[1]

1 Department of Oncology, CRUK/MRC Oxford Institute for Radiation Oncology, University of Oxford, UK
2 Division of Radiation and Cancer Biology, Department of Radiation Oncology, Stanford University, CA, USA

Keywords
DNA damage response; hypoxia; reoxygenation; replication restart; replication stress; ribonucleotide reductase

Correspondence
E. M. Hammond, Department of Oncology, CRUK/MRC Oxford Institute for Radiation Oncology, University of Oxford, Oxford OX3 7DQ, UK
Tel: +44 1865 617320
E-mail: ester.hammond@oncology.ox.ac.uk

(Received 6 November 2017, revised 5 December 2017, accepted 22 December 2017)

doi:10.1111/febs.14377

The term hypoxia refers to any condition where insufficient oxygen is available and therefore encompasses a range of actual oxygen concentrations. The regions of tumours adjacent to necrotic areas are at almost anoxic levels and are known to be extremely therapy resistant (radiobiological hypoxia). The biological response to radiobiological hypoxia includes the rapid accumulation of replication stress and subsequent DNA damage response, including both ATR- and ATM-mediated signalling, despite the absence of detectable DNA damage. The causes and consequences of hypoxia-induced replication stress will be discussed.

Introduction

Oxygen is an essential factor that controls numerous developmental processes and normal tissue homeostasis. At a cellular level, oxygen is required for oxidative metabolism, energy supply through the generation of ATP and cell survival [1]. In solid tumours, regions of low oxygen (hypoxia) occur as a result of a high metabolic demand and inadequate oxygen supply. The abnormally formed/inefficient vasculature found in tumours is one of the primary causes of this imbalance between oxygen delivery and consumption [2,3]. The presence of hypoxic regions in tumours is clinically significant as they lead to resistance to therapy, genomic instability and an increase in the invasion and metastatic potential [4,5]. Hypoxia-driven genomic instability has been attributed, in part, to the repression of the DNA repair pathways, including homologous recombination (HR) and base excision repair, observed in these conditions [6–9]. A gradient of oxygen tensions occurs throughout tumours, reaching near anoxia in areas adjacent to necrotic regions. These extremely low oxygen tensions (< 0.1% O_2) are often referred to as radiobiological hypoxia and have been associated with the induction of DNA replication stress (RS) and the subsequent activation of DNA damage response (DDR) signalling [10–14]. In conditions of radiobiological hypoxia, cells have increased

Abbreviations
APC, anaphase promoting complex; ATM, ataxia-telangiectasia mutated; ATR, ataxia-telangiectasia and RAD3-related; BrdU, 5-bromo-2′-deoxyuridine; DDR, DNA damage response; DNA-PK, DNA-dependent protein kinase; dNTP, deoxyribonucleotide; DSB, double-strand break; HR, homologous recombination; MDM2, mouse double minute 2 homolog; NHEJ, nonhomologous end joining; O_2, oxygen; PI3KK, phosphatidylinositol-4,5-bisphosphate 3-kinase; RNR, ribonucleotide reductase; RPA, replication protein A; RRM, ribonucleotide reductase catalytic subunit M; RS, DNA replication stress; SCF, Skp, Cullin, F-box containing.

resistance to radiation-induced DNA damage and therefore radiotherapy. Numerous *in vitro* studies have demonstrated that the DNA damaging effect of radiation is absolutely dependent on the presence of oxygen at the time of exposure [5,15,16]. In accordance with this finding, patients with more hypoxic tumours have a worse response to radiotherapy [3]. Characterising the biological response to radiobiological hypoxia, including RS and the DDR, offers opportunities to identify novel therapeutic targets to improve radiotherapy response.

Replication stress

DNA replication is one of the most important and well-regulated biological processes, which ensures that the genome will be duplicated just once per cell cycle, and that replication is complete before the initiation of mitosis [17]. The importance of the DNA replication process is highlighted by the fact that not only the sequence of events, but also the majority of proteins involved in this process are highly conserved in eukaryotes [18]. RS is defined as the slowing or stalling of replication fork progression during DNA replication and is characterised by the accumulation of long stretches of ssDNA [4]. This ssDNA is usually formed, either because the replicative helicases continue to unwind the DNA while the replicative polymerases are stalled, or because the newly synthesised DNA is degraded by the action of nucleases [19,20]. Replication protein A (RPA) is the first responder to RS and acts by binding and stabilising the ssDNA tracks [21]. The ssDNA, once coated with RPA, creates a primer-template structure that serves as a signalling platform for the activation of the RS response (Fig. 1) [22]. Specifically, after binding to ssDNA, RPA recruits and interacts with several factors involved in the ataxia-telangiectasia and RAD3-related (ATR)-dependent DDR pathway. In brief, RPA first interacts with ATR-interacting protein (ATRIP), thereby recruiting and activating the ATR kinase at the replication fork, with additional cooperation from various stress response proteins including the Rad9-Rad1-Hus1 (9-1-1) complex, the ATR-activator TOBP1 and Ewing tumour-associated antigen ETAA1 [22–26]. Once activated, ATR signals through phosphorylation of downstream targets to initiate the cell cycle checkpoints and prevent cells with unreplicated DNA progressing through the cell cycle. In addition to its functions in cell cycle progression, the replication checkpoint acts locally at the replication fork. ATR is essential for preventing fork collapse. For example, SMARCAL1 (SWI/SNF-related, matrix-associated, actin-dependent regulator of chromatin, subfamily A-like 1) is phosphorylated by ATR at replication forks and maintains fork stability [27,28]. Signalling from the ATR kinase provides time to resolve stress, and allow the accumulation of resources such as deoxyribonucleotides (dNTPs), histones and RPA around stalled forks, in order to complete replication [29,30]. In general, ATR-mediated fork stabilisation ensures that forks will restart and continue faithful replication once the stress has been resolved. However, some lesions can be bypassed as the replication machinery may continue replicating by repriming after the lesion [31]. This generates ssDNA gaps that are 'filled' by lesion-specific polymerases or by fork remodelling [32]. Moreover, sometimes, despite the RS response, stalled forks fail to restart and eventually collapse, resulting in double-strand break (DSB) formation. Recently, RPA exhaustion was described as a key factor in replication fork breakage. Specifically, it was proposed that the suppression of firing of dormant origins by the replication checkpoint maintains an adequate supply of RPA to ensure genomic integrity at the site of DSB [33]. DSBs which occur during RS, can be formed either by passive fork breakage or after the activation of endonucleases (such as Mus81), which cleave exposed structures (such as retained ssDNA or reversed forks) [34]. Two main pathways are responsible for the repair of the DSBs: nonhomologous end joining (NHEJ), which is error-prone and can occur throughout the cell cycle, and HR, which is error-free and occurs in the S and G_2 phases of the cell cycle [35]. In addition to ATR signalling, the DDR includes activation of two other members of the PI3KK family: the ataxia-telangiectasia mutated (ATM) and DNA-dependent protein (DNA-PK) kinases [36]. It is generally considered that the DDR activates the ATR pathway in response to RS and/or at single-stranded DNA breaks (SSBs), whereas in the event of DSBs, ATM and DNA-PK mediated cascades are the primary responders [22,37]. Importantly, ATM acts as the principle responder to DSBs, whereas DNA-PK is activated when DSBs are repaired through the NHEJ pathway [38]. DNA-PK has recently been shown to respond to RS through phosphorylation and recruitment to the replication fork [39]. Regardless of the unique actions of the above kinases in the event of DNA damage, there is considerable crosstalk and collaboration between them. In particular, the ATR and ATM kinases share many common downstream targets and functions, and have been shown to activate each other in some cases [22]. Of note, ATM activation has also been described in the absence of DNA damage, for example in response to hypoxia, heat, hypotonic and oxidative stress, and chromatin modifiers [40,41].

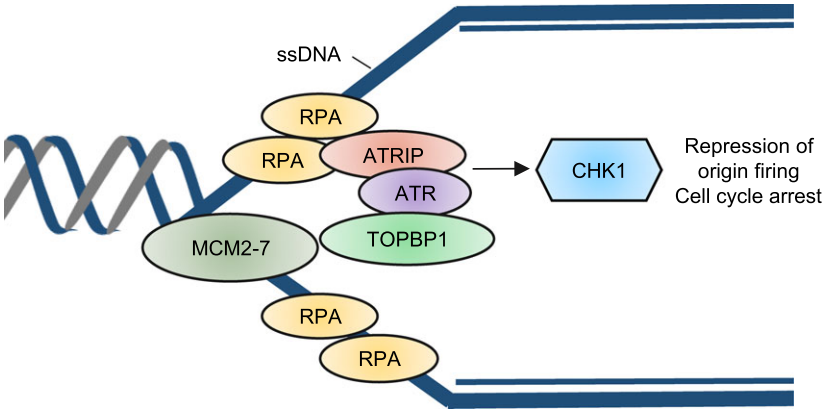


Fig. 1. Molecular signalling during replication stress. DNA is unwound by the MCM helicases forming a ssDNA. RPA binds and coats ssDNA at the replication fork. RPA interacts with ATRIP which recruits and the ATR kinase to the replication fork. ATR phosphorylates downstream targets including CHK1 leading to cell cycle arrest and suppression of dormant origin firing. Additional factors, such as TOPBP1, assist in the coordinated RS programme to prevent cell cycle progression.

Hypoxia-induced replication stress

The first evidence that certain levels of hypoxia lead to impaired DNA replication came from 5-bromo-2′-deoxyuridine (BrdU) incorporation assays, which demonstrated that in radiobiological levels of hypoxia, BrdU incorporation was significantly decreased [10]. Since this observation, the induction of RS in hypoxia has been further evidenced by the detection of specific RS-induced phosphorylation events (RPA-S33, γH2AX and CHK1-S345) and using DNA fibre analysis [42,43]. Importantly, these more recent studies verified that hypoxia-induced RS is indeed oxygen dependent, i.e. not all levels of hypoxia lead to RS [43]. Strikingly, even prolonged exposure to hypoxia does not lead to detectable SSB or DSB formation, as visualised using the 53BP1 foci assay or comet assay [12,13]. Perhaps not surprisingly, the ATR kinase was found to respond to hypoxia-induced RS and hypoxic cells have been shown to have increased sensitivity to ATR inhibitors [44–47]. However, as previously mentioned despite the lack of detectable DNA damage, ATM is also active in hypoxic conditions as evidenced by ATM-dependent phosphorylation of both itself and downstream targets such as KAP-1 [48]. ATM activation in hypoxia occurs independently of the DSB-associated MRN complex, further confirming the lack of DNA damage in these conditions [48]. Additionally, ATM remains diffuse throughout the nucleus in hypoxia and does not form specific foci. Recently, we demonstrated that ATM activation in hypoxia is, in part, dependent on the presence of RS. Specifically, hypoxia increases heterochromatic marks including trimethylation of H3 at lysine 9 (H3K9me3), which, in combination with RS, leads to activation of ATM signalling [13].

DNA fibre analysis has been particularly informative in characterising hypoxia-induced RS as changes in replication kinetics are visualised at the single molecule level [42]. In response to hypoxia (< 0.1% O_2) we observed an increase in the numbers of stalled replication forks and a decrease in new origin firing. In addition, the replication rates at ongoing forks in hypoxia showed a significant reduction but not complete abrogation [43,49]. DNA fibre analysis in noncancer cells demonstrated that hypoxia-induced RS is not restricted to cancer cells but likely occurs in all cells [43]. The level of hypoxia in tumours is extremely dynamic due to fluctuations in blood flow as a result of blockages and aberrant structures. As a result, hypoxic regions undergo cycling hypoxia, which includes periods of reoxygenation [50]. This knowledge led us to ask what would happen to DNA replication in cells experiencing hypoxia-induced RS once oxygen was restored. DNA replication can restart in response to reoxygenation, but this is dependent on how long cells experienced hypoxia-induced RS before reoxygenation. Relatively short periods of hypoxia (8 h) followed by reoxygenation allow restart of replication forks, whereas after longer periods (> 12 h) replication restart does not occur [14,43] (Fig. 2). These data suggested that prolonged hypoxia renders cells replication incompetent. A number of genes involved in DNA replication and repair have been found to be repressed in hypoxic conditions including members of the minichromosome maintenance complex (MCM) family [51,52]. The MCM2–7 complex is loaded onto chromatin in the G_1 phase of the cell cycle and provides

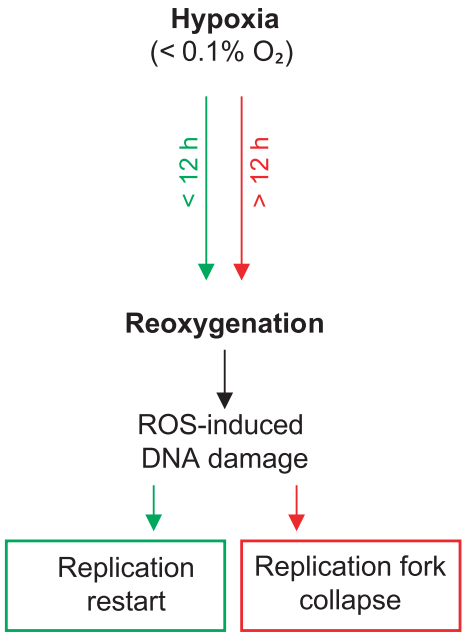


Fig. 2. Replication restart in response to reoxygenation. Hypoxia followed by reoxygenation incurs ROS-dependent DNA damage regardless of time in hypoxic conditions. Longer exposure to hypoxia (> 12 h) renders cells incompetent for fork restart which is in part due to the repression of the expression of the MCM helicases and their dissociation from chromatin. Determination of the exact time frame in which hypoxia renders replication forks incompetent for restart is technically challenging as DNA fibres generated in these conditions (> 8–12 h) are generally of poor quality.

the essential helicase activity necessary for duplex unwinding during replication [20]. MCM3, MCM4 and MCM5 were all repressed at the transcriptional level in response to hypoxia and most importantly, several members of this complex, MCM5, MCM6 and MCM7, were all shown to dissociate from chromatin after prolonged exposure to hypoxia [14,43,53]. Once the MCM complex is removed from the chromatin in S phase it cannot be reloaded in this phase and therefore DNA replication cannot continue/restart. These data led to the hypothesis that cells that have experienced hypoxia-induced RS for prolonged periods of time (> 12 h) cannot restart replication due to disassembly of the replisome [43]. However, this hypothesis is challenging to verify experimentally as it would require the re-expression of numerous factors in hypoxic conditions.

Since the somewhat surprising finding that ATM is activated in response to hypoxia-induced RS it has also been linked to DNA replication in hypoxic conditions [40,48]. Inhibition/depletion of ATM in hypoxia leads to slower replication rates and the accumulation of DNA damage in S phase, suggesting that the role of hypoxia-induced ATM activity is to promote replication by protecting replication fork stability [13]. Interestingly, inhibition of ATM was found to increase origin firing and in all likelihood, this is due to increased firing of dormant origins. Pharmacologic inhibition of Chk1 had no hypoxia-specific effect on DNA replication, although a significant increase in origin firing was observed after reoxygenation when Chk1 was inhibited [43]. siRNA-mediated knockdown of Chk2, however, had no effect on origin firing following reoxygenation-induced replication restart [54]. Similarly, replication restart following reoxygenation was not altered by ATM inhibition [13].

The source of RS in hypoxia – nucleotide imbalance

Previous studies suggested that nucleotide imbalance might be significant in hypoxic conditions leading us to hypothesis that this might be the cause of RS [14,22,43]. The biosynthesis of dNTPs involves both *de novo* and salvage pathways. In both cases, the first step of nucleotide biosynthesis requires the action of ribonucleotide reductase (RNR). RNR is an enzyme consisting of two homodimeric subunits, RRM1 and RRM2 or RRM2B, which are encoded by three genes on different chromosomes. The RRM1 dimer constitutes the large α subunit, which contains the catalytic site, whereas the β subunit is encoded by either RRM2 or RRM2B. Importantly, the β subunit contains an oxygen-requiring di-iron tyrosyl radical site essential for catalysis. The importance of RNR is further emphasised by the many different levels of regulation, including allosteric and transcriptional control, cell cycle specific proteolysis in mammalian cells and inhibition through small proteins in yeast [55]. A critical difference between RRM2 and RRM2B is that the expression of RRM2 is tightly cell cycle regulated. Unlike RRM2B, RRM2 contains a KEN box in the N terminus of the protein, which is recognised by SCF and APC complexes, leading to RRM2 cell cycle specific degradation [56,57]. Interestingly, an ATR-dependent downregulation of cyclin F has been shown to increase RRM2 stability in response to DNA damage [57]. The RRM1/RRM2 holoenzyme is mostly responsible for providing dNTPs for S phase DNA replication and repair in proliferating cells [55]. In contrast, the RRM1/RRM2B holoenzyme is believed to generate dNTPs for DNA repair in quiescent cells, as well as for mtDNA replication [58–61]. Importantly, humans with RRM2B mutations have mitochondrial diseases, including mtDNA depletion syndrome, mitochondrial neurogastrointestinal encephalopathy and

autosomal-dominant progressive external ophthalmoplegia [62–64]. Interestingly, mice lacking *RRM2B* are not embryonic lethal, but die early after weaning due to renal failure after attenuation of the dNTP pools and increased apoptosis [65].

Recently, we demonstrated that RNR switches isoforms from RRM2 to RRM2B allowing ongoing replication in hypoxic conditions [49,66]. The functional activity of RNR in hypoxia is retained through increased oxygen-entering frequency and increased stabilisation of the tyrosyl radical in the RRM2B subunit. This activity of RNR allows for the preservation of fork integrity through maintaining replication rates albeit significantly slower. Inhibition of RRM2B in cells experiencing hypoxia results in detrimental consequences for cell fate and loss of RRM2B in a xenograft model showed delayed tumour growth and increased radiosensitivity, highlighting the biological importance of the hypoxic induction of RRM2B [49]. However, due to the low activity of the RRM1/RRM2B enzyme, insufficient dNTPs are generated to maintain replication at the rates observed in normoxic conditions, explaining the occurrence of RS in hypoxia (Fig. 3). RRM2B transcriptional induction was shown to be p53-dependent and -independent of the hypoxia-inducible factor 1α. However, it is important to note that a reduced but still apparent hypoxic induction of RRM2B protein levels was observed in p53-deficient cells, suggesting additional p53-independent mechanisms of RRM2B stabilisation in hypoxia. Interestingly, it has been shown that ATM is capable of stabilising RRM2B through direct phosphorylation at serine 72, which inhibits hyperubiquitination and degradation by the E3 ubiquitin-protein ligase, mouse double minute 2 homolog (MDM2) [67]. Given that MDM2 expression is decreased in hypoxia, this may also contribute to the stabilisation of RRM2B under these conditions [68]. Moreover, nitric oxide, which is reported to be elevated in hypoxia, has been shown to increase RRM2B in p53-deficient cells [69]. Since all these mechanisms are relevant to hypoxic stress, further investigation is needed to verify if they could be responsible for the p53-independent RRM2B induction in hypoxia. Of note, the basal levels of RRM2B expression show no significant association with p53 status [70]. Since p53 is often mutated or deleted in human tumours, the involvement of mechanisms that lead to p53-independent basal expression of RRM2B, as well as protein stabilisation under hypoxia, suggest that RRM2B can perform its hypoxic role even in the absence of functional p53 [71]. The existence of alternative mechanisms that lead to RRM2B overexpression and stabilisation in hypoxia again highlights the importance of RRM2B protein in these conditions.

RRM2B as a clinical target

Ribonucleotide reductase activity is highly associated with cancer growth rates, and overexpression of the RNR subunits has in turn been correlated with many cancer types [72,73]. RRM2B typically showed gains in many different cancers including breast, colon, ovarian, prostate and uterine cancers as well as glioblastoma [72]. The copy number changes correlated with increased *RRM2B* expression in breast and prostate cancers, which supports a potential role for RRM2B as a tumour promoter [72]. In the same TCGA study, *RRM2* and *RRM1* showed low and rare copy number changes, respectively, in the malignancies examined. RNR has long been recognised as an important target for anticancer therapy [74]. Small-molecule inhibitors that target RNR can be classified into two categories depending on which subunit they target. Nucleoside analogues are used to target the α subunit (RRM1), as it is the subunit responsible for nucleotide binding, whereas redox active metal chelators target the β subunit (RRM2 and RRM2B) by inhibiting tyrosyl radical formation [72]. A well-known RNR inhibitor,

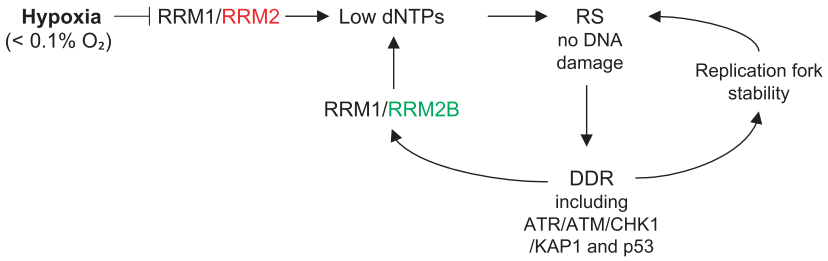


Fig. 3. Hypoxic conditions lead to replication stress. Nucleotide levels rapidly decrease in response to hypoxia (< 0.1% O_2) due to the oxygen dependency of the RNR enzyme. A RS response is then induced. RS initiates activation of the ATM and ATR kinases to coordinate the hypoxic DDR albeit in the absence of detectable DNA damage. The isoform switch and activity of RRM1/RRM2B allows for replication rates to continue at significantly reduced rates.

hydroxyurea (HU) inhibits the reduction of nucleoside diphosphates to dNDPs by scavenging the iron from the tyrosyl radical site, which is involved in RNR catalytic function. 3-aminopyridine-2-carboxaldehyde thiosemicarbazone (3-AP), also known as triapine, represents a far more specific and potent inhibitor of RNR by also targeting the tyrosyl radical site of the β subunit. Interestingly, hypoxic cells treated with either HU or 3-AP showed significant loss of viability compared to untreated cells (K. Purshouse, I. P. Foskolou, E. M. Hammond unpublished data). These data suggest that targeting RNR activity specifically in hypoxic tumour cells might be an effective therapeutic strategy. Although designing specific RRM2B inhibitors has long been proposed [65], the high sequence homology and the similarities in the mechanism of action with RRM2, have proven to be challenging obstacles. Interestingly, new approaches such as genetic strategies offer promising avenues for future drug development; for example delivery of siRNA against RRM2 by phosphorothionate oligodeoxynucleotides (GTI-2040) is in clinical trials for various solid tumours [75–78].

Conclusion

The activation of RS and the DDR is associated with the early stages of cancer development; hypoxia is a physiologically relevant factor proposed to contribute to this [79,80]. Hypoxia-induced RS leads to activation of the DDR pathway, including ATR and ATM signalling and this occurs in the absence of detectable DNA damage and reduced DNA repair capacity [4]. These findings suggest that the initiation of the DDR in response to hypoxia-induced RS is an effective way of protecting replication forks and avoiding further genomic instability. Inhibition of key components of the RS and DDR pathways, for example ATR, Chk1 and ATM, leads to the accumulation of DNA damage in hypoxia [53]. Although the sources of hypoxia-induced RS are likely multifactorial, the oxygen dependency of RNR is a key contributing factor [34]. Targeting RNR activity specifically in hypoxic tumour cells might be an effective therapeutic strategy in combination with radiotherapy.

Acknowledgements

This work was supported by a Cancer Research UK (CRUK) grant awarded to EMH, a CRUK Oxford Centre Prize DPhil Studentship (C38302/A12981) to IPF, MRC Institute DPhil Studentship to NN and a National Institute for Health Research (NIHR) Academic Clinical Fellowship to KP. The views expressed are those of the authors and not necessarily those of the NHS, the NIHR or the Department of Health. MMO is a Cancer Research Institute Irvington Fellow supported by the Cancer Research Institute.

Conflict of interest

The authors have no conflicts of interest.

Author contributions

All authors contributed to the writing of this manuscript.

References

1 Rankin EB & Giaccia AJ (2016) Hypoxic control of metastasis. *Science* **352**, 175–180.
2 Patiar S & Harris AL (2006) Role of hypoxia-inducible factor-1alpha as a cancer therapy target. *Endocr Relat Cancer* **13** (Suppl 1), S61–S75.
3 Vaupel P & Mayer A (2007) Hypoxia in cancer: significance and impact on clinical outcome. *Cancer Metastasis Rev* **26**, 225–239.
4 Bristow RG & Hill RP (2008) Hypoxia and metabolism. Hypoxia, DNA repair and genetic instability. *Nat Rev Cancer* **8**, 180–192.
5 Gray LH, Conger AD, Ebert M, Hornsey S & Scott OC (1953) The concentration of oxygen dissolved in tissues at the time of irradiation as a factor in radiotherapy. *Br J Radiol* **26**, 638–648.
6 Kumareswaran R, Ludkovski O, Meng A, Sykes J, Pintilie M & Bristow RG (2012) Chronic hypoxia compromises repair of DNA double-strand breaks to drive genetic instability. *J Cell Sci* **125** (Pt 1), 189–199.
7 Luoto KR, Kumareswaran R & Bristow RG (2013) Tumor hypoxia as a driving force in genetic instability. *Genome Integr* **4**, 5.
8 Glazer PM, Hegan DC, Lu Y, Czochor J & Scanlon SE (2013) Hypoxia and DNA repair. *Yale J Biol Med* **86**, 443–451.
9 Leszczynska KB, Göttgens EL, Biasoli D, Olcina MM, Lent J, Anbalagan S, Bernhardt S, Giaccia AJ & Hammond EM (2016) Mechanisms and consequences of ATMIN repression in hypoxic conditions: roles for p53 and HIF-1. *Sci Rep* **6**, 21698.
10 Hammond EM, Denko NC, Dorie MJ, Abraham RT & Giaccia AJ (2002) Hypoxia links ATR and p53 through replication arrest. *Mol Cell Biol* **22**, 1834–1843.
11 Hammond EM, Dorie MJ & Giaccia AJ (2004) Inhibition of ATR leads to increased sensitivity to hypoxia/reoxygenation. *Cancer Res* **64**, 6556–6562.
12 Hammond EM & Giaccia AJ (2004) The role of ATM and ATR in the cellular response to hypoxia and reoxygenation. *DNA Repair (Amst)* **3**, 1117–1122.

13 Olcina MM, Foskolou IP, Anbalagan S, Senra JM, Pires IM, Jiang Y, Ryan AJ & Hammond EM (2013) Replication stress and chromatin context link ATM activation to a role in DNA replication. *Mol Cell* **52**, 758–766.
14 Pires IM, Bencokova Z, McGurk C & Hammond EM (2010) Exposure to acute hypoxia induces a transient DNA damage response which includes Chk1 and TLK1. *Cell Cycle* **9**, 2502–2507.
15 Horan AD, Giandomenico AR & Koch CJ (1999) Effect of oxygen on radiation-induced DNA damage in isolated nuclei. *Radiat Res* **152**, 144–153.
16 Zhang H, Koch CJ, Wallen CA & Wheeler KT (1995) Radiation-induced DNA damage in tumors and normal tissues. III. Oxygen dependence of the formation of strand breaks and DNA-protein crosslinks. *Radiat Res* **142**, 163–168.
17 Li JJ & Deshaies RJ (1993) Exercising self-restraint: discouraging illicit acts of S and M in eukaryotes. *Cell* **74**, 223–226.
18 Branzei D & Foiani M (2010) Maintaining genome stability at the replication fork. *Nat Rev Mol Cell Biol* **11**, 208–219.
19 Mimitou EP & Symington LS (2011) DNA end resection–unraveling the tail. *DNA Repair (Amst)* **10**, 344–348.
20 Pacek M & Walter JC (2004) A requirement for MCM7 and Cdc45 in chromosome unwinding during eukaryotic DNA replication. *EMBO J* **23**, 3667–3676.
21 Glanzer JG, Liu S, Wang L, Mosel A, Peng A & Oakley GG (2014) RPA inhibition increases replication stress and suppresses tumor growth. *Cancer Res* **74**, 5165–5172.
22 Cimprich KA & Cortez D (2008) ATR: an essential regulator of genome integrity. *Nat Rev Mol Cell Biol* **9**, 616–627.
23 Zou L & Elledge SJ (2003) Sensing DNA damage through ATRIP recognition of RPA-ssDNA complexes. *Science* **300**, 1542–1548.
24 Lee YC, Zhou Q, Chen J & Yuan J (2016) RPA-binding protein ETAA1 is an ATR activator involved in DNA replication stress response. *Curr Biol* **26**, 3257–3268.
25 Haahr P, Hoffmann S, Tollenaere MA, Ho T, Toledo LI, Mann M, Bekker-Jensen S, Räschle M & Mailand N (2016) Activation of the ATR kinase by the RPA-binding protein ETAA1. *Nat Cell Biol* **18**, 1196–1207.
26 Bass TE, Luzwick JW, Kavanaugh G, Carroll C, Dungrawala H, Glick GG, Feldkamp MD, Putney R, Chazin WJ & Cortez D (2016) ETAA1 acts at stalled replication forks to maintain genome integrity. *Nat Cell Biol* **18**, 1185–1195.
27 Lopes M, Cotta-Ramusino C, Pellicioli A, Liberi G, Plevani P, Muzi-Falconi M, Newlon CS & Foiani M (2001) The DNA replication checkpoint response stabilizes stalled replication forks. *Nature* **412**, 557–561.
28 Couch FB, Bansbach CE, Driscoll R, Luzwick JW, Glick GG, Bétous R, Carroll CM, Jung SY, Qin J, Cimprich KA *et al.* (2013) ATR phosphorylates SMARCAL1 to prevent replication fork collapse. *Genes Dev* **27**, 1610–1623.
29 Gunjan A & Verreault A (2003) A Rad53 kinase-dependent surveillance mechanism that regulates histone protein levels in *S. cerevisiae*. *Cell* **115**, 537–549.
30 Toledo LI, Altmeyer M, Rask MB, Lukas C, Larsen DH, Povlsen LK, Bekker-Jensen S, Mailand N, Bartek J & Lukas J (2013) ATR prohibits replication catastrophe by preventing global exhaustion of RPA. *Cell* **155**, 1088–1103.
31 Elvers I, Johansson F, Groth P, Erixon K & Helleday T (2011) UV stalled replication forks restart by re-priming in human fibroblasts. *Nucleic Acids Res* **39**, 7049–7057.
32 Mailand N, Gibbs-Seymour I & Bekker-Jensen S (2013) Regulation of PCNA-protein interactions for genome stability. *Nat Rev Mol Cell Biol* **14**, 269–282.
33 Toledo L, Neelsen KJ & Lukas J (2017) Replication catastrophe: when a checkpoint fails because of exhaustion. *Mol Cell* **66**, 735–749.
34 Zeman MK & Cimprich KA (2014) Causes and consequences of replication stress. *Nat Cell Biol* **16**, 2–9.
35 McCabe N, Hanna C, Walker SM, Gonda D, Li J, Wikstrom K, Savage KI, Butterworth KT, Chen C, Harkin DP *et al.* (2015) Mechanistic rationale to target PTEN-deficient tumor cells with inhibitors of the DNA damage response kinase ATM. *Cancer Res* **75**, 2159–2165.
36 Goldstein M & Kastan MB (2015) The DNA damage response: implications for tumor responses to radiation and chemotherapy. *Annu Rev Med* **66**, 129–143.
37 Jackson SP & Bartek J (2009) The DNA-damage response in human biology and disease. *Nature* **461**, 1071–1078.
38 Collis SJ, DeWeese TL, Jeggo PA & Parker AR (2005) The life and death of DNA-PK. *Oncogene* **24**, 949–961.
39 Ying S, Chen Z, Medhurst AL, Neal JA, Bao Z, Mortusewicz O, McGouran J, Song X, Shen H, Hamdy FC *et al.* (2016) DNA-PKcs and PARP1 bind to unresected stalled DNA replication forks where they recruit XRCC1 to mediate repair. *Cancer Res* **76**, 1078–1088.
40 Olcina MM, Grand RJ & Hammond EM (2014) ATM activation in hypoxia – causes and consequences. *Mol Cell Oncol* **1**, e29903.
41 Blackford AN & Jackson SP (2017) ATM, ATR, and DNA-PK: the trinity at the heart of the DNA damage response. *Mol Cell* **66**, 801–817.

42 Foskolou IP, Biasoli D, Olcina MM & Hammond EM (2016) Measuring DNA replication in hypoxic conditions. *Adv Exp Med Biol* **899**, 11–25.
43 Pires IM, Bencokova Z, Milani M, Folkes LK, Li JL, Stratford MR, Harris AL & Hammond EM (2010) Effects of acute versus chronic hypoxia on DNA damage responses and genomic instability. *Cancer Res* **70**, 925–935.
44 Hammond EM & Giaccia AJ (2006) Hypoxia-inducible factor-1 and p53: friends, acquaintances, or strangers? *Clin Cancer Res* **12**, 5007–5009.
45 Pires IM, Olcina MM, Anbalagan S, Pollard JR, Reaper PM, Charlton PA, McKenna WG & Hammond EM (2012) Targeting radiation-resistant hypoxic tumour cells through ATR inhibition. *Br J Cancer* **107**, 291–299.
46 Leszczynska KB, Dobrynin G, Leslie RE, Ient J, Boumelha AJ, Senra JM, Hawkins MA, Maughan T, Mukherjee S & Hammond EM (2016) Preclinical testing of an Atr inhibitor demonstrates improved response to standard therapies for esophageal cancer. *Radiother Oncol* **121**, 232–238.
47 Fokas E, Prevo R, Hammond EM, Brunner TB, McKenna WG & Muschel RJ (2014) Targeting ATR in DNA damage response and cancer therapeutics. *Cancer Treat Rev* **40**, 109–117.
48 Bencokova Z, Kaufmann MR, Pires IM, Lecane PS, Giaccia AJ & Hammond EM (2009) ATM activation and signaling under hypoxic conditions. *Mol Cell Biol* **29**, 526–537.
49 Foskolou IP, Jorgensen C, Leszczynska KB, Olcina MM, Tarhonskaya H, Haisma B, D'Angiolella V, Myers WK, Domene C, Flashman E *et al.* (2017) Ribonucleotide reductase requires subunit switching in hypoxia to maintain DNA replication. *Mol Cell* **66**, 206–220 e9.
50 Michiels C, Tellier C & Feron O (2016) Cycling hypoxia: a key feature of the tumor microenvironment. *Biochim Biophys Acta* **1866**, 76–86.
51 Hammond EM, Mandell DJ, Salim A, Krieg AJ, Johnson TM, Shirazi HA, Attardi LD & Giaccia AJ (2006) Genome-wide analysis of p53 under hypoxic conditions. *Mol Cell Biol* **26**, 3492–3504.
52 Chan N, Ali M, McCallum GP, Kumareswaran R, Koritzinsky M, Wouters BG, Wells PG, Gallinger S & Bristow RG (2014) Hypoxia provokes base excision repair changes and a repair-deficient, mutator phenotype in colorectal cancer cells. *Mol Cancer Res* **12**, 1407–1415.
53 Olcina M, Lecane PS & Hammond EM (2010) Targeting hypoxic cells through the DNA damage response. *Clin Cancer Res* **16**, 5624–5629.
54 Olcina MM, Grand RJ & Hammond EM (2014) ATM activation in hypoxia – causes and consequences. *Mol Cell Oncol* **1**, 8.
55 Nordlund P & Reichard P (2006) Ribonucleotide reductases. *Annu Rev Biochem* **75**, 681–706.
56 Chabes AL, Bjorklund S & Thelander L (2004) S phase-specific transcription of the mouse ribonucleotide reductase R2 gene requires both a proximal repressive E2F-binding site and an upstream promoter activating region. *J Biol Chem* **279**, 10796–10807.
57 D'Angiolella V, Donato V, Forrester FM, Jeong YT, Pellacani C, Kudo Y, Saraf A, Florens L, Washburn MP & Pagano M (2012) Cyclin F-mediated degradation of ribonucleotide reductase M2 controls genome integrity and DNA repair. *Cell* **149**, 1023–1034.
58 Bourdon A, Minai L, Serre V, Jais JP, Sarzi E, Aubert S, Chrétien D, de Lonlay P, Paquis-Flucklinger V, Arakawa H *et al.* (2007) Mutation of RRM2B, encoding p53-controlled ribonucleotide reductase (p53R2), causes severe mitochondrial DNA depletion. *Nat Genet* **39**, 776–780.
59 Guittet O, Håkansson P, Voevodskaya N, Fridd S, Gräslund A, Arakawa H, Nakamura Y & Thelander L (2001) Mammalian p53R2 protein forms an active ribonucleotide reductase in vitro with the R1 protein, which is expressed both in resting cells in response to DNA damage and in proliferating cells. *J Biol Chem* **276**, 40647–40651.
60 Pontarin G, Ferraro P, Bee L, Reichard P & Bianchi V (2012) Mammalian ribonucleotide reductase subunit p53R2 is required for mitochondrial DNA replication and DNA repair in quiescent cells. *Proc Natl Acad Sci USA* **109**, 13302–13307.
61 Pontarin G, Ferraro P, Håkansson P, Thelander L, Reichard P & Bianchi V (2007) p53R2-dependent ribonucleotide reduction provides deoxyribonucleotides in quiescent human fibroblasts in the absence of induced DNA damage. *J Biol Chem* **282**, 16820–16828.
62 Kollberg G, Darin N, Benan K, Moslemi AR, Lindal S, Tulinius M, Oldfors A & Holme E (2009) A novel homozygous RRM2B missense mutation in association with severe mtDNA depletion. *Neuromuscul Disord* **19**, 147–150.
63 Shaibani A, Shchelochkov OA, Zhang S, Katsonis P, Lichtarge O, Wong LJ & Shinawi M (2009) Mitochondrial neurogastrointestinal encephalopathy due to mutations in RRM2B. *Arch Neurol* **66**, 1028–1032.
64 Tyynismaa H, Ylikallio E, Patel M, Molnar MJ, Haller RG & Suomalainen A (2009) A heterozygous truncating mutation in RRM2B causes autosomal-dominant progressive external ophthalmoplegia with multiple mtDNA deletions. *Am J Hum Genet* **85**, 290–295.
65 Kimura T, Takeda S, Sagiya Y, Gotoh M, Nakamura Y & Arakawa H (2003) Impaired function of p53R2 in Rrm2b-null mice causes severe renal failure through attenuation of dNTP pools. *Nat Genet* **34**, 440–445.

66 Foskolou IP & Hammond EM (2017) RRM2B: an oxygen-requiring protein with a role in hypoxia. *Mol Cell Oncol* **4**, e1335272.
67 Chang L, Zhou B, Hu S, Guo R, Liu X, Jones SN & Yen Y (2008) ATM-mediated serine 72 phosphorylation stabilizes ribonucleotide reductase small subunit p53R2 protein against MDM2 to DNA damage. *Proc Natl Acad Sci USA* **105**, 18519–18524.
68 Alarcón R, Koumenis C, Geyer RK, Maki CG & Giaccia AJ (1999) Hypoxia induces p53 accumulation through MDM2 down-regulation and inhibition of E6-mediated degradation. *Cancer Res* **59**, 6046–6051.
69 Guittet O, Tebbi A, Cottet MH, Vésin F & Lepoivre M (2008) Upregulation of the p53R2 ribonucleotide reductase subunit by nitric oxide. *Nitric Oxide* **19**, 84–94.
70 Cho EC & Yen Y (2016) Novel regulators and molecular mechanisms of p53R2 and its disease relevance. *Biochimie* **123**, 81–84.
71 Wasylishen AR & Lozano G (2015) Attenuating the p53 pathway in human cancers: many means to the same end. *Cold Spring Harb Perspect Med* **6**, a026211.
72 Aye Y, Li M, Long MJ & Weiss RS (2015) Ribonucleotide reductase and cancer: biological mechanisms and targeted therapies. *Oncogene* **34**, 2011–2021.
73 Elford HL, Freese M, Passamani E & Morris HP (1970) Ribonucleotide reductase and cell proliferation. I. Variations of ribonucleotide reductase activity with tumor growth rate in a series of rat hepatomas. *J Biol Chem* **245**, 5228–5233.
74 Crona M, Codó P, Jonna VR, Hofer A, Fernandes AP & Tholander F (2016) A ribonucleotide reductase inhibitor with deoxyribonucleoside-reversible cytotoxicity. *Mol Oncol* **10**, 1375–1386.
75 Juhasz A, Vassilakos A, Chew HK, Gandara D & Yen Y (2006) Analysis of ribonucleotide reductase M2 mRNA levels in patient samples after GTI-2040 antisense drug treatment. *Oncol Rep* **15**, 1299–1304.
76 Leighl NB, Laurie SA, Chen XE, Ellis P, Shepherd FA, Knox JJ, Goss G, Burkes RL, Pond GR, Dick C *et al.* (2009) A phase I/II study of GTI-2040 plus docetaxel as second-line treatment in advanced non-small cell lung cancer: a study of the PMH phase II consortium. *J Thorac Oncol* **4**, 1163–1169.
77 Lee Y, Vassilakos A, Feng N, Lam V, Xie H, Wang M, Jin H, Xiong K, Liu C, Wright J *et al.* (2003) GTI-2040, an antisense agent targeting the small subunit component (R2) of human ribonucleotide reductase, shows potent antitumor activity against a variety of tumors. *Cancer Res* **63**, 2802–2811.
78 Oh YK & Park TG (2009) siRNA delivery systems for cancer treatment. *Adv Drug Deliv Rev* **61**, 850–862.
79 Bartkova J, Horejsí Z, Koed K, Krämer A, Tort F, Zieger K, Guldberg P, Sehested M, Nesland JM, Lukas C *et al.* (2005) DNA damage response as a candidate anti-cancer barrier in early human tumorigenesis. *Nature* **434**, 864–870.
80 Gorgoulis VG, Vassiliou LV, Karakaidos P, Zacharatos P, Kotsinas A, Liloglou T, Venere M, Ditullio RA Jr, Kastrinakis NG, Levy B *et al.* (2005) Activation of the DNA damage checkpoint and genomic instability in human precancerous lesions. *Nature* **434**, 907–913.